Università degli Studi di Ferrara

DOTTORATO DI RICERCA IN CO-TUTELA con
« Université Pierre et Marie Curie » di Parigi
(Sorbonne Université)
in
"Scienze Farmaceutiche" e "Chimie Moléculaire"

CICLO XXIII

COORDINATORI Prof. Stefano Mandredini e Prof. Emmanuel Lacôte

Enantioselective Approaches and Domino Sequences for the Synthesis of Compounds of Biological Interest

Settore Scientifico Disciplinare CHIM/06

Sostenuto l' 8 Aprile 2011

Davanti alla commissione costituita da:

Prof. Pollini Gian Piero e Prof. Poli Giovanni: Direttori della Tesi

Prof.ssa Ongeri Sandrine e Prof.ssa Costi Maria Paola: Controrelatori

M. Karoyan Philippe et M. Trapella Claudio: Esaminatori

Dottorando
Dott.ssa Pelà Michela

Tutori
Prof. Pollini Gian Piero

Prof. Poli Giovanni

Anni 2008/2011

Università degli Studi di Ferrara

THESE DE DOCTORAT DE
L'UNIVERSITE PIERRE ET MARIE CURIE

Spécialité

Chimie Moléculaire, ED : 406
(Ecole doctorale)

Présentée par

Mme Pelà Michela

Pour obtenir le grade de

DOCTEUR de l'UNIVERSITÉ PIERRE ET MARIE CURIE

Sujet de la thèse :

Enantioselective Approaches and Domino Sequences for the Synthesis of Compounds of Biological Interest

soutenue le 8 Avril 2011

devant le jury composé de :

M. Poli Giovanni et M. Pollini Gian Piero: Directeurs de thèse

Mme Ongeri Sandrine et Mme Costi Maria Paola : Rapporteurs

M. Karoyan Philippe et M. Trapella Claudio : Examinateurs

Université Pierre & Marie Curie - Paris 6
Bureau d'accueil, inscription des doctorants et base de données
Esc G, 2ème étage
15 rue de l'école de médecine
75270-PARIS CEDEX 06

Tél. Secrétariat : 01 42 34 68 35
Fax : 01 42 34 68 40
Tél. pour les étudiants de A à EL : 01 42 34 69 54
Tél. pour les étudiants de EM à MON : 01 42 34 68 41
Tél. pour les étudiants de MOO à Z : 01 42 34 68 51
E-mail : scolarite.doctorat@upmc.fr

Contents

List of abbreviations

Ac	acetyl
Ar	aryl
Bn	benzyl
Boc	*tert*-butoxycarbonyl
n-Bu	butyl
d. r.	diastereomeric ratio
DBU	1,8-Diazabicyclo[5.4.0]undec-7-ene
DHP	3,4-dihydro-2H-pyran
DMF	*N,N*-dimethylformamide
DMSO	dimethyl sulfoxide
ee	enantiomeric excess
equiv.	equivalent
Et	ethyl
h	hour
LiHMDS	Lithium bis(trimethylsilyl)amide
L-Sélectride	Lithium tri-*sec*-butylborohydride
Me	methyl
min	minute
Ph	phenyl
iPr	isopropyl
*p*TsOH	*p*-toluenesulphonic acid
Y	yield
NMR	nuclear magnetic resonance
TBAB	tetra-*n*-butylammonium bromide
TBAF	tetra-*n*-butylammonium fluoride
TBS	*tert*-butyldimethylsilyl
tBu	*tert*-butyl
THF	tetrahydrofuran
TMEDA	tetramethylethylene diamine
WSC	1-Ethyl-3-(3'-dimethylaminopropyl) carbodiimide · HCl

General Introduction

Ryōji Noyori in "Asymmetric Catalysis in Organic Synthesis", John Wiley&Sons, New York, 1994 wrote: "*Life depends on chiral recognition, because living systems interact with enantiomers in decisively different manner".*

We know that the majority of biological processes take place as a consequence of the different ways in which enantiomers with different configuration react with receptors and life itself is in many ways chiral. Nature provides a vast diversity of chiral species in several classes of compounds, including "*inter alia"* aminoacids, carbohydrates, terpenes, carboxylic acids and alkaloids, several in great abundance, and the chiral information is derived from enantiomerically pure building blocks enzymatically synthesized by various organisms.

Interestingly, chiral biomolecules usually exist in Nature prevalently as one of the two possible enantiomeric forms, *e.g*., amino acids in the *L*-form and sugars in the *D*-form. Chirality is an important factor in determining bioactivity. The recognition that enantiomers often have different bioactivity and metabolic fates[1] in a number of chiral chemicals with important pharmacological activity led to a significant increase in the development of chiral pharmaceuticals, chirality becoming a major concern in the modern pharmaceutical industry.[2]

This interest can be attributed largely to a deeper awareness that enantiomers of a racemic drug may have different pharmacological activities, as well as different pharmacokinetic and pharmacodynamic effects.

Each racemic drug could interact differently and metabolize each enantiomer by a separate pathway to produce different pharmacological activity.

Thus, one isomer may produce the desired therapeutic effect, the other one being

[1] D.E. Drayer, *Clin. Pharmacol. Theor*., **1986**, *40* 125.
[2] S. Lam and G. Malikin, *Chirality*, **1992**, *4*, 395; I.W. Wainer (Editor*), Drug Stereochemistry Analytical Methods and Pharmacology*, Marcel Dekker, Inc., New York, New York, **1993**.

inactive or, in worst cases, noxious. For example, the (*L*)-Thyroxine, an amino acid produced by thyroid gland, is known to speed up metabolic processes, causing nervousness and loss of weight, while its enantiomer, (*D*)-Thyroxine served to lower the cholesterol levels.

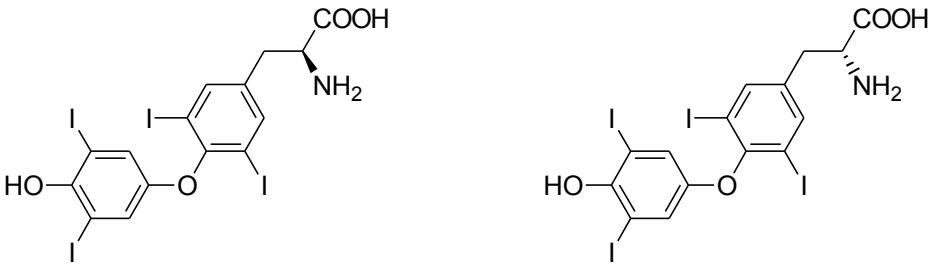

(L)-Thyroxine (D)-Thyroxine

Figure 1

The use of thalidomide (n-phthalyl-glutamic acid imide), which was marketed as the racemate, led to a tragedy in the 1960s in Europe. The sedative-hypnotic drug thalidomide prescribed to pregnant women to counter morning sickness exhibited irreversible neurotoxicity and mutagenic effects. It was discovered only after hundred of babies were born deformed that the *S*-enantiomer was teratogenic. Studies later suggested that these effects were caused by the *S*-enantiomer and that the *R*-enantiomer contained the desired therapeutic activity.[3]

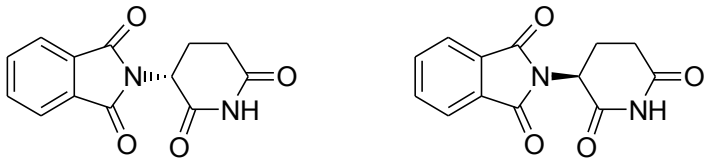

R- Thalidomide *S*- Thalidomide

Figure 2

In 1992 the U.S. Food and Drug Administration issued a guideline for chiral drugs: only the therapeutically active isomer could be marketed and each enantiomer should be studied separately for its pharmacological and metabolic pathways.[4] In addition, a

[3] Stephens TD, Fillmore BJ., Hypothesis: Thalidomide Embryopathy – Proposed Mechanism of Action. *Teratology* **2000**; 61: 189-195.
[4] S.C. Stinson, *Chemical and Engineering News*, **1995**, 70, 44.

rigorous justification is required for market approval of a racemate of chiral drugs. Currently, a large number of chiral drugs are marketed as racemic mixtures.[5] Nevertheless, to avoid the possible undesirable effects of a chiral drug, it is imperative that only the pure, therapeutically active form should be prepared and marketed.

When a chiral molecule is synthesized in an achiral environment using achiral starting materials, an equal mixture of the two possible enantiomers (i.e. a racemic mixture) is produced. The special problem of the separation of the enantiomers could be solved using a chiral resolving agent. This technique relies on the fact that while enantiomers have identical physical properties, diastereomers generally have different properties. Another technique is to use chiral chromatography. In this process, the racemate is run through a column filled with a chiral substance. The enantiomers will interact differently with the substance and will then elute at different rates.

As more and more enantiomerically enriched active agents are required today, the selective synthesis of enantiomers is the subject of many research projects aimed at the discovery of reactions or reaction sequences in which one configuration of one or more new stereogenic elements is selectively formed. In an asymmetric synthesis, an achiral molecule is enantioselectively converted into a chiral molecule or a chiral molecule is diastereoselectively converted into a new chiral molecule that contains at least one more chirality element. In an asymmetric synthesis the enantiomers (or diastereomers) of a chiral product are formed in different yields.

Thus, the study of stereoselectivity has evolved from issues of diastereoselectivity, through auxiliary-based methods for the synthesis of enantiomerically pure compounds to asymmetric catalysis. In the latter instance, enantiomers (not diastereomers) are the products, and highly selective reactions and modern purification techniques allow preparation - in a single step - of chiral substances in 99% ee for many reaction types.

- ✓ *Physical resolution of racemates* for example using HPLC (High Performance Liquid Chromatography) with specific chiral columns;

[5] B. Lin, X. Zhu, B. Koppenhoeffer and U. Epperlein, *LC·GC*, **1997***,15* 40. P. van Eikeren, in S. Ahuja (Editor*) Chiral Separations Applications and Technology*, American Chemical Society, Washington, D.C., **1997**, Ch. 2.

- ✓ Indirect enantiomeric resolution, *via* *chiral auxiliary-based approaches,* involves the coupling of the enantiomers with an auxiliary chiral reagent to convert them into diastereomers. The diastereomers can then be separated by cromatography or other achiral separation techniques;
- ✓ *Enzymatic catalysis* in which the action of an enzymatic transformation is exploited to obtain enantioenriched compounds;
- ✓ *Catalytic enantioselective trasformations* using chiral pool as catalytic compounds (for example the best know catalyst is the (*L*)-Proline). [6]

[6] G.Lin, Y. Li, A.S.C. Chan, *Principles and applications of Asymmetric Synthesis,* **2001**, Wiley-Interscience.

Chapter 1

"Ferrara's Project"

1. Introduction

1.1 G-protein coupled receptor (GPCR): structure, biological activation and signal transduction

Many drugs produce therapeutic activities through interaction with G-protein-coupled receptors (GPCRs), which actually represent the most important biological target for drug discovery. [7, 8]

GPCR (G-protein coupled receptor)s constitue a superfamily of integral membrane proteins consisting of seven transmembrane helices connected by loops with a *N*-terminal extremity always located on the extracellular side, the *C*-terminus being extended into the cytoplasm. GPCRs can be divided into different families on the basis of their structural and genetic properties.

- ✓ Receptors of *Family 1* are characterized by several highly conserved amino acids and a disulphide bridge that connects the first and second extracellular loops (ECLs). Most of these receptors at the carboxy-terminal tail present palmitoylated cysteine residue that bind to the membrane. They are also characterized by the presence of amino acids such as proline that produces a distortion of the helical transmembrane domain.

- ✓ *Family 2* GPCRs are characterized by a relatively long amino terminus, which contains several cysteines forming a network of disulphide bridges. Their morphology is similar to some family 1 receptors but lacking the palmitoylation site. Moreover, the conserved residues and motifs are different from the conserved residues in the family 1 receptors.

[7] Gilchrist, A., *Expert Opin. Ther. Targets,* **2004**, 8, 495–498
[8] Saito, Y., and Civelli, O., *Int. Rev. Neurobiol.* **2005**, 65, 179–209

- ✓ Receptor of the *Family 3* are characterized by a long amino terminus and carboxyl tail. The ligand-binding domain is located in the amino terminus. None of the features that characterize family 1 and 2 receptors are present in Family 3 receptors.

These receptors are activated by an external signal in form of a ligand or other signal mediator, including peptide (e.g. Neuropeptide S) and non-peptide neurotransmitters, hormones, growth factors, odorant molecules and light. The conformational change created in the receptor caused activation of a G-protein. Further effect depends on the type of G protein.

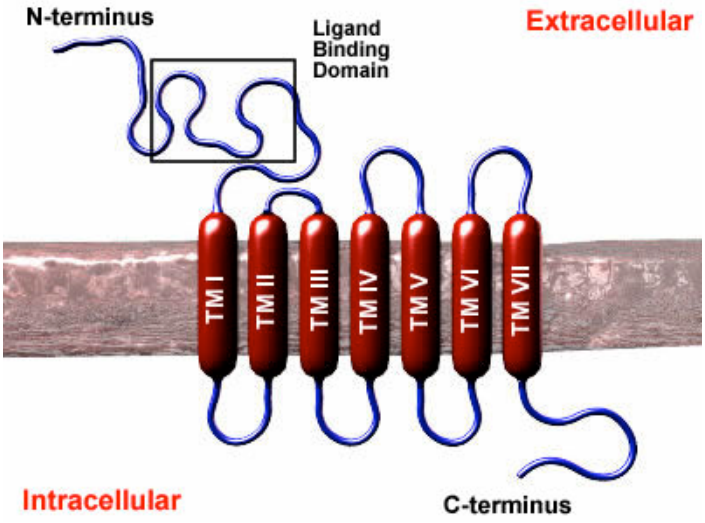

Figure 3

The transduction of the signal through the membrane by the receptor is not completely understood. It is known that the inactive G protein is bound to the receptor in its inactive state. (Figure 4)

- ❖ GPCR bound to Gαβγ complex; "G-proteins" are a trimer of α, β, and γ subunits (known as Gα, Gβ, and Gγ, respectively);
- ❖ Gα complex bound to Guanosine diphosphate (G**D**P) when the protein is inactive;
- ❖ Ligand binds to extracelluar part of GPCR (1);

- Upon receptor activation, there is a consequent allosterically activation of the G-protein by facilitating the exchange of a molecule of GDP for GTP at the G-protein's α-subunit (2);
- Once the G protein is activated, the subunits of the G-protein dissociate from the receptor, Gα looses affinity for βγ dimer to yield a Gα-GTP monomer and a Gβγ dimer, which are now free to modulate the activity of other intracellular proteins (3);
- Cascade events:
    - βγ dimer stays bound to the membrane and interacts with Effectors based on the specific βγ subunits like Adenylyl Cyclase (4);
    - Gα GTP complex enters the cytosol and interacts with Effectors, such as PLC-β (4);
- Hydrolysis of GTP, linked to Gα subunit, provides Gα-GDP (5) product that is inactive but more related to the βγ dimer;
- The trimer protein are reformed (Gαβγ) (6);
- Gαβγ complex binds to GPCR.

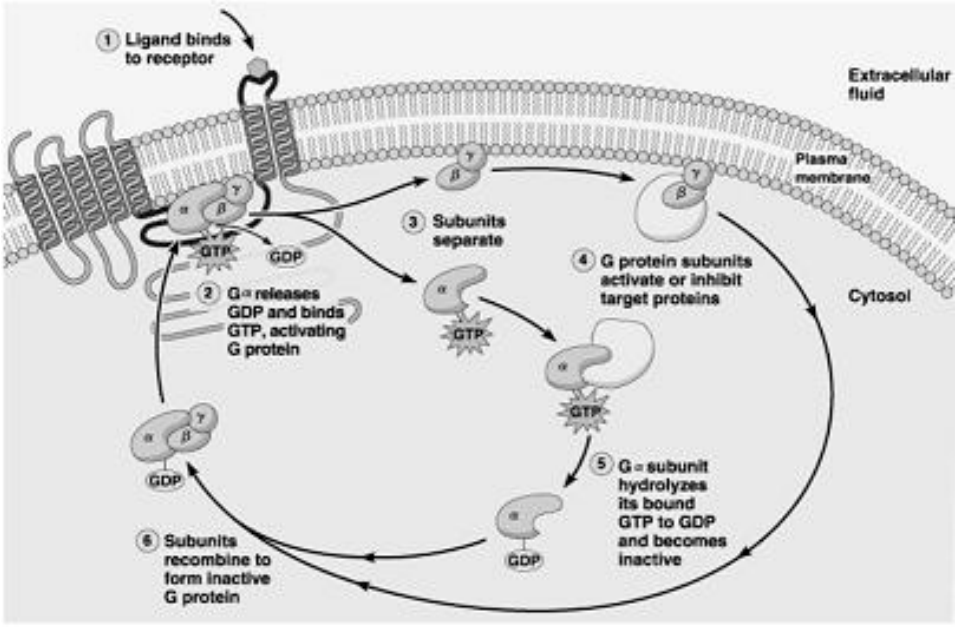

Figure 4

There is another subclassification of "G-protein" in particular at the α subunit: Gαs, Gαi and Gαq. Activation each of them produces different cascade events.

In Figure 5a the mechanism of signal transduction is described: Gαs protein is activated by a ligand; a subsequent activation of adenylate cyclase takes place increasing the AMPc concentration.

The section 5b outlines the mechanism after activation of Gαq: the released phospholipase C (PLC) provokes the cleavage of the membrane lipid phosphatidylinosityl-bisphosphate (PIP2) into diacylglycerol and IP3. The latter serves mainly to open calcium channels of the endoplasmic reticulum (ER) leading to the release of Ca^{2+} into the cell with consequent increase of its intracellular concentration.

These profiles representing the two activated pathways by NPS (neuropeptide S) after interaction with its receptor are shown below.

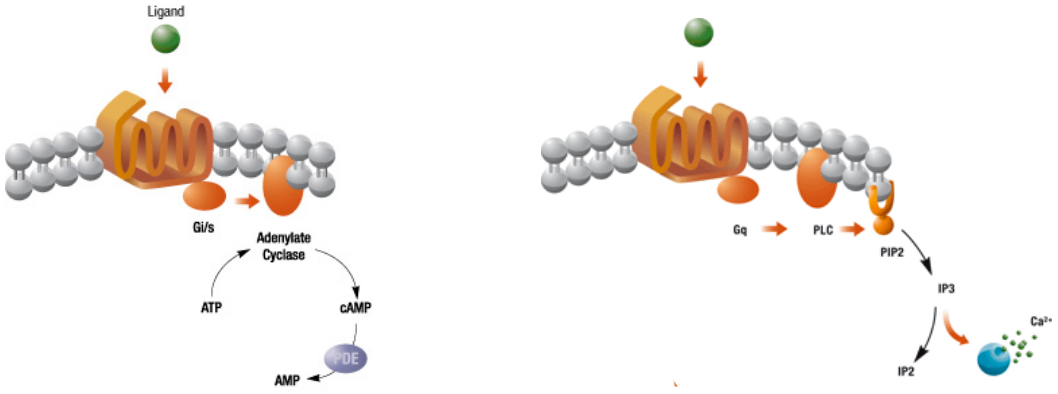

a. b.

Figure 5

1.2 NPS/NPSR system

At least 800 different genes codifying for putative GPCRs have been identified in the human genome, ~360 of which encode transmitter GPCRs [9]. Moreover, the endogenous

[9] Vassilatis, D. K., Hohmann, J. G., Zeng, H., Li, F., Ranchalis, J. E., Mortrud, M. T., Brown, A., Rodriguez, S. S., Weller, J. R., Wright, A. C., Bergmann, J. E., and Gaitanaris, G. A. *Proc. Natl. Acad. Sci. U. S. A.,* **2003,** 100, 4903–4908

ligand is known for only ~240 receptors, whereas the others are still orphans. The first step in understanding the function and the potential of an orphan receptor as drug target is the identification of its endogenous ligand. In the last decade, the *reverse pharmacology technique* [10], *i.e.* the use of a recombinant orphan GPCR as a target for identifying its endogenous ligand, has been validated as a successful approach for the identification of novel transmitter systems. In particular, several novel peptide receptor systems have been identified through this approach, including nociceptin/orphanin FQ, prolactin-releasing peptide, urotensin II and many others. The latest neuropeptides identified by the reverse pharmacology approach was *Neuropeptide S (NPS)*: a crucial discovery firstly reported in the patent literature.[11] A subsequent, elegant study by Xu et al.[12] demonstrated that hNPS (as well as the rat and mouse isoforms of this peptide) selectively binds and activates a previous orphan GPCR, known as GPR154, that was renamed NPS receptor, then abbreviated as NPSR.

Several splice variants and multiple single nucleotide polymorphisms have been reported for the human NPSR. The most intensely investigated NPSR isoforms are hNPSR Asn107 and hNPSR Ile107. This receptor polymorphism seems to have functional implications since the hNPSR Ile107 receptor displayed similar binding affinity but higher NPS potency (by approx. 10-fold) than hNPSR Asn107.[13] It is worthy of mention that the rat and mouse NPSR contain Ile at position 107.[14]

The primary sequence of human (h) NPS, a 20-residue peptide, which is highly conserved across species, is reported (Figure 6).

SFRNGVGTGMKKTSFQRAKS

H-Ser-Phe-Arg-Asn-Gly-Val-Gly-Thr-Gly-Met-Lys-Lys-Thr-Ser-Phe-Gln-Arg-Ala-Lys-Ser-OH

Figure 6

[10] Civelli, O. , *Trends Pharmacol. Sci.,* **2005,** 26, 15–19

[11] Sato, S., Shintani, Y., Miyajima, N., and Yoshimura, K. (April 18, **2002**) Japan Patent WO 0231145

[12] Xu, Y. L., Reinscheid, R. K., Huitron-Resendiz, S., Clark, S. D., Wang, Z., Lin, S. H., Brucher, F. A., Zeng, J., Ly, N. K., Henriksen, S. J., de Lecea, L., and Civelli, O. *Neuron,* **2004,** 43, 487–497.

[13] Reinscheid, R. K., Xu, Y. L., Okamura, N., Zeng, J., Chung, S., Pai, R., Wang, Z., and Civelli, O. *J. Pharmacol. Exp. Ther.* **2005,** 315, 1338–1345

[14] Reinscheid, R. K., Xu, Y. L. *FEBS J.* **2005**, 272, 5689–5693

The *N*-terminal serine residue, which is present in all the species analyzed so far, gave the name to this novel neuropeptide (Neuropeptide S). hNPS is cleaved from a larger precursor protein (ppNPS) which is expressed in few discrete brain areas. On the contrary, the receptor NPSR is widely distributed in the brain. This profile of receptor expression suggests the involvement of the NPS–NPSR system in the regulation of multiple central functions.

In cells expressing the recombinant NPSR receptor, NPS selectively binds and activates its receptor, producing intracellular calcium mobilization and an increase of cAMP levels. This indicates that the increase cellular excitability, after NPSR stimulation, it is due to the activation of both Gq and Gs protein. *In vivo* studies in rodents showed that the supraspinal administration of NPS produced a rather unique pattern of actions: anxiolytic-like effects associated with the stimulation of locomotor activity and clear arousal promoting effects.[5] Thus, NPS could be defined as an ***activating anxiolytic***.[7]

In addition, NPS has been reported to inhibit food intake, facilitate memory and elicit antinociceptive effects, while recent evidence suggests an involvement of the NPS/NPSR system in drug addiction.[15]

[15] Guerrini, R., Salvadori, S., Rizzi, A., Regoli, D., Calò, G. *Med. Res. Rev.*; **2010**, 30(5):751-77.

1.3 Structure-activity relationship study of NPS leading to identified peptide and non peptide ligands

1.3.1. Peptide ligands of NPSR

The development of novel ligands for NPSR is required in order to determine the role played by the NPS-NPS receptor system in the regulation of different biological functions and ultimately to predict the therapeutic potential of novel drugs interacting with this receptor.

Thanks to structure-activity relationship studies reported for the first time by our research group, we were able to identify the main requirements for biological activity in the primary structure of NPS.[16]

Thus, single residue replacement, either by an alanine residue (Ala-scan) or by the corresponding enantiomer (D-scan) with *N*- and *C*-terminal truncation, demonstrated that the *N*-terminus of the peptide was of crucial importance for biological activity. In particular, the sequence Phe^2-Arg^3-Asn^4 is likely to act as message domain crucial for receptor binding and its activation, while the sequence Gly^5-Val^6-Gly^7 is important for inducing the bioactive conformation of the peptide.

In parallel, we also performed a conformation/activity relationship study[17] that demonstrated that helicity can be tolerated in the *C*-terminal part of NPS and this conformational structure is not required for bioactivity and it is not tolerated around position Gly^7.

[16] Roth, A. L.; Marzola, E.; Rizzi, A.; Arduin, M.; Trapella, C.; Corti, C.; Vergura, R.; Martinelli, P.; Salvadori, S.; Regoli, D.; Corsi, M.; Cavanni, P.; Calo`, G.; Guerrini, R.. *J. Biol. Chem.* **2006**, *281*, 20809-20816.
[17] Tancredi, T.; Guerrini, R.; Marzola, E.; Trapella, C.; Calo, G.; Regoli, D.; Reinscheid, R. K.; Camarda, V.; Salvadori, S.; Temussi, P. A., *J. Med. Chem.,* **2007**, *50*, 4501–4508.

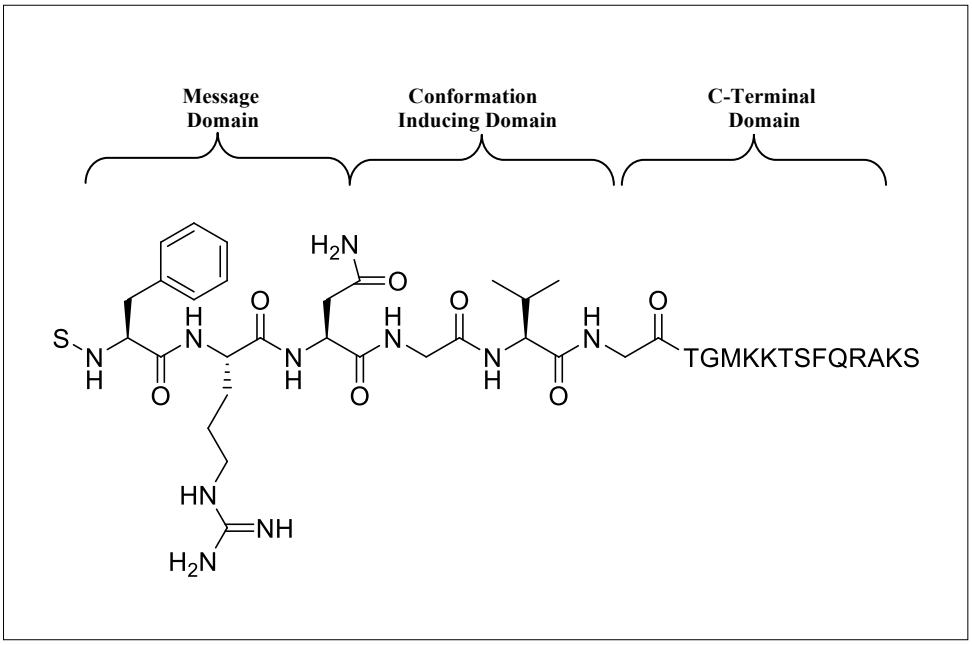

Figure 7

Conformational changes induced by substituting Gly[5] with the achiral R helix promoting amino acid Aib or with D-Ala seem to provoke a decreased agonist efficacy, as indicated by structure–activity studies performed at position 5. Therefore, we planned a SAR study mainly focusing at Gly[5] position by replacing with a series of *L*- and *D*- amino acids characterized by hydrophobic aromatic and aliphatic side chains.[18] As a result, we demonstrated that substitution of Gly[5] with *D*-amino acids bearing a short lipophilic-branched side chain could generate a fairly potent, pure and selective NPSR antagonists.

a. H-Ser-Phe-Arg-Asn-Gly-Val-Gly-Thr-Gly-Met-Lys-Lys-Thr-Ser-Phe-Gln-Arg-Ala-Lys-Ser-OH

b. H-Ser-Phe-Arg-Asn-(D)Val-Val-Gly-Thr-Gly-Met-Lys-Lys-Thr-Ser-Phe-Gln-Arg-Ala-Lys-Ser-OH

c. H-Ser-Phe-Arg-Asn-(D)Cys (tBu)-Val-Gly-Thr-Gly-Met-Lys-Lys-Thr-Ser-Phe-Gln-Arg-Ala-Lys-Ser-OH

Figure 8

[18] R.Guerrini, V.Camarda, C.Trapella, G.Calò, A.Rizzi, C.Ruzza, S.Fiorini, E.Marzola, R. K.Reinscheid, D.Regoli, S.Salvadori, *J. Med. Chem.* **2009,** *52,* 524–529.

Above, the structures of first two NPSR-peptide antagonists actually known in literature are reported, namely: [D-Val^5]NPS (Figure 8b) and [D-Cys(tBu)^5]NPS (Figure 8c) whose pharmacology activity has been evaluated in a calcium mobilization assay using HEK293 cells stably expressing mouse NPSR (HEK293mNPSR) and the fluorometric imaging plate reader FlexStation II.

1.3.2 Non-peptide ligands of NPSR

Non-peptide derivatives have been widely used to examine in details and improve the knowledge of the NPS system[19]. However, at the beginning of this work only ligands featuring an oxazol-piperazine scaffold were known able to bind the NPSR receptor.

A series of compounds with a claimed activity at NPSR has been recently reported in a patent application by Takeda Pharmaceuticals Inc [20] without the support of pharmacological or biological data. In the patent, structures containing a 3-oxo-tetrahydro-oxazolo[3,4-*a*]pyrazine scaffold mainly substituted in position 1 and 7, have been described to possess NPSR antagonistic activity.

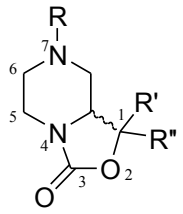

Figure 9

Two of these compounds, namely (**SHA 66** and **SHA 68**), differing exclusively for the presence of a fluoro substituent at the *para* position of the benzyl moiety (**SHA 68**),

[19] Reinscheid R.K.. *Peptides* **2007***, 28,* 830–837; Reinscheid R.K. and Xu, Y.L.. *Neuroscientist,* **2005**, *11*, 532–538; Guerrini R., Salvadori S., Rizzi A., et al.. *Medicinal Research Reviews*, **2010**, *30* (5), 751-77.

[20] Fukatzu K, Nakayama Y, Tarui N, Mori M, Matsumoto H, Kurasawa O, Banno H.; Takeda Pharmaceuticals; **2004**, PCT/JP04/12683.

were prepared by Okamura et al.[21] who studied their pharmacological proprieties as potential NPSR antagonists *in vitro* and *in vivo*. The two closely related bicyclic piperazines have been described as potent and selective antagonists at NPSR *in vitro*, able to antagonize NPS-induced effects *in vivo*.

Thus, **SHA 68** shoved selectivity for this receptor and was able to block NPS-induced Ca^{2+} mobilization in central and peripheral site after binding. However, its pharmacokinetic profile indicated a limited BBB penetration.

SHA 68 (see Fig. 10b) i.e. the racemic mixture (9*R/S*)-3-oxo-1,1-diphenyl-tetrahydro-oxazolo[3,4-*a*]pyrazine-7-carboxylic acid 4-fluoro-benzylamide represents the first generation of non-peptide NPSR antagonists.

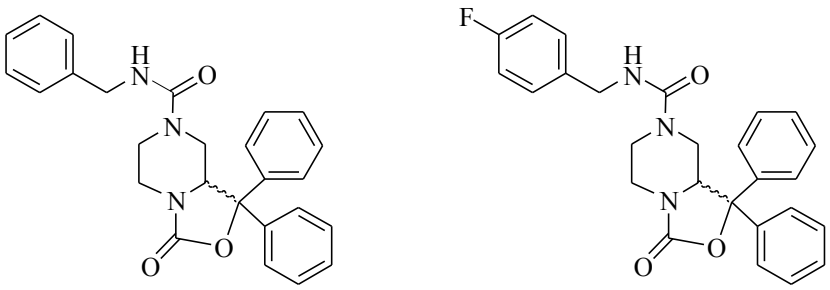

a. (±) SHA-66 **b. (±) SHA-68**

Figure 10

Structure–activity studies performed at position 7 of SHA 68[22] have indicated that a potent NPSR antagonist activity required a free urea moiety since alkylation of the urea nitrogen or its replacement with carbon or oxygen atoms generated derivatives with a decreased activity. In addition, compounds with α-methyl substitution or elongated alkyl chains showed reduced potency, indicating a limited tolerance for position 7 substituents. Interestingly, removal of the fluorine atom at the *para* position of the phenyl ring generated a compound (SHA 66) displaying similar potency in comparison

[21] Okamura N, Habay SA, Zeng J, Chamberlin AR, Reinscheid RK.; *J. Pharmacol. Exp. Ther.,* **2008**, 325, 893–901.
[22] Y. Zhang, B. P. Gilmour, H. A. Navarro, S. P. Runyon, *Bioorg. Med. Chem. Lett.,* **2008**, 18, 4064–4067.

to the parent compound, indicating that the fluorine atom does not affect receptor binding. [6,7]

Very recently, new series of NPSR antagonists has been developed by the same group of researchers (Melamed et al..[23] and Trotter et al..[24]) in order to identified new antagonists of the Neuropeptide S receptor (NPSR) with high potency, good permeability into the brain trough the brain-blood-barrier (BBB), namely: (Figure 11):

- a *quinolinone* class of potent NPSR antagonists that readily cross the blood–brain barrier (**NPSR-QA1**).
- a *tricyclic imidazole* antagonist of NPSR, represented by **NPSR-PI1,** that demonstrates potent in vitro NPSR antagonism and central exposure *in vivo*.

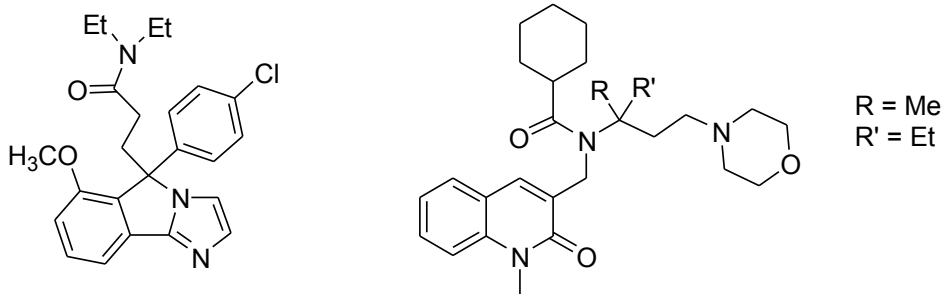

NPSR-PI1 **NPSR-QA1**

Figure 11

In both cases, the racemic mixture of **NPSR-PI1** and **NPSR-QA1** was separated using chiral column chromatography affording the two potent enantiomeric compounds showed in Figure 11, but the absolute configuration of these antagonists remained unknown.

[23] J. Y. Melamed, A.E. Zartman , N.R. Kett , A.L. Gotter, V.N. Uebele, D.R. Reiss, C.L. Condra, C. Fandozzi, L.S. Lubbers, B.A. Rowe, G.B. McGaughey, M.Henault, R. Stocco, J.J. Renger, G.D. Hartman, M.T. Bilodeau, B.W. Trotter, *Bioorg. Med. Chem. Lett.,* **2010**, 20, 4700–4703.

[24] B. W. Trotter, K. K. Nanda, P.J. Manley, V. N. Uebele, C. L. Condra, A. L. Gotter, K. Menzel, M. Henault, R. Stocco, J.J. Renger, G. D. Hartman, M. T. Bilodeau**,** *Bioorg. Med. Chem. Lett.,* **2010**, 20, 15, 4704-4708 .

2. Aim of the project

The NPS-NPSR system is a quite recent discovery and many studies are still required to deeply understand its biological functions and better define the therapeutic potential of selective NPSR ligands.

The availability of selective NPSR antagonists is an important target in this field and my work has been mostly addressed to their discovery.

In details, this work has been maily focused in the asymmetric synthesis of chiral 2,4-disubstituted- and 2,4,6-trisubstitued-piperazines starting from cheap, commercially available materials. The piperazine moiety is a well recognized "privileged scaffold" in medicinal chemistry,[25] being the common structural feature of a wide range of biologically active natural and synthetic products.

The variety of synthetic methods that allow for the fast and efficient assembly of piperazine skeletons reported in the literature has been comprehensively surveyed in four excellent reviews. [26]

In this project, the asymmetric construction of the substituted piperazine ring has been accomplished through two efficient methodologies featuring a different way for the introduction of the required chirality, namely:

- ✓ using readily available optical active natural materials such as aminoacids (alanine) as starting materials;
- ✓ using a chiral auxiliary reagent to obtain separable diastereomers.

The first class of compounds showing antagonism activity for the NPS receptor has been reported in the literature by the Takeda's group. The synthetic pathway has been previously described by Schanen and coworkers in 1996.[27]

---

[25] a) Horton, D. A.; Bourne, G. T.; Smythe, M. L., *Chem. Rev.,* **2003**, *103*, 893–930; b) Tullberg, M.; Grøtli, M.; Luthman, K. *J. Org. Chem.,* **2007**, *72*, 195–199.

[26] a) Dinsmore, C. J.; Beshore, D. C. *Tetrahedron*, **2002**, 58, 3297–3312; Dinsmore, C. J.; b) Beshore, D. C. *Org. Prepar. Proced. Int.,* **2002**, 34, 367–404; c) Quirion, J.-C. Asymmetric Synthesis of Substituted Piperazines. In Targets in Heterocyclic Systems; Attanasi, O. A., Spinelli, D., Eds.; Italian Society of Chemistry: Roma, **2008**; Vol. 12, pp 438–459; d) De Risi C., Pelà M., Pollini G.P., Trapella C., Zanirato V., *Tetrahedron: Asymmetry,* **2010**, *21*, 255-274.

[27] V. Schanen, M.P.Cherrier, S.Jose de Melo, J.C. Quirion, H.P. Husson, *Synthesis*,**1996**, 833-837.

3. Synthesis

3.1 Synthesis of Takeda's compound

In order to obtain the first non-peptide antagonist of NPS for pharmacological evaluation we planned to prepare the "**Takeda compound**" following the Schanen's synthetic approach[27] even if some modifications.

Thus, the starting move was the reaction between *R*-(-)phenylglycinol **1** and *N*-Boc-(*D*)-Alanine **2** to produce amide **3** under standard condensation conditions for the peptide bond formation (activation *via* dicyclohexylcarbodiimide) introducing a defined stereogenic centre at the beginning of the piperazine synthon construction, differently from the Schanen's approach.

The two carbonyl functions of the intermediate **3** could be selectively reduced with $LiAlH_4$ in diethylether leading to the formation of **4** and its hydroxyl function was subsequently protected with *tert*-butyldimethylsilyl chloride in THF producing the amine **5**. Its condensation reaction with with bromoacetic acid was conveniently accomplished *via* dicyclohexylcarbodiimide activation (Scheme 1) leading to the bromoacetylated derivative **6** which was smoothly cyclized to the piperazinone **7** by treatment with NaH in a mixture of DMF/THF.

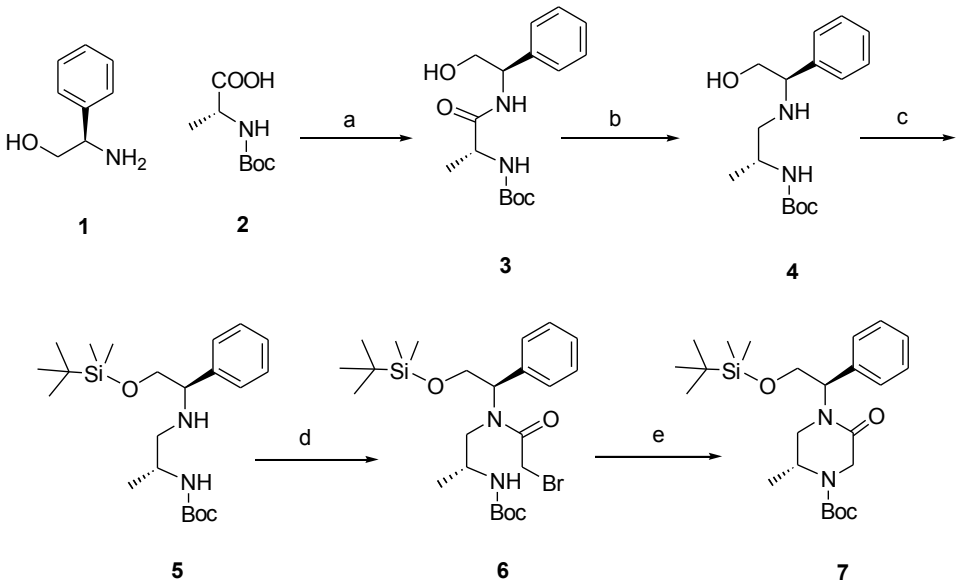

Reagents and conditions : (a) *N*-Boc-(D)-Ala-OH, CH_2Cl_2, WSC, room temp., Y=64%; (b) $LiAlH_4$, Et_2O, 0°C, Y=100%; (c) TBDMS-Cl, imidazole, DMF, 0°C, Y=76%; (d) Bromoacetic acid, CH_2Cl_2, WSC, room temp., Y=35%; (e) NaH 60%, THF/DMF, room temp., Y=74%.

Scheme 1

Removal of the silyl protective group of **7** was easily achieved by action of fluorine ions giving rise to **8** which was treated with borane dimethyl sulfide complex in order to reduce selectively the lactam moiety producing the piperazine derivative **9**. It was well known that the alkylation at position 2 of the piperazine ring system does not occur in the presence of the free hydroxyl function.[27] Therefore, the alcoholic functionality has been protected as the corresponding methyl ether **10** using NaH and MeI**.** A solution of this compound in freshly distilled THF was treated with *sec*-BuLi/TMEDA at -78 °C and reacted with diisopropyl ketone furnishing exclusively the *trans*-1,1-diisopropyl-7-(2-methoxy-1-phenyl-ethyl)-5-methyl-hexahydro-oxazolo[3,4-*a*]pyrazin-3-one **11** . Informations about the conformation of the piperazine ring was obtained by NMR analysis that showed coupling constants between the proton on C_2 and the adjacent methylene protons (on C_3) of 12 and 5 Hz. These data confirm that proton in C_2 was in axial position and consequently the alkylated substituent in equatorial conformation. Interestingly, the exclusive formation of *trans*-2,6-disubstitued product has been already

observed by Beak[28] in the piperidine series. Thus, the synthesis of the first example of a non-peptide compound able to interact with the NPSR, also named "**Takeda Compound**", was completed in nine steps with very low overall yield (~4%).

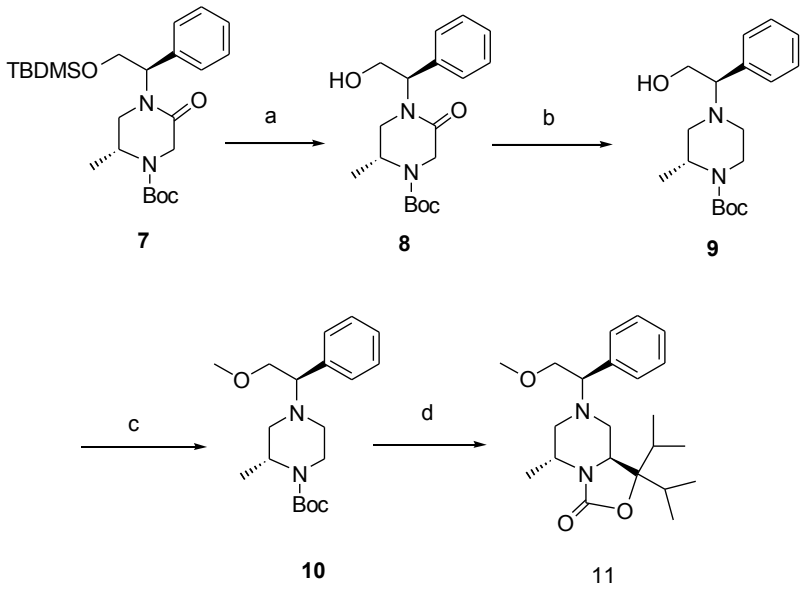

Reagents and conditions : (a) TBAF, THF, room temp. Y=72%; (b) $(CH_3)_2S*BH_3$, THF, 0°C,Y=88%; (c) NaH 60%, MeI, THF/DMF, 0°C,Y=62%; (d) *sec*-BuLi, TMEDA, isopropyl ketone, THF,-78°C, Y=48%.

Scheme 2

3.2 Synthesis of SHA-68 compound in racemic mixture

While this work was in progress, two small molecules described in the Takeda patent were also synthesized and tested by Okamura et al.[21] namely, the closely related bicyclic piperazines **SHA 66** and **SHA 68** that are potent and selective antagonists at NPSR *in vitro* and are able to antagonize NPS-induced effects *in vivo*.

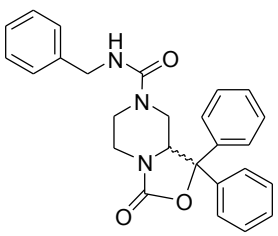

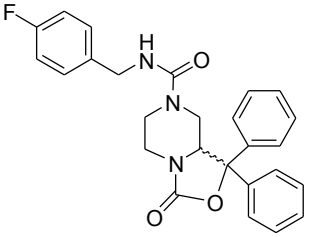

[28] Beak, P.,; Lee, W.K.; *J. Org. Chem.,* **1993,** 58, 1109.

SHA 66 **SHA 68**

Figure 12

The low overall yield of the synthetic process to prepare **11** and the interesting data related to the two new compounds described by Okamura et al.,[21] prompted us to explore an asymmetric synthesis of the two enantiomers of the Neuropeptide S receptor (NPSR) antagonist (9*R*/*S*)-3-oxo-1,1-diphenyl-tetrahydro-oxazolo[3,4-a]pyrazine-7-carboxylic acid 4-fluoro-benzylamide (**(*R/S*)-SHA 68**) to complete their structural characterization and to confirm the pharmacological evaluation. Initially, in order to confirm the published data, we decided to synthesize (***R/S*)-SHA 68** in racemic form envisaging a very easy pathway starting from a cheap, commercially available *N*-benzylpiperazine, already possessing a synthetically suitable substituent at one of the two nitrogen of the heterocyclic skeleton.

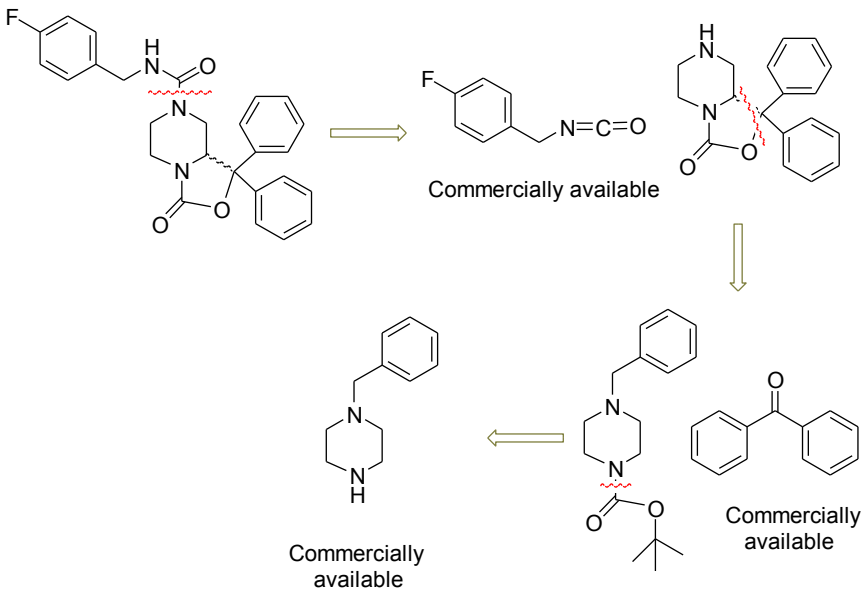

Scheme 3

The first step was the orthogonal protection of second nitrogen of the piperazine scaffold. As the corresponding *tert*-butoxycarbonyl group (Boc) and this operation was easily achieved under standard condition to produce quantitatively the intermadiate **13**. The construction of the second heterocycle condensed to the piperazine ring **14** was

smoothly accomplished in good yield (76%) by treatment **13** with *sec*-butyllithium/N,N,N',N'-tetramethylethylene diamine (TMEDA), at -78°C, followed by trapping of the intermediate anion with benzophenone. As already observed by Okamura et al., removal of the benzyl-protecting group of **14** was unsuccessful *via* palladium catalysed hydrogenolysis, but occurred smoothly through a simultaneous substitution *in situ* of the *N*-benzyl function with the fluorenyl methylenoxycarbonyl protective group (Fmoc-) by adding FmocCl to an acetonitrile solution of **14** at room temperature. After approximately 10 min, the precipitated **15** could be isolated by filtration with 70% yield. The last step of this pathway to obtain **(*R/S*)-SHA 68** compound required removal of the Fmoc-protecting group by treatment of **15** with 1,8-diazabicyclo[5.4.0]undec-7-ene (DBU) followed by reaction with the commercially available *p*-fluorobenzyl isocyanate.

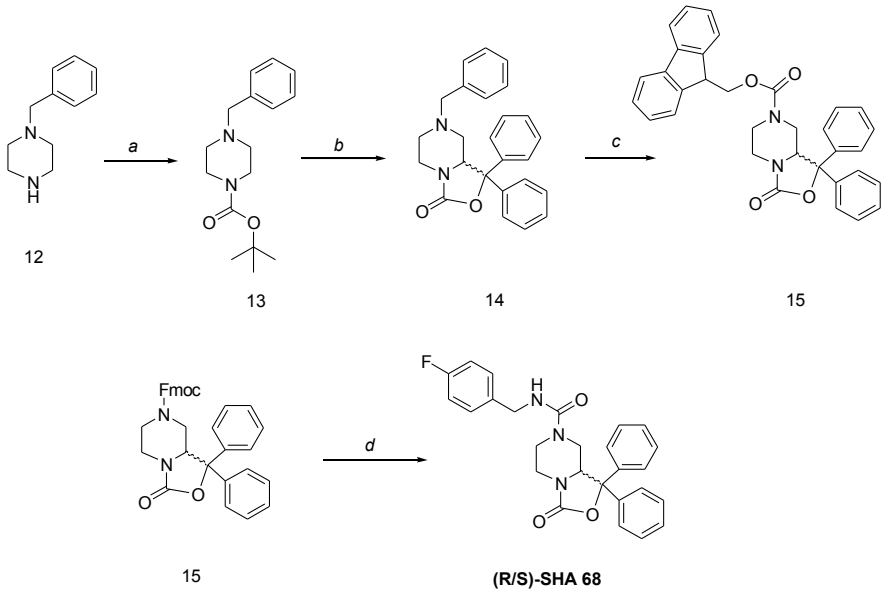

Reagents and conditions: (a) Boc_2O, H_2O/*tert*-butanol, NaOH (2N), room temp.; (b) *sec*-BuLi, TMEDA, benzophenone, THF, -78°C, Y=49%; (c) Fmoc-Cl, CH_3CN, 100°C, Y=65%; (d) DBU, 4-Fluorobenzyl-isocyanate, THF, room temp., Y=59%.

Scheme 4

Quenching of the reaction mixture after 15 min allowed to obtain **(*R/S*)-SHA 68** in almost quantitative yield after purification *via* flash cromatography (Scheme 4).

The structure of **(*R/S*)-SHA 68** was fully characterized by ^{1}H and ^{13}C NMR and mass spectrometry.

3.3 Asymmetric Synthesis of (*R*)-SHA 68 and (*S*)-SHA 68

Enantioselective synthesis of chiral compound is an important goal for organic and medicinal chemists and different strategies are available for the synthesis of optically active compounds.

In this project aimed at the construction of optical active piperazine compounds as a new class of non-peptide NPSR antagonists, we envisaged the chiral auxiliary approach as a convenient pathway for their asymmetric synthesis as outlined retrosynthetically in scheme 5.

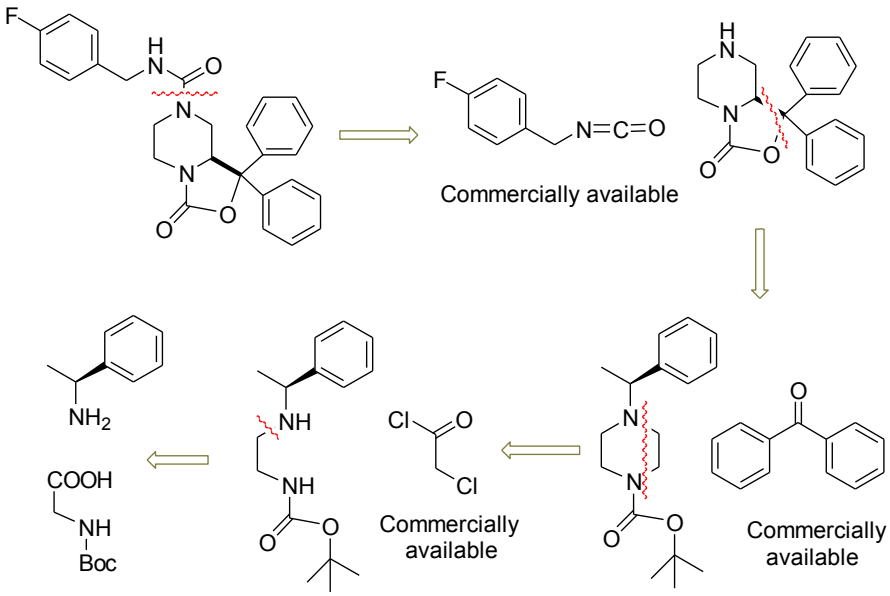

Scheme 5

The piperazine scaffold was synthesized in seven steps utilizing as chiral auxiliaries the readily available *S*-phenyl-ethylamine and *R*-phenyl-ethylamine. In the following schemes are reported the synthetic pathway for only the *S*-enantiomer, the same results being obtained with the other one. WSC-promoted condensation of *N*-Boc-glycine with

the chiral amine give the amide **16**, which underwent $LiAlH_4$ reduction of the carbonyl moieties to give **17**, which was acylated by action of chloro acetyl chloride in the presence of $NaHCO_3$ to furnish **18**. Its subsequent cyclization was performed by treatment with NaH at room temperature to produce the piperazinone derivative **19**, which was subsequently reduced in a good yield at the lactame function employing borane dimethyl sulfide complex.

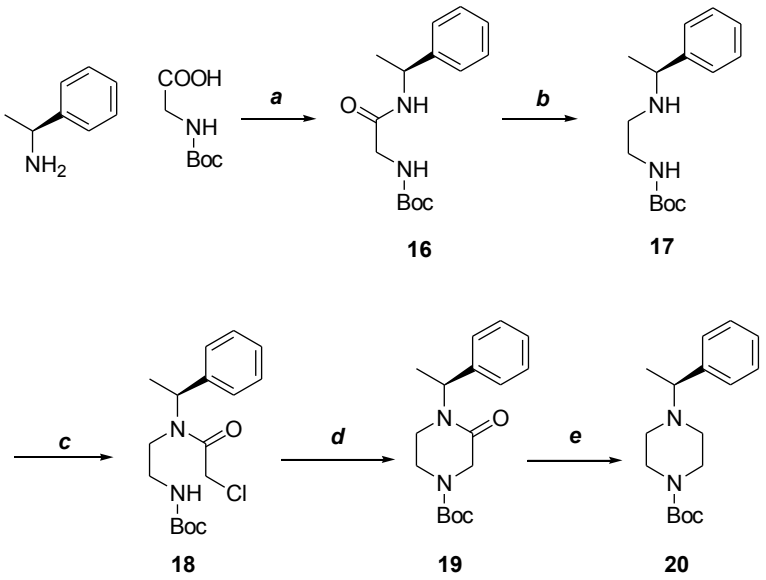

Reagents and conditions : (a) Boc-Gly-OH, CH_2Cl_2, WSC, room temp., Y=60%; (b) $LiAlH_4$, Et_2O, 0°C, Y=90%; (c) Chloroacetyl-chloride, $NaHCO_3$, AcOEt, 0°C, Y=100%; (d) NaH 60%, THF/DMF, room temp., Y=45%; $(CH_3)_2S*BH_3$, THF, 0°C, Y=87%.

Scheme 6

First attempts to build up the second heterocycle through the key alkylation step was rather unexpectedly unsuccessful although we payed careful attention to the choice of reagents (benzophenone, TMEDA and THF were freshly distilled and a new bottle of *sec*-BuLi was opened and used immediately) and reaction conditions (anhydrous and under nitrogen).

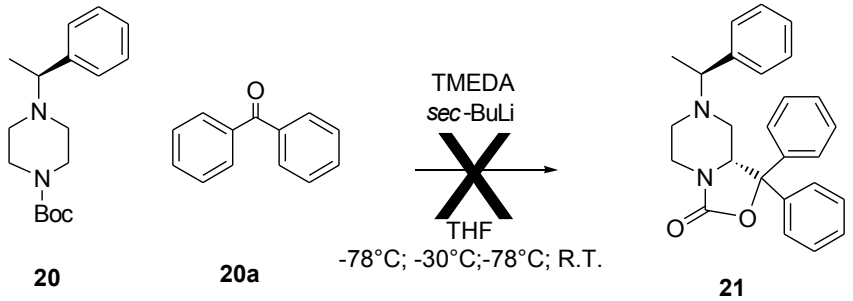

Scheme 7

Beside starting material, the only detectable reaction product characterized by NMR and mass spettroscopy was the secondary alcohol derived by reduction of benzophenone, which is likely to be produced by action of a residual piperazine-borane complex formed during the previous carbonyl reductive step.

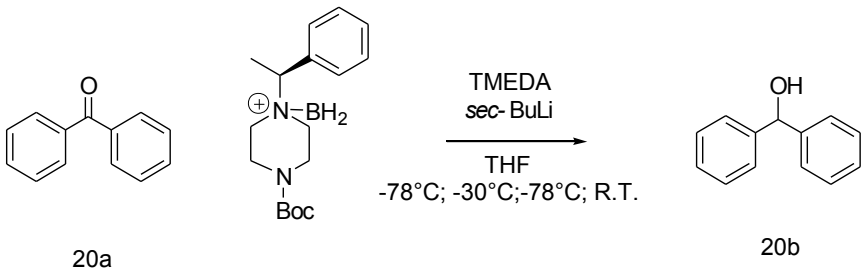

Scheme 8

This hypothesis has been confirmed since the dihydropyrazine **19a** was obtained using $LiAlH_4$ instead of borane dimethyl sulfide complex.

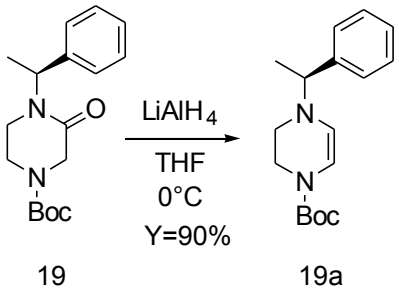

Scheme 9

The formation of this unexpected product could be accounted for considering the basic character of H^-.

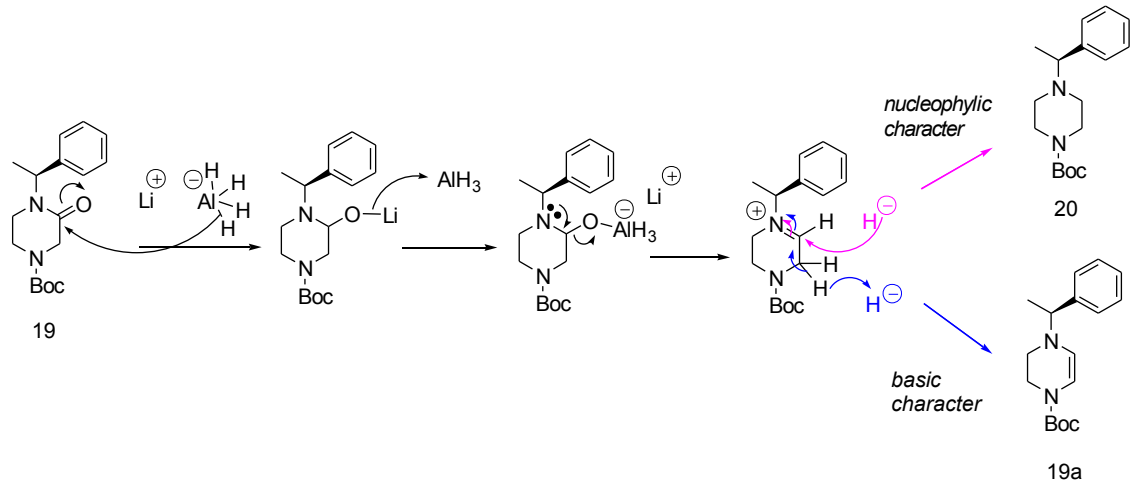

Scheme 10

Moreover, since the *Boc*-protective group too seemed to be the responsible for the unexpected formation of **20**, we decided to remove it using a solution of trifluoroacetic acid (TFA) in CH_2Cl_2. The reduction of amide group carried out on the derived free amine **19b** using $LiAlH_4$ gave the desired piperazine **19c,** subsequently protected at the second nitrogen atom as the *Boc*-derivative **20** in quantitative yield.

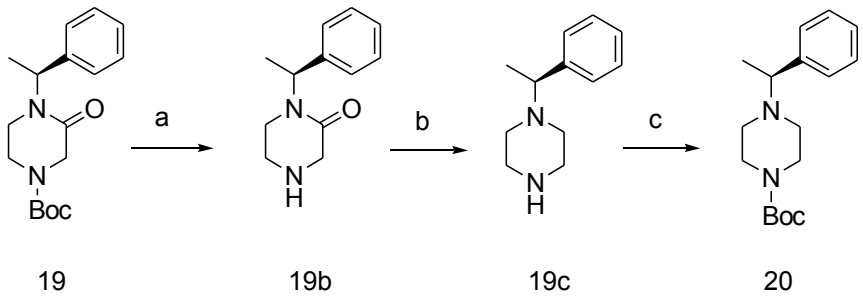

Reagents and conditions: (a) TFA, CH_2Cl_2, 0°C, Y=97%; (b) $LiAlH_4$, Et_2O, 0°C, Y=87%; (c) Boc_2O, H2O/*tert*-butanol, NaOH (2N), room temp., Y=100%.

Scheme 11

While this work was in progress, an interesting paper by Reginato et al.[29] described the selective reduction of 2-oxo-piperazines as strategy to perform the easy alkylation at the carbon C2. Thus, treatment of **20** with *sec*-butyllithium/TMEDA at -78 °C, followed by trapping of the intermediate anion with benzophenone, the smooth formation of two diastereoisomers, **21a** and **21b,** occurred in good yield (76%) and the mixture was easily separated by flash cromatography.

Further steps were similar to the ones previously used for the preparation of **(*R/S*)-SHA 68**. The amine debenzylation was accomplished by addition of FmocCl to an acetonitrile solution of **21a** and **21b** at room temperature. After 10 min, crude **22a** and **22b** were isolated as a white solids by filtration and used without further purification.

Compounds **22a** and **22b** were treated with DBU and the urea moiety was formed using *p*-fluoro-benzylisocyanate to give the final products **(*S*)-SHA 68** and **(*R*)-SHA 68** in almost quantitative yield (Scheme 12).

[29] G.Reginato, B.Credico, D.Andreotti, A.Mingardi, A.Paio, D.Donati, B.Pezzati, Al. Mordini, *Tetrahedron: Asymmetry,* **2010**, 21, 191–194;

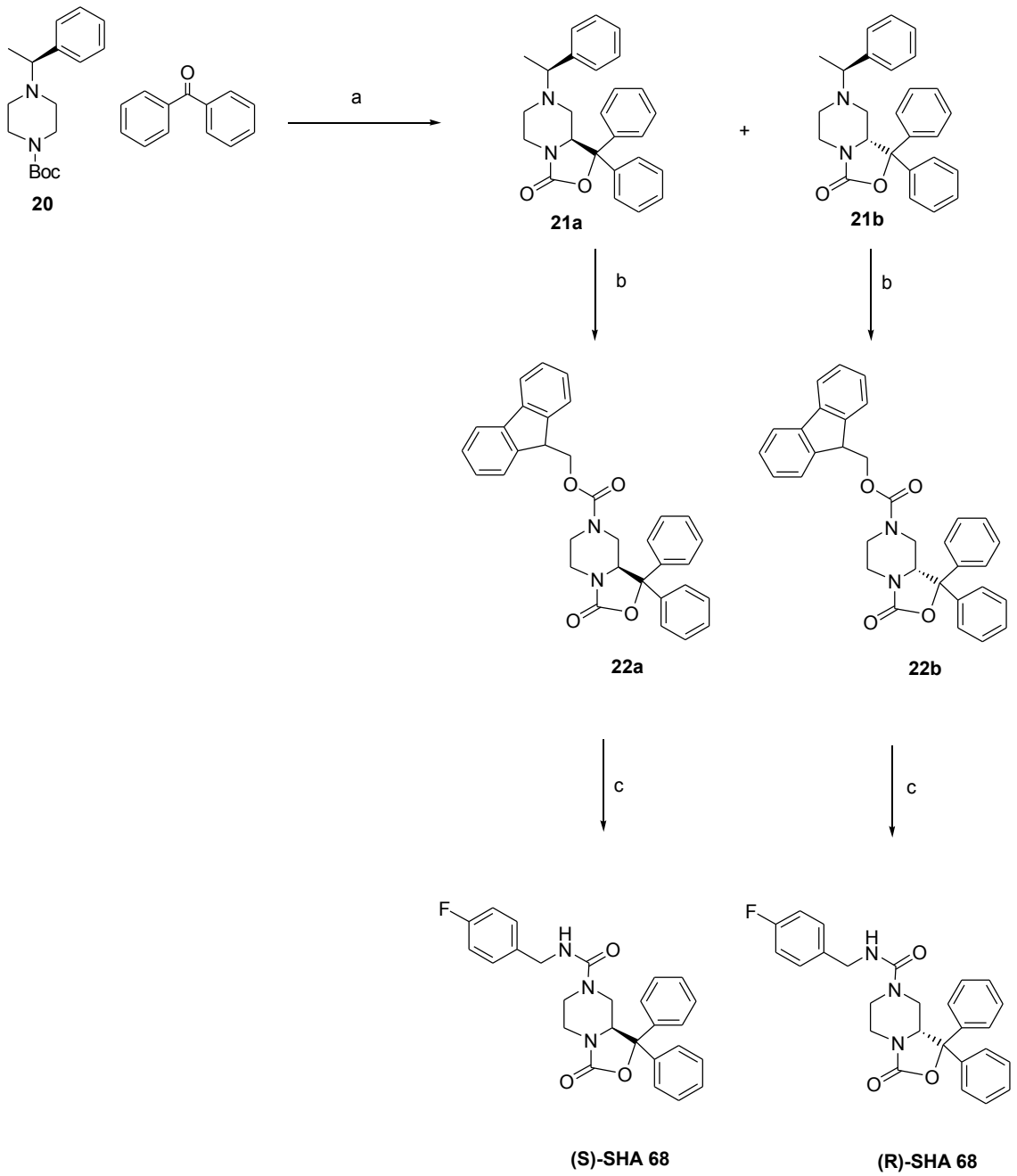

Reagents and conditions: (a) Benzophenone, *sec*-BuLi, TMEDA, THF, -78°C, Y=45%; (b) Fmoc-Cl, CH_3CN, 100°C, Y=67%; (c) DBU, *p*-fluorobenzyl-isocyanate, THF, room temp, 76% and 83% yields.

Scheme 12

4. Chiral chromatography profiles

The structures of the two diastereoisomers **21a** and **21b** and the two optical active compounds were fully characterized by ^{1}H, ^{13}C , DEPT, COSY, HMQC, HMBC, NOE, NMR and mass spectrometry. The enantiomeric excess of **(*R*)-SHA 68** and **(*S*)-SHA 68**

were determined by chiral HPLC analysis. The Figure 6 shows the chromatograms for the single enantiomers **(*S*)-SHA 68** (first eluted component, red line) and **(*R*)-SHA 68** (second eluted species, blue line), no trace of **(*R*)-SHA 68** in the chromatogram corresponding to the elution of **(*S*)-SHA 68**, nor of **(*S*)-SHA 68** in that of **(*R*)-SHA 68** could be detected. The optical purity of the two enantiomers was further supported by values of the reported peaks area .

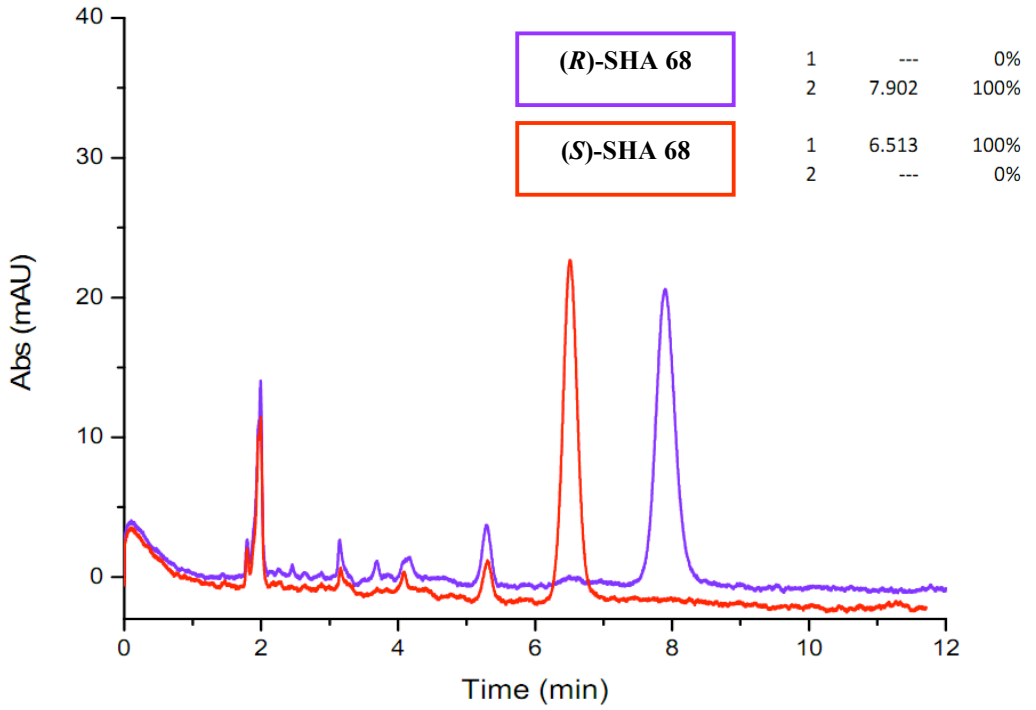

Figure 13

In Figure 14 we compare the chromatographic analytical profiles of the two enantiomers with the racemate.

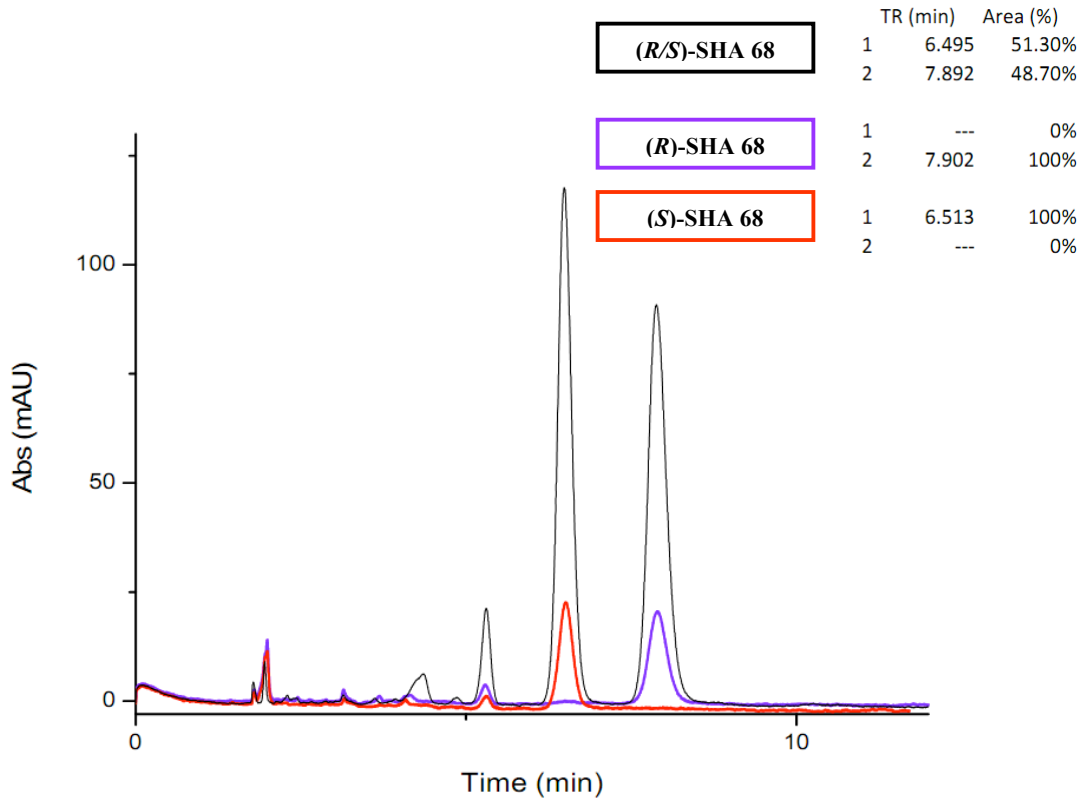

Figure 14

5. NMR spectrometry profile

In Figure 8 the enlarged [^{1}H]NMR spectra of the C9 proton region of the **(*R*)-SHA 68** is reported. Evaluation of the coupling constants between the proton Hx on C9 and the two adjacent protons Ha/Hb on C8 was useful to define the conformation of the enantiomer. The coupling constant values of Hx with Ha/Hb protons were 11.2 and 3.7 Hz for **(*R*)-SHA 68**. These data confirms that the proton on C9 was in axial position and consequently the alkylated substituent in equatorial position.

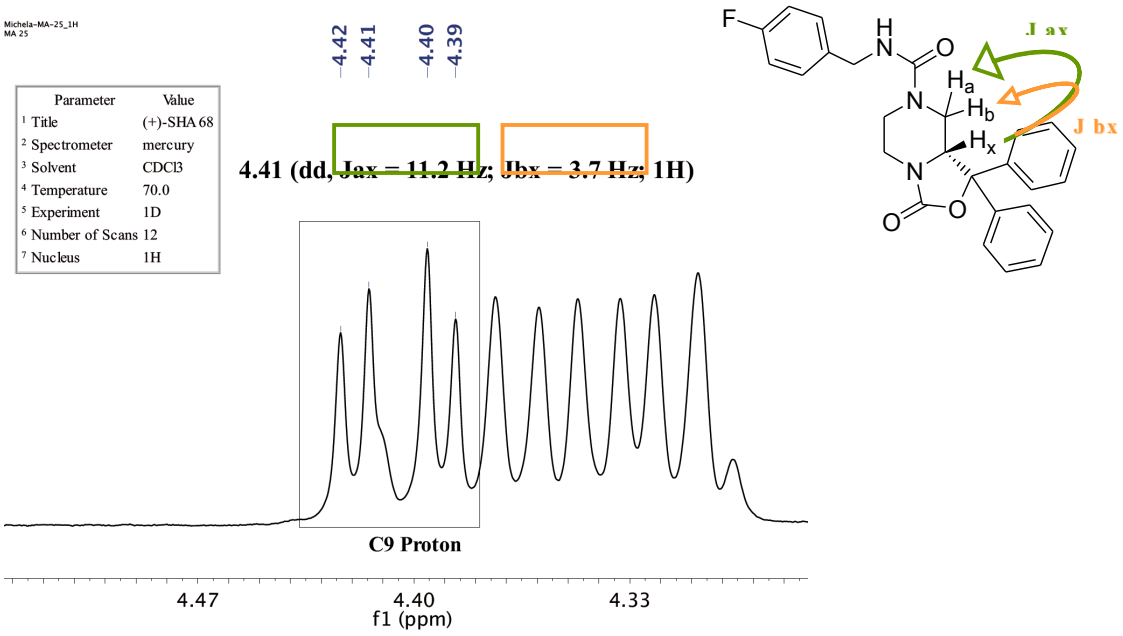

Figure 15

6. X ray spectroscopy analysis

In order to define the absolute configuration of the C9 chiral centre crystals of the diastereoisomer **21b** were produced using ethanol/ethyl acetate as crystallization solvents. The absolute configuration of the enantiomer (***R*)-SHA 68** has been assigned by reference to the configurations of the two stereogenic centers present in the diastereoisomer **21b**.

As shows in figure 16, knowing the unchanged chiral centre C10 (in configuration ***S***) of the compound **21b** we can determine the configuration of the chiral centre C9, that shows a configuration ***R***.

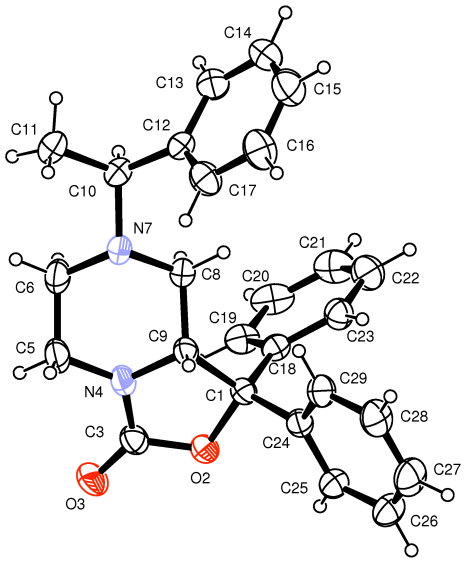

Figure 16

Figure 17 represents another angulation of the X ray structure of the diestereoisomer (*S, R*) **21b**; the piperazine ring assumes a perfect chair conformation and we can confirm that the proton bind at C9 is placed in axial position as demonstrate by NMR analysis.

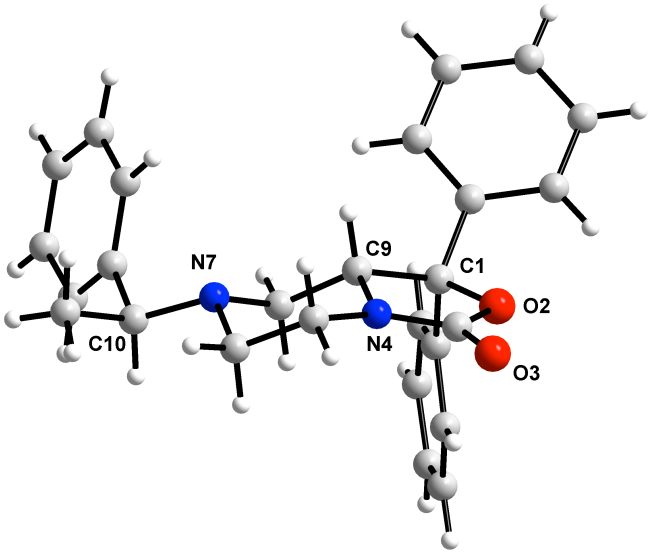

Figure 17

7. Biological activity

Next, in collaboration with the pharmacology researchers of the "Università degli Studi di Ferrara" we planned a study able to furnish information about the biological activity of this new class of compounds.

We evaluated and compared the *in vitro* NPSR antagonist properties of **(*R/S*)-SHA 68**, **(*R*)-SHA 68** and **(*S*)-SHA 68**. The three compounds were tested in calcium mobilization studies performed on HEK293 cells expressing the murine NPSR or the two isoforms of the human receptor (hNPSRAsn107 and hNPSRIle107).[13]

The natural peptide NPS was able to induce calcium mobilization in a concentration dependent manner in HEK 293 mNPSR (pEC_{50} 8.97 ± 0.11; E_{max} 250 ± 11%), hNPSRAsn107 (pEC_{50}: 9.07 ± 0.11; E_{max} 316 ± 13%) and hNPSRIle107 (pEC_{50}: 9.17 ± 0.15; E_{max} 333 ± 17%).

(*R/S*)-SHA 68 inhibited in a concentration dependent manner the stimulatory effect of NPS showing similar high values of potency ($pK_B \cong 8$). These values of potency are superimposable to those previously published. [21,30]

(*R*)-SHA 68 was also able to antagonize in a concentration dependent manner the stimulatory effect of NPS displaying values of potency similar or slightly higher than the racemic mixture.

By contrast, **(*S*)-SHA 68** showed a slight inhibitory effect only at micromolar concentrations.

The values of potency of the three compounds, in the three cells lines, are summarized in Table 1.

[30] C. Ruzza, A. Rizzi, C. Trapella, M. Pelà, V. Camarda, V. Ruggieri, M. Filaferro, C. Cifani, R. K. Reinscheid, G. Vitale, R. Ciccocioppo, S. Salvadori, R. Guerrini, G. Calò, *Peptides,* **2010**, 31, 915-925.

	mNPSR	hNPSR Ile107	hNPSR Asn107
	pK_B	pK_B	pK_B
(*R/S*)-SHA 68	8.16	8.03	7.99
(*R*)-SHA 68	**8.29**	**8.18**	**8.28**
(*S*)-SHA 68	<6	<6	<6

Table 1

Collectively, these results demonstrated that **(*R*)-SHA 68** is the active enantiomer while the contribution of **(*S*)-SHA 68** to the biological activity of the racemic mixture is negligible. As already mentioned in the introduction, the relevance of ligand chirality for NPSR binding is also corroborated by the fact that the biological activity of chemically different molecules, such as the quinoline[23] and the tricyclic imidazole[24] compounds, could be attributed to a single bioactive enantiomer.

(*R*)-SHA 68 was demonstrated to be the active enantiomer.

8. Conclusions

The present study described the enantioselective synthesis of 2,4-disubstituted and 2,4,6-trisubstitued chiral piperazines.

Initially, envisaged the synthesis of (***R/S***)**-SHA 68** in racemic form in order to confirm the chemical and biological published data through an efficient synthetic scheme which can be easily scaled up to multi-grams.

Later, we focused our attention to the asymmetric synthesis of the two enantiomers **(*R*)-SHA 68** and **(*S*)-SHA 68** starting from cheap commercially available reagents.

In order to define the conformation of the piperazine ring we performed a series of NMR experiments leading to define a chair conformation where the substituent in C9 was placed in equatorial position.

To know the absolute configuration of this new chiral centre X ray analysis was performed on suitable crystals obtained by the diastereoisomer **21b.** The new stereogenic centre showed (*R)* configuration

Furthermore, we studied these molecules from a pharmacological point of view; evaluating and comparing the *in vitro* NPSR antagonist properties of **(*R/S*)-SHA 68**, **(*R*)-SHA 68** and **(*S*)-SHA 68**.

The results demonstrated that **(*R*)-SHA 68** is the active enantiomer while the contribution of **(*S*)-SHA 68** to the biological activity of the racemic mixture is negligible.

(*R*)-SHA 68 was demonstrated to be the antagonist of the receptor of the neuropeptide S.

Nowadays, this molecule represents the standard non peptide NPSR antagonist and surely will be used to investigate the biological functions controlled by the NPS / NPSR system and to evaluate the therapeutic potential of innovative drugs acting as NPSR selective ligands.

Chapter 2

“Paris’ Project”

I. Introduction

In the frame of the synthesis of biological active chiral compounds I have spend nine months at the Pierre et Marie Curie University in Paris under the supervision of Professor Giovanni Poli, focusing the attention on the synthesis of natural product (-)-Steganacin. This stage allowed me to view a different approach for the selective generation of new structures using a palladium catalysed domino reactions instead of the use of chiral auxiliaries used for the synthesis of **(*R*)** and **(*S*)-SHA 68**.

The isolation and structure determination of a novel class of dibenzocyclooctadiene lignan lactones, represented by the antileukemic esters steganacin **23** and steganangin **23a**, was reported in 1973 by Kupchan and his collaborators. [31]

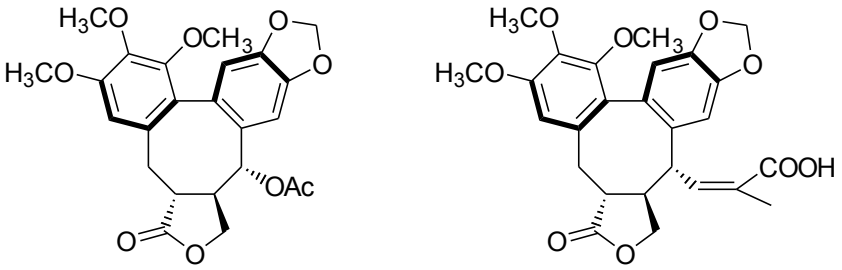

23
Steganacin

23a
Steganagin

Figure 18

Steganacin and steganangin were isolated from a plant of South Africa, *Steganotaenia araliacea* Hochst (Figure 18), which was found to show significant antitumor activity *in vivo* against P388 leukemia in mice.

[31] M. Kupchan, R.W. Britton, M.F. Ziegler, C.J. Gilmore, R.J. Restivo, R.F. Bryan, *Journal of the American Society,* **1973**, 95:4, 21, 1335-1336.

In vitro both compounds inhibit the assembly of tubulin into microtubules by interacting with the colchicine binding site and have been shown to possess cytotoxic activity against several cancer cell lines.[32]

Figura 19

Steganacin also causes a slow depolymerization of preformed microtubules. This molecule inhibits the binding of colchicine to tubulin and thus resembles Podophyllotoxin, which also competitively inhibits colchicine binding (Figure 20).[33]

Steganacin presents a trimethoxybenzene ring and probably interacts with that portion of the colchicine binding site that recognizes the trimethoxybenzene ring of Colchicine.

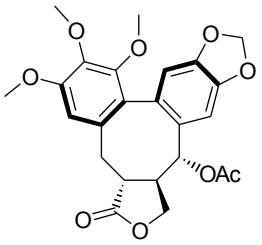

23
Steganacin

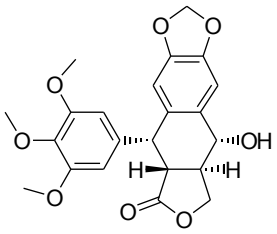

23b
Podophyllotoxin

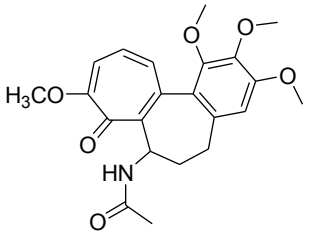

23c
Colchicine

Figure 20

[32] a) L. Wilson, *Biochemistry,* **1970**, *9*, 4999; b) R. W. J. Wang, L. I. Rebbun, and M. S. Kupchan, *Cancer Res.,* **1977**, 37, 3071.
[33] For the synthesis of an aza-analogue of podophyllotoxin from our group see: Poli, G.; Giambastiani, G. *J. Org. Chem.* **2002**, *67*, 9456-9459.

The tubulin, the globular protein target for the Steganacin, is the fundamental unit of the structures of the cytoskeleton: microtubules.

This protein is present in the cytoplasm in α / β form of the dimer and both monomers are able to recognize and bind GTP, but only the β subunit is able to hydrolyze this substrate to GDP. So, the β dimer bounds to GDP and the other one (α monomer) bounds GTP, the final protofilament appears to be polarized as this affinity is higher in the β subunit.

The process of formation of the microtubule can be divided into five distinct phase (Figure 21).

- ✓ The first process is the *nucleation* in which there is aggregation between different tubulin structure to form a protofilaments that rappresents the constitutional unit.
- ✓ In the second step is observed the *aggregation* of the protofilaments in the abundance of GTP.
- ✓ When the concentration of GTP is low, the *breakdown* of microtubules is observed. In this phase the (-)-Steganacin explics this action hydrolyzing GTP to GDP with consequently disassembly of the microtubles.
- ✓ This step is characterized by *stabilization*: a balance between the release speed of the tubulin to the negative terminal of microtubules (tubulins in the microtubule long hydrolyzed GTP and lost affinity for tubulin which they are linked) and the speed of the addition of tubulin to the positive terminal by nucleation. The length of the filament in this way is constant.
- ✓ Therefore, in the presence of high concentrations of GTP a *dynamic instability* process is observed and short or very long microtubles is formed.

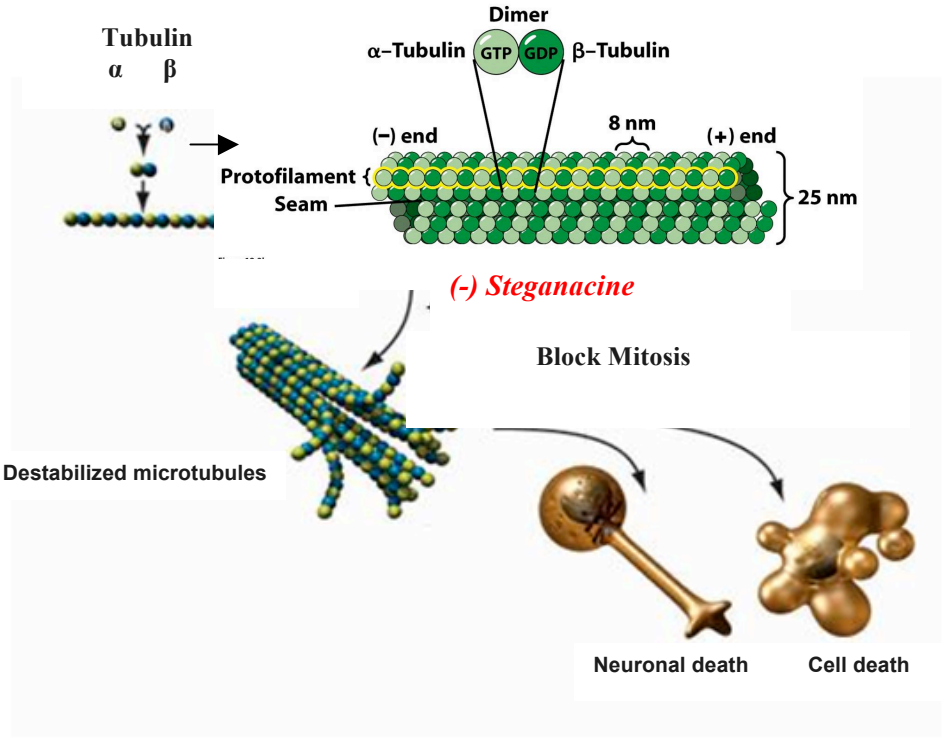

Figure 21

The interest of chemists for the **(-)-Steganacin 23** was initially motivated by its antitumor activity; it is for this reason that in literature we found different total syntheses of this molecule. [34]

Also, different analogues of steganacin were prepared: in 1989 Koga and co-workers published the synthesis of an aza-analogue of this compound that presented a nitrogen in position 3; [35] in the 2006 different triazole derivatives were reported in the literature [36] and the same years an hybrid structure with allocolchicine was studied.[37, 38]

[34] a) Kende, A. S.; Liebeskind, L. S. *J. Am. Chem. Soc.,* **1976**, *98*, 267-268. b) Becker, D.; Hughes, L. R.; Raphael, R. A. *J. Chem. Soc., Perkin Trans. 1*, **1977**, *14*, 1674-1681. c) Ziegler, F. E.; Fowler, K. W.; Sinha, N. D. *Tetrahedron Lett.,* **1978**, *19*, 2767-2770. d) Ziegler, F. E.; Chliwner, I.; Fowler, K. W.; Kanfer, S. J.; Kuo, S. J.; Sinha, N. D. *J. Am. Chem. Soc.,* **1980**, *102*, 790-798. e) Magnus, P.; Schultz, J.; Gallagher, T. *J. Chem. Soc., Chem. Commun.,* **1984**, 1179-1180. f) Ishiguro, T.; Mizuguchi, H.; Tomioka, K.; Koga, K. *Chem. Pharm. Bull.,* **1985**, *33*, 609-617.

[35] a) Tomioka, K.; Kubota, Y.; Kawasaki, H.; Koga, K. *Tetrahedron Lett.* **1989**, *30*, 2949-2952. b) Kubota, Y.; Kawasaki, H.; Tomioka, K.; Koga, K. *Tetrahedron* **1993**, *49*, 3081-3090.

[36] a) Beriozkina, T.; Appukkuttan, P.; Mont, N.; Van der Eycken, E. *Org. Lett.* **2006**, *8*, 487-490. b) Imperio, D.; Pirali, T.; Galli, U.; Pagliai, F.; Cafici, L.; Canonico, P. L.; Sorba, G.; Genazzani, A. A.; Tron, G. C. *Bioorg. Med. Chem.* **2007**, *15*, 6748-6757. c) Mont, N.; Pravinchandra Mehta, V.; Appukkuttan, P.; Beryozkina, T.; Toppet, S.; Van Hecke, K.; Van Meervelt, L.; Voet, A.; DeMaeyer, M.; Van der Eycken, E. *J. Org. Chem.* **2008**, *73*, 7509-7516.

[37] Joncour, A.; Décor, A.; Liu, J.-M.; Tran Huu Dau, M.-E.; Baudoin, O. *Chem. Eur. J.,* **2007**, 13, 5450-5465.

In the last two decades of the last century a detailed SAR[39] study was performed for the steganacin-type lignan lactones. Here are some critical structural features for the potency:

- ✓ the dioxolane moiety is fundamental for the cytotoxic activity;
- ✓ the lactone ring is not essential, although it contributes to potency;
- ✓ the acetate is not essential as stegane is equally active;
- ✓ the trimethoxyphenyl ring is essential for cytotoxic and antitubulic activities.

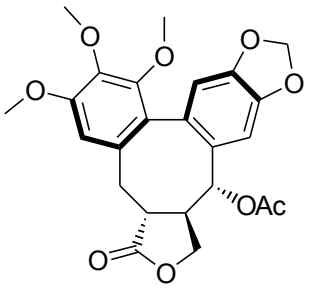

23

Figure 22

In order to investigate the biological activity of this natural product and the importance of chirality, different enatioselective total syntheses[40] were performed.

Although these syntheses take advantage of different process to obtain the target molecule, the common key steps are invariably the formation of the lacton moiety and the oxidative coupling between the two aromantic rings.

---

[38] Pour une revue, voir : Appukkuttan, P.; Van der Eycken, E. *Eur. J. Org. Chem.* **2008**, 5867-5886.

[39] F. Zavala, D. Guenard, L. Robin, E. Brown, *J. Med. Chem.,* **1980**, *23*, 546; b) K. Tomioka, T. Ishiguro, H. Mizuguchi, N. Komeshima, K. Koga, S. Tsukagoshi, T. Tsuruo, T. Tashiro, S. Tanida, T. Kishi, *J. Med. Chem.*, **1991**, 34, 54; c) K. Tomioka, H. Kawasaki, K. Koga, *Chem. Pharm. Bull.,* **1990**, 38, 1898.

[40] a) Tomioka, K.; Ishiguro, T.; Koga, K. *Tetrahedron Lett.,* **1980**, *21*, 2973-2976. b) Tomioka, K.; Ushiguro, T.; Iitaka, Y.; Koga, K. *Tetrahedron,* **1984**, *40*, 1303-1312.

II. Aim of the project

From a structural point of view the (-)-Steganacin presents a γ-lactonic skeleton condensed to an eight membered ring, three contiguous stereogenic centers and a biarylic portion.

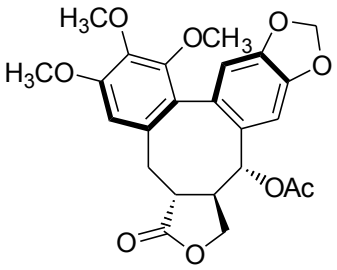

23

(-)-Steganacin

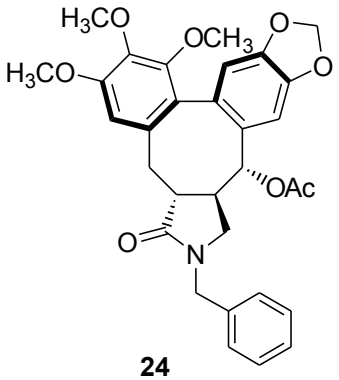

24

aza analogue of the (-)-Steganacin

Figure 23

Aim of this project is the synthesis of an **aza-analogue of Steganacin** in which the lactone structure is replaced by a γ-lactam moiety.

In 2009, Kammerer et al.[41] reported an original regio- and stereoselective synthesis of aryl substituted pyrrolidones by a phosphine-free Pd-catalyzed allene carbopalladation/allylic alkylation sequence.

To test and validate the potential of this domino "carbopalladation allene / allylic alkylation" sequence in a synthetic target application, we decided to synthesize a new aza analogue of **(-)-Steganacin** (Scheme 13).

[41] C. Kammerer , G. Prestat, D. Madec, G. Poli, *Chem. Eur. J.,* **2009**, *15*, 4224-4227.

III. Synthesis

III.I Retrosynthetic analysis

According to our retrosynthetic plan, **(-)-Aza-steganacin 24** could be derived from double bond oxidative cleavage of alkene **25** followed by a diastereoselective reduction of the resulting ketone. Intermediate **25** was envisaged to derive from a biaryl oxidative coupling of **26**, which could in turn originate from allene **27** via domino carbopalladation / allylic alkylation sequence followed by an appropriate benzylation step. Intermediate **27** was thought to derive from amination of allenol **28**, which can in turn easily originate from commercially available propargyl alcohol **29** (Scheme 13).

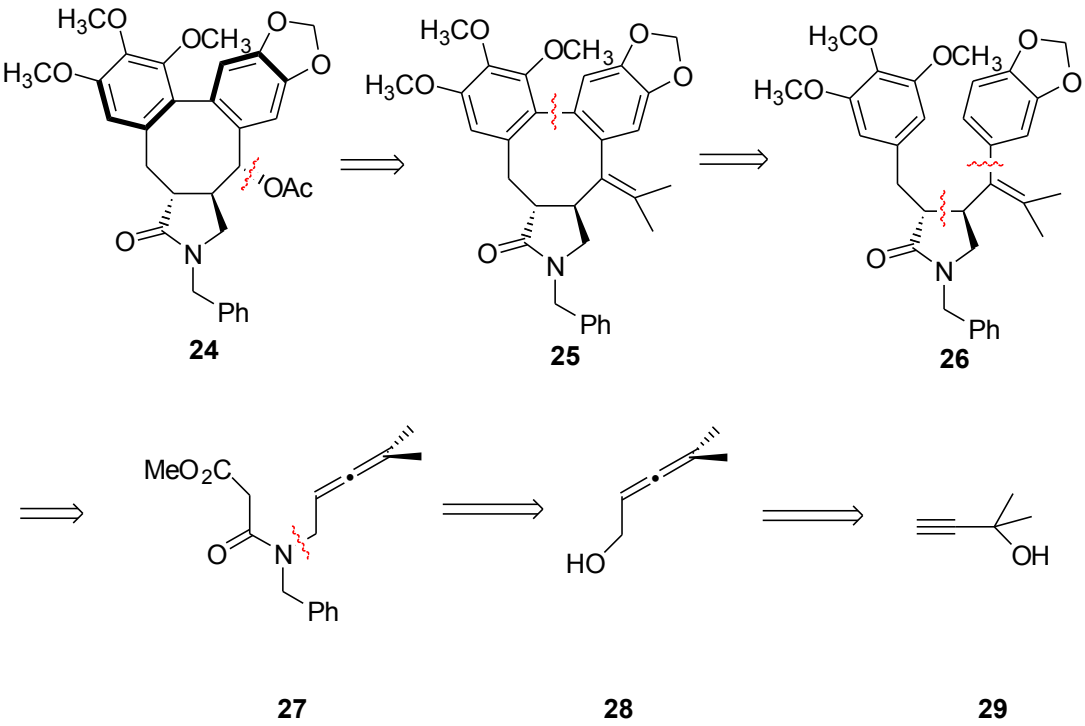

Scheme 13

III.II Synthesis of allenol intermediate

Preparation of allenol **28** was first tackled.[42] Accordingly, the hydroxyl function of propargyl alcohol **29** was protected as tetrahydropyranyl (THP) ether **30** so as to render it an active leaving group. Subsequent hydroxymethylation of the terminal acetylene **30** to give propargyl alcohol **31** was obtained by deprotonation with *n*-BuLi and subsequent treatment with excess *para*-formaldehyde. Following treatment with $LiAlH_4$ generated the desired allenol **28**. (Scheme 14)

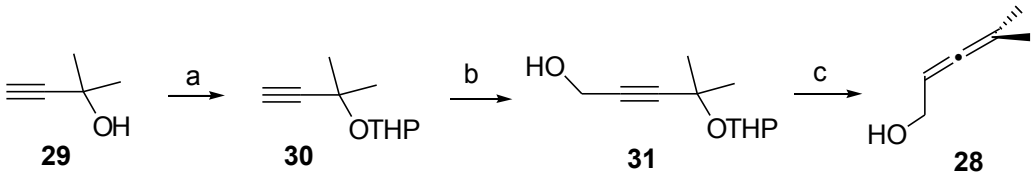

Reagents and conditions: a) DHP (1.2 eq), pTsOH (1 mol%), CH_2Cl_2, 0°C, 6h Y=71%; b) *n*-BuLi (1.1 eq), $(H_2CO)n$ (3 eq) Et_2O, -78°C, room temp., 12h, Y=94%; c) $LiAlH_4$ (3 eq.), Et_2O, 0°C, o.n. Y=66%.

Scheme 14

The mechanism of this reaction involves $LiAlH_4$ mediated deprotonation of the propargyl alcohol to yield the corresponding aluminum alkoxide. Subsequent intramolecular hydride delivery to the triple bond via a S_N2' mechanism generates, after hydrolysis of aluminium salt, the desired allenyl alcohol (Scheme 15).

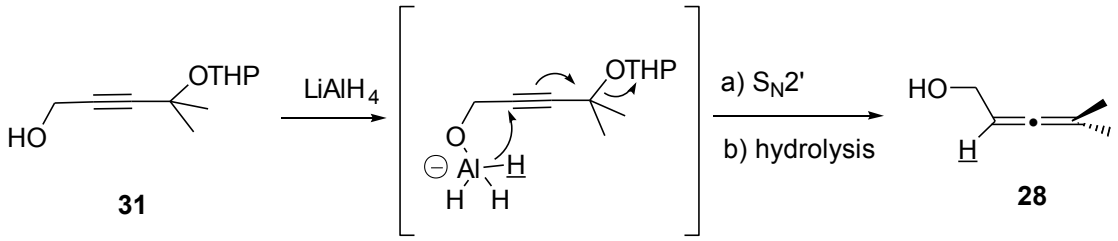

Scheme 15

[42] Cowie, J. S.; Landor, P. D.; Landor, S. R., *J. Chem. Soc., Perkin Trans.,* **1973**, *1,* 720-724.

A limitation of this synthetic protocol is due to the fact that all the intermediates along the sequence are rather volatile. As a consequence, much attention has to be paid to limit product loss during purification.

III.III Synthesis of cyclization precursor

We decided, for the subsequent amination of allenol **28**, to consider a protocol involving the transient generation of an electrophilic π-allyl vinylidene intermediate. Indeed, a couple of related examples have been previously reported for the synthesis of enantioenriched α-allenic amines[43].

Accordingly, we chose to activate the allenyl alcohol **28** as the corresponding phenyl-acetate, so as to combine a high reactivity in its oxidative addition to Pd(0) and a relatively high molecular weight of the allylic precursor. In the event, treatment of allenyl alcohol **28** with phenylacetyl chloride in the presence of Et_3N gave the desired phenyl-acetate **32** in 84% yield.

In order to synthesized the lactam moiety we planned a Pd(0)-catalyzed amidation of the allylic ester **32**. Thus, the amidation reaction of ester **32** with *N*-benzyltrifluoroacetamide, previously deprotonated by sodium hydride, was carried out in the presence of a catalytic amount of Pd $(PPh_3)_4$ in THF. After 24h at 55° C, the desired trifluoroacetamide **33** was obtained in a yield of 60%.

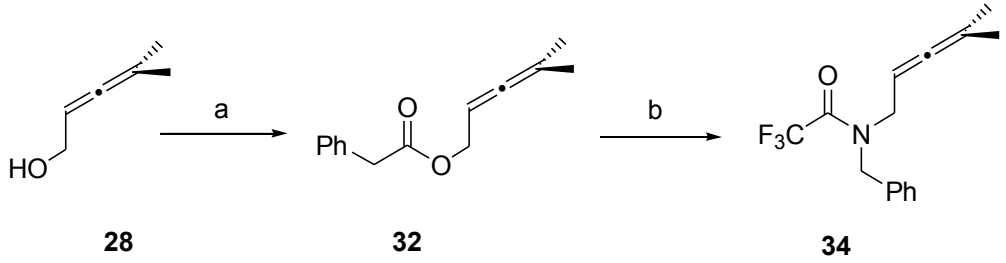

28 **32** **34**

Reagents and conditions: a) Phenyl-acetyl chloride (3 eq.), Et_3N (3 eq.), CH_2Cl_2, 0°C, o.n., Y=84%; b) LiHMDS (1.3 eq.), $BnNHCOCF_3$ (1.2 eq.), $Pd(PPh_3)_4$ (2.5% mol), THF, room temp., o.n., Y=60%.

Scheme 16

[43] a) Trost, B. M.; Fandrick, D. R.; Dinh, D. C., *J. Am. Chem. Soc,.* **2005**, *127*, 14186-14187; b) Imada, Y.; Nishida, M.; Kutsuwa, K.; Murahashi, S.-I.; Naota, T., *Org. Lett.,* **2005**, *7*, 5837-5839.

From a mechanistic point of view, the allenyl precursor is expected to coordinate to the Pd(0) complex via the internal double bond and oxidatively add to the metal to yield a fugitive π-allyl vinylidene intermediate. Attack to the distal position of this latter by the nitrogen nucleophile generates the desired allenyl-amine product and regenerates the catalytic species (Pd^0) (Scheme 17).

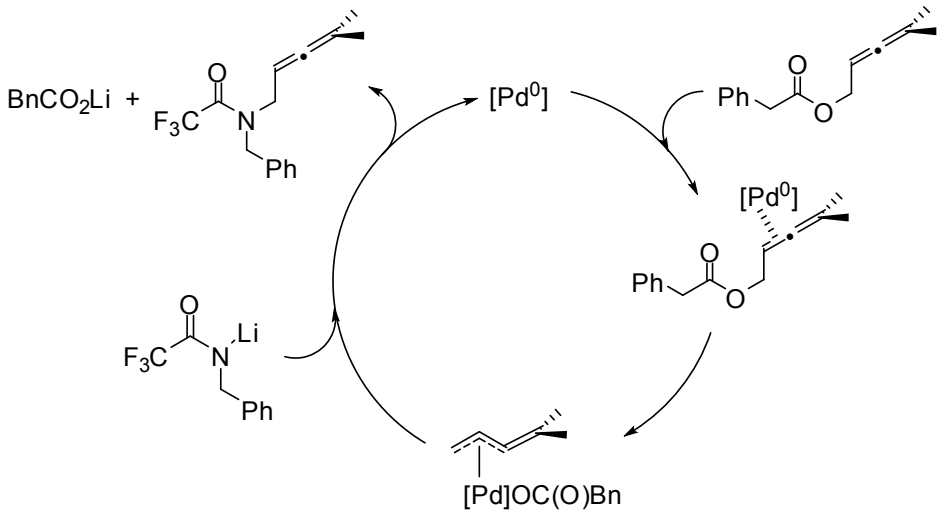

Scheme 17

Cleavage of the trifluoroacetamide group was effected in a mixture of methanol / water, saturated with potassium carbonate.[44] After 16h at 50°C, the free amine **35** was isolated in 85% yield. Subsequent treatment of **35** with 3-chloro-3-methyl oxopropionate in the presence of triethylamine in dichloromethane afforded the desired cyclization precursor **27** in 76% yield. (Scheme 18)

[44] Rückle, T.; Biamonte, M.; Grippi-Vallotton, T.; Arkinstall, S.; Cambet, Y.; Camps, M.; Chabert, C.; Church, D. J.; Halazy, S.; Jiang, X.; Martinou, I.; Nichols, A.; Sauer, W.; Gotteland, J.-P., *J. Med. Chem.,* **2004**, *47*, 6921-6934.

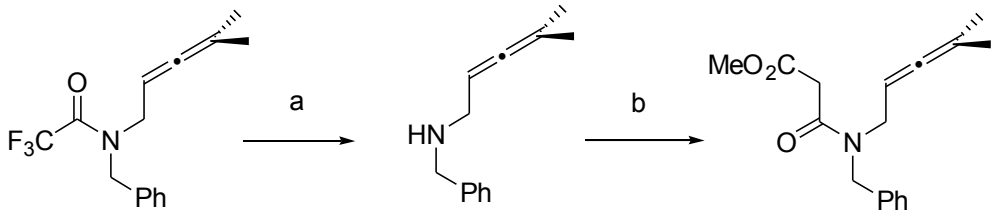

34 **35** **27**

Reagents and conditions: a) Satd K_2CO_3 MeOH / H_2O (10:1), 50 °C, 16h, Y=85%; b) methyl 3-chloro-3-oxopropanoate (3 eq.), Et_3N (3 eq.), CH_2Cl_2, room temp., 16 h, Y=76%.

Scheme 18

III.IV Phosphine-free Pd-catalyzed Domino Sequence and benzylation reaction

The key domino carbopalladation / allylation sequence was next tackled. To this purpose, we directly selected the reaction conditions optimized by our group in the methodological study,[41] as they were the result of a through optimization work. Thus, after a relative straightforward experimentation we found satisfactory conditions for this key step. In the event, a phosphine-free Pd^0 complex was generated in DMSO from $PdCl_2(CH_3CN)_2$, by using *n*-BuLi (2 equiv) as an *in situ* reducing agent [45] and the aromatic iodide **36** was added in the presence of TBAB. After treatment with NaH 60%, the malonamide **27** was added to the reaction mixture and after 16 hours the desired styryl pyrrolidone **37** was obtained in 74% yield as a single diastereoisomer. As in the previous methodological study, the domino sequence turned out to be completely regio- and stereoselective in favor of the 5-*exo trans* product.

[45] a) E. Negishi, T. Takahashi, K. Akiyoshi, *J. Chem. Soc. Chem. Commun.,* **1986**, 1338 – 1339; b) M. Bottex, M. Cavicchioli, B. Hartmann, N. Monteiro, G. Balme, *J. Org. Chem.* **2001**, 66, 175 – 179.).

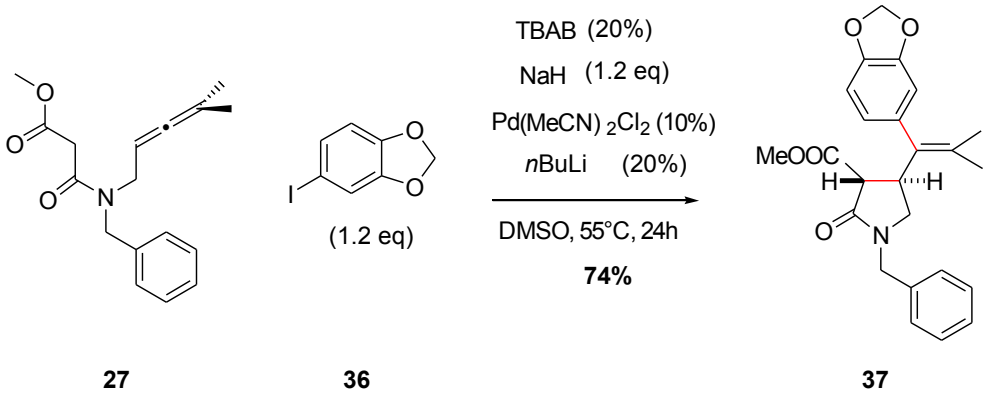

27 **36** **37**

Scheme 19

A mechanistic sequence for the carbopalladation/allylic alkylation domino sequence is proposed in Scheme 20: *Oxidative addition* of the Pd^0 complex to the aryl iodide, forms the electrophilic aryl palladium(II) complex. *Coordination* of one of the double bonds of the deprotonated allene to the electrophilic complex (Pd^{II}) and subsequent *carbopalladation* affords the corresponding σ-allyl complex. *Isomerisation* of this latter generates the corresponding electrophilic π-allyl complex, which is intramolecularly trapped by the deprotonated active methylene in a 5-*exo* cyclization mode. *Decoordination* of the thus formed Pd(0) complex releases the final product and the active catalytic species therby closing the catalytic cycle.

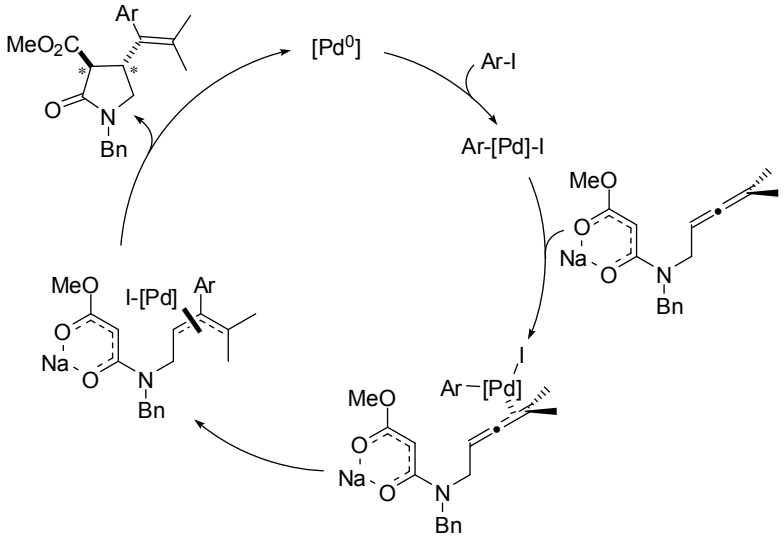

Scheme 20

The anion of 4-styryl pyrrolidin-2-one **37** was treated with the desired benzyl bromide in degassed DMF. After 24 hours at 100°C the product **38** was obtained with a yield of 73% as a single diastereoisomer having a *trans* relative configuration between the two benzyl substituents. This diastereoselectivity can be rationalized by assuming approach of the electrophile from the less hindered enolate face.

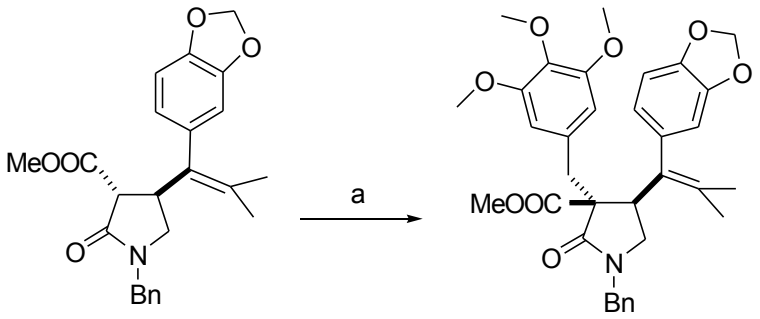

37 **38**

Reagents and conditions: a) 5-Bromomethyl-1,2,3-trimethoxy-benzene (3 eq.), NaH 60% (1.2 eq.), degassed DMF, 100 °C, 24h, Y=73%.

Scheme 21

III.V Removal of the methoxycarbonyl group

In order to remove the methoxycarbonyl group several strategies were tried.

In the first assay, compound **38** was subjected to Krapcho decarbometoxylation reaction[46] in the presence of sodium chloride and water in DMSO. Unfortunately, after 24h at 150°C, only traces of desired product 4 have been observed.

So, we decided to change pathway and try an ester hydrolysis / decarboxylation sequence. Accordingly, treatment of **38** with 20 equivalents of KOH in EtOH[47] for 4h at 80°C gave the corresponding acid and the transesterification product in a 70:30 report.

Using methanol as the co-solvent for the hydrolysis gave the desired acid with only 25% conversion.

[46] a) Krapcho, A. P., *Synthesis,* **1982**, 805-822; b) Krapcho, A. P., *Synthesis,* **1982**, 893-914; c) Krapcho, A. P., *Arkivoc,* **2007**, 1-53; d) Krapcho, A. P., *Arkivoc,* **2007**, 54-120.
[47] R. Shintani, M. Murakami, T. Hayashi, *Org. Lett.,* **2009**, 11, 2, 457-459.

Finally, heating compound **38** at reflux for 20 minutes in the presence of 20 equivalents of KOH in ethylene glycol gave the desired decarboxylated product **26** in 60% yield. (Scheme 22)

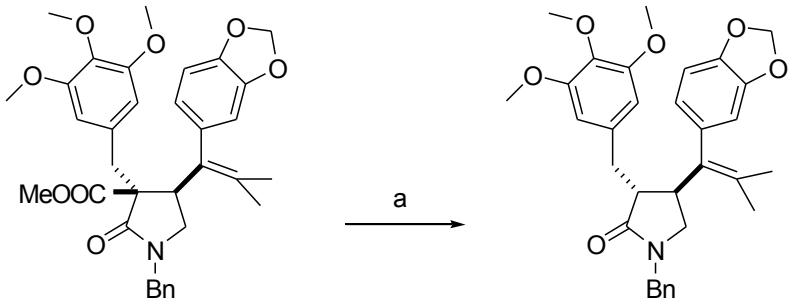

38 **26**

Reagents and conditions: a) KOH (20 eq.), ethylene glycol, 180-190 °C, 20 min. Y=60%

Scheme 22

III.VI Further steps

Unfortunately, I did not have time enough in Paris to study the final assembling of **26** toward the target. In any case, the concluding part of this synthesis would entail an oxidative coupling between the two arylic portions of the **26** to build up the characteristic eight membered biaryl ring system (intermediate **25**). Then, an oxidative cleavage of the double bond followed by a diastereoselective reduction of the resulting ketone **39** and final alcohol acetylation **40** should afford the desired **(-)-Steganacin aza-analogue 24**.

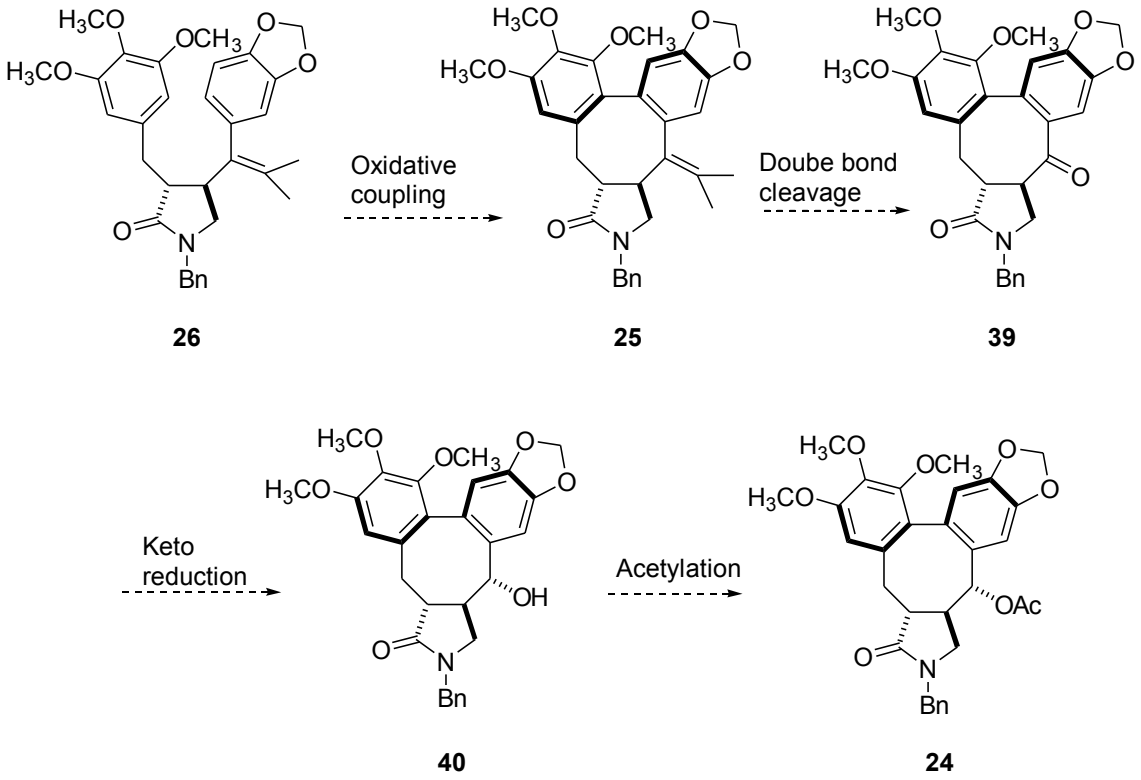

26 **25** **39**

40 **24**

Scheme 23

III. Conclusion

In this work I accomplished the synthesis of an advanced intermediate of Stegancine. The sequence entails fifteen steps, seven of which are needed to obtain the key malonamidic intermediate **27** from the propargyl alcohol **29** in a 19% of overall yield.

The crucial catalytic domino (carbopalladation/allylic alkylation) process (**27** + **36** → **37**) was could be validated and took place in 74% yield.

After benzylation of this key intermediate, several strategies to remove the methoxycarbonyl group were tested, the best solution being hydrolysis in ethylene glycol at high temperatures.

Four further steps should be necessary to complete the synthesis of the desired **(-)-Steganacin aza-analogue 24**. The next study will focus on the non-phenolic oxidative coupling between the two aromatic moieties.

References

[1] D.E. Drayer, *Clin. Pharmacol. Theor*., **1986**, *40,* 125.

[2] S. Lam, G. Malikin, *Chirality*, **1992**, *4*, 395; I.W. Wainer (Editor*), Drug Stereochemistry Analytical Methods and Pharmacology*, Marcel Dekker, Inc., New York, New York, **1993**.

[3] Stephens TD, Fillmore BJ., Hypothesis: Thalidomide Embryopathy – Proposed Mechanism of Action. *Teratology* **2000**; 61: 189-195.

[4] S.C. Stinson, *Chemical and Engineering News*, **1995**, 70, 44.

[5] B. Lin, X. Zhu, B. Koppenhoeffer and U. Epperlein, *LC·GC*, **1997***,15* 40. P. van Eikeren, in S. Ahuja (Editor*) Chiral Separations Applications and Technology*, American Chemical Society, Washington, D.C., **1997**, Ch. 2.

[6] G.Lin, Y. Li, A.S.C. Chan, *Principles and applications of Asymmetric Synthesis,* **2001**, Wiley-Interscience.

[7] Gilchrist, A., *Expert Opin. Ther. Targets,* **2004**, 8, 495–498

[8] Saito, Y., and Civelli, O., *Int. Rev. Neurobiol.* **2005**, 65, 179–209

[9] Vassilatis, D. K., Hohmann, J. G., Zeng, H., Li, F., Ranchalis, J. E., Mortrud, M. T., Brown, A., Rodriguez, S. S., Weller, J. R., Wright, A. C., Bergmann, J. E., and Gaitanaris, G. A. *Proc. Natl. Acad. Sci. U. S. A.,* **2003,** 100, 4903–4908

[10] Civelli, O. , *Trends Pharmacol. Sci.,* **2005,** 26, 15–19

[11] Sato, S., Shintani, Y., Miyajima, N., and Yoshimura, K. (April 18, **2002**) Japan Patent WO 0231145

[12] Xu, Y. L., Reinscheid, R. K., Huitron-Resendiz, S., Clark, S. D., Wang, Z., Lin, S. H., Brucher, F. A., Zeng, J., Ly, N. K., Henriksen, S. J., de Lecea, L., and Civelli, O. *Neuron,* **2004,** 43, 487–497.

[13] Reinscheid, R. K., Xu, Y. L., Okamura, N., Zeng, J., Chung, S., Pai, R., Wang, Z., and Civelli, O. *J. Pharmacol. Exp. Ther.* **2005,** 315, 1338–1345

[14] Reinscheid, R. K., Xu, Y. L. *FEBS J.* **2005**, 272, 5689–5693

[15] Guerrini, R., Salvadori, S., Rizzi, A., Regoli, D., Calò, G. *Med. Res. Rev.*; **2010**, 30(5):751-77.

[16] Roth, A. L.; Marzola, E.; Rizzi, A.; Arduin, M.; Trapella, C.; Corti, C.; Vergura, R.; Martinelli, P.; Salvadori, S.; Regoli, D.; Corsi, M.; Cavanni, P.; Calo`, G.; Guerrini, R.. *J. Biol. Chem.* **2006**, *281*, 20809-20816.

[17] Tancredi, T.; Guerrini, R.; Marzola, E.; Trapella, C.; Calo, G.; Regoli, D.; Reinscheid, R. K.; Camarda, V.; Salvadori, S.; Temussi, P. A., *J. Med. Chem.,* **2007**, *50*, 4501–4508.

[18] R.Guerrini, V.Camarda, C.Trapella, G.Calò, A.Rizzi, C.Ruzza, S.Fiorini, E.Marzola, R. K.Reinscheid, D.Regoli, S.Salvadori, *J. Med. Chem.* **2009,** *52,* 524–529.

[19] a) Reinscheid R.K.. *Peptides* **2007***, 28,* 830–837; b) Reinscheid R.K. and Xu, Y.L.. *Neuroscientist,* **2005**, *11*, 532–538; c) Guerrini R., Salvadori S., Rizzi A., et al.. *Medicinal Research Reviews*, **2010**, *30* (5), 751-77.

[20] Fukatzu K, Nakayama Y, Tarui N, Mori M, Matsumoto H, Kurasawa O, Banno H.; Takeda Pharmaceuticals; **2004**, PCT/JP04/12683.

[21] Okamura N, Habay SA, Zeng J, Chamberlin AR, Reinscheid RK.; *J. Pharmacol. Exp. Ther.,* **2008**, 325, 893–901.

[22] Y. Zhang, B. P. Gilmour, H. A. Navarro, S. P. Runyon, *Bioorg. Med. Chem. Lett.,* **2008**, 18, 4064–4067.

[23] J. Y. Melamed, A.E. Zartman , N.R. Kett , A.L. Gotter, V.N. Uebele, D.R. Reiss, C.L. Condra, C. Fandozzi, L.S. Lubbers, B.A. Rowe, G.B. McGaughey, M.Henault, R. Stocco, J.J. Renger, G.D. Hartman, M.T. Bilodeau, B.W. Trotter, *Bioorg. Med. Chem. Lett.,* **2010**, 20, 4700–4703.

[24] B. W. Trotter, K. K. Nanda, P.J. Manley, V. N. Uebele, C. L. Condra, A. L. Gotter, K. Menzel, M. Henault, R. Stocco, J.J. Renger, G. D. Hartman, M. T. Bilodeau**,** *Bioorg. Med. Chem. Lett.,* **2010**, 20, 15, 4704-4708 .

[25] a) Horton, D. A.; Bourne, G. T.; Smythe, M. L., *Chem. Rev.,* **2003**, *103*, 893–930; b) Tullberg, M.; Grøtli, M.; Luthman, K. *J. Org. Chem.,* **2007**, *72*, 195–199.

[26] a) Dinsmore, C. J.; Beshore, D. C. *Tetrahedron*, **2002**, 58, 3297–3312; Dinsmore, C. J.; b) Beshore, D. C. *Org. Prepar. Proced. Int.,* **2002**, 34, 367–404; c) Quirion, J.-C.

Asymmetric Synthesis of Substituted Piperazines. In Targets in Heterocyclic Systems; Attanasi, O. A., Spinelli, D., Eds.; Italian Society of Chemistry: Roma, **2008**; Vol. 12, pp 438–459; d) De Risi C., Pelà M., Pollini G.P., Trapella C., Zanirato V., *Tetrahedron: Asymmetry,* **2010**, *21*, 255-274.

[27] V. Schanen, M.P.Cherrier, S.Jose de Melo, J.C. Quirion, H.P. Husson, *Synthesis*,**1996**, 833-837.

[28] Beak, P.,; Lee, W.K.; *J. Org. Chem.,* **1993,** 58, 1109.

[29] G.Reginato, B.Credico, D.Andreotti, A.Mingardi, A.Paio, D.Donati, B.Pezzati, Al. Mordini, *Tetrahedron: Asymmetry,* **2010**, 21, 191–194;

[30] C. Ruzza, A. Rizzi, C. Trapella, M. Pelà, V. Camarda, V. Ruggieri, M. Filaferro, C. Cifani, R. K. Reinscheid, G. Vitale, R. Ciccocioppo, S. Salvadori, R. Guerrini, G. Calò, *Peptides,* **2010**, 31, 915-925.

[31] M. Kupchan, R.W. Britton, M.F. Ziegler, C.J. Gilmore, R.J. Restivo, R.F. Bryan, *Journal of the American Society,* **1973**, 95:4, 21, 1335-1336.

[32] a) L. Wilson, *Biochemistry,* **1970**, *9*, 4999; b) R. W. J. Wang, L. I. Rebbun, and M. S. Kupchan, *Cancer Res.,* **1977**, 37, 3071.

[33] For the synthesis of an aza-analogue of podophyllotoxin from our group see: Poli, G.; Giambastiani, G. *J. Org. Chem.* **2002**, *67*, 9456-9459.

[34] a) Kende, A. S.; Liebeskind, L. S. *J. Am. Chem. Soc.,* **1976**, *98*, 267-268. b) Becker, D.; Hughes, L. R.; Raphael, R. A. *J. Chem. Soc., Perkin Trans. 1*, **1977**, *14*, 1674-1681. c) Ziegler, F. E.; Fowler, K. W.; Sinha, N. D. *Tetrahedron Lett.,* **1978**, *19*, 2767-2770. d) Ziegler, F. E.; Chliwner, I.; Fowler, K. W.; Kanfer, S. J.; Kuo, S. J.; Sinha, N. D. *J. Am. Chem. Soc.,* **1980**, *102*, 790-798. e) Magnus, P.; Schultz, J.; Gallagher, T. *J. Chem. Soc., Chem. Commun.,* **1984**, 1179-1180. f) Ishiguro, T.; Mizuguchi, H.; Tomioka, K.; Koga, K. *Chem. Pharm. Bull.,* **1985**, *33*, 609-617.

[35] a) Tomioka, K.; Kubota, Y.; Kawasaki, H.; Koga, K. *Tetrahedron Lett.* **1989**, *30*, 2949-2952. b) Kubota, Y.; Kawasaki, H.; Tomioka, K.; Koga, K. *Tetrahedron* **1993**, *49*, 3081-3090.

[36] a) Beriozkina, T.; Appukkuttan, P.; Mont, N.; Van der Eycken, E. *Org. Lett.* **2006**, *8*, 487-490. b) Imperio, D.; Pirali, T.; Galli, U.; Pagliai, F.; Cafici, L.; Canonico, P. L.; Sorba, G.; Genazzani, A. A.; Tron, G. C. *Bioorg. Med. Chem.* **2007**, *15*, 6748-6757. c) Mont, N.; Pravinchandra Mehta, V.; Appukkuttan, P.; Beryozkina, T.; Toppet, S.; Van Hecke, K.; Van Meervelt, L.; Voet, A.; DeMaeyer, M.; Van der Eycken, E. *J. Org. Chem.* **2008**, *73*, 7509-7516.

[37] Joncour, A.; Décor, A.; Liu, J.-M.; Tran Huu Dau, M.-E.; Baudoin, O. *Chem. Eur. J.,* **2007**, 13, 5450-5465.

[38] Pour une revue, voir : Appukkuttan, P.; Van der Eycken, E. *Eur. J. Org. Chem.* **2008**, 5867-5886.

[39] F. Zavala, D. Guenard, L. Robin, E. Brown, *J. Med. Chem.,* **1980**, *23*, 546; b) K. Tomioka, T. Ishiguro, H. Mizuguchi, N. Komeshima, K. Koga, S. Tsukagoshi, T. Tsuruo, T. Tashiro, S. Tanida, T. Kishi, *J. Med. Chem.*, **1991**, 34, 54; c) K. Tomioka, H. Kawasaki, K. Koga, *Chem. Pharm. Bull.,* **1990**, 38, 1898.

[40] a) Tomioka, K.; Ishiguro, T.; Koga, K. *Tetrahedron Lett.,* **1980**, *21*, 2973-2976. b) Tomioka, K.; Ushiguro, T.; Iitaka, Y.; Koga, K. *Tetrahedron,* **1984**, *40*, 1303-1312.

[41] C. Kammerer , G. Prestat, D. Madec, G. Poli, *Chem. Eur. J.,* **2009**, *15*, 4224-4227.

[42] Cowie, J. S.; Landor, P. D.; Landor, S. R., *J. Chem. Soc., Perkin Trans.,* **1973**, *1,* 720-724.

[43] a) Trost, B. M.; Fandrick, D. R.; Dinh, D. C., *J. Am. Chem. Soc,*. **2005**, *127*, 14186-14187; b) Imada, Y.; Nishida, M.; Kutsuwa, K.; Murahashi, S.-I.; Naota, T., *Org. Lett.,* **2005**, *7*, 5837-5839.

[44] Rückle, T.; Biamonte, M.; Grippi-Vallotton, T.; Arkinstall, S.; Cambet, Y.; Camps, M.; Chabert, C.; Church, D. J.; Halazy, S.; Jiang, X.; Martinou, I.; Nichols, A.; Sauer, W.; Gotteland, J.-P., *J. Med. Chem.,* **2004**, *47*, 6921-6934.

[45] a) E. Negishi, T. Takahashi, K. Akiyoshi, *J. Chem. Soc. Chem. Commun.,* **1986**, 1338 – 1339; b) M. Bottex, M. Cavicchioli, B. Hartmann, N. Monteiro, G. Balme, *J. Org. Chem.* **2001**, 66, 175 – 179.).

[46] a) Krapcho, A. P., *Synthesis,* **1982**, 805-822; b) Krapcho, A. P., *Synthesis,* **1982**, 893-914; c) Krapcho, A. P., *Arkivoc,* **2007**, 1-53; d) Krapcho, A. P., *Arkivoc,* **2007**, 54-120.

[47] R. Shintani, M. Murakami, T. Hayashi, *Org. Lett.,* **2009**, 11, 2, 457-459.

Chapter 3

Experimental Section

General Methods

Depending on the reaction, dichloromethane was distilled on CaH_2 or dried on a Mbraun solvent purification system MB SPS-800. Diethyl ether and THF were distilled on sodium/benzophenone or dried on a MBraun solvent purification system MB SPS-800. DMF was distilled over $MgSO_4$ under reduced pressure or was dried on a MBraun solvent purification system MB SPS-800. Acetonitrile was dried on a MBraun solvent purification system MB SPS-800. DMSO was distilled over CaH_2 under reduced pressure.

Flash chromatography was conducted on silica gel (0.040-0.063 mm unless stated) (Polygram SIL G/UV254). Analytical Thin Layer Chromatographies (TLC) were performed on Merck precoated 60 F^{254} platesor.

One-dimensional and two dimensional NMR spectra were recorded on a VARIAN 400 MHz instrument or a Bruker Avance 400 spectrometer (BBFO probe), using the residual peak of deuterated chloroform as internal standard (7.27 ppm for ^{1}H NMR and 77.2 ppm for ^{13}C NMR). Chemical shifts are reported in ppm and coupling constants *J* in Hertz. Abbreviations used for peak multiplicity are: s,singlet; br s, broad singlet; d, doublet; t, triplet; q, quadruplet; quint., quintuplet; m, multiplet.

IR spectra were recorded on a Bruker Tensor 27 (Pike) apparatus and only the strongest or the structurally most important peaks were listed.

MS analyses were performed on a ESI-Micromass ZMD 2000 and high resolution mass spectrometry was performed on a Thermo Fisher Scientific LTQOrbitrap (ESI).

Optical rotation data were recorded on a Perkin-Elmer polarimeter 241.

Melting points were measured using a Stuart Scientific SMP3 apparatus.

The purity of the tested compounds (R/S)-SHA 68, (R)-SHA 68 and (S)-SHA 68 has been assessed by RP-HPLC.

Chiral chromatography analysis

A micro HPLC (Agilent 1100 micro series, Agilent Technologies) equipped with a micro diode array detector was employed. A 150mm × 2mm stainless steel column packed with Lux Cellulose-1 (cellulose tris 3,5-dimethylphenylcarbamate from Phenomenex) was used for all the measurements. The average size of the packing material was 3 µm. The mobile phase was a binary mixture of hexane/isopropyl alcohol (80/20 v/v). Flow rate was 200uL/min. Injection volume was 3µL. Analyte solutions were filtered with PFTE filters (0.45µm, Supelco, Bellefonte, PA, USA) before injection. All chromatograms were recorded at 230 nm. The retention times for the first (**(*S*)-SHA 68**) and second (**(*R*)-SHA 68**) eluted enantiomers were 6.5 and 7.9 min, respectively.

Crystal structure determination of compound 21b

The crystal data of compound **21b** were collected at room temperature using a Nonius Kappa CCD diffractometer with graphite monochromated Mo-Kα radiation. The data sets were corrected for Lorentz and polarization effects. The structure was solved by direct methods and refined using full-matrix least-squares with all non-hydrogen atoms anisotropically and hydrogens included on calculated positions, riding on their carrier atoms. All calculations were performed using SHELXL-97 and PARST implemented in WINGX system of programs.

Crystal Data: $C_{26}H_{26}N_2O_2$, orthorhombic, space group $P2_12_12_1$, a = 11.2339(2), b = 11.6808(3), c = 16.4783(5) Å, V = 2162.30(9) Å^3, Z = 4, D_c = 1.224 g cm^{-3}, intensity data collected with $\theta \leq 26°$, 4215 independent reflections measured, 3460 observed reflections [$I > 2\sigma(I)$], final R index = 0.0365 (observed reflections), R_w = 0.0904 (all reflections), S = 1.048. The absolute configuration has not been established by anomalous dispersion effects in diffraction measurements on the crystal. The enantiomer has been assigned by reference to an unchanging chiral centre in the synthetic procedure view of compound **21b** is shown in Figure 16.

CCDC deposition number: 810351.

Synthesis of Takeda's compound

1) [1-(2-Hydroxy-1-phenyl-ethylcarbamoyl)-ethyl]-carbamic acid *tert*-butyl ester (3)

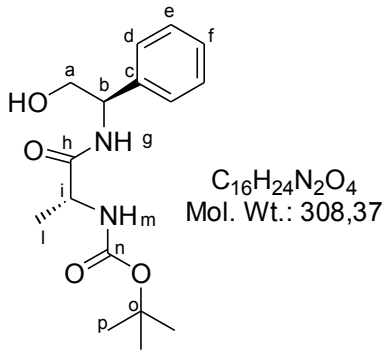

$C_{16}H_{24}N_2O_4$
Mol. Wt.: 308,37

To a stirred solution of (D)-Boc-Ala-OH (2 g, 14.6 mmol) in CH_2Cl_2 (20 mL), WSC (1.86 g, 9.8 mmol) and (*R*)-phenylaminoglycinol (2.76 g, 14.6 mmol) were added. After 24 h at room temperature the reaction was monitored by TLC (EtOAc/light petroleum 4:1). The organic layer was washed with brine (10 mL) and the product was purified by crystallization with ethyl ether to obtain **3** in 43% yield.

^{1}H NMR (CD_3OD, 400 MHz): 7.35-7.29 (m, 5H, Hd,e,f); 4.95 (bs, 1H, Hb); 4.15 (q, *J*= 7.0 Hz, 1H, Hi); 3.79-3.68 (m, 2H, Ha); 1.44 (s, 9H, H_p); 1.32 (d, *J*= 7.0 Hz, 3H, H_l).

^{13}C NMR (CD_3OD, 100MHz): δ = 175.8 (C_h), 155.7 (Cn), 141.2 (C_c), 129.6 (C_d or C_e), 128.5 (C_f), 128.1 (C_d or C_e), 80.8 (C_o), 66.3 (C_a), 57.1 (C_b), 51.8 (C_i), 28.9 (C_p), 18.4 (C_l).

MS (ESI): $[M+H]^+$ = 309.

$[\alpha]_D^{20}$ = -17 (c = 0.121g/100 ml, methanol).

2) [2-(2-Hydroxy-1-phenyl-ethylamino)-1-methyl-ethyl]-carbamic acid *tert*-butyl ester (4)

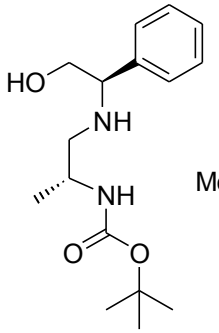

$C_{16}H_{26}N_2O_3$
Mol. Wt.: 294,39

To a stirred suspension of $LiAlH_4$ (296 mg, 7.792 mmol) at 0°C in anhydrous THF, a solution of **3** (800 mg, 2.59 mmol) was added drop wise. The reaction was monitored by TLC (EtOAc/light petroleum 4:1) and after 24 hours the excess of hydride was quenched with water and the salts were filtered trough a celite pad. The solvent was evaporated in vacuo and the crude product **4** was obtained in quantitative yield and used in the next step without further purification.

3) {2-[2-(*tert*-Butyl-dimethyl-silanyloxy)-1-phenyl-ethylamino]-1-methyl ethyl} carbamic acid *tert*-butyl ester (5)

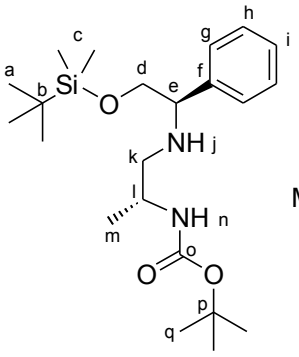

$C_{22}H_{40}N_2O_3Si$
Mol. Wt.: 408,65

To a stirred solution of **4** (980 mg, 3.33 mmol) in DMF (10 mL) at 0°C, imidazole (453 mg, 6.66 mmol) was added. After 10 min, *tert*-buthyldimethysilil chloride (551 mg, 3.6 mmol) solubilized in DMF (5ml) was slowly added. The reaction was monitored by TLC (EtOAc/light petroleum 4:1) and after 3 h at room temperature the reaction was termined. The excess of *tert*-buthyldimethysilil chloride was hydrolized by adding

water. After complete elimination of solvent reaction with low pressure pomp the residue was eluited with Et_2O and washed with 10 ml of water. The combined organic phases were concentrate to dryness to obtain 1.03 gr of **5** in 76% yield.

^{1}H NMR ($CDCl_3$, 400 MHz): δ = 7.32-7.25 (m, 5H, Hg,h,i); 5.00-4.96 (m, 1H, Hl); 4.59 (bs, 1H, Hn); 4.23 (bs, 1H, Hj); 3.87 (dd, 1H, *J*= 4.4Hz, Hd or Hd'); 3.77(dd, 1H, *J*= 4.0Hz, Hk or Hk'); 3.73 (dd, 1H, *J*= 3.6Hz, Hk' or Hk); 3.65 (dd, 1H, *J*= 4.0Hz, Hd' or Hd); 3.55-3.50 (m, 1H, He); 1.44 (s, 9H, Hq); 1.07 (s, 3H, Hm); 0.89 (s, 9H, Ha); 0.01 (s, 6H, Hc).

^{13}C NMR ($CDCl_3$, 100MHz): δ = 155.85 (Co), 141.01 (Cf), 128.39 (Ch or Cg), 127.75 (Cg or Ch), 127.34 (Ci), 70.69 (Cp), 68.46 (Cd), 66.29 (Ck), 64.14 (Ce), 54.66 (Cl), 28.51 (Cq), 25.98 (Ca), 19.27 (Cm), 18.34 (Cb), -5.37 (Cc).

MS (ESI): $[M+H]^+$ = 409.

$[\alpha]_D^{20}$ = - 9 (c = 0.24 g/100 ml, Chloroform).

4) (2-{(2-Bromo-acetyl)-[2-(*tert*-butyl-dimethyl-silanyloxy)-1-phenyl-ethyl]-amino} -1-methyl-ethyl)-carbamic acid *tert*-butyl ester (6)

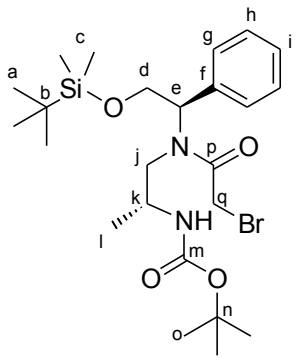

$C_{24}H_{41}BrN_2O_4Si$
Mol. Wt.: 529,58

To a stirred solution of bromoacetic acid (681 mg, 4.9 mmol) in CH_2Cl_2 (20 mL), WSC (470 mg, 2.45 mmol) and the silyl intermediate **5** (1 g, 2.45 mmol) were added. After 24 h at room temperature the reaction was monitored by TLC (EtOAc/light petroleum 2:8).

The organic phase was concentrate to dryness and the crude product was purified by column chromatography (EtOAc/ light petroleum 2:8) to yield **6** (450 mg, 35%).

^{1}H NMR ($CDCl_3$, 400 MHz): δ = 7.35-7.25 (m, 5H, Hg,h,i), 5.15-5.13 (m, 2H, Hd), 4.13-4.10 (m, 4H, Hj and Hq), 3.87 (m, 1H, He), 2.84-2.76 (m, 2H, NH and Hk), 1.38 (s, 9H, Hq), 0.87 (s, 12H, Ha and Hl); 0.08 (s, 6H, Hc).

^{13}C NMR ($CDCl_3$, 100MHz): δ = 170.15 (Cp), 155.35 (Cm), 135.6 (Cf), 129.08 (Ch or Cg), 128.87 (Ci), 127.87 (Cg or Ch), 70.69 (Cn), 62.05 (Cd), 61.78 (Ce), 47.48 (Ch), 46.30 (Cj), 41.94 (Cq), 28.45 (Co), 25.85 (Ca), 19.06 (Cl), 18.21 (Cb), -5.37 (Cc).

MS (ESI): $[M+H]^+$ = 409.

$[\alpha]_D^{20}$ = - 33 (c = 0.10 g/100 ml, Chloroform).

5) 4-[2-(*tert*-Butyl-dimethyl-silanyloxy)-1-phenyl-ethyl]-2-methyl-5-oxo-piperazine -1-carboxylic acid *tert*-butyl ester (7)

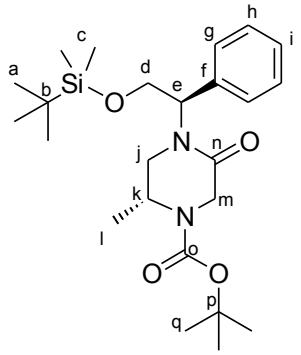

$C_{24}H_{40}N_2O_4Si$
Mol. Wt.: 448,67

To a stirred suspension of NaH 60% (61 mg, 2.55 mmol) in a mixture of THF/DMF 1/1 (10 mL) at 0°C, a solution of **6** (450 mg, 0.85 mmol) in THF/DMF 1/1 (10 mL) was added. After 24 h the reaction was quenched by adding NH_4Cl satured solution (5 mL) and the solvent was removed in vacuo. The residue was dissolved in EtOAc (10 mL) and washed twice with water (5 mL). The organic layer was dried, evaporated under reduced pressure and the crude product purified by flash chromatography (eluent: EtOAc/light petroleum 2:8) to obtain **7** in 74% yield.

^{1}H NMR ($CDCl_3$, 400 MHz): δ = 7.31-7.25 (m, 5H, Hg,h,i), 5.76 (dd, 1H, *J*= 5.6Hz, He), 4.30 (d, 1H, *J*= 18.4Hz, part of AB system, Hd), 3.80 (d, 1H, *J*= 18.6Hz, part of AB system, Hd'), 4.18-3.91 (m, 3H, Hj and Hk), 3.17 (m, 2H, Hm), 1.42 (s, 9H, Hq), 1.24 (s, 3H, Hl), 0.86 (s, 9H, Ha), 0.06 (s, 6H, Hc).

MS (ESI): $[M+H]^+$ =449

6) 4-(2-Hydroxy-1-phenyl-ethyl)-2-methyl-5-oxo-piperazine-1-carboxylic acid tert-butyl ester (8)

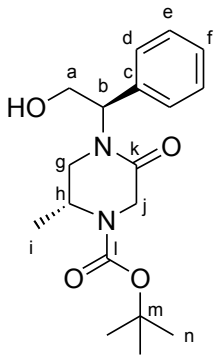

$C_{18}H_{26}N_2O_4$
Mol. Wt.: 334,41

To a solution of compoud **7** (268 mg, 0.598 mmol) in 10 ml of anhydrous THF, cooled at 0°C, was added TBAF (566 mg, 1.795 mmol). The reaction was stirred at room temperature for 1 h and after this time the solvent was removed under vacuum. The residue was diluited with EtOAc and washed twice with water. The organic layer was dried and concentrated under reduced pressure to give the crude product, which was purified by flash chromatography to obtain compound **8** (144 mg, yield 72%).

^{1}H NMR ($CDCl_3$, 400 MHz): δ = 7.35-7.25 (m, 5H, Hd,e,f), 5.7 (q, 1H, *J*= 6.8Hz, Hh), 4.35 (d, 1H, *J*= 18.4Hz, part of AB system, Ha), 3.85 (d, 1H, *J*= 18.6Hz, part of AB system, Ha'), 4.10 (s, 2H, Hj), 3.14 (dd, 1H, *J*=12.6, 4.2Hz, Hd), 2.93 (dd, 1H, *J*=12.5, 2.6Hz, Hd'), 2.66 (bs, 1H, OH), 1.43 (s, 9H, Hn), 1.18 (d, 3H, *J*= 6.8Hz, Hi).

^{13}C NMR ($CDCl_3$, 100MHz): δ = 167.56 (Ck), 153.56 (Cl), 135.72 (Cc), 128.94 (Cd or Ce), 128.37 (Cf) , 128.19 (Ce or Cd), 80.73 (Cm), 61.85 (Ca), 58.99 (Cb), 48.02 (Cg), 45.24 (Cj), 45.17 (Ch), 28.42 (Cl), 16.00 (Cb).

MS (ESI): $[M+H]^+ = 335$.

$[\alpha]_D^{20}$ = - 33 (c = 0.10 g/100 ml, Chloroform).

7) 4-(2-Hydroxy-1-phenyl-ethyl)-2-methyl-piperazine-1-carboxylic acid tert-butyl ester (9)

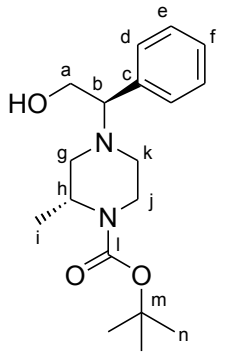

$C_{18}H_{28}N_2O_3$
Mol. Wt.: 320,43

Under argon atmosphere 144 mg (0.431 mmol) of compound **8** were suspended in anhydrous THF, the reaction mixture was cooled at 0°C and under vigorously stirring $(CH_3)_2S*BH_3$ (124 µl, 1.293 mmol) was added drop wise. The reaction mixture was heated at reflux for 30 minutes. After this time the reaction was acidified (citric acid sat.) and quenched with NaOH 2N, the THF was removed in vacuo and the aqueous layer extracted twice with EtOAc (10ml each). The organic layer was dried, concentrated in vacuo and purified by flash chromatography (EtOAc/light petroleum, 3/1) to afford compound **9** in 88% yield.

^{1}H NMR ($CDCl_3$, 400 MHz): δ = 7.37-7.22 (m, 5H, Hd,e,f), 4.25 (bs, 1H, OH), 4.00-3.96 (m, 2H, Ha), 3.85-3.78 (m, 2H, Hj), 3.25-3.20 (m, 1H, Hb), 3.10-3.05 (m, 1H, Hh), 2.87-2.80 (m, 2H, Hk), 2.28-2.20 (m, 2H, Hg), 1.39 (s, 9H, Hn), 1.18 (d, 3H, *J*= 6.8Hz, Hi).

^{13}C NMR ($CDCl_3$, 100MHz): δ = 154.26 (Cl), 133.28 (Cc), 129.34 (Cd or Ce), 128.90 (Cf), 128.75 (Ce or Cd), 80.73 (Cm), 69.87 (Cb), 60.26 (Ca), 51.85 (Cg), 50.70 (Ck), 46.19 (Ch), 38.27 (Cj), 28.37 (Cl), 15.47 (Cb).

MS (ESI): $[M+H]^+$ = 321.

$[\alpha]_D^{20}$ = - 36 (c = 0.10 g/100 ml, Chloroform).

8) 4-(2-Methoxy-1-phenyl-ethyl)-2-methyl-piperazine-1-carboxylic acid tert-butyl ester (10)

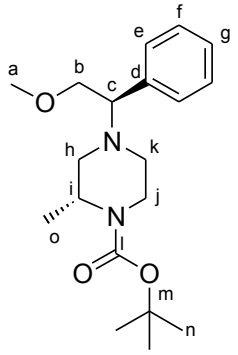

$C_{19}H_{30}N_2O_3$
Mol. Wt.: 334,45

A solution of the compound **9** (121 mg, 0.378 mmol) in a mixture of THF/DMF 1/1 (10 mL) at 0°C, was added drop wise to a stirred suspension of sodium hydride 60% (27.21 mg, 1.134 mmol) in 5 ml a mixture of THF/DMF 1/1. The reaction mixture was left in the same conditions for half an hour, then a solution of methyl iodide (70.61 µl, 1.134 mmol) in a mixture of THF/DMF 1/1 was added. After 24 h at room temperature, the reaction was termined, the DMF was removed under vacuum and the residue was diluited with 5 ml of Brine and extracted three times with EtOAc. The organic layers were combined, dried and evaporated under reduced pressure to give a crude product than purified by flash chromatography (EtOAc/light petroleum 1:4) to obtain compound **10** (78 mg, yield 62%).

^{1}H NMR ($CDCl_3$, 400 MHz): δ = 7.30-7.25 (m, 5H, He,f,g), 4.15-4.10 (m, 1H, Hc), 3.84-3.68 (m, 2H, Hb or Hh or Hk or Hj), 3.60-3.41 (m, 2H, Hb or Hh or Hk or Hj),

3.28 (s, 3H, Ha), 3.18-2.99 (m, 2H, Hb or Hh or Hk or Hj), 2.49-2.41 (m, 1H, Hi), 2.18-2.02 (m, 2H, Hb or Hh or Hk or Hj), 1.42 (s, 9H, Hn), 1.16 (d, 3H, *J*= 6.8Hz, Ho).

MS (ESI): $[M+H]^+ = 335$.

$\mathbf{[\alpha]_D^{20}}$ = - 57 (c = 0.098 g/100 ml, Chloroform).

9) 1,1-Diisopropyl-7-(2-methoxy-1-phenyl-ethyl)-5-methyl-hexahydro-oxazolo[3,4-a]pyrazin-3-one (11)

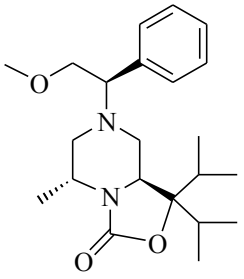

$C_{22}H_{34}N_2O_3$
Mol. Wt.: 374,52

To a stirred solution of **10** (80 mg, 0.239 mmol) in anhydrous THF (5 mL), TMEDA (180 µl, 1.195 mmol) was added. The reaction was cooled at -78°C and *sec*-BuLi 1.4M in exane (513 µl, 0.718 mmol) was added. The reaction was heated at -35°C and after 2 h a solution of diisopropyl ketone (102 µl, 0.718 mmol) in anhydrous THF (7 mL) was added drop wise. The reaction became green and was stirred at room temperature for 24 h. After this time the reaction was monitorated by TLC (EtOAc/light petroleum 1:4) and quenched by adding NH_4Cl satured solution (5 mL). The solvent was removed in vacuo and the aqueous phase extracted 3 times with EtOAc (10 mL). The combined organic layer was dried and evaporated to dryness. The crude product was purified by flash chromatography using EtOAc/light petroleum 1:4 as eluent to obtain **11** in 48% yield.

MS (ESI): $[M+H]^+ = 375$.

Synthesis of SHA-68 compound in racemic mixture

10) 4-Benzyl-piperazine-1-carboxylic acid tert-butyl ester (13)

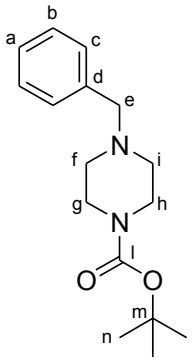

$C_{16}H_{24}N_2O_2$
Mol. Wt.: 276,37

A solution of *N*-benzyl-piperazine (1.96ml, 11.35 mmol) in a mixture of water and *tert*-butanol 1:2 (90 ml), cooled at 0°C, was treated with di-*tert*-butyl-dicarbonate (2.72 g, 12.48 mmol) in presence of NaOH 1N. The reaction mixture was stirred at room temperature and it was monitorated by TLC (EtOAc/light petroleum 1:1); after an hour the reaction was termined. The solvent was removed under vacuum and the crude material dissolved in EtOAc; the organic layer was washed twice with citric acid, dried and concentrated to obtain the product **13** in quantitative yield. The compound **13** was used in the next step without further purification.

^{1}H NMR ($CDCl_3$, 400 MHz): δ = 7.30-7.27 (m, 5H, Ha,b,c), 3.50 (s, 2H, He), 3.42 (t, 4H, *J*= 5.2, Hg and Hh), 2.34 (t, 4H, *J*= 5.2, Hf and Hi), 1.44 (s, 9H, Hn).

^{13}C NMR ($CDCl_3$, 100MHz): δ = 154.84 (Cl), 137.88 (Cd), 129.21 (Cb or Cc), 128.32 (Ca), 127.21 (Cc or Cb), 79.59 (Cm), 63.11 (Cf, Ci), 52.91 (Cg, Ch), 42.41 (Ce), 28.48 (Cn).

MS (ESI): $[M+H]^+ = 277$

11) 7-Benzyl-1,1-diphenyl-hexahydro-oxazolo[3,4-*a*]pyrazin-3-one (14)

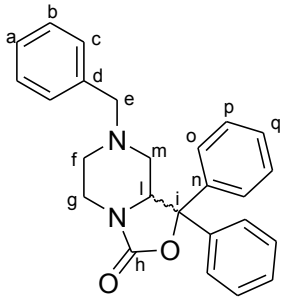

$C_{25}H_{24}N_2O_2$
Mol. Wt.: 384,47

To a stirred solution of **13** (2 g, 7.24 mmol) in anhydrous THF (10 mL), TMEDA (2.94 ml; 19.54 mmol) was added. The reaction was cooled at -78°C and *sec*-BuLi 1.4M in exane (14 ml, 19.54 mmol) was added. The reaction was heated at -35°C and after 2 h a solution of benzophenone (2.60 g; 14.28 mmol) in anhydrous THF (10 mL) was added drop wise. The reaction became green and was stirred at room temperature for 24 h. After this time the reaction was monitorated by TLC (EtOAc/light petroleum 1:2) and quenched by adding NH_4Cl satured solution (5 mL). The solvent was removed in vacuo and the aqueous phase extracted 3 times with EtOAc (15 mL). The combined organic layer was dried and evaporated to dryness. The crude product was purified by flash chromatography using EtOAc/light petroleum 1:2 as eluent to obtain 1.34 g of **14** in 49% yield.

^{1}H NMR ($CDCl_3$, 400 MHz): δ = 7.52-7.21 (m, 15Ha,b,c,o,p,q), 4.55 (ddd, 1H, *J*= 10.6, 3.6Hz, Hl), 3.80 (dd, 1H, *J*= 13.6, 3.4, 1.2Hz, Hg), 3.50 (d, 1H, *J*= 13.2Hz, part of AB system, He), 3.30 (d, 1H, *J*= 13.2Hz, part of AB system, He'), 3.10 (dt, 1H, *J*=12.6, 3.6 Hz, Hg'), 2.69 (td, 1H, *J*=11.2, 3.6, 1.6Hz, Hf), 2.57 (dd, 1H, *J*=11.2, 3.6, 1.6Hz, Hm), 1.95 (dt, 1H, *J*=12, 3.6 Hz, Hf'), 1.60 (t, 1H, *J*=12Hz, Hm').

^{13}C NMR ($CDCl_3$, 100MHz): δ = 156.13 (Ch), 142.35 (Cn), 138.77 (Cn'), 137.34 (Cd), 128.99 (Carom), 128.62 (Carom), 128.51 (Carom), 128.43 (Carom), 128.33 (Carom), 127.94 (Carom), 127.44 (Carom), 126.05 (Carom), 125.86 (Carom) 85.36 (Ci), 63.03 (Ce), 61.27 (Cl), 55.57 (Cm), 50.67 (Cf), 41.59 (Cg).

MS (ESI): $[M+H]^+ = 384.7$

12) 3-Oxo-1,1-diphenyl-tetrahydro-oxazolo[3,4-a]pyrazine-7-carboxylic acid 9H-fluoren-9-ylmethyl ester (15)

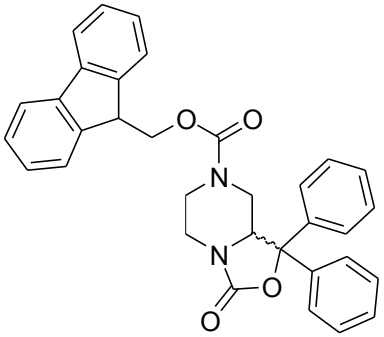

$C_{33}H_{28}N_2O_4$
Mol. Wt.: 516,59

To a solution of **14** (1.34 g; 3.48 mmol) in acetonitrile (20ml) was added FmocCl (991 mg; 3.84 mmol) in one portion, and the mixture was brought to reflux at 90°C. After approximately 10 min, a white precipitate formed in the reaction flask. The suspension was allowed to stir at reflux for an additional 5 h, after which the mixture was cooled and vacuum filtered. The precipitate was washed with an additional portion of cold acetonitrile (20 ml). The crude white solid **15** (1.08 g, 65%) was then used without further purification.

MS (ESI): $[M+H]^+ = 517.1$

13) 3-Oxo-1,1-diphenyl-tetrahydro-oxazolo[3,4-*a*]pyrazine-7-carboxylic acid 4-fluoro-benzylamide (*R/S* -SHA-68)

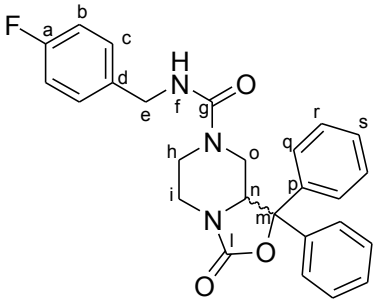

$C_{26}H_{24}FN_3O_3$
Mol. Wt.: 445,49

To a mixture of **14** (1.18 g; 2.28 mmol) and 4-fluorobenzyl isocyanate (581 µl; 4.56 mmol) in THF (20 ml) was added 1,8- diazabicyclo[5.4.0]undec-7-ene (375 µl; 2.51 mmol) drop-wise. The reaction was stirred for 15 min at room temperature, quenched by addition of saturated aqueous NH_4Cl (10 ml), extracted with ethyl acetate (40 ml), dried (Na_2SO_4), filtered, and concentrated. The product was purified by crystallization with ethyl ether to obtain in a solid form **(*R/S*)-SHA 68** in 59% yield.

m.p. = 85-86°C

^{1}H NMR ($CDCl_3$, 400 MHz): δ = 7.51-6.98 (m, 14H, Hb,c,q,r,s), 4.80 (bs, 1H, Hf), 4.41 (dd, 1H, *J*= 11.2, 3.6Hz, Hn), 4.43-4.30 (m, 2H, He), 4.02 (ddd, 1H, *J*= 13.2, 3.6, 1.2Hz, Ho'), 3.83 (dd, 1H, *J*= 13.2, 2.4Hz, Hi), 3.63 (td, *J*=13.2, 3.6, 2.0Hz, Hh'), 3.07 (dt, 1H, *J*=12.4, 3.6Hz, Hi), 2.91 (dt, 1H, *J*=12.4, 3.6Hz, Hh), 2.15 (dd, 1H, *J*=13.6, 11.2Hz, Ho).

^{13}C NMR ($CDCl_3$, 100MHz): δ = 163.47 (Ca), 161.02 (Cd), 157.08 (Cg), 156.06 (Cl), 141.81 (Cp or Cp), 138.29 (Cp or Cp'), 129.52 (Cb), 128.79 (Cq or Cq'), 128.70 (Cq or Cq'), 128.33 (Cc or Cc'), 125.96 (Cr or Cr'), 125.83 (Cr or Cr'), 115.74 (Cs or Cs'), 115.52 (Cs or Cs'), 85.81 (Cm), 60.51 (Cn), 46.54 (Co), 44.50 (Ce), 43.78 (Ch), 41.34 (Ci).

^{19}F-NMR ($CDCl_3$): δ = -114.699

MS (ESI): $[M+H]^+$ = 446

Asymmetric Synthesis of (*R*)-SHA 68 and (*S*)-SHA 68

14) [(1-Phenyl-ethylcarbamoyl)-methyl]-carbamic acid *tert*-butyl ester (16).

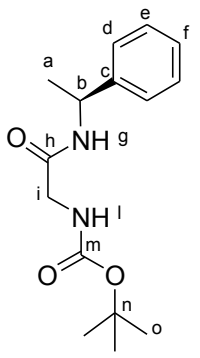

$C_{15}H_{22}N_2O_3$
Mol. Wt.: 278,35

To a stirred solution of Boc-Gly-OH (5 g, 28.5 mmol) in CH_2Cl_2 (50 mL), WSC (3.64 g, 19 mmol) and (S)-phenylethyl amine (3.45 g, 28.5 mmol) were added. After 24 h at room temperature the reaction was monitored by TLC (EtOAc/light petroleum 2:1). The organic layer was washed with 10% citric acid (20 mL), 5% $NaHCO_3$ (20 mL) and brine (20 mL). The organic phase was dried, concentrated in vacuo and purified by flash chromatography (EtOAc/light petroleum 2:1) to obtain **16** in 60% yield.

^{1}H NMR ($CDCl_3$, 400 MHz): δ = 7.31-7.24 (m, 5H, Hd,e,f); 6.62 (bs, 1H, Hg); 5.31 (bs, 1H, Hl); 5.11 (q, *J*= 6.8 Hz, 1H, Hb); 3.75 (m, 2H, Hi); 1.47 (d, *J*= 6.8 Hz, 3H, Ha); 1.42 (s, 9H, Ho).

^{13}C NMR ($CDCl_3$, 100MHz): δ = 168.6 (Ch), 156.2 (Cm), 143.0 (Cc), 128.7 (Cd or Ce), 127.4 (Cf), 126.1 (Cd or Ce), 80.2 (Cn), 48.7 (Cb), 44.6 (Cl), 28.3 (Co), 21.9 (Ca).

MS (ESI): $[M+H]^+$ =279.

$[\alpha]_D^{20}$ = -41 (c = 0.121g/100 ml, chloroform).

15) [2-(1-Phenyl-ethylamino)-ethyl]-carbamic acid *tert*-butyl ester (17).

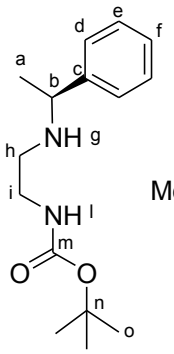

$C_{15}H_{24}N_2O_2$
Mol. Wt.: 264,36

To a stirred suspension of $LiAlH_4$ (0.85g, 22.38mmol) at 0°C in anhydrous THF, a solution of **16** (3.11 g, 11.19 mmol) was added drop wise. The reaction was monitored by TLC (EtOAc/light petroleum 3:1) and after 24 hours the excess of hydride was quenched with water and the salts were filtered trough a celite pad. The solvent was evaporated in vacuo to yield **17** (2.66 g, 10.07 mmol) in 90% yield.

^{1}H NMR ($CDCl_3$, 400 MHz): δ = 7.32-7.27 (m, 5H, Hd,e,f); 4.96 (bs, 1H, Hl); 3.75 (q, *J*=6.6 Hz, 1H, Hb); 3.16-3.13 (m, 2H, Hi); 2.59-2.51 (m, 2H, Hh); 1.75 (bs, 1H, Hg); 1.42 (s, 9H, Ho); 1.35 (d, *J*=6.6 Hz, 3H, Ha).

MS (ESI): $[M+H]^+ = 265$.

$[\alpha]_D^{20}$ = -29° (c = 0.11 g/100 mL, chloroform).

16) {2-[(2-Chloro-acetyl)-(1-phenyl-ethyl)-amino]-ethyl}-carbamic acid *tert*-butyl ester (18).

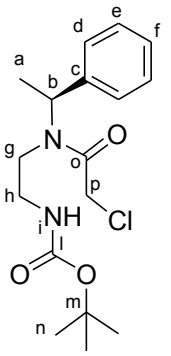

$C_{17}H_{25}ClN_2O_3$
Mol. Wt.: 340,84

To a stirred solution of **17** (1.94 g, 7.34 mmol) in EtOAc (50 mL) at 0°C, of satured solution of $NaHCO_3$ (5 mL) was added. After 10 min, chloroacetyl chloride (1.17 mL, 14.68 mmol) was added drop wise. The reaction was monitored by TLC (EtOAc/light petroleum 3:1) and after 24 h at room temperature, $NaHCO_3$ (2 mL) was added to the organic phase. The organic layer was separated and the aqueous phase was extracted twice with EtOAc (50 mL). The combined organic phases were concentrate to dryness to obtain **18** in quantitative yield.

^{1}H NMR ($CDCl_3$, 400 MHz): δ = 7.22-6.98 (m, 5H, $H_{d,e,f}$); 5.59-5.43 (q, *J*=8 Hz, 1H, H_b); 4.85 (bs, 1H, H_i); 4.10-3.97 (m, 2H, H_h); 3.76 (s, 2H, H_p); 3.18-3.15 (m, 2H, H_g); 1.40-1.25 (d, *J*=8 Hz, 3H, H_a); 1.06 (s, 9H, H_n).

^{13}C NMR ($CDCl_3$, 100MHz): δ = 170.12 (Co), 155.85 (Cl), 139.47 (Cc), 128.45 (Cd o Ce), 128.20 (Cd o Ce), 128.03 (Cf), 80.69 (Cm), 59.44 (Cp), 42.86 (Cb), 41.14 (Cg or Ch), 38.24 (Cg or Ch), 27.48 (Cn), 19.98 (Ca).

MS (ESI): $[M+H]^+$ = 341.

17) 3-Oxo-4-(1-phenyl-ethyl)-piperazine-1-carboxylic acid *tert*-butyl ester (19).

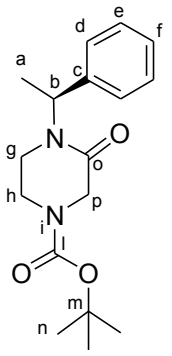

$C_{17}H_{24}N_2O_3$
Mol. Wt.: 304,38

To a stirred suspension of 60% NaH (1.14 g, 28.61 mmol) in a mixture of THF/DMF 1/1 (20 mL) at 0°C, a solution of **18** (3.25 g, 9.54 mmol) in THF/DMF 1/1 (10 mL) was added. After 24 h the reaction was quenched by adding NH_4Cl satured solution (15 mL) and the solvent was removed in vacuo. The residue was dissolved in EtOAc (50 mL) and washed twice with water (20 mL). The organic layer was dried, evaporated under reduced pressure and the crude product purified by flash chromatography (eluent: EtOAc/light petroleum 1:1) to obtain **19** in 45% yield.

^{1}H NMR ($CDCl_3$, 400 MHz): δ = 7.36-7.28 (m, 5H, Hd,e,f), 6.08 (q, 1H, *J*= 8Hz, Hb); 4.20 (d, 1H, *J*= 20Hz, part of AB system, Hp), 4.10 (d, 1H, *J*= 20Hz, part of AB system, Hp'), 3.62 (bs, 1H, Cg), 3.27 (bs, 1H, Cg'), 3.19 (bs, 1H, Ch); 2.83 (bs, 1H, Ch'), 1.52 (d, *J*= 8Hz, 3H, Ca), 1.45 (s, 9H, Cn).

^{13}C NMR ($CDCl_3$, 100MHz): δ = 165.44 (Co), 153.78 (Cl), 139.41 (Cc), 128.63 (Cd), 127.68 (Ce), 127.36 (Cf), 80.69 (Cm), 50.08 (Cb), 47.98 (Cg), 40.24 (Ch), 28.32 (Cn), 15.34 (Ca).

MS (ESI): $[M+H]^+$ = 305.

$[\alpha]_D^{20}$ = -116.0 ° (c = 0.318 g/100 mL, chloroform).

18) 1- (1-Phenyl-ethyl)-piperazin-2-one (19b).

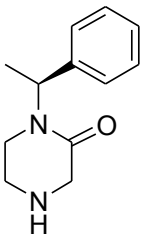

$C_{12}H_{16}N_2O$
Mol. Wt.: 204,27

1.31g of compound (**19**) (4.30 mmol) was solubilized in CH_2Cl_2 and 3.30 ml of TFA (43.04 mmol) was added at 0°C, the reaction was completed in 1 hour. $NaHCO_3$ satured was added and the acqouos phase was extractet several time with EtOAc and the organic phases were combined, dried and evaporated under vacuum to give compound (**19b**) in 97% yield.

MS (ESI): $[M+H]^+ = 205$

19) 1-(1-Phenyl-ethyl)-piperazine (19c).

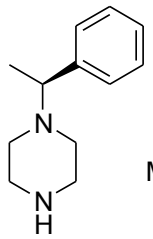

$C_{12}H_{18}N_2$
Mol. Wt.: 190,28

To a stirred suspension of $LiAlH_4$ (331 mg, 8.73 mmol) at 0°C in anhydrous THF, a solution of **19b** (890 mg, 4.36 mmol) was added drop wise. The reaction was monitored by TLC (EtOAc/light petroleum 1:1) and after 24 hours the excess of hydride was quenched with water and the salts were filtered trough a celite pad. The solvent was evaporated in vacuo to yield **19c** in 87% yield.

MS (ESI): $[M+H]^+ = 191$

20) 4- (1-Phenyl- ethyl)-piperazine-carboxylic acid *tert*-butyl ester (20).

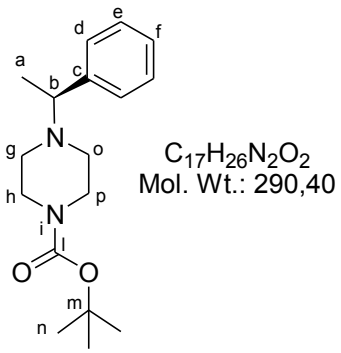

A solution of **19c** (520 mg; 2.73 mmol) in a mixture of water and *tert*-butanol 1:2 (60 ml), cooled at 0°C, was treated with di-*tert*-butyl-dicarbonate (650 mg, 3 mmol) in presence of NaOH 2N. The reaction mixture was stirred at room temperature for 12 hours and monitorated by TLC (EtOAc/light petroleum 1:1); after an hour the reaction was termined. The solvent was removed under vacuum and the crude material dissolved in EtOAc; the organic layer was washed twice with citric acid, dried and concentrated in vacuo.

The product **20** was obtained by flash cromatography (EtOAc/ light petroleum 1:2) in quantitative yield.

^{1}H NMR ($CDCl_3$, 400 MHz): δ = 7.31-7.25 (m, 5H, Hd,e,f), 3.41-3.35 (m, 5H, Hb,g,o), 2.39-2.34 (m, 4H, Hh,p), 1.43 (s, 9H, Hn), 1.35 (d, 3H, *J*= 7, Ha).

MS (ESI): $[M+H]^+$ =291

$[\alpha]_D^{20}$ = + 42.4° (C = 0.0125g/100 ml, cloroformio).

21) 1,1-Diphenyl-7-(1-phenyl-ethyl)-hexahydro-oxazolo[3,4-*a*] pyrazin-3-one (21a and 21b).

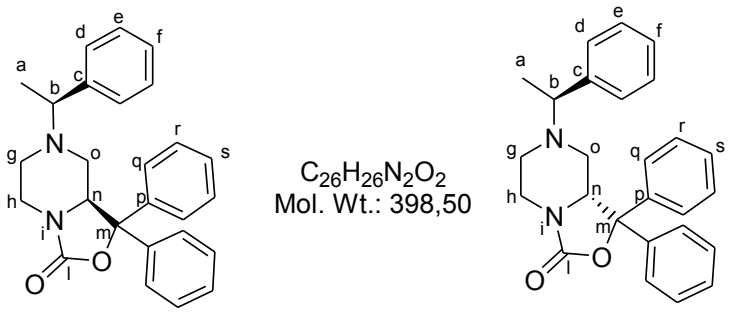

To a stirred solution of **20** (380 mg, 1.31 mmol) in anhydrous THF (5 mL), TMEDA (0.53 mL, 3.54 mmol) was added. The reaction was cooled at -78°C and *sec*-BuLi 1.4M in exane (2.53 mL, 3.54 mmol) was added. The reaction was heated at -35°C and after 2 h a solution of benzophenone (480 mg, 2.62 mmol) in anhydrous THF (7 mL) of was added drop wise. The reaction became green and was stirred at room temperature for 24 h. After this time the reaction was monitorated by TLC (EtOAc/light petroleum 1:2) and quenched by adding NH_4Cl satured solution (20 mL). The solvent was removed in vacuo and the aqueous phase extracted 3 times with EtOAc (30 mL). The combined organic layer was dried and evaporated to dryness. The crude diastereomers mixture was purified by flash chromatography using EtOAc/light petroleum 1:2 as eluent to obtain the fast running diastereomer **21a** in 40% yield and the low running distereomer **21b** in 45% yield.

<u>Compound 21a:</u>

^{1}H NMR ($CDCl_3$, 400 MHz): δ = 7.50 - 7.14 (m, 15H, Hd,e,f,,q,r,s), 4.44 (dd, 1H, *J* = 10.9, 3.6 Hz, Hn), 3.82 (ddd, 1H, *J* = 12.8, 3.5, 1.6 Hz, Hh'), 3.48 (q, 1H, *J* = 6.8 Hz,Hb), 3.11 (ddd, 1H, *J* = 13.0, 12.0, 3.81 Hz, Hh), 2.76 (td, 1H, *J* = 12, 3.6 Hz, Hg), 2.44 (ddd, 1H, *J* = 11.5, 3.5, 1.6 Hz, Ho'), 2.02 (td, 1H, *J* = 11.7, 3.6 Hz, Hg'), 1.50 (t, 1H, *J*= 11.2Hz, Ho), 1.27 (d, 3H, *J* = 6.8 Hz, Ha).

^{13}C NMR ($CDCl_3$, 100MHz): δ = 156.20 (Cl), 142.48 (Cp or Cp'), 142.28 (Cp or Cp'), 138.81 (Cc), 128.65 (C arom.), 128.51 (C arom.), 128.32 (C arom.), 127.98 (C arom.),

127.59 (C arom.), 127.28 (C arom.), 126.11 (C arom.), 125.92 (C arom.), 125.84 (C arom.), 85.39 (Cm), 63.86 (Cb), 61.67 (Cn), 53.24 (Co), 47.58 (Cg), 42.11 (Ch), 17.16 (Ca).

MS ESI [$M+H^+$]= 399.

$[\alpha]_D^{20}$= -132°(c = 0.11 g/100 mL, chloroform).

Compound 21b:

^{1}H NMR ($CDCl_3$, 400 MHz): δ = 7.55 - 7.14 (m, 15H, Hd,e,f,,q,r,s), 4.51 (dd, 1H, *J* = 10.9, 3.6 Hz, Hn), 3.74 (ddd, 1H, *J* = 12.8, 3.5, 1.6 Hz, Hh'), 3.34 (q, 1H, *J* = 6.8 Hz, Hb), 3.04 (ddd, 1H, *J* = 13.0, 12.1, 3.6 Hz, Hh), 2.70 - 2.61 (m, 2H, Ho',g'), 1.86 (td, 1H, *J* = 12, 3.6 Hz, Hg), 1.46 (t, 1H, *J*= 11.2Hz, Ho), 1.22 (d, 3H, *J* = 7.2 Hz, Ha).

^{13}C NMR ($CDCl_3$, 100MHz): δ = 156.17 (Cl), 142.85 (Cp or Cp'), 142.52 (Cp or Cp'), 138.91 (Cc), 128.69 (C arom.), 128.58 (C arom.), 128.50 (C arom.), 128.35 (C arom.), 128.01 (C arom.), 127.51 (C arom.), 127.37 (C arom.), 126.19 (C arom.), 125.95 (C arom.), 85.50 (Cm), 64.52 (Cb), 61.56 (Cn), 52.66 (Co), 49.30 (Cg), 42.07 (Ch), 19.34 (Ca).

MS ESI [$M+H^+$]= 399.

$[\alpha]_D^{20}$= +216 (c = 0.108 g/100 mL, chloroform).

22) 3-Oxo-1,1-diphenyl-tetrahydro-oxazolo[3,4-*a*]pyrazine-7-carboxylic acid 9*H*-fluoren-9-ylmethyl ester (22a and 22b).

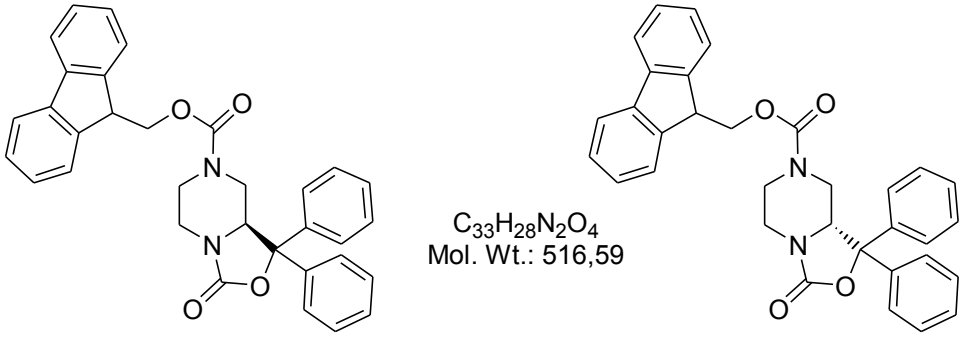

To a stirred solution of **21a** or **21b** (200 mg, 0.52 mmol) in acetonitrile (10 mL) at reflux, Fmoc-Cl (148 mg, 0.57 mmol) dissolved in acetonitrile (7 mL) was added. The reaction, monitored by TLC (EtOAc/light petroleum 1:2), was completed in 12 h. The desired precipitate was filtered off to obtain **22a** or **22b** in about 67% yield and pure enough to be used in the next reaction.

23) 3-Oxo-1,1-diphenyl-tetrahydro-oxazolo[3,4-*a*]pyrazine-7-carboxylic acid 4-fluoro-benzylamide ((*S*)-SHA 68 and (*R*)-SHA 68).

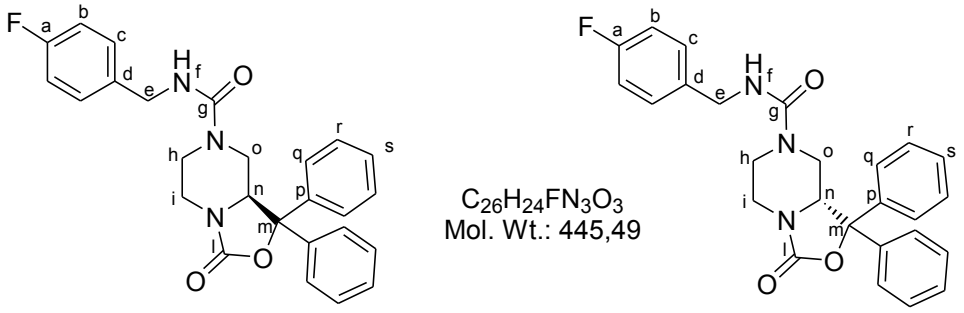

To a stirred solution of **22a** or **22b** (55 mg, 0.11 mmol) in anhydrous THF (15 mL) *p*-fluoro-benzylisocianate (34.4 mg, 0.228 mmol) and DBU (19.2 mg, 0.126 mmol) were added. The reaction was monitored by TLC (EtOAc/light petroleum 1:2) and by mass spectrometry. After 24 h the reaction was treated and the organic phase was dried and

evaporate to dryness to give **(*S*)-SHA 68** and **(*R*)-SHA 68** in 83% and 76% yield respectively, after column chromatography using EtOAc/light petroleum 1/1 as eluent.

^{1}H NMR ($CDCl_3$, 400 MHz): δ = 7.51-6.98 (m, 14H, Hb,c,q,r,s), 4.95 (bs, 1H, Hf), 4.43 (dd, 1H, *J*= 11.2, 3.6Hz, Hn), 4.43-4.30 (m, 2H, He), 4.03 (ddd, 1H, *J*= 13.5, 3.5, 1.2Hz, Ho'), 3.81 (dd, 1H, *J*= 13.1, 2.7 Hz, Hi), 3.69 (td, *J*=13.2, 3.6, 2.0Hz, Hh'), 3.05 (dt, 1H, *J*=12.7, 3.7Hz, Hi), 2.91 (dt, 1H, *J*=12.4, 3.6Hz, Hh), 2.14 (dd, 1H, *J*=13.3, 11.2Hz, Ho).

^{13}C NMR ($CDCl_3$, 100MHz): δ =163.47 (Ca), 161.02 (Cd), 157.20 (Cg), 156.11 (Cl), 141.81 (Cp or Cp), 138.30 (Cp or Cp'), 129.48 (Cb), 128.82 (Cq or Cq'), 128.72 (Cq or Cq'), 128.37 (Cc or Cc'), 125.99 (Cr or Cr'), 125.83 (Cr or Cr'), 115.70 (Cs or Cs'), 115.48 (Cs or Cs'), 85.90 (Cm), 60.55 (Cn), 46.58 (Co), 44.47 (Ce), 43.76 (Ch), 41.37 (Ci).

MS ESI [$M+H^+$]= 445.9.

(*S*)-SHA 68 :

$[\alpha]_D^{20}$= -91 (c= 0.12 g/100 mL, MeOH).

(*R*)-SHA 68

$[\alpha]_D^{20}$= +92 (c= 0.1 g/100 mL, MeOH).

Synthesis of (-)-Steganacin aza analogue

24) 2-[(1,1-Dimethylprop-2-yn-1-yl)oxy]tetrahydro-2*H*-pyran (30)

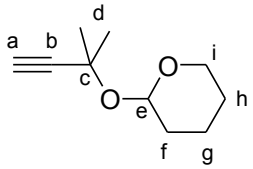

$C_{10}H_{16}O_2$
Mol. Wt.: 168,23

3,4-Dihydro-2*H*-pyran (30.1 mL, 330 mmol, 1.1 equiv.) was added dropwise to a solution of 3-methylbut-1-yn-3-ol **29** (29 mL, 300 mmol, 1 equiv.) and *p*-toluenesulfonic acid (571 mg, 3 mmol, 1 mol%) in dichloromethane (300 mL), cooled to 0°C. The resulting mixture was stirred at 0°C for 5h and solid potassium carbonate K_2CO_3 was then introduced. Dichloromethane was evaporated under reduced pressure and the residue was distilled over silicon oil to afford the expected protected alcohol **30** in 71% yield (35.8 g) as a colorless oil.

b.p.: 70°C (23 mmHg)

^{1}H NMR ($CDCl_3$, 400 MHz): δ = 5.08-5.06 (m, 1H, He), 3.98-3.93 (m, 1H, Hi'), 3.54-3.48 (m, 1H, Hi), 2.43 (s, 1H, Ha), 1.87-1.51 (m, 12H, Hd, f, g, h).

^{13}C NMR ($CDCl_3$, 100 MHz): δ = 96.2 (Ce), 86.5 (Cb), 72.0 (Ca), 71.0 (Cc), 63.4 (Ci), 32.0 (Cf), 30.7 (Cd'), 29.9 (Cd), 25.5 (Cg or Ch), 20.5 (Cg or Ch).

IR (neat): 3293, 2985, 2940, 2869, 2108 cm^{-1}

HRMS (ESI+) *m/z* calcd for $C_{10}H_{16}O_2Na_1$ ($M+Na^+$) 191.10425. Found: 191.10426.

Commercially available product.

25) 4-Methyl-4-(tetrahydro-2*H*-pyran-2-yloxy)pent-2-yn-1-ol (31)

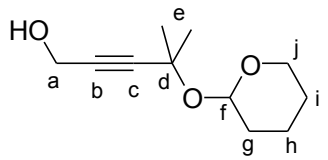

$C_{11}H_{18}O_3$
Mol. Wt.: 198,26

n-Butyllithium (41 mL, 97 mmol, 1.1 equiv., 2.38 M solution in hexanes) was added dropwise to a solution of protected propargyl alcohol **30** (14.8 g, 88 mmol, 1 equiv.) in freshly distilled diethyl ether (140 mL), cooled to -78°C. The temperature of the solution was carefully maintained below -50°C during the addition. The reaction mixture was stirred at -78°C during 45 min and paraformaldehyde (7.95 g, 264 mmol, 3 equiv.) was then added. The reaction was vigorously stirred and allowed to slowly reach room temperature overnight. The reaction medium was smoothly quenched with a mixture of ice and water, and the aqueous layer was extracted with diethyl ether. The combined organic layers were washed with brine, dried on $MgSO_4$ and concentrated in vacuo. The crude product was purified by flash chromatography on silica gel eluting with a gradient of pentane/Et_2O 85:15 to 70:30. The expected alcohol **31** was obtained in 94% yield (10.5 g) as a yellow oil.

^{1}H NMR ($CDCl_3$, 400 MHz): δ = 5.06-5.04 (m, 1H, Hf), 4.25 (d, *J* = 6.0 Hz, 2H, Ha), 3.95-3.91 (m, 1H, Hj'), 3.52-3.46 (m, 1H, Hj), 3.26 (t, *J* = 6.0 Hz, 1H, HOH), 1.85-1.45 (m, 12H, He, g, h, i).

^{13}C NMR ($CDCl_3$, 100 MHz): δ = 95.7 (Cf), 87.5 (Cc), 82.7 (Cb or Cd), 71.0 (Cb or Cd), 63.0 (Cj), 50.7 (Ca), 31.9 (Cg), 30.5 (Ce'), 30.0 (Ce), 25.4 (Ch or Ci), 20.1 (Ch or Ci).

IR (neat): 3414, 2938, 2866, 1440, 1361 cm^{-1}

HRMS (ESI+) *m/z* calcd for $C_{11}H_{18}O_3Na_1$ ($M+Na^+$) 221.11482. Found: 221.11437.

26) 4-Methylpenta-2,3-dien-1-ol (28)

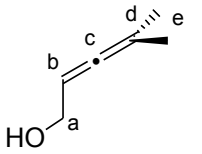

$C_6H_{10}O$
Mol. Wt.: 98,14

Propargyl alcohol **31** (6.6 g, 33 mmol, 1 equiv.) diluted in freshly distilled diethyl ether (60 mL) was added dropwise to a suspension of powdered lithium and aluminium hydride $LiAlH_4$ (3.81 g, 100 mmol, 3 equiv.) in distilled diethyl ether (100 mL), cooled to 0°C. The resulting reaction mixture was allowed to reach room temperature over 5h (the completion of the reaction was monitored by ^1H NMR). The excess lithium and aluminium hydride was hydrolyzed at 0°C by adding successively water (3.2 mL), an aqueous NaOH solution (3.2 mL, 15% w/w) and water (7 mL) again. The biphasic mixture was then stirred vigorously during 1h. The resulting white suspension was filtered on celite and washed several times with diethyl ether. The combined organic layers were dried on $MgSO_4$ and concentrated in vacuo. The crude product was purified by flash chromatography on silica gel eluting with pentane/Et_2O 80:20 to afford the expected allenol **28** in 66% yield (2.17 g) as a pale yellow oil.

^{1}H NMR ($CDCl_3$, 400 MHz): δ = 5.20 (tsept, *J*= 3.0, 5.5 Hz, 1H, Hb), 4.08 (d, *J*= 5.5 Hz, 2H, Ha), 1.73 (d, *J*= 3.0 Hz, 6H, He), 1.45 (br s, 1H, HOH).

^{13}C NMR ($CDCl_3$, 50 MHz): δ = 200.7 (Cc), 98.7 (Cd), 90.1 (Cb), 61.1 (Ca), 20.7 (Ce).

IR (neat): 3307, 2981, 2909, 2856, 1968 cm^{-1}

HRMS (ESI+) *m*/*z* calcd for $C_6H_{11}O_1$ ($M+H^+$) 99.08044. Found: 99.08017.

Data in agreement with: Richey, H. G. Jr.; Moses, L. M. *J. Org. Chem.* 1983, *48*, 4013-4017. Commercially available product.

27) Phenyl-acetic acid 4-methyl-penta-2,3-dienyl ester (32)

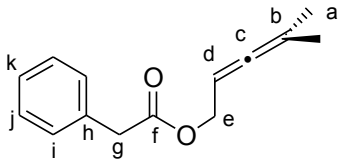

$C_{14}H_{16}O_2$
Mol. Wt.: 216,28

Triethylamine (9.22 mL, 66 mmol, 3 equiv.) were successively added to a solution of allenyl alcohol **31** (2.17 g, 22 mmol, 1 equiv.) in dichloromethane (110 mL). Phenacyl chloride (8.7 mL, 66 mmol, 3 equiv.) was then introduced dropwise at 0°C and the resulting mixture was stirred for 2.5h at room temperature. The reaction was quenched with a saturated solution of NH_4Cl and the aqueous layer was extracted with dichloromethane. The combined organic layers were washed with a saturated solution of $NaHCO_3$, dried on $MgSO_4$ and carefully concentrated in vacuo. The crude product was purified by flash chromatography on silica gel eluting with cyclohexane/AcOEt 95:5 to afford the expected allenol **32** in 84% yield (4 g) as a pale yellow oil.

^{1}H NMR ($CDCl_3$, 400 MHz): δ = 7.32-7.28 (m, 5H, Hi,j,k), 5.08 (m, 1H, Hd), 4.53 (d, 2H, *J*= 7.0 Hz, He), 3.64 (s, 2H, Hg), 1.68 (d, 6H, *J*= 3.0 Hz, Ha).

^{13}C NMR ($CDCl_3$, 100 MHz): δ = 203.64 (Cc), 171.6 (Cf), 134.4 (Ck), 129.8 (Cd), 129.0 (Cj or Ci), 127.4 (Cj or Ci), 97.7 (Cb), 85.1 (Cd), 63.9 (Ce), 41.7 (Cg), 20.5 (Ca).

IR (neat): 2984, 2940, 2912, 1972, 1739, 1218 cm^{-1}

HRMS (ESI+) *m/z* calcd for $C_{14}H_{16}O_2Na_1$ ($M+Na^+$) 239.2648. Found: 239.1043.

28) *N*-benzyl-2,2,2-trifluoroacetamide (33)

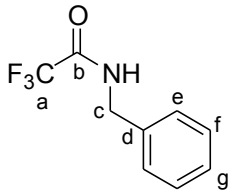

$C_9H_8F_3NO$
Mol. Wt.: 203,16

Trifluoroacetic anhydride (6.25 mL, 45 mmol, 1 equiv.) was added dropwise at 0°C to a solution of 4-*N*,*N*-dimethylaminopyridine (DMAP) (550 mg, 4.5 mmol, 10 mol%) and benzylamine (10.8 mL, 99 mmol, 2.2 equiv.) in dichloromethane (150 mL). The resulting mixture was stirred at room temperature overnight. The reaction was quenched with a saturated solution of NH_4Cl and the aqueous layer was extracted with dichloromethane. The combined organic layers were washed with a saturated solution of $NaHCO_3$, dried on $MgSO_4$ and concentrated in vacuo. The crude product was recrystalized in toluene to afford 7.51 g of the expected product **33** (82 %) as white crystals.

m.p.: 73°C

^{1}H NMR ($CDCl_3$, 400 MHz): δ = 7.53-7.23 (m, 5H, He, f, g), 6.51 (br s, 1H, HNH), 4.55 (d, 2H, *J*= 6.0 Hz, Hc).

^{13}C NMR ($CDCl_3$, 100 MHz): δ = 157.3 (Cb), 136.0 (Cd), 129.1 (Ce or Cf), 128.4 (Cg), 128.1 (Ce or Cf), 116.0 (Ca), 44.0 (Cc).

IR (neat): 3292, 3091, 3035, 1697, 1557, 1164 cm^{-1}

HRMS (ESI+) *m/z* calcd for $C_9H_8O_1N_1F_3Na_1$ ($M+Na^+$) 226.04502. Found: 226.04506.

Commercially available product.

29) *N*-benzyl-(4'-methylpenta-2',3'-dienyl)-trifluoroacetamide (34)

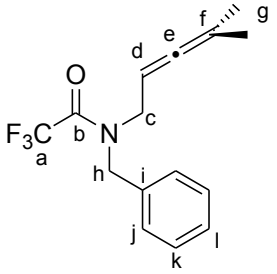

$C_{15}H_{16}F_3NO$
Mol. Wt.: 283,29

LiHMDS (9.02 ml, 9.02 mmol, 1.3 equiv., 1M in THF) was slowly added to a solution of *N*-benzyltrifluoroacetamide **33** (1.69 g, 8.33 mmol, 1.2 equiv.) in dry THF (18 mL) at 0°C. The resulting mixture was stirred at room temperature for 10 min. Allenyl ester **32** (1.5 g, 6.9 mmol, 1 equiv.) diluted in dry THF (8 mL) was added via cannula, followed by $Pd(PPh_3)_4$ (200 mg, 0.17 mmol, 2.5 mol%). The resulting yellow mixture was stirred at 55°C for 4h and the completion of the reaction was monitored by TLC. The reaction was quenched with a saturated solution of NH_4Cl and the aqueous layer was extracted with diethyl ether. The combined organic layers were dried on $MgSO_4$ and concentrated in vacuo. The crude material was purified by flash chromatography on silica gel eluting with a gradient of pentane/Et_2O 98:2 to 95:5 to afford 1.17 g of the expected product **34** (60%) as a colorless oil and as a 63:37 mixture of rotamers.

Major rotamer:

1H NMR (CDCl3, 400 MHz): δ = 7.41-7.22 (m, 5H, Hj,k,l), 4.94 (m, 1H, Hd), 4.67 (s, 2H, Hh), 3.86 (d, 2H, *J*= 6.0 Hz, Hc), 1.75 (d, 6H, *J*= 3.0 Hz, Hg).

^{13}C NMR ($CDCl_3$, 100 MHz): δ = 203.3 (Ce), 157.3 (Cb), 135.6 (Ci), 129.0 (Cj or Ck), 128.5 (Cj or Ck), 127.5 (Cl), 116.8 (Ca), 98.8 (Cf), 84.2 (Cd), 48.6 (Ch), 45.9 (Cc), 20.3 (Cg).

Minor rotamer:

1H NMR (CDCl3, 400 MHz): δ = 7.41-7.22 (m, 5H, Hj, k, l), 4.94 (m, 1H, Hd), 4.62 (s, 2H, Hh), 3.87 (d, 2H, *J*= 6.0 Hz, Hc), 1.71 (d, 6H, *J*= 3.0 Hz, Hg).

^{13}C NMR ($CDCl_3$, 100 MHz): δ = 202.6 (Ce), 157.0 (Cb), 135.0 (Ci), 129.0 (Cj or Ck), 128.3 (Cl), 128.1 (Cj or Ck), 116.8 (Ca), 98.6 (Cf), 83.0 (Cd), 49.9 (Ch), 44.8 (Cc), 20.4 (Cg).

Mixture of rotamers:

IR (neat): 2911, 1970, 1688, 1451, 1200, 1137 cm^{-1}

30) *N*-Benzyl-4-methylpenta-2,3-dien-1-amine (35)

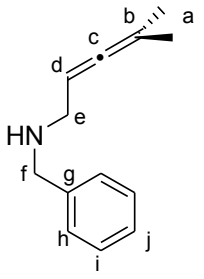

$C_{13}H_{17}N$
Mol. Wt.: 187,28

Allenyl trifluoroacetamide **34** (1.19 g, 4.19 mmol, 1 equiv.) was diluted in a mixture of methanol (28 mL) and water (3 mL) and potassium carbonate K_2CO_3 was added until saturation of the solution. The resulting mixture was heated at 50°C and the completion of the reaction was monitored by TLC. After 16h, water was added to the reaction mixture and methanol was removed in vacuo. The resulting aqueous phase was extracted with dichloromethane, and the combined organic layers were dried on $MgSO_4$ and concentrated in vacuo. The crude product was purified by flash chromatography on silica gel eluting with a gradient of cyclohexane/AcOEt 90:10 to pure AcOEt to afford the expected amine **35** in 85% yield (690 mg) as a pale yellow oil.

^{1}H NMR ($CDCl_3$, 400 MHz): δ = 7.34-7.25 (m, 5H, Hh, i, j), 5.08 (m, 1H, Hd), 3.83 (s, 2H, Hf), 3.23 (d, 2H, *J*= 6.0 Hz, He), 1.73 (d, 6H, *J*= 3.0 Hz, Ha), 1.64 (br s, 1H, HNH).

^{13}C NMR ($CDCl_3$, 100 MHz): δ = 201.9 (Cc), 140.4 (Cg), 128.5 (Ch or Ci), 128.4 (Ch or Ci), 127.0 (Cj), 96.5 (Cb), 87.9 (Cd), 53.0 (Cf), 48.2 (Ce), 20.8 (Ca).

IR (neat): 3315, 2978, 2907, 1967, 1603, 1451 cm^{-1}

HRMS (ESI+) *m/z* calcd for $C_{13}H_{18}N_1$ ($M+H^+$) 188.14338. Found: 188.14331.

Data in agreement with: Shibata, T.; Kadowaki, S.; Takagi, K. *Heterocycles* 2002, *57*, 2261-2266.

31) *N*-Benzyl-(4'-methylpenta-2',3'-dienyl)-3-methoxy-3-oxopropionamide (27)

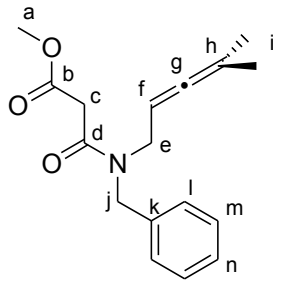

$C_{17}H_{21}NO_3$
Mol. Wt.: 287,35

Triethylamine (1.5 mL, 10.8 mmol, 3 equiv.) was added to a solution of allenylamine **35** (670 mg, 3.58 mmol, 1 equiv.) in distilled dichloromethane (36 mL). Methyl 3-chloro-3-oxopropionate (1.15 mL, 10.8 mmol, 3 equiv.) was introduced dropwise at 0°C and the reaction was stirred at room temperature for 16h. The reaction was quenched with a saturated solution of NH_4Cl and the aqueous layer was extracted with dichloromethane. The combined organic layers were washed with a saturated solution of $NaHCO_3$, dried on $MgSO_4$ and concentrated in vacuo. The crude product was purified by flash chromatography on silica gel (0.015-0.040 mm) eluting with pentane/Et_2O 75:25 to afford the expected product **27** in 76% yield (780 mg) as a pale yellow oil and as a 71:29 mixture of rotamers.

Major rotamer:

^{1}H NMR ($CDCl_3$, 400 MHz): δ = 7.39-7.19 (m, 5H, Hl, m, n), 4.90 (m, 1H, Hf), 4.61 (s, 2H, Hj), 3.78 (s, 3H, Ha), 3.74 (d, 2H, *J*= 5.0 Hz, He), 3.55 (s, 2H, Hc), 1.72 (d, 6H, *J*= 3.0 Hz, Hi).

^{13}C NMR ($CDCl_3$, 100 MHz): δ = 202.1 (Cg), 168.4 (Cb or Cd), 166.5 (Cb or Cd), 137.2 (Ck), 128.7 (Cm or Cl), 128.2 (Cm or Cl), 127.5 (Cn), 99.4 (Ch), 84.8 (Cf), 52.6 (Ca), 48.5 (Cj), 46.7 (Ce), 41.0 (Cc), 20.5 (Ci).

Minor rotamer:

^{1}H NMR ($CDCl_3$, 400 MHz): δ = 7.39-7.19 (m, 5H, Hl, m, n), 4.97 (m, 1H, Hf), 4.55 (s, 2H, Hj), 3.98 (d, 2H, *J*= 6.5 Hz, He), 3.72 (s, 3H, Ha), 3.46 (s, 2H, Hc), 1.67 (d, 6H, *J*= 3.0 Hz, Hi).

^{13}C NMR ($CDCl_3$, 100 MHz): δ = 203.2 (Cg), 168.1 (Cb or Cd), 166.3 (Cb or Cd), 136.3 (Ck), 129.1 (Cm or Cl), 127.8 (Cn), 126.5 (Cm or Cl), 97.1 (Ch), 84.3 (Cf), 52.6 (Ca), 50.7 (Cj), 45.5 (Ce), 41.4 (Cc), 20.6 (Ci).

Mixture of rotamers:

IR (neat): 2910, 1968, 1741, 1647, 1435 cm^{-1}

HRMS (ESI+) *m/z* calcd for $C_{17}H_{21}O_3N_1Na_1$ ($M+Na^+$) 310.14136. Found: 310.14166.

32) 5-iodo-1,3-benzodioxole (36)

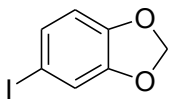

$C_7H_5IO_2$
Mol. Wt.: 248,02

Benzodioxole (1.7 mL, 15 mmol, 1 equiv.) was added to a solution of *N*-iodosuccinimide (3.54 g, 15.75 mmol, 1.05 equiv.) in distilled acetonitrile, in a flask

protected from light. Trifluoroacetic acid (1.16 mL, 15 mmol, 1 equiv.) was then added dropwise and the resulting mixture was stirred at 50°C for 72h (the completion of the reaction was monitored by ^{1}H NMR). The reaction was quenched with a saturated solution of $Na_2S_2O_3$ and the resulting precipitate was filtered off. The aqueous layer was extracted with diethyl ether and the combined organic layers were washed with a saturated solution of NaCl, dried on $MgSO_4$ and concentrated in vacuo. The crude product was purified by flash chromatography on silica gel (0.015-0.040 mm) eluting with pure pentane to afford 2.78 g of the expected product **36** (75%) as a pale yellow oil.

^{1}H NMR ($CDCl_3$, 400 MHz): δ = 7.14 (m, 2H, Hc,e), 6.61 (d, 1H, *J*= 8.0 Hz, Hf), 5.96 (s, 2H, Ha).

^{13}C NMR ($CDCl_3$, 100 MHz): δ = 148.9 (Cb or Cg), 148.8 (Cb or Cg), 130.7 (Ce), 117.8 (Cc), 110.6 (Cf), 101.5 (Ca), 82.3 (Cd).

IR (neat): 2889, 2775, 1498, 1469, 1225, 1030 cm^{-1}

Commercially available product.

33) (3,4-*trans*)-1-Benzyl-3-(methoxycarbonyl)-4-(1'-(1,3-benzodioxol-5-yl)-2'-methylprop-1'-en-1'-yl)-pyrrolidin-2-one (37)

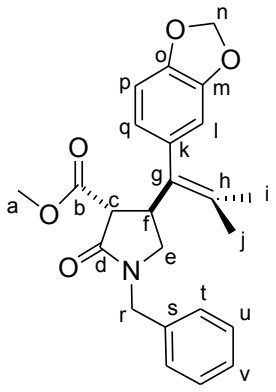

$C_{24}H_{25}NO_5$
Mol. Wt.: 407,46

Sodium hydride (16 mg, 0.4 mmol, 1.2 equiv., 60% dispersion in mineral oil) was added to a solution of allenyl amide **27** (94 mg, 0.33 mmol, 1 equiv.) in freshly distilled DMSO (3 mL) under argon atmosphere. The resulting mixture was stirred at room temperature for 20 min. In another flask, *n*-butyllithium (29 µL, 0.07 mmol, 20 mol%, 2.28 M solution in hexanes) was added dropwise to a solution of dichlorobis(acetonitrile) palladium $PdCl_2(MeCN)_2$ (8.6 mg, 0.03 mmol, 10 mol%) in freshly distilled DMSO (2 mL) under argon atmosphere. The resulting solution, initially yellow, became dark orange. The 5-iodo-1,3-benzodioxole (98 mg, 0.4 mmol, 1.2 equiv.) and tetrabutylammonium bromide (21.3 mg, 0.06 mmol, 20 mol%) were then successively added, and the solution containing the enolate of **27** was added via cannula. The resulting mixture was stirred at 55°C. The completion of the reaction was monitored by TLC and the reaction was quenched with a saturated solution of NH_4Cl. The aqueous layer was extracted with dichloromethane. The combined organic layers were washed with a saturated solution of NaCl, dried on $MgSO_4$ and concentrated in vacuo. The crude product was purified by flash chromatography on silica gel eluting with cyclohexane/AcOEt 75:25 to afford the expected product **37** (99 mg, 74% yield) as a yellow oil.

^{1}H NMR ($CDCl_3$, 400 MHz): δ = 7.33-7.27 (m, 3H, Hu, v), 7.16 (d, 2H, *J*= 7.0 Hz, Ht), 6.76 (d, 1H, *J*= 8.0 Hz, Hp), 6.37 (s, 1H, Hl), 6.32 (d, 1H, *J*= 8.0 Hz, Hq), 5.96 (s, 2H, Hn), 4.53 (d, 1H, *J*= 15.0 Hz, part of AB system, Hr'), 4.19 (d, 1H, *J*= 15.0 Hz, part of AB system, Hr), 4.10 (m, 1H, Hf), 3.82 (s, 3H, Ha), 3.42 (d, 1H, *J*= 10.0 Hz, Hc), 3.32 (t, 1H, *J*= 9.0 Hz, He'), 3.05 (t, 1H, *J*=9.0 Hz, He), 1.81 (s, 3H, Hi or Hj), 1.42 (s, 3H, Hi or Hj).

^{13}C NMR ($CDCl_3$, 100 MHz): δ = 170.2 (Cb), 169.1 (Cd), 147.6 (Co), 146.2 (Cm), 135.6 (Cs), 133.6 (Ch), 132.7 (Ck), 131.1 (Cg), 128.5 (Cu), 127.7 (Ct), 127.4 (Cv), 122.7 (Cq), 110.1 (Cl), 108.2 (Cp), 100.8 (Cn), 52.7 (Cc), 52.4 (Ca), 48.3 (Ce), 46.5 (Cr), 38.9 (Cf), 22.6 (Ci or Cj), 19.5 (Ci or Cj).

IR (neat): 2913, 1737, 1689, 1485, 1430, 1331, 1230 cm^{-1}

HRMS (ESI+) *m*/*z* calcd for $C_{24}H_{25}O_5N_1Na_1$ ($M+Na^+$) 430.16249. Found: 430.16220

34) 4-(1-Benzo[1,3]dioxol-5-yl-2-methyl-propenyl)-1-benzyl-2-oxo-3-(3,4,5-trimethoxy-benzyl)-pyrrolidine-3-carboxylic acid methyl ester (38)

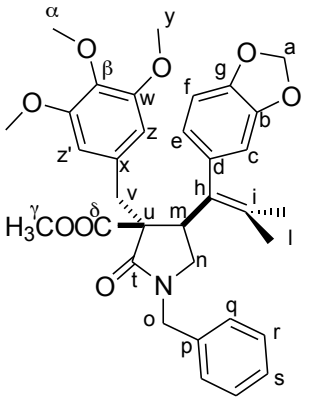

$C_{34}H_{37}NO_8$
Mol. Wt.: 587,66

Sodium hydride (11 mg, 0.27 mmol, 1.2 equiv., 60% dispersion in mineral oil) was added to a solution of pyrrolidin-2-one **37** (93 mg, 0.23 mmol, 1 equiv.) in freshly distilled and degassed DMF (4 mL) under argon atmosphere. The resulting mixture was stirred at 40°C for 20 min and 3,4,5-trimethoxybenzyl bromide (179 mg, 0.68 mmol, 3 equiv.) was introduced. The reaction mixture was stirred at 100°C for 24h. The reaction was quenched with a saturated solution of NH_4Cl and the aqueous layer was extracted with diethyl ether. The combined organic layers were washed with a large volume of water, dried on $MgSO_4$ and concentrated in vacuo. The crude product was purified by flash chromatography on silica gel eluting with cyclohexane/AcOEt 70:30 to afford the expected product **38** in 73% yield (98 mg) as a white foam.

^{1}H NMR ($CDCl_3$, 400 MHz): δ = 7.27-7.24 (m, 3H, Hr,s), 7.05 (dd, 2H, *J*= 2.5, 6.5 Hz, Hq), 6.67 (m, 2H, Hf and He), 6.58 (s, 1H, Hc), 6.49 (s, 2H, Hz), 5.91 (s, 2H, Ha), 4.48 (d, 1H, *J*= 14.8 Hz, part of AB system, Ho'), 4.30 (d, 1H, *J*= 14.8 Hz, part of AB system, Ho), 3.84 (s, 3H, Hα), 3.80 (s, 6H, Hy), 3.53 (d, 1H, *J*= 14.1 Hz, part of AB system, Hv'), 3.51 (t, 1H, *J*= 8.4Hz, Hn), 3.31 (t, 1H, *J*=8.9 Hz, Hm), 3.23 (s, 3H, Hγ), 3.11 (d, 1H, *J*= 14.1Hz, part of AB system, Hv), 2.80 (t, 1H, *J*= 8.4Hz, Hn), 1.52 (s, 3H, Hl), 1.40 (s, 3H, Hl').

^{13}C NMR ($CDCl_3$, 100 MHz): δ = 172.6 (Cδ), 170.6 (Ct), 153.1 (Cw), 147.2 (Cb), 146.1 (Cg), 137.2 (Cx), 135.8 (Cp or Cβ), 135.6 (Cp or Cβ), 133.7 (Cd), 131.0 (Ch), 130.3 (Ci), 128.6 (Cq or Cr or Cs), 127.9 (Cq or Cr or Cs), 127.6 (Cq or Cr or Cs), 123.6 (Ce), 110.8 (Cc), 108.0 (Cf), 107.6 (Cz), 100.9 (Ca), 61.1 (Cu), 60.5 (Cα), 56.1 (Cy), 51.7 (Cγ), 48.2 (Cn), 47.2 (Co), 42.2 (Cm), 38.1 (Cv), 23.1 (Cl o Cl'), 20.5 (Cl o Cl').

35) 4-(1-Benzo[1,3]dioxol-5-yl-2-methyl-propenyl)-1-benzyl-3-(3,4,5-trimethoxy-benzyl)-pyrrolidin-2-one (26)

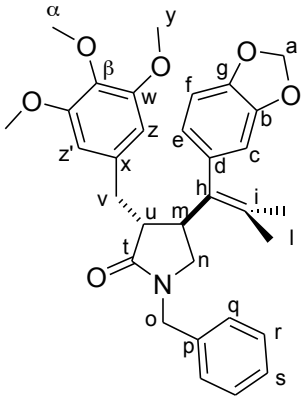

$C_{32}H_{35}NO_6$
Mol. Wt.: 529,62

Ester **38** (111 mg, 0.19 mmol, 1 equiv.) was solubilized in ethylene glycol (10 mL) and 20 equivalents of potassium hydroxide (KOH) (211 mg, 3.78 mmol) was added. The resulting mixture was heated at 180-190°C and the completion of the reaction was monitored by TLC. After 20 minutes, the reaction was quenched with HCl 20% and the resulting aqueous phase was extracted with diethyl ether, and the combined organic layers were dried on $MgSO_4$ and concentrated in vacuo. The crude product was purified by flash chromatography on silica gel eluting with a gradient of cyclohexane/AcOEt 70:30 to pure AcOEt to afford the expected pyrrolidin-2-one **26** in 60% yield (60 mg).

^{1}H NMR ($CDCl_3$, 400 MHz): δ = 7.26-7.21 (m, 3H, Hr,s), 7.03 (dd, 2H, *J*= 2.5, 6.5 Hz, Hq), 6.73 (m, 1H, *J*= 8.0 Hf), 6.48 (s, 2H, Hz), 6.42 (s, 1H, Hc), 6.36 (d, 1H, *J*= 8.0 Hz, He), 5.96 (s, 2H, Ha), 4.46 (d, 1H, *J*= 14.5 Hz, part of AB system, Ho'), 3.84 (s, 6H, Hy), 3.80 (s, 3H, Hα), 3.69 (m, 1H, Hm), 3.46 (d, 1H, *J*= 14.5 Hz, part of AB system, Ho), 3.21 (m, 2H, Hn and Hv), 2.95 (m, 2H, Hu and Hn'), 2.79 (m, 1H, Hv'), 1.57 (s, 3H, Hl), 1.45 (s, 3H, Hl').

^{13}C NMR ($CDCl_3$, 100 MHz): δ = 175.2 (Ct), 153.2 (Cw), 147.4 (Cb), 146.1 (Cg), 136.5 (Cx), 134.2 (Cp and Cβ), 133.7 (Cd), 132.2 (Ch), 128.6 (Ci), 128.1 (Cq or Cr or Cs), 127.5 (Cq or Cr or Cs), 122.5 (Cq or Cr or Cs), 110.2 (Cc), 108.1 (Cf), 105.9 (Cz), 101.0 (Ca), 61.0 (Cα), 56.3 (Cy), 49.2 (Cn), 48.3 (Cu), 46.7 (Co), 38.7 (Cm), 33.1 (Cv), 23.0 (Cl or Cl'), 20.7 (Cl or Cl').

Supporting Information

All the spectra were elaborated using MestreNova 6.0.2 software, and FID data are available on request:

^{1}H-NMR spectrum of compound **21a**

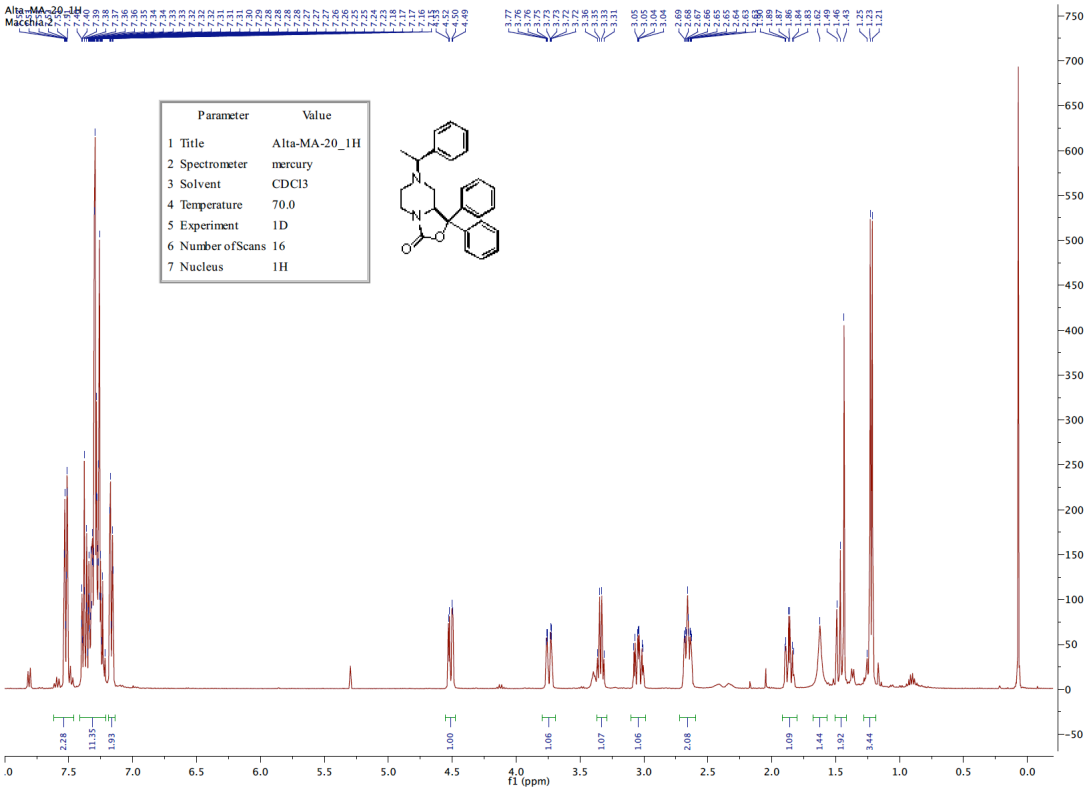

^{13}C-NMR spectrum of compound **21a**

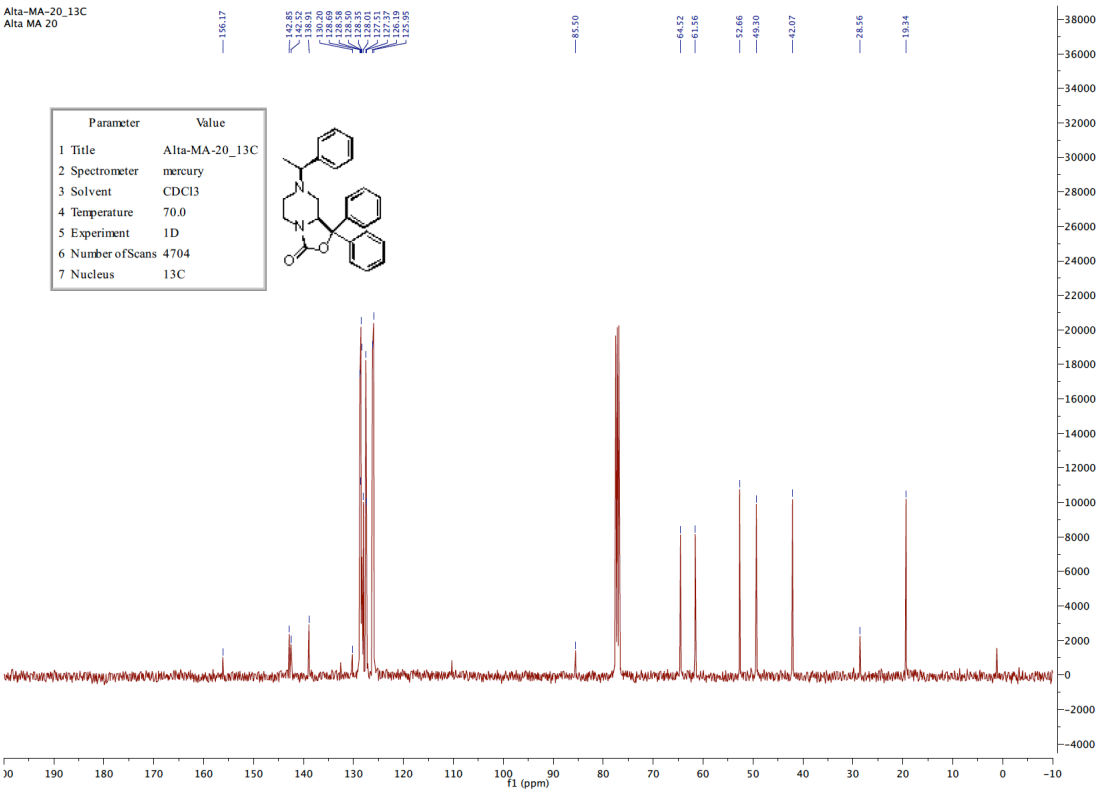

DEPT-NMR spectrum of compound **21a**

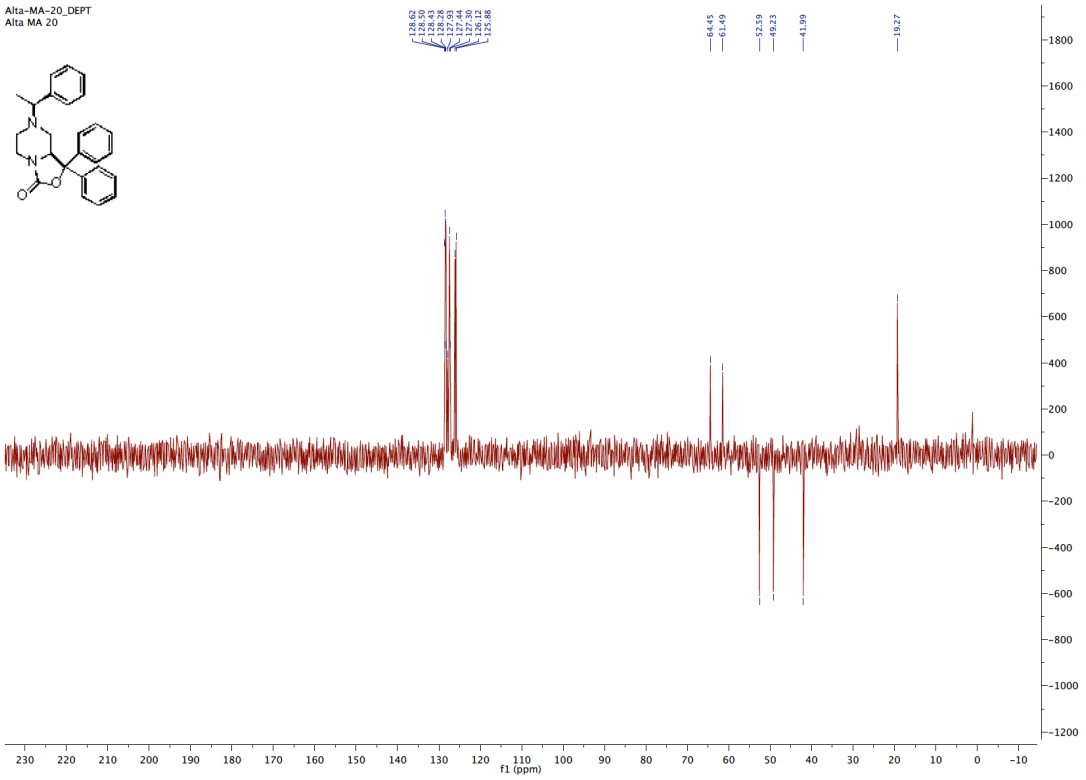

COSY-NMR spectrum of compound **21a**

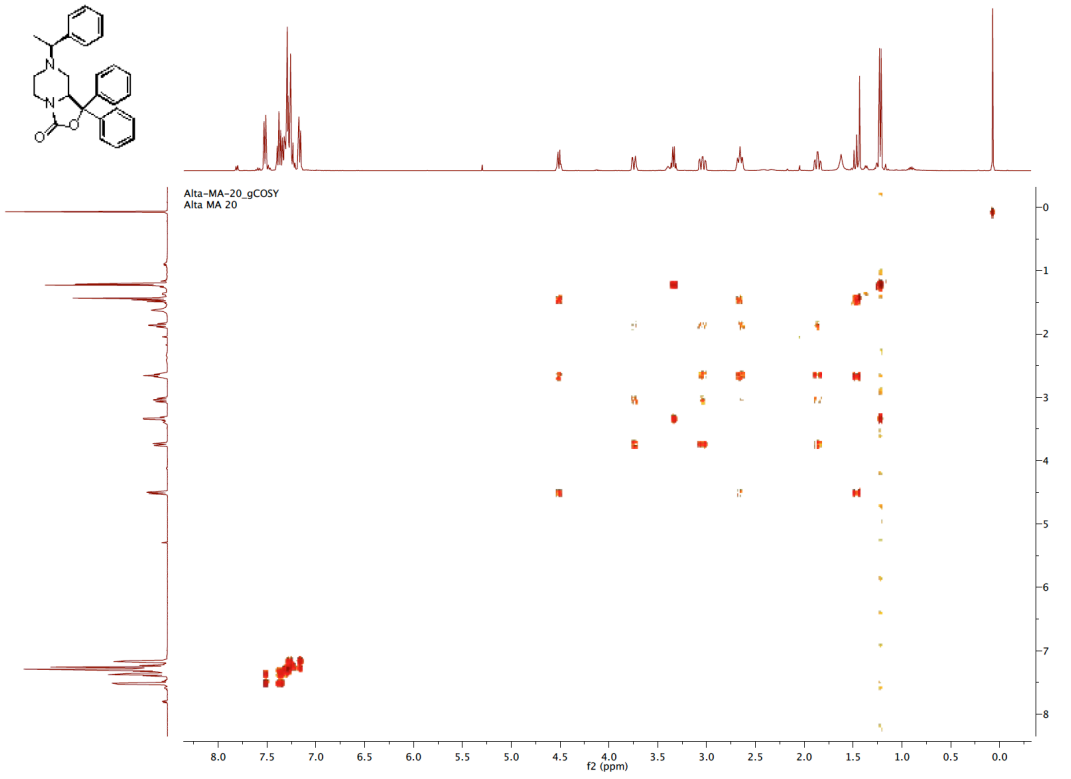

HMBC-NMR spectrum of compound **21a**

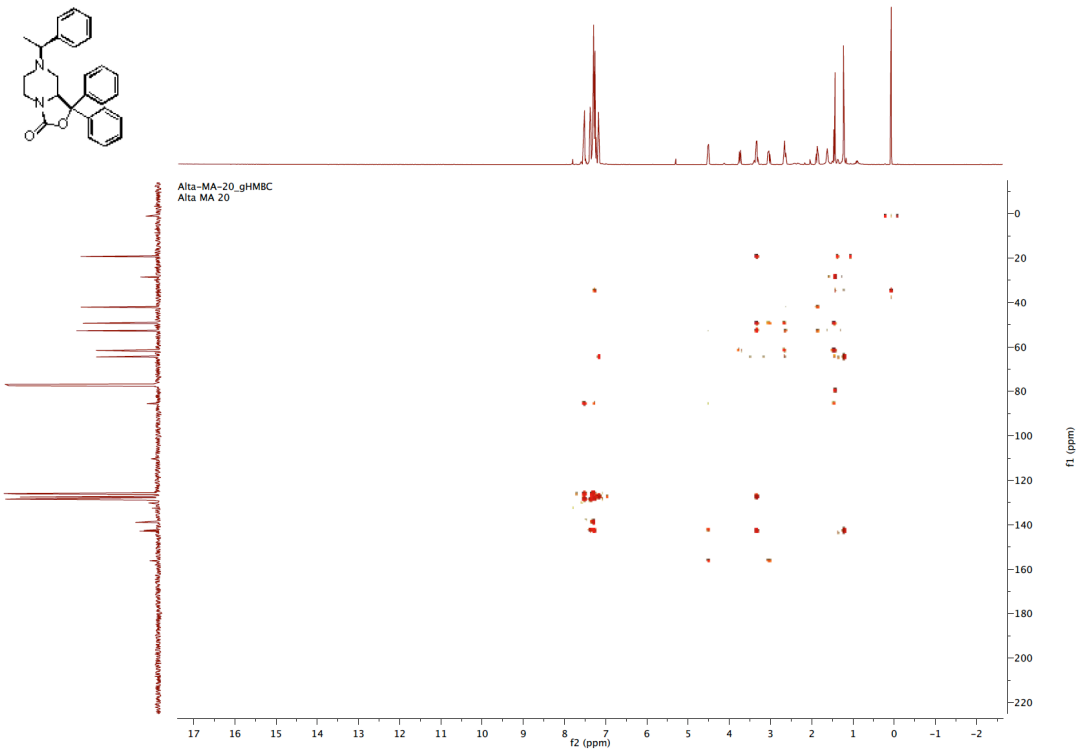

HMQC-NMR spectrum of compound **21a**

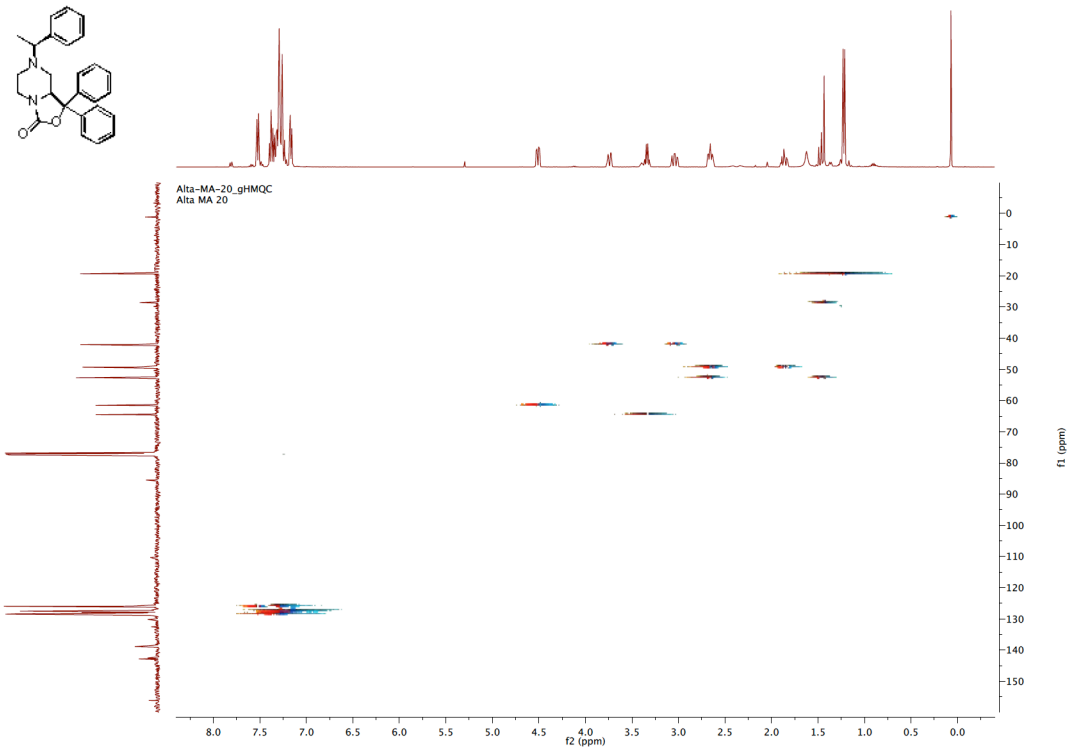

^{1}H-NMR spectrum of compound **21b**

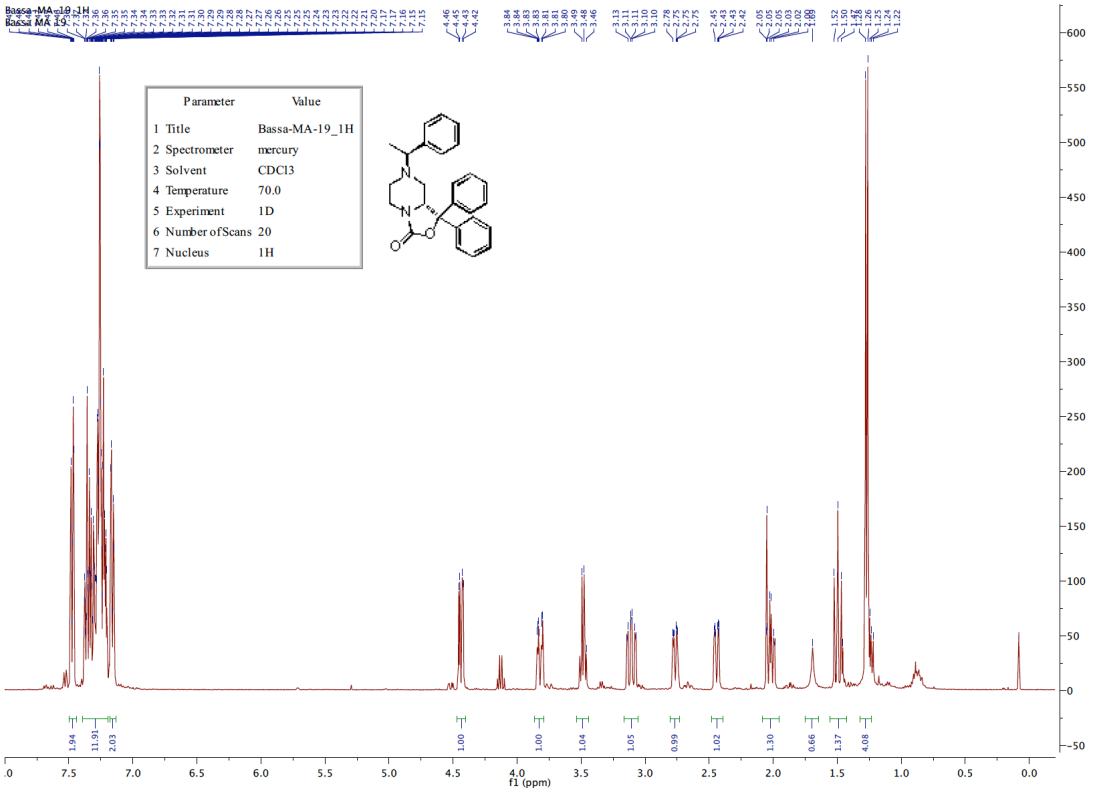

^{13}C-NMR spectrum of compound **21b**

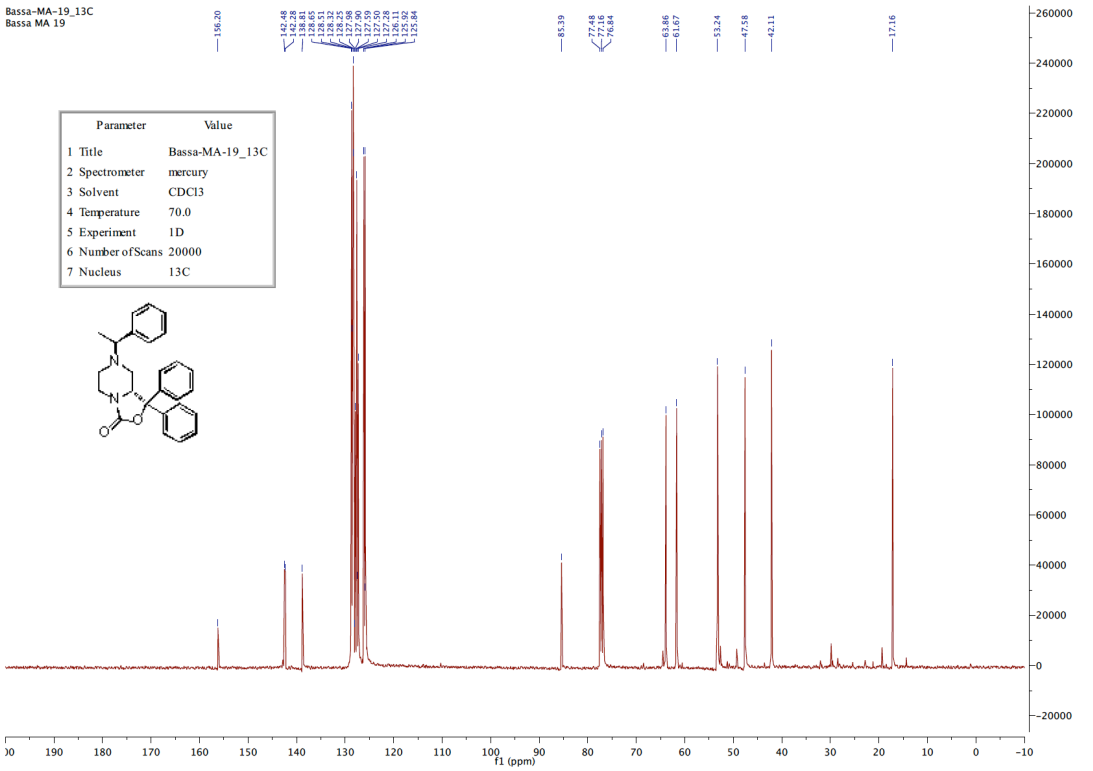

DEPT-NMR spectrum of compound **21b**

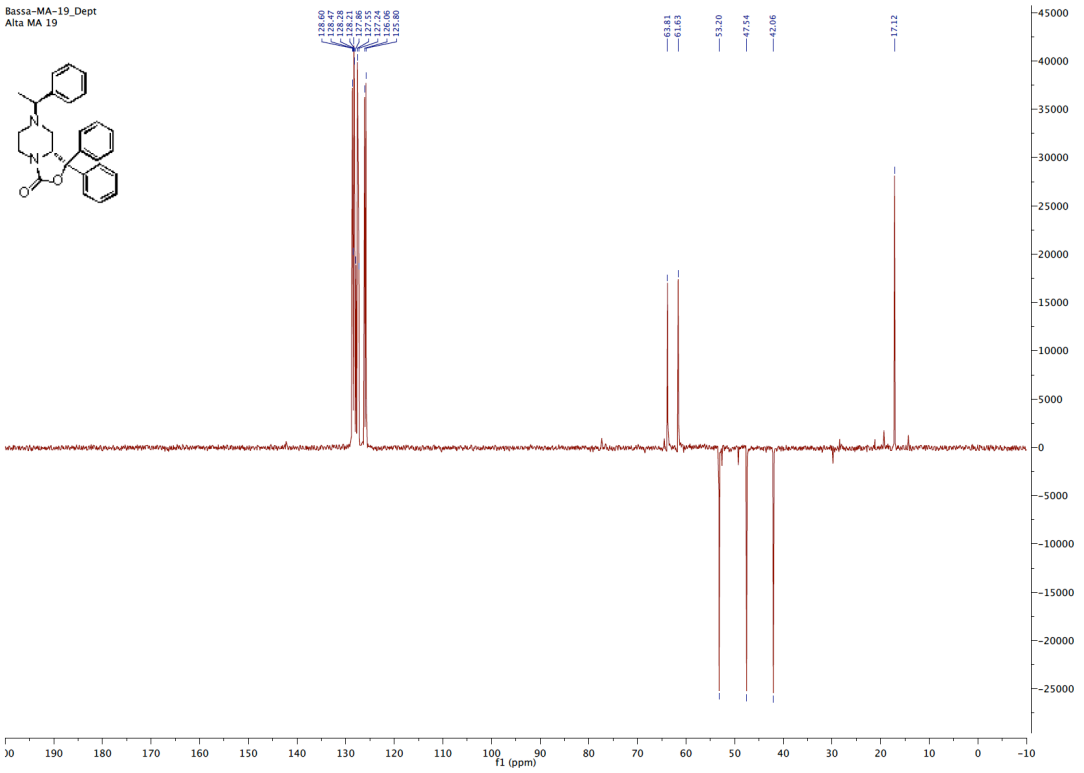

COSY-NMR spectrum of compound **21b**

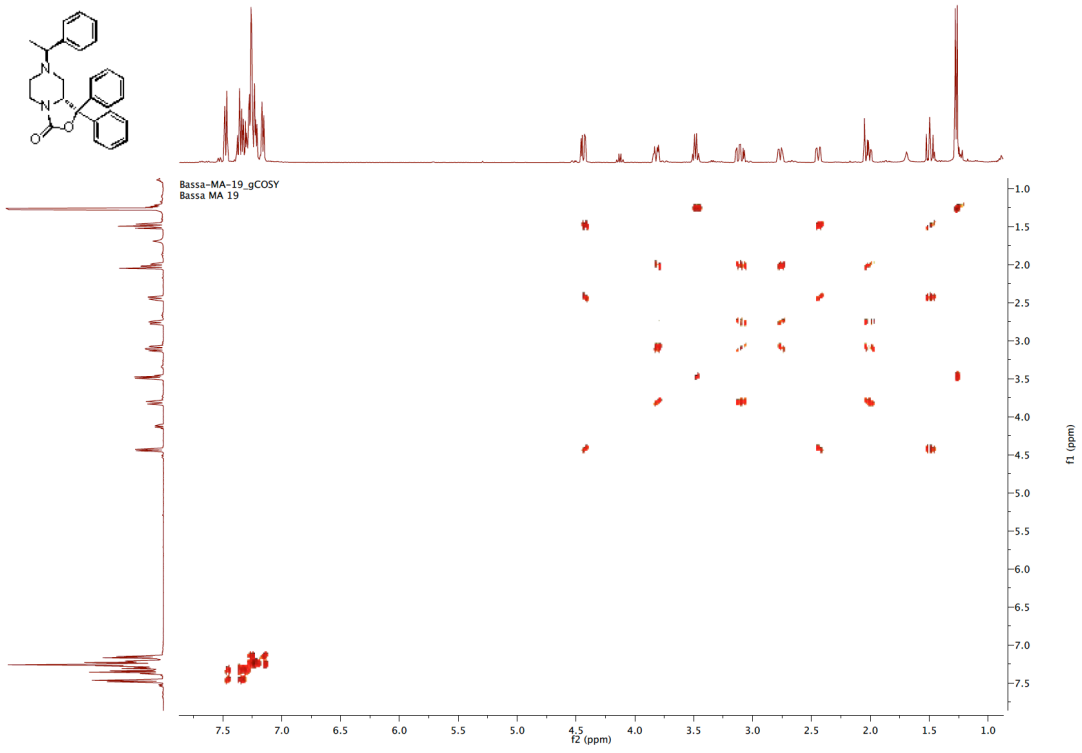

HMBC-NMR spectrum of compound **21b**

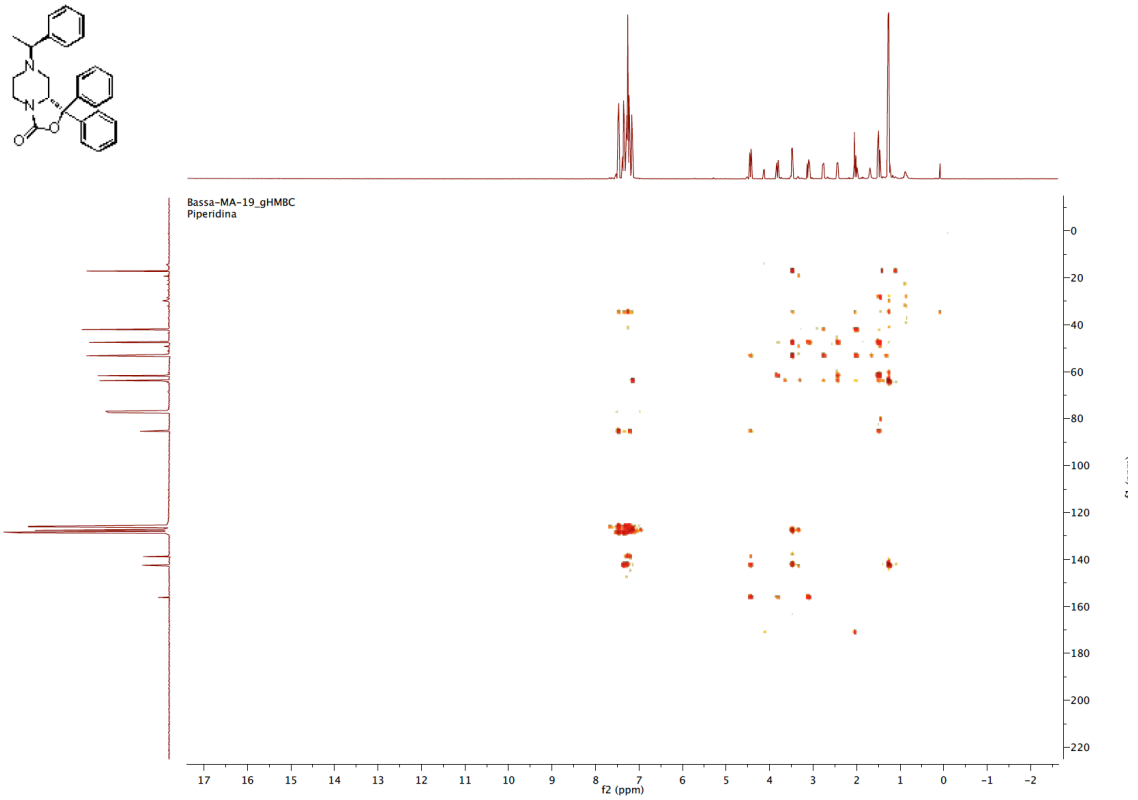

HMQC-NMR spectrum of compound **21b**

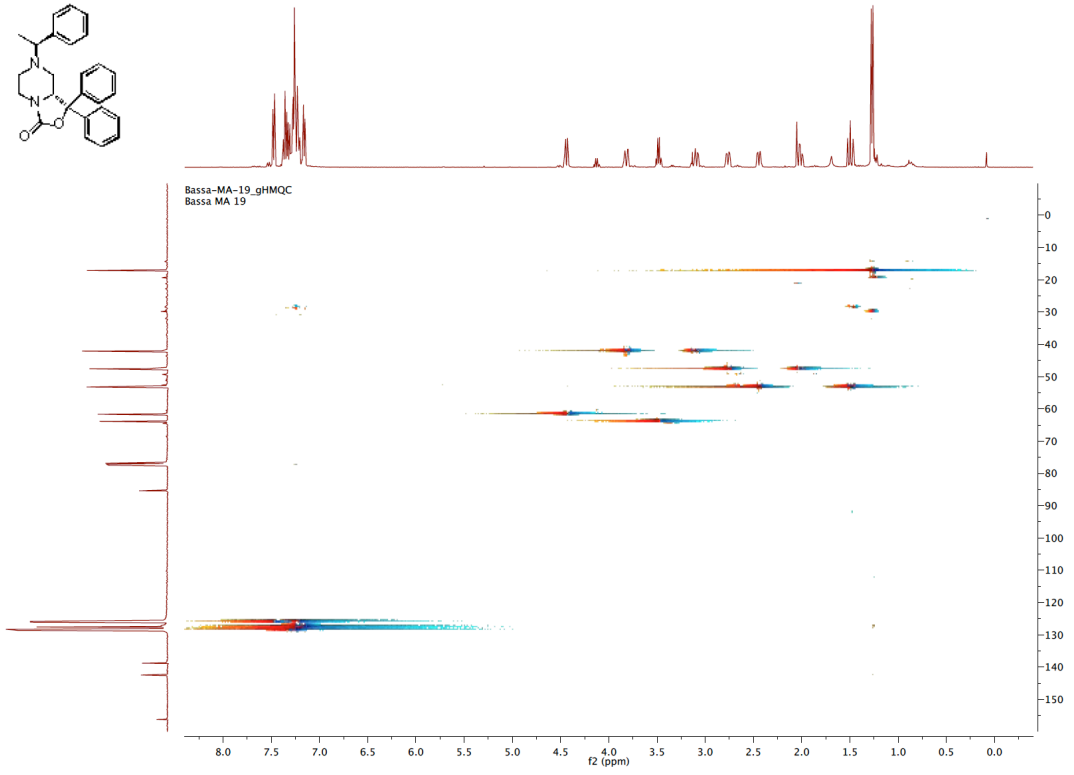

^{1}H-NMR spectrum of compound **(*S*)-SHA68**

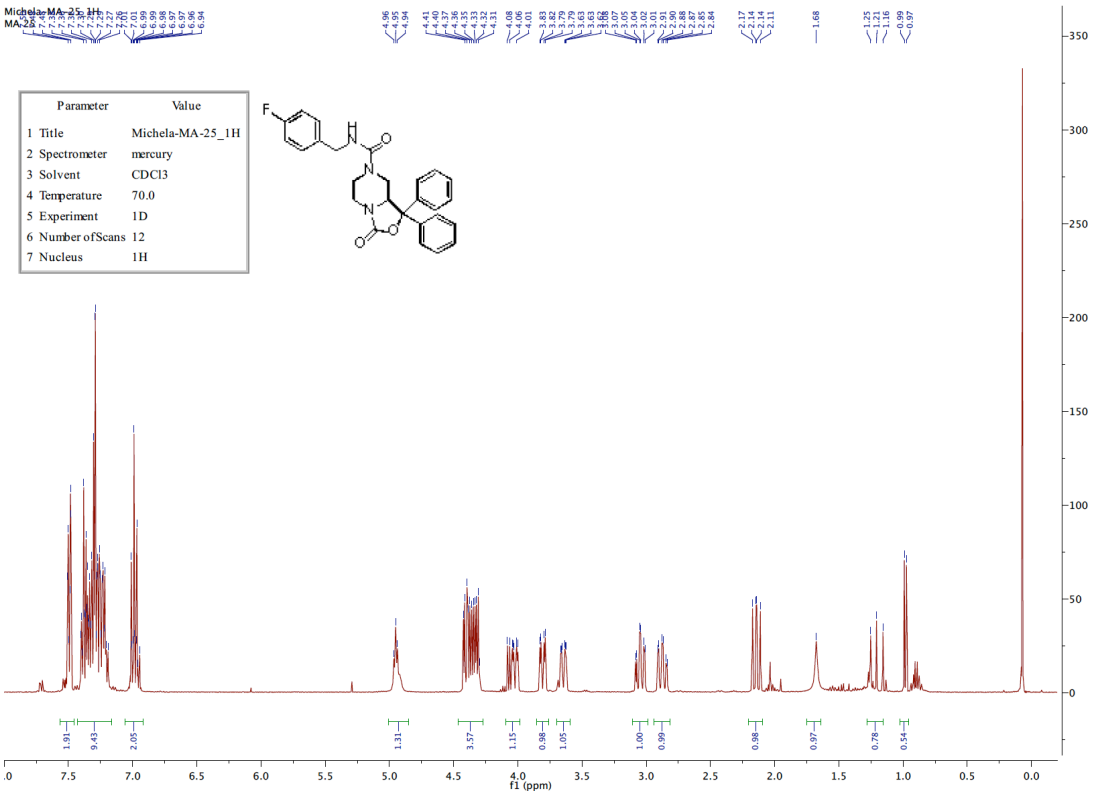

^{13}C-NMR spectrum of compound **(*S*)-SHA68**

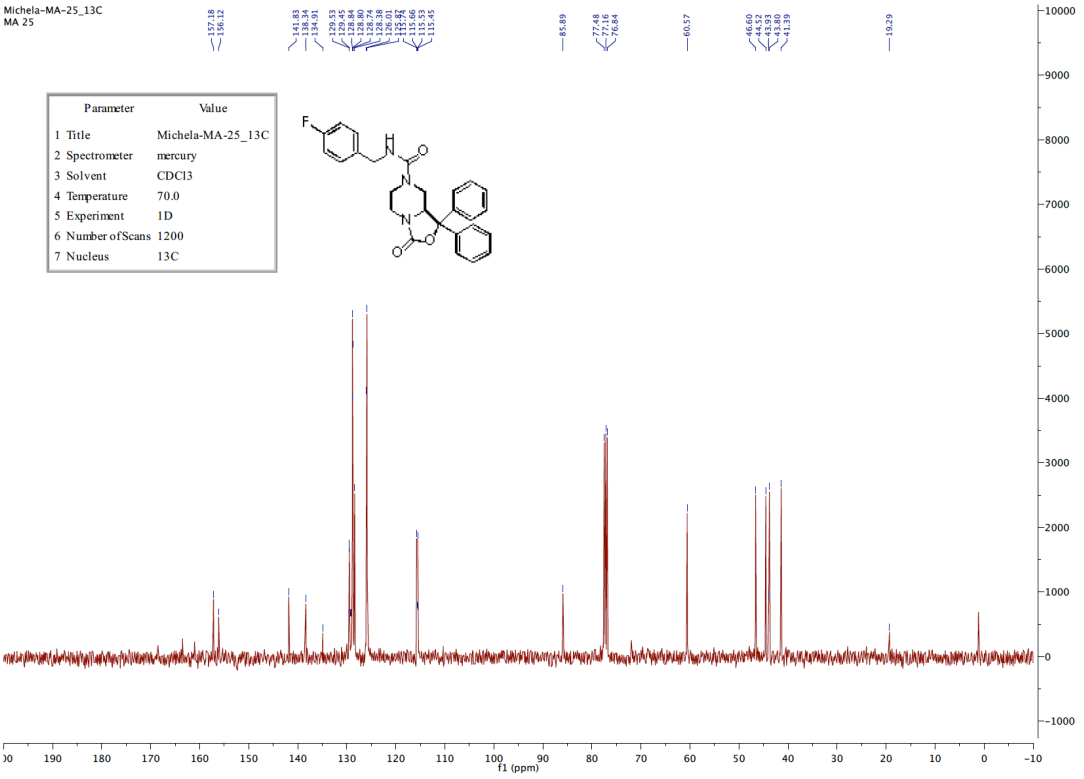

DEPT-NMR spectrum of compound **(*S*)-SHA68**

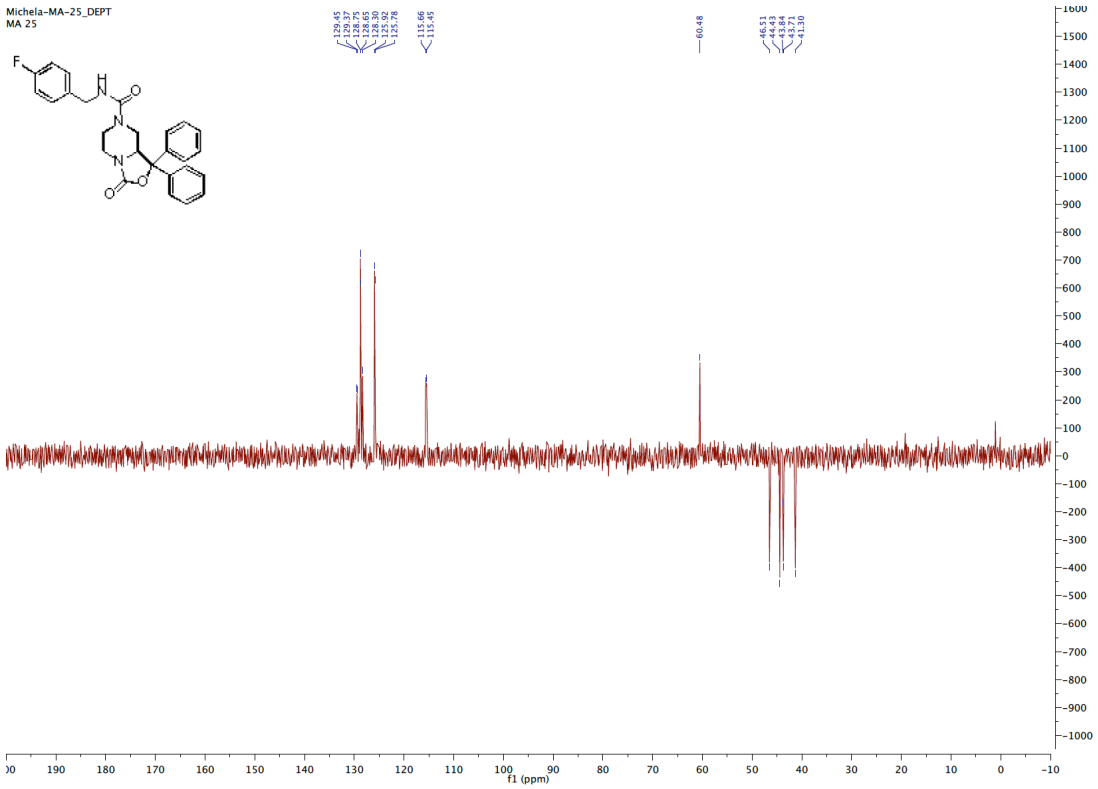

COSY-NMR spectrum of compound **(*S*)-SHA68**

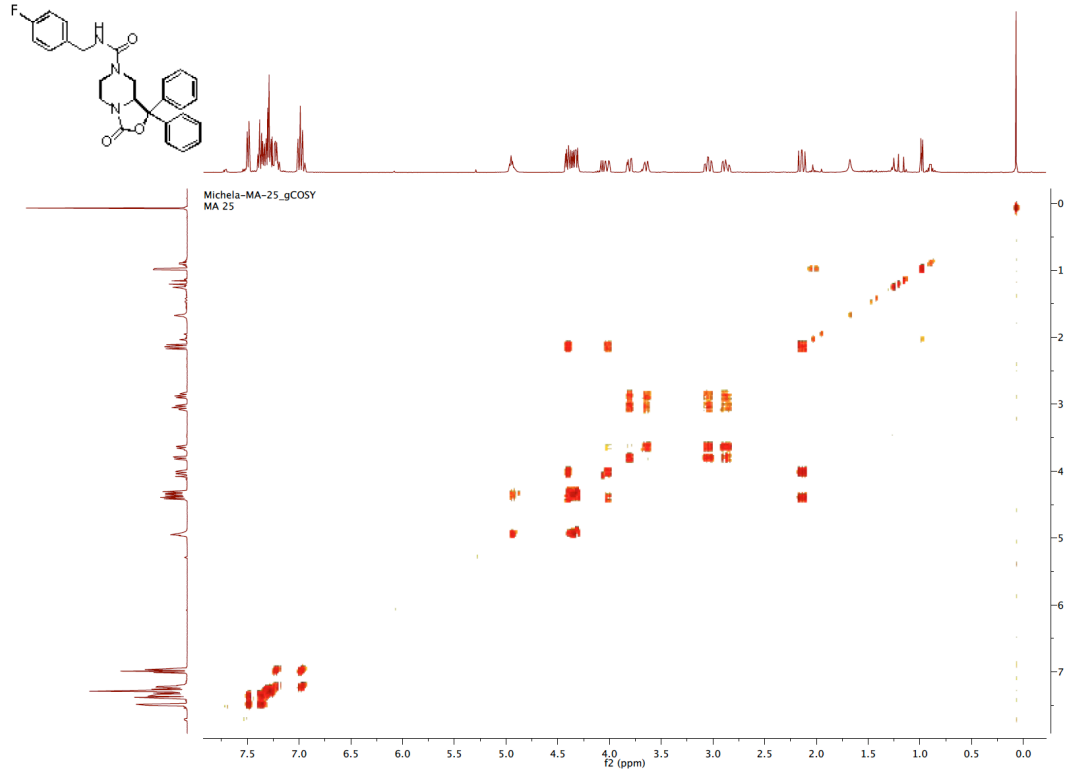

HMBC-NMR spectrum of compound **(*S*)-SHA68**

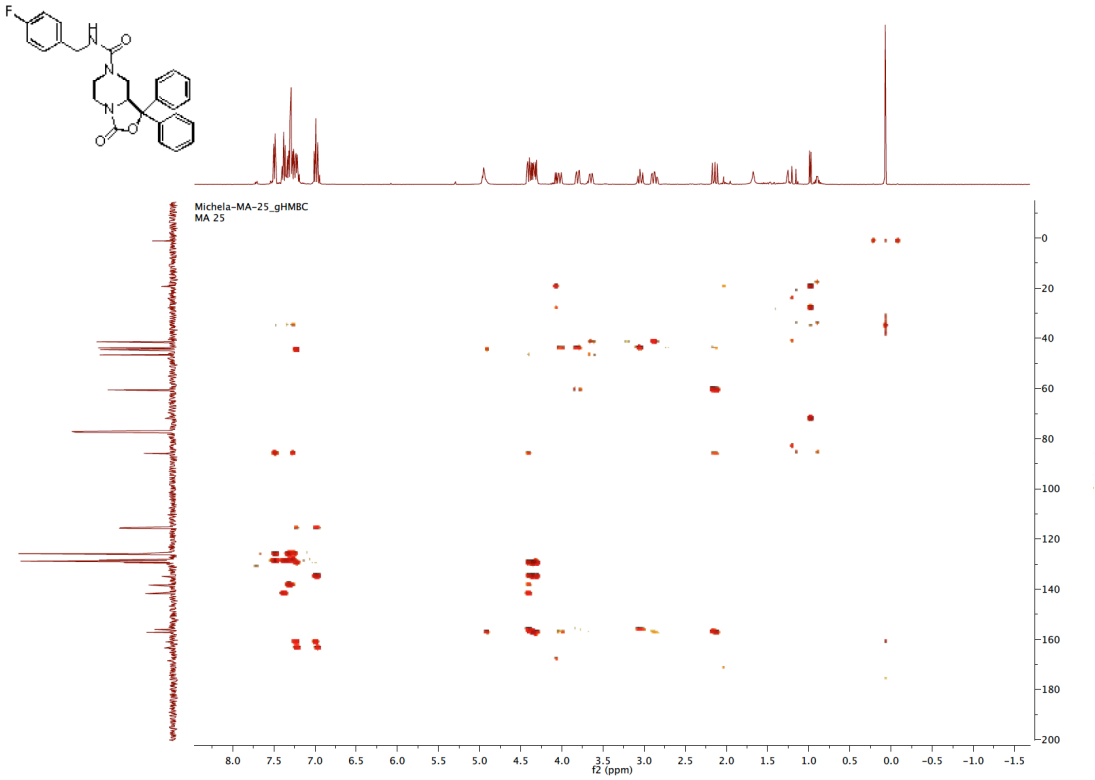

HMQC-NMR spectrum of compound **(*S*)-SHA68**

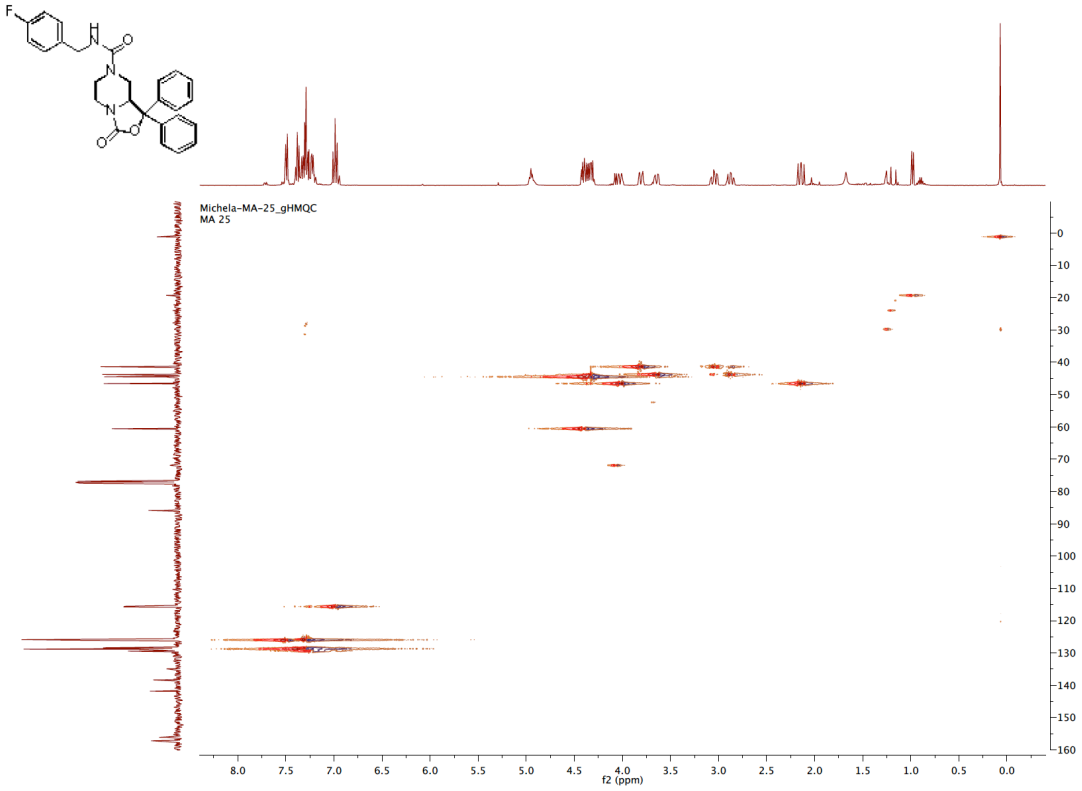

^{19}F-NMR spectrum of compound **(*S*)-SHA68**

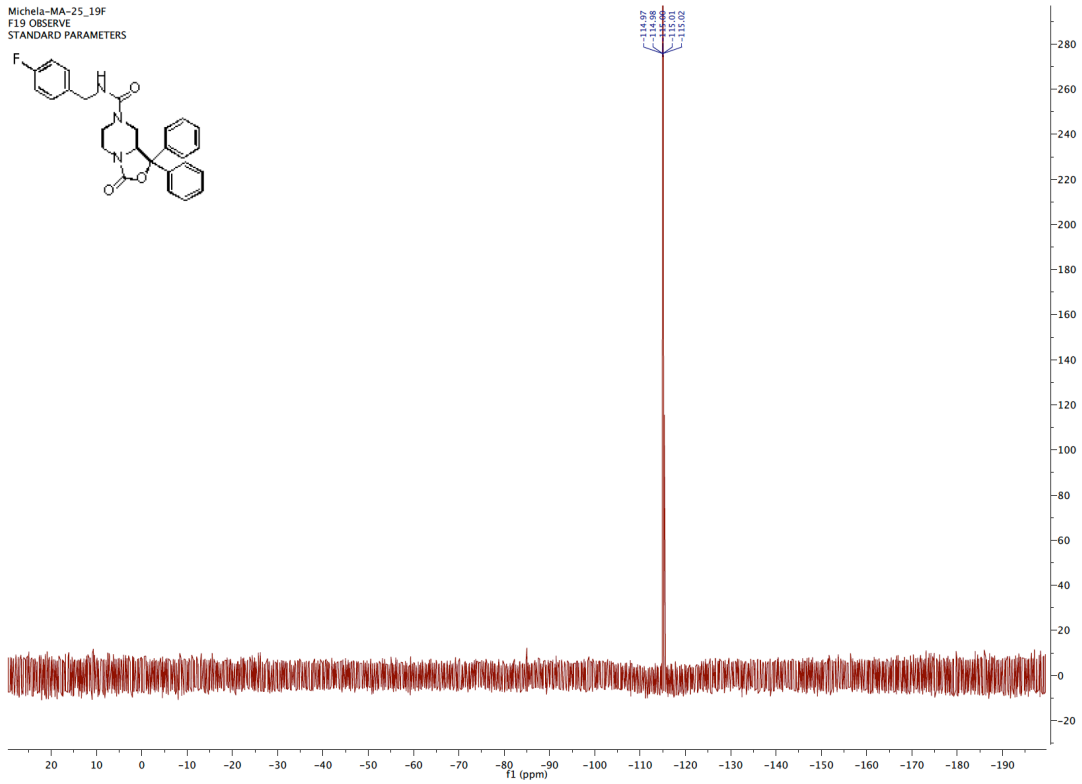

^{1}H-NMR spectrum of compound **(*R*)-SHA68**

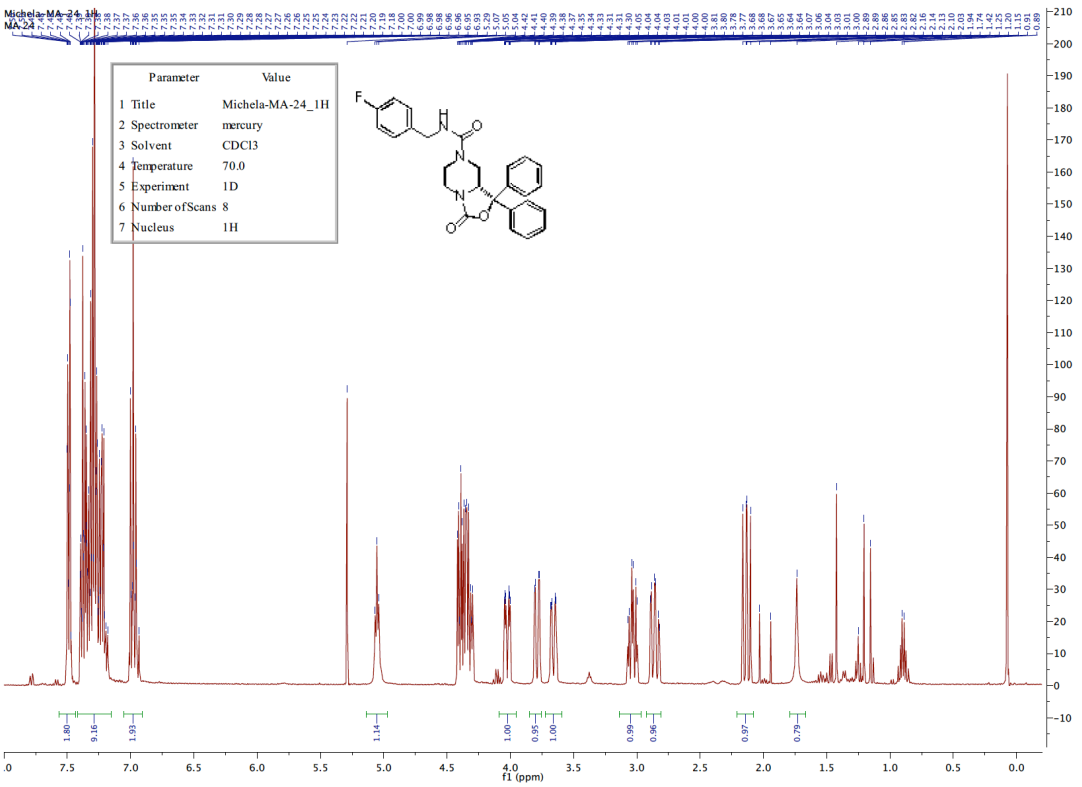

^{13}C-NMR spectrum of compound **(*R*)-SHA68**

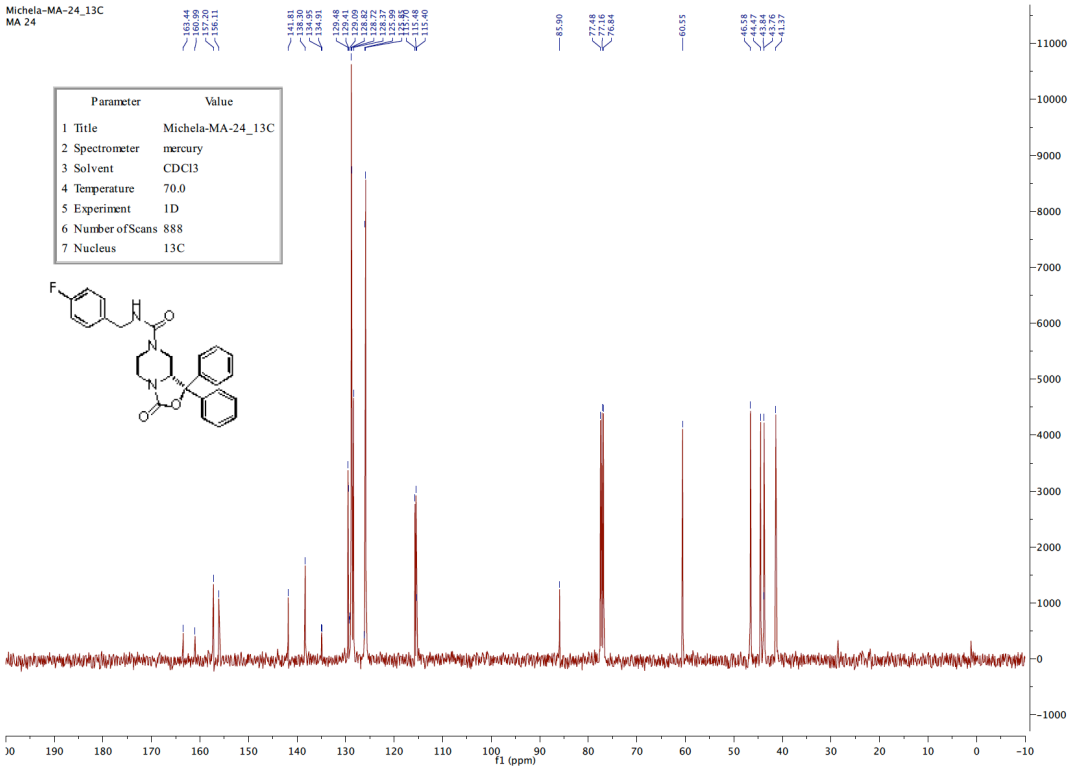

DEPT-NMR spectrum of compound **(*R*)-SHA68**

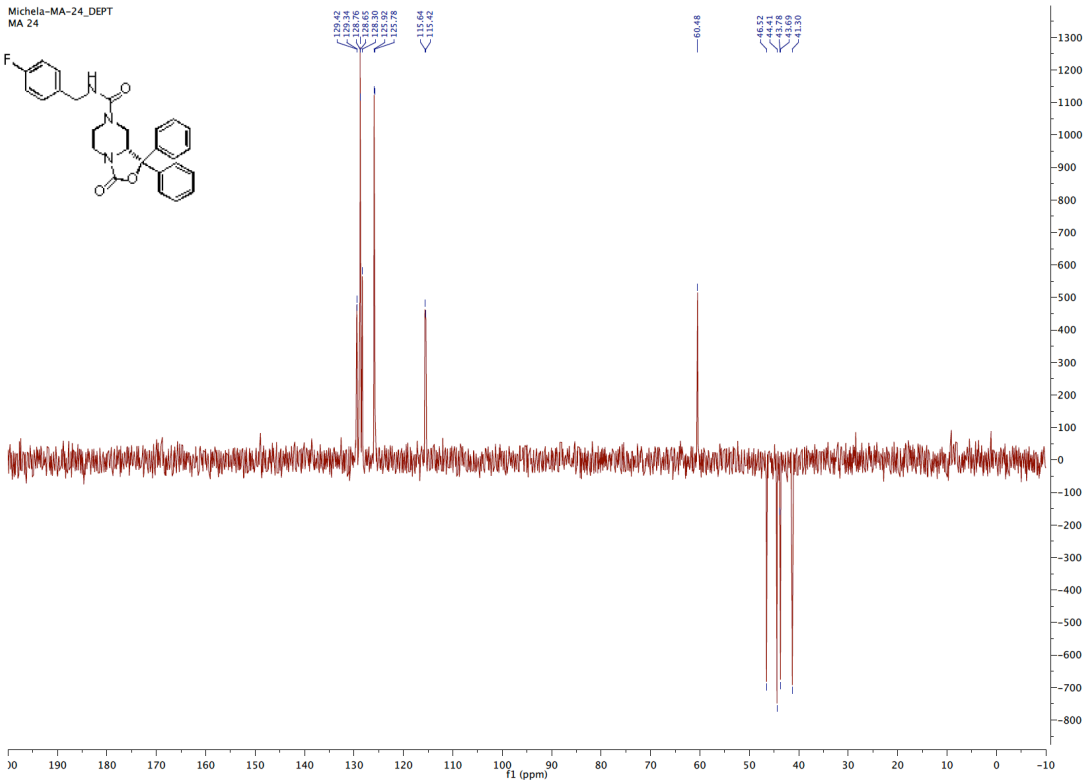

COSY-NMR spectrum of compound **(*R*)-SHA68**

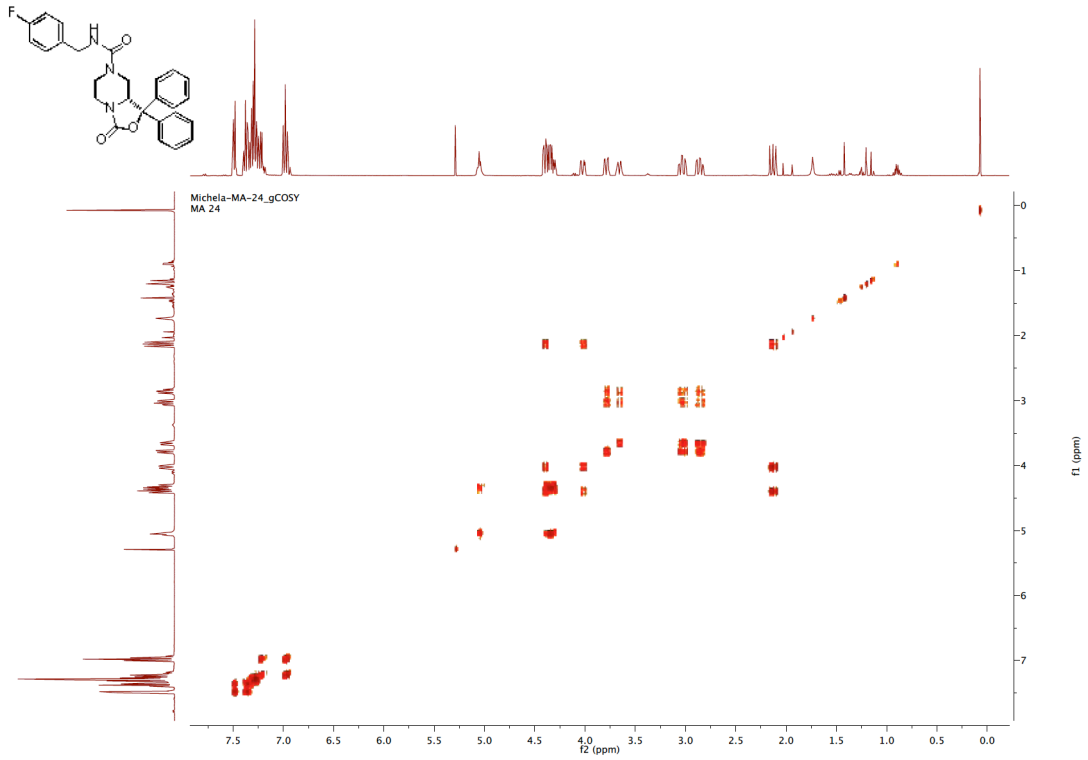

HMQC-NMR spectrum of compound **(*R*)-SHA68**

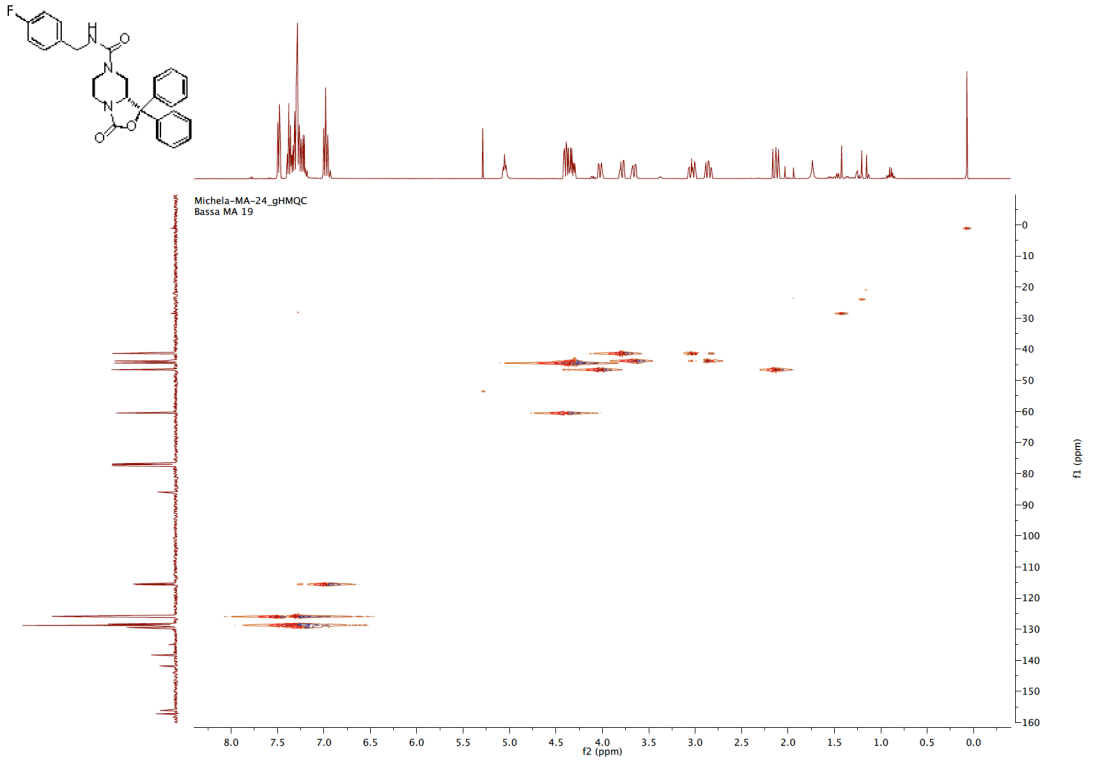

HMBC-NMR spectrum of compound **(*R*)-SHA68**

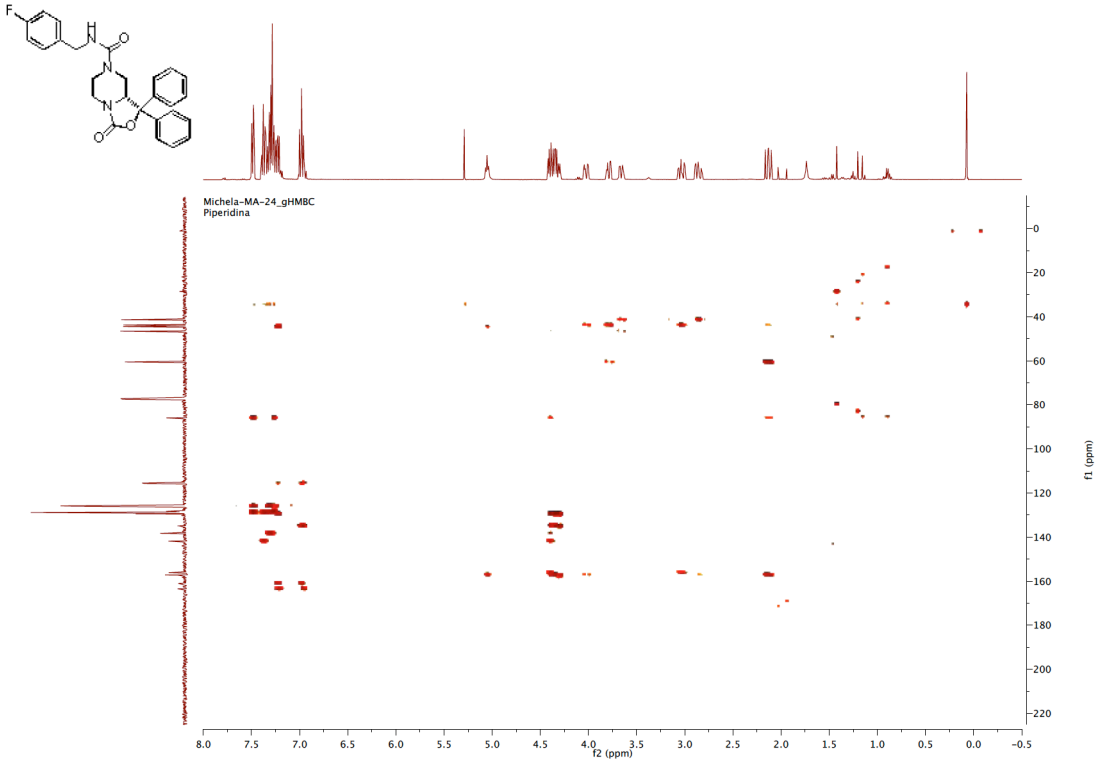

^{19}F-NMR spectrum of compound **(*R*)-SHA68**

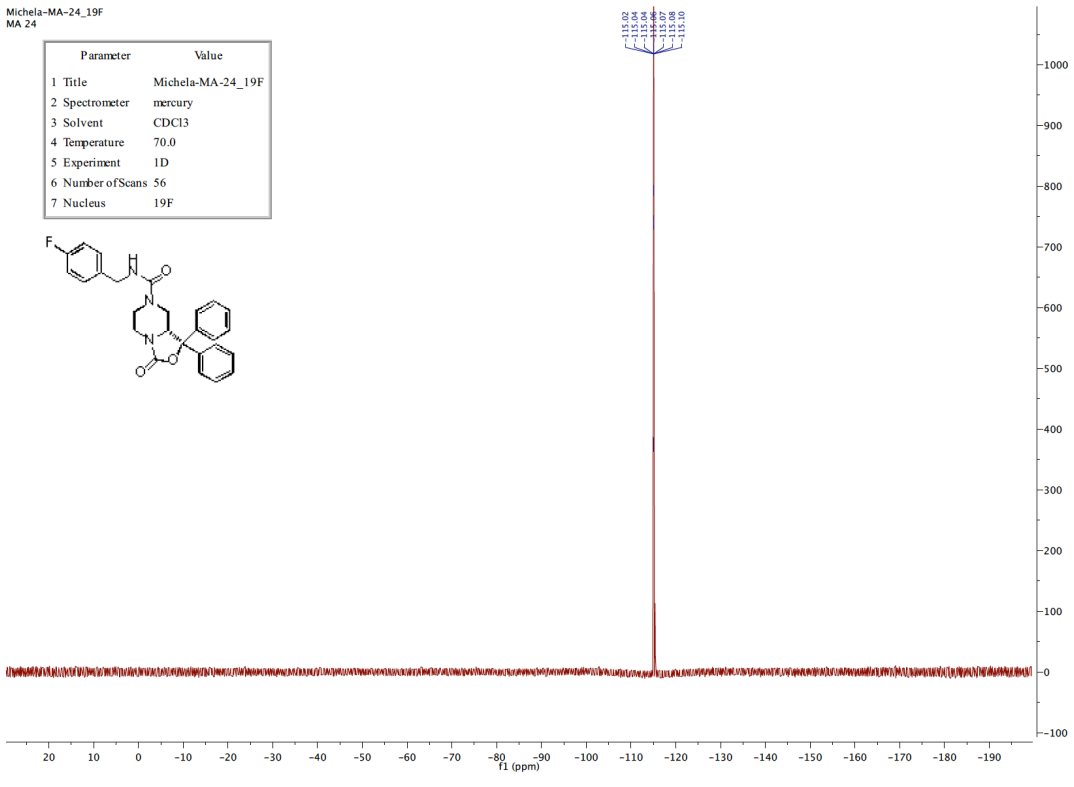

Chiral chromatography analysis

Column:	Lux 3u Cellulose-1, 150 x 2mm, Phenomenex
Mobile phase:	80% Hexane : 20% Isopropanol
Flow:	200µl/min
Injection volume:	3µl

All chromatograms were recorded at 230 nm.

		Ritention Time (min)	Area (%)
(*R/S*) SHA 68	1	6.495	51.30%
	2	7.892	48.70%
(*R*) SHA 68	1	------	0%
	2	7.902	100%
(*S*) SHA 68	1	6.513	100%
	2	------	0%

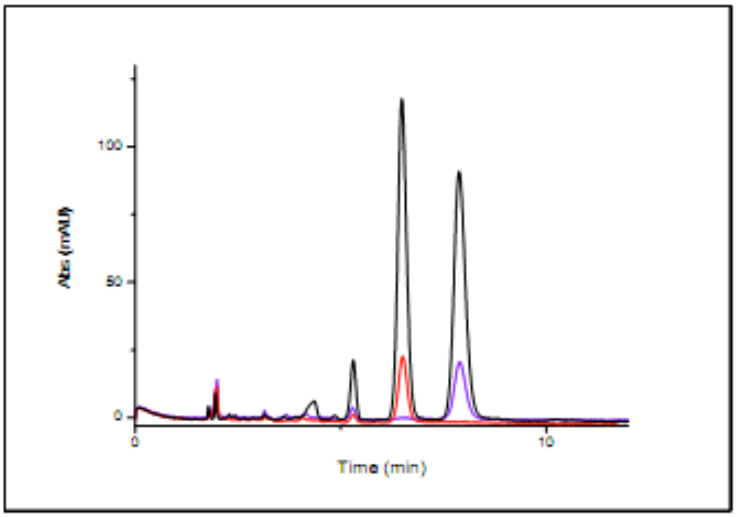

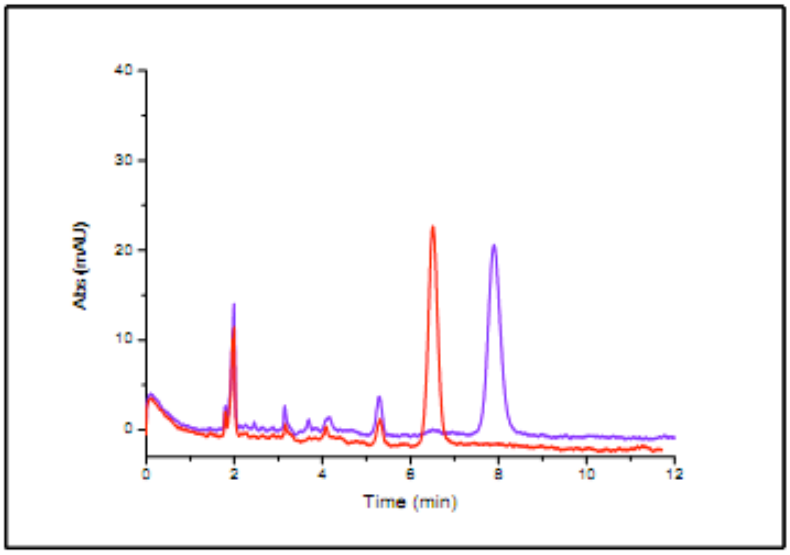

Résumé de Thése

Le travail effectué durant ces trois ans commence avec la synthèse énantiosélective d'un composé capable de se lier au récepteur NPSR.

Le Neuropeptide S et ses NPSR récepteurs constituent une nouvelle découverte.[12] Une fois que le récepteur NPSR a été activé par son agoniste endogène (NPS), un peptide de 20 acides aminés, s'en suit la mobilisation du Ca^{2+} intracellulaire et l'augmentation du taux d'AMPc. Le système NPS / NPSR est impliqué dans plusieurs fonctions biologiques, dont la régulation des cycles veille-sommeil, l'ingestion d'aliments, l'anxiété et l'activité locomotrice**.**

(*R/S*)-SHA-68 [21]est le premier antagoniste non peptidique sélectif au récepteur NPSR. Actuellement, seuls les composés à structure ossazolo-pipérazinique ont été reconnus capables de se lier au récepteur NPSR. **(*R/S*)-SHA- 68** en est le principal analogue (l'acide 4-7-fluorobenzilammide-carboxy-(9*R/S*)-3-oxo-1,1-diphényl-tétrahydro-ossazolo[3,4-*a*]-pyrazine).

Cette molécule présente un centre stéréogène mais actuellement, elle est utilisée en tant que mélange racémique. Les excellentes propriétés pharmacologiques de ce ligand nous ont conduit vers la synthèse énantiosélective, la purification et la caractérisation de deux composés optiquement purs afin d'évaluer séparément leur activité pharmacologique. Après l'obtention des deux énantiomères, leur caractérisation et la vérification de leur pureté optique, nous avons été en mesure de comprendre la conformation et la configuration absolue de l'énantiomère (*R*) en raison des informations cristallographiques. Des études pharmacologiques menées dans les laboratoires du Dr. Calò de l'Università degli Studi di Ferrara ont permis de démontrer que **(*R*)-SHA 68** est le seul énantiomère capable d'antagoniser l'activité du ligand endogène du récepteur NPSR.

Dans le cadre d'une convention de co-tutelle de thèse établie entre l'Université Pierre et Marie Curie de Paris et l'Università degli Studi di Ferrara, on a eu l'opportunité de

développer une collaboration avec l'équipe du Prof. Giovanni Poli, au sein de laquelle j'ai pu effectuer un stage de neuf mois.

L'équipe du Prof. Poli s'intéresse en particulier aux réactions catalysées au palladium-appliquées à la synthèse de γ-lactones et de γ-lactames à partir de précurseurs alléniques.

Il nous est paru intéressant appliquer cette chimie à la synthèse d'un nouvel analogue azoté de la (-)-Stéganacine. Ce produit naturel, isolé pour la première fois en 1973 de la plante *Steganotaenia araliacea*,[31] appartient à la famille des lignanes et plus particulièrement des dibenzocyclooctadiènes. L'intérêt pour la (-)-Stéganacine est dû à son activité antitumorale[34] et à sa structure complexe. Elle est composée d'une γ-lactone accolée à un cycle à huit chaînons et d'un motif bis-arylique polyoxygéné présentant un axe de chiralité configurationnellement stable à température ambiante. Par ailleurs, cette molécule présente trois centres stéréogènes contigus à stéréochimie relative *trans*, *trans*.

À partir de l'alcool propargylique disponible dans le commerce, l'intermédiaire désiré est obtenu en 7 étapes avec un rendement global de 19%.

La réaction clef de cette stratégie synthétique est la séquence domino « carbopalladation d'allène / alkylation allylique » qui a été optimisée dans les laboratoires du Prof. Poli.[41] Cette réaction nous a permis d'obtenir le γ-lactame désiré avec un rendement de 74%.

Une réaction de benzylation et de decarboxylation nous ont ensuite permis d'obtenir le substrat pour l'étude de l'étape de couplage oxydant biarylique pour former le cycle à huit chaînons.

La coupure oxydante de la double liaison exocyclique, suivie d'une réduction diastéréosélective de la cétone générée et une étape finale d'acylation devraient enfin permettre d'accéder à l'analogue azoté de la stéganacine.

Riassunto della Tesi

Il lavoro svolto in questi tre anni inizia con la sintesi asimmetrica di un composto in grado di legare il recettore NPSR.

Il Neuropeptide S e il suo recettore NPSR costituiscono un sistema di recente scoperta.[12]

In seguito all'attivazione del recettore NPSR da parte del suo agonista endogeno NPS, un peptide di 20 aminoacidi, si osserva una mobilitazione del Ca^{2+} intracellulare e un aumento dei livelli di cAMP nella cellula. Il sistema NPS/NPSR è implicato in diverse funzionalità biologiche tra cui la regolazione dei cicli sonno-veglia, del food-intake, dell'ansia e dell'attività locomotoria.

(*R/S*) SHA-68 [21]è il primo antagonista non peptidico selettivo per il recettore NPSR; lo stato dell'arte fino ad ora evidenzia, tra i ligandi non peptidici, solo molecole a struttura ossazolo-piperazinica in grado di legare il recettore NPSR. *(R/S*) SHA-68 è il capostipite di questa famiglia, la 4-fluorobenzilammide dell'acido 7-carbossi-(9*R/S*)-3-oxo-1,1-difenil-tetraidro-ossazolo [3,4-*a*] pirazina, e pur possedendo un centro stereogenico, viene al momento usato come miscela racemica.

Le ottime proprietà farmacologiche di tale ligando hanno spinto le nostre ricerche verso la sintesi enantioselettiva, la purificazione e la caratterizzazione dei due composti otticamente puri al fine di valutarne separatamente l'attività farmacologica.

In seguito all'ottenimento dei 2 enantiomeri, grazie all'utilizzo di un ausiliario chirale, alla loro caratterizzazione e alla verifica del loro grado di purezza mediante HPLC con colonne chirali, siamo stati in grado di risalire alla conformazione e configurazione assoluta di uno dei due composti otticamente puri risultata essere (*R*). Queste informazioni sono supportate dai dati cristallografici fornitici dal Prof. Bertolasi dell'Università degli Studi di Ferrara. Gli studi farmacologici svolti presso i laboratori del Dr. Calò della medesima università ci hanno permesso inoltre di affermare che solo l'enantiomero **(*R*)-SHA 68** è in grado di legare ed antagonizzare l'attività del neuropeptide S sul recettore NPSR.

Grazie alla convenzione di tesi in cotutela stabilita tra l'Università degli Studi di Ferrara e l'Université Pierre et Marie Curie di Parigi, abbiamo avuto l'opportunità di sviluppare una collaborazione con l'équipe del Prof. Giovanni Poli, presso la quale ho svolto uno stage di nove mesi.

Il gruppo di ricerca del Prof. Poli s'interessa in particolare di reazioni catalizzate dal Palladio applicate alla sintesi di γ-lattoni e di γ-lattami a partire da precursori allenici. Ci è quindi sembrato interessante applicare questa chimica alla sintesi di un analogo azotato della (-)-Steganacina.

La (-)-Steganacina è una sostanza naturale isolata per la prima volta nel 1973 dalla pianta *Steganotaenia araliacea*, [31] appartiene alla famiglia dei lignani. L'intesse per la (-)-Steganacina è dovuto alla sua attività antitumorale[34] poiché è in grado di interagire con il meccanismo di polimerizzazione-depolimerizzazione della tubulina e alla struttura chimica complessa. Questa molecola infatti presenta un nucleo γ-lattonico, un ciclo a 8 termini, una porzione biarilica e tre centri stereogenici contigui a stereochimica relativa *trans*, *trans*. A partire dall'alcool propargilico disponibile in commercio, l'intermedio desiderato si ottiene in 7 passaggi con una resa totale del 19%.

La reazione chiave di questo approccio sintetico è la sequenza domino « carbopalladazione dell'allene / alchilazione allilica » che è stata messa a punto nel laboratori del Prof. Poli.[41] Questa reazione ci ha permesso di ottenere il γ-lattame desiderato con una resa del 74%.

Una reazione di benzilazione e di decarbossilazione ci hanno portato all'ottenimento del substrato necessario per lo studio dello step di coupling ossidativo biarilico per la formazione del ciclo a 8 termini.

L'ossidazione del doppio legame esociclico, seguita da una riduzione diastereoselettiva del chetone generato e il passaggio finale di acilazione dovrebbero fornire l'**analogo azotato della (-)-Steganacina** di nostro interesse.

Abstract of the thesis

Neuropeptide S (NPS) is the endogenous ligand of the previously orphan G-protein coupled receptor, recently named NPSR.[12] NPS is a small peptide of 20 amino acids and rapresents the endogenous ligand of NPSR. In cells expressing the recombinant NPSR receptor, NPS selectively binds and activates its receptor, producing intracellular calcium mobilization and an increase of cAMP levels. The NPS-NPSR receptor system regulates important biological functions such as sleep/waking, locomotion, anxiety and food intake.

(*R/S*) SHA-68 [21] is the first non-peptide antagonist of NPSR receptor; actually only a class of molecules able to interact with NPSR are reported in the literature and they are the same oxazol-piperazine structure.

Initially, in order to confirm the published data, we decided to synthesize **SHA 68** in racemic form following the Okamura's methodology[21].

The high selectivity of (**R/S**)**-SHA 68** for NPSR and its good antagonist activity prompted us to synthesize the enantiomers of this non-peptide compound, starting from cheap commercially available reagents as chiral auxiliary.

In order to define the conformation of the piperazine ring in this two enantiomers we performed a series of NMR experiments leading to define a chair conformation where the substituent in C9 was placed in equatorial position.

To know the absolute configuration of the new chiral centre X ray analysis was performed on suitable crystals that show us the *R* configuration of the new stereogenic centre.

From a pharmacological point of view **(*R*)-SHA 68** was demonstrated to be the antagonist of the receptor of the Neuropeptide S.

This new class of non-peptide NPSR antagonists provides additional tools for *in vitro* and *in vivo* studies required to elucidate the NPSR conformation, adding new informations to well know NPS-NPSR system.

In the frame of the synthesis of biological active chiral compounds I have spend nine months at the Pierre et Marie Curie University in Paris under the supervision of Professor Giovanni Poli, focusing the attention on the synthesis of natural product (-)-Steganacin. This stage allowed me to view a different approach for the selective generation of new structures using a palladium catalysed domino reactions instead of the use of chiral auxiliaries used for the synthesis of **(*R*)** and **(*S*)-SHA 68**.

Steganacin was isolated from *Steganotaenia araliacea* a South Africa's plant.[31] The interest of chemists for the **(-)-Steganacin** was initially motivated by its antitumor activity; [34] it is for this reason that in literature we found different total syntheses of this molecule.

From a structural point of view the (-)-Steganacin presents a γ-lactonic skeleton condensed to an eight membered ring, a biarylic portion and three contiguous stereogenic centers with a relative stereochemistry *trans*, *trans*.

Aim of this project is the synthesis of an **aza-analogue of Steganacin** in which the lactone structure is replaced by a γ-lactam moiety.

The synthetic process starts from a commercially available propargyl alcohol to afford in seven steps the desired cyclization precursor in 19 % yield.

The key step of our project was previously studied in the laboratories of Prof. Giovanni Poli and reported in literature by Kammerer et al. in 2009.[41] This is an original regio- and stereoselective synthesis of aryl substituted pyrrolidones by a phosphine-free Pd-catalyzed allene carbopalladation/allylic alkylation sequence. This reaction allowed us to obtain the key intermediate in 74% yield.

After benzylation of this key intermediate, several strategies to remove the methoxycarbonyl group were tested, the best solution being hydrolysis in ethylene glycol at high temperatures. The next study will focus on the non-phenolic oxidative coupling between the two aromatic moieties to formed an eight membered ring.

Then, an oxidative cleavage of the double bond followed by a diastereoselective reduction of the resulting ketone and final alcohol acetylation should afford the desired **(-)-Steganacin aza-analogue**.

Bioorganic & Medicinal Chemistry 17 (2009) 5080–5095

Contents lists available at ScienceDirect

Bioorganic & Medicinal Chemistry

journal homepage: www.elsevier.com/locate/bmc

Structure–activity studies on the nociceptin/orphanin FQ receptor antagonist 1-benzyl-*N*-{3-[spiroisobenzofuran-1(3*H*),4′-piperidin-1-yl]propyl} pyrrolidine-2-carboxamide

Claudio Trapella [a,†], Carmela Fischetti [b,c,†], Michela Pela' [a], Ilaria Lazzari [a], Remo Guerrini [a,*], Girolamo Calo' [b], Anna Rizzi [b], Valeria Camarda [b], David G. Lambert [c], John McDonald [c], Domenico Regoli [b], Severo Salvadori [a]

[a] Department of Pharmaceutical Sciences and Biotechnology Center, University of Ferrara, via Fossato di Mortara 19, 44100 Ferrara, Italy
[b] Department of Experimental and Clinical Medicine, Section of Pharmacology and National Institute of Neuroscience, University of Ferrara, via Fossato di Mortara 19, 44100 Ferrara, Italy
[c] Department of Cardiovascular Sciences (Pharmacology and Therapeutics Group), Division of Anaesthesia, Critical Care and Pain Management, University of Leicester, Leicester Royal Infirmary, Leicester, LE1 5WW, UK

ARTICLE INFO

Article history:
Received 27 March 2009
Revised 20 May 2009
Accepted 23 May 2009
Available online 2 June 2009

Keywords:
SAR studies
NOP receptor antagonists
Receptor and [^{35}S]GTPγS binding
Mouse vas deferens
Calcium mobilization
Tail withdrawal assay

ABSTRACT

Twelve derivatives of the nociceptin/orphanin FQ (N/OFQ) receptor (NOP) antagonist 1-benzyl-*N*-{3-[spiroisobenzofuran-1(3*H*),4′-piperidin-1-yl]propyl} pyrrolidine-2-carboxamide (Comp 24) were synthesised and tested in binding experiments performed on CHO_{hNOP} cell membranes. Among them, a novel interesting NOP receptor antagonist (compound **35**) was identified by blending chemical moieties taken from different NOP receptor ligands. In vitro in various assays, Compound **35** consistently behaved as a pure, highly potent (pA_2 in the range 8.0–9.9), competitive and NOP selective antagonist. However compound 35 was found inactive when challenged against N/OFQ in vivo in the mouse tail withdrawal assay. Thus the usefulness of the novel NOP ligand compound 35 is limited to in vitro investigations.

1. Introduction

Nociceptin/orphanin FQ (N/OFQ)[1,2] modulates different biological functions via activation of the N/OFQ peptide receptor (NOP).[3] Few non-peptide molecules have been reported to selectively interact with the NOP receptor: these include the NOP agonist Ro 64-6198,[4] and the antagonists J-113397[5] and SB-612111[6] (see Chart 1). However, the chemical synthesis of such molecules, which are characterized by two chiral centres, is extremely complex, time consuming and of low yield, making the availability of these tools to the scientific community very limited.

Recently, a novel non-peptide NOP antagonist, 1-benzyl-*N*-{3-[spiroisobenzofuran-1(3*H*),4′-piperidin-1-yl]propyl} pyrrolidine-2-carboxamide, has been reported by Banyu researchers (as Comp **24**).[7] Comp **24** binds with high affinity (pIC_{50} 9.57) to the human recombinant NOP receptor showing an impressive selectivity (>3000-fold) over classical opioid receptors. Comp **24** behaves as a pure NOP antagonist in the [^{35}S]GTPγS assay with very high potency (pIC_{50} 9.82). Moreover, in vivo in mice Comp **24** at 10 mg/kg sc completely reverses the locomotor inhibitory effect elicited by a NOP receptor agonist.[7] Recently this molecule was synthesized and characterized in our laboratories confirming its excellent in vitro pharmacological profile in terms of high antagonist potency and selectivity of action over classical opioid receptors.[8] Moreover, in the mouse tail withdrawal assay, Comp **24** at 10 mg/kg ip did not modify per se tail withdrawal latencies but prevented the pronociceptive and antinociceptive effects of 1 nmol N/OFQ given supraspinally and spinally, respectively.[8] Collectively, these studies demonstrate that Comp **24** behaves as a pure, highly potent, selective and competitive NOP antagonist.

Interestingly, Comp 24 displays some chemical characteristics typical of N/OFQ related peptides (see Chart 1), these include: (i) a spacer of 12 atoms between the two phenyl rings which matches

Abbreviations: EtOAc, ethyl acetate; Bn-Cl, benzyl chloride; Boc_2O, di-*tert*-butyldicarbonate; BSA, bovine serum albumin; *n*-BuLi, normal butyllithyum; DCC, *N*,*N*′-dicicloexyl-carbodiimide; DCM, methylen chloride; DMF, *N*,*N*′-dimetilformammide; DPN, diprenorphine; Et_3N, triethylamine; Et_2O, diethylether; EtPt, light petroleum boiling fraction 40–60°; HOBt, 1-hydroxy-benzotriazole; *i*-PrOH, isopropanol; MeOH, methanol; rt, room temperature; NSB, non-specific binding; TBAF, tetrabutylamonium fluoride; TBDMS-Cl, *tert*-butyldimethylsilylchloride; TFA, trifluoro acetic acid; THF, tetrahydrofurane; TLC, thin layer chromatography; WSC, 1-ethyl-(3-dimethyl-amino-propyl)-carbodiimmide hydrochloride.

* Corresponding author. Tel.: +39 0532 455 988; fax: +39 0532 455953.
E-mail address: r.guerrini@unife.it (R. Guerrini).

† Both authors equally contributed to this work.

0968-0896/$ - see front matter © 2009 Elsevier Ltd. All rights reserved.
doi:10.1016/j.bmc.2009.05.068

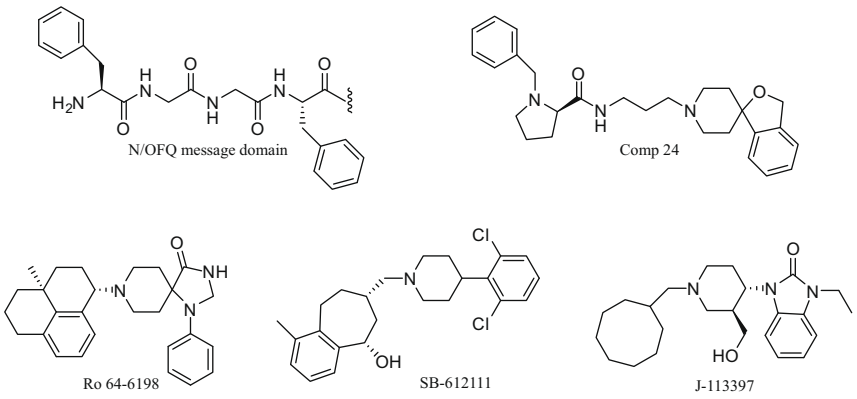

Chart 1. Chemical formulae of nociceptin/orphanin FQ receptor ligands.

the Phe-Gly-Gly-Phe sequence of the N/OFQ message domain; (ii) an amide bond which is quite uncommon in non-peptide NOP ligands; (iii) a *N*-benzyl amino acid, a chemical moiety also present in the N-terminal of the NOP receptor peptide antagonists [Nphe[1]]N/OFQ(1-13)-NH_2[9] and UFP-101.[10] Based on these considerations, in the present study, the importance of the *N*-benzyl D-Pro of Comp 24 was assessed by replacement with L- or D-Phe, and Nphe. In addition, the amide bond of Comp 24 was substituted with other amide bond isosters. Moreover, the spiroisobenzofurane nucleus of Comp 24 was replaced with chemical moieties derived from other non-peptide NOP ligands that is, Ro 64-6198,[4] SB-612111[6] and J-113397[5] (Chart 1). The novel molecules were evaluated for their ability to bind the human recombinant NOP receptor expressed in CHO cell (CHO_{hNOP}) membranes. The molecule with the highest affinity, that is, compound **35** has been further characterized in vitro at the recombinant human NOP in [^{35}S]GTPγS binding and calcium mobilization assays and at native NOP receptors expressed in isolated animal (mouse, rat, guinea-pig) tissues. Finally compound **35** was assayed in vivo against the effects elicited by N/OFQ in the mouse tail withdrawal assay.

2. Chemistry

Compound **24** was synthesized following procedures reported by Goto et al.[7] The key intermediate **5** (Scheme 1) was obtained starting from commercially available benzanilide **1** that reacts with *n*-butyllithium at −78 °C and subsequentially with the *N*-benzyl-

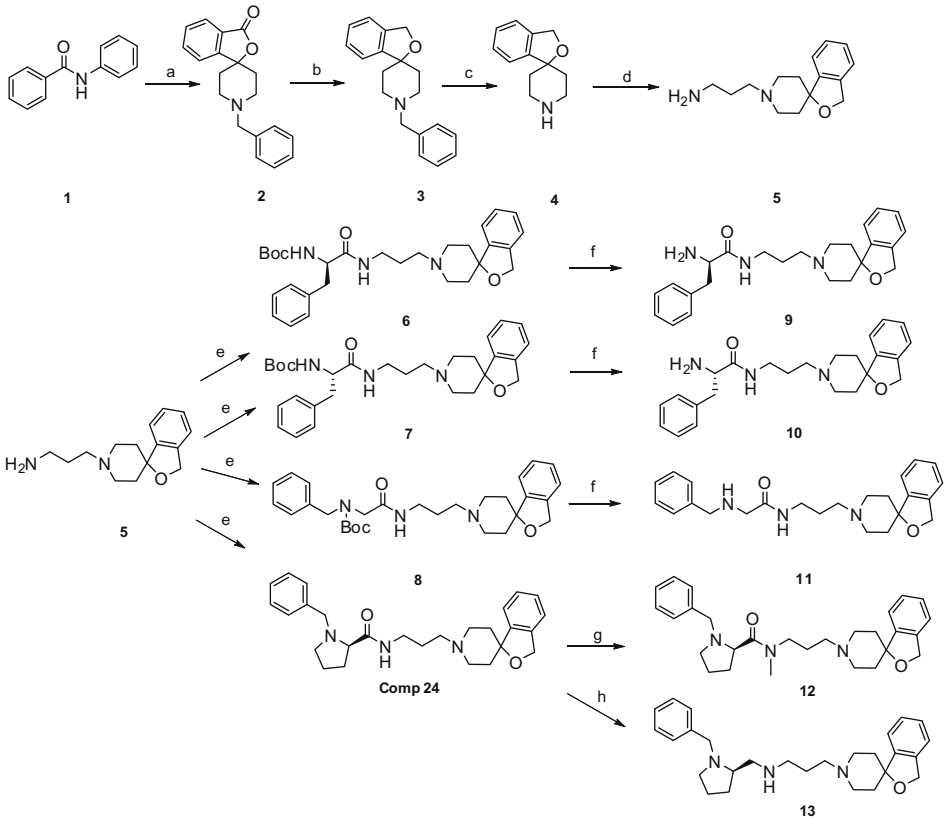

Scheme 1. Reagents and conditions: (a) *n*-BuLi 2.5 M, −78 °C, *N*-benzyl-piperidine-4-one, 0 °C, THF; (b) $(CH_3)_2S^*BH_3$, THF, 0 °C to reflux; (c) H_2, C/Pd 10%, EtOH, overnight; (d) *N*-Boc-3-bromo-propyl amine DMF, 60 °C, 3 h, then DCM TFA 1 h; (e) L-Phe, D-Phe, Nphe or *N*-Bn-D-Pro, DMF, HOBt. WSC, 0 °C to rt, 24 h; (f) TFA, 0 °C, 1 h; (g) $(CH_3)_2S^*BH_3$, THF, 0 °C to reflux O.N.; (h) CH_3I, NaH, DMF, 0 °C to rt, O.N.

piperidone to give the spiroisobenzofuran-2-one **2**. Compound **2** was reduced with borane dimethyl sulfide complex in THF to give the corresponding isobenzofurane **3**. The deprotection of the piperidine nitrogen using H_2 in presence of palladium on charcoal 10% afforded the desired spiroisobenzofurane piperidine **4** in good yield.

Alkylation with *N*-Boc-3-bromo-propyl amine followed by TFA treatment gave the free amine **5.** The substitution in compound 24 of the D-Pro amino acid with the D-Phe, L-Phe and Nphe was achieved using compound **5** and the corresponding protected aminoacid for the coupling reaction, removing the Boc protected group from the amino function with TFA at 0 °C. This allowed us to obtain compounds **9**, **10** and **11** (Scheme 1).

The *N*-methyl alkylation or the reduction of the amide bond of compound **24** produced the final compounds **12** and **13**.

The substitution of the amide bond in Comp 24 with ester or ether bond was achieved following Scheme 2. 3-Bromo-1-propanol, was protected as TBDMS derivative (**14)** and reacted with **4** in DMF at 60 °C in the presence of potassium carbonate to obtain compound **15**. Treatment of **15** with TBAF in THF allows us to obtain the corresponding alcohol **16** which was condensed with the *N*-Bn-D-Pro using the Steglich esterification[11] to obtain the desired ester **17**

All the attempt to prepare the tosylate of **16** using tosyl chloride and Et_3N, generated the corresponding chloride **18**, which is employed in the esterification reaction[12] with Bn-D-prolinol **19** using tetrabutyl ammonium iodide as an exchanging agent to obtain the ether **20.**

The replacement of the amide bond present in Comp 24 with a olefin moiety was the most difficult procedure, in particular, all the attempts to prepare the desired olefin via Wittig[13] or Horner–Wadsworth–Emmons[14] reaction on the *N*-Bn-Prolinale[15] using the (3-carboxy-propyl)-triphenylphosphonium bromide **21**, failed. In contrast, using the dimethylsulfynil anion[16,17] to generate the corresponding ylide allowed us to obtain the corresponding olefin **22** in moderate yield.

Compound **22** was reacted with **4** in the presence of WSC/HOBt and the amide bond of **23** reduced using borane dimethylsulfide complex to obtain the desired olefin derivative **25** as a inseparable mixture of *E/Z* isomers (Scheme 3).

The synthesis of compound **28** (Scheme 4) started from the commercially available 1-phenyl-1,3,8-triaza-spiro[4.5]decan-4-one **26** that was alkylated using the conditions previously reported for **5** with *N*-Boc-3-bromo-propyl amine to obtain in a good yield the derivative **27**. Deprotection of *tert*-butoxycarbonil moiety and the coupling with *N*-Bn-D-Pro allowed us to obtain the chimeric compound **28** as depicted in Scheme 4.

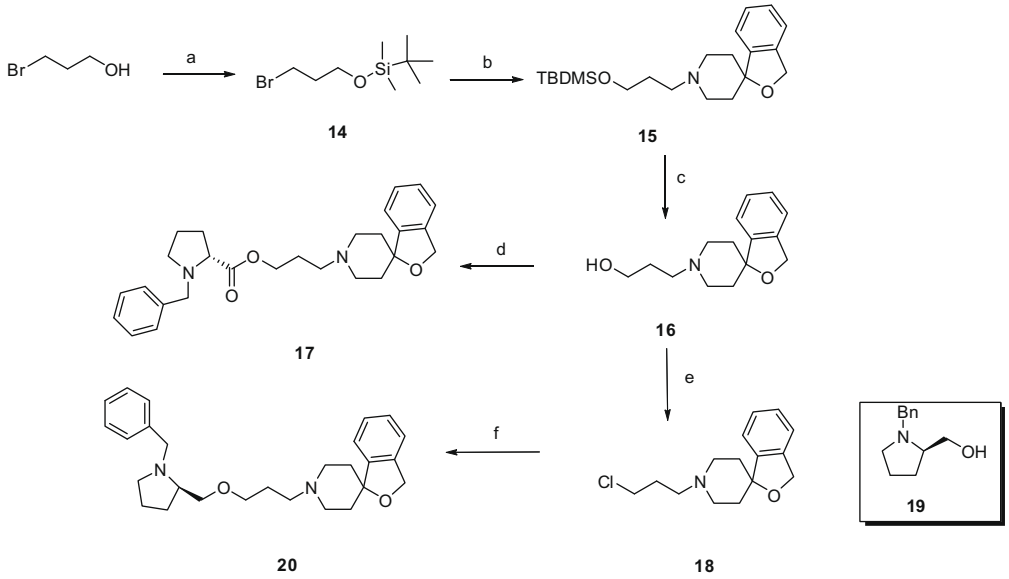

Scheme 2. Reagents and conditions: TNDMS-Cl, imidazole, THF, rt, 24 h; (b) (**4**), K_2CO_3, DMF, 60 °C, O.N.; (c) TBAF, THF, 24 h; (d) *N*-Bn-D-Pro, HOBt, WSC, DMF, rt, O.N.; (e) tosyl chloride, Et_3N, CH_2Cl_2, 0 °C to rt, O.N.; (f) (**15**) TBAI, NaH, DMF, 0 °C to rt, O.N.

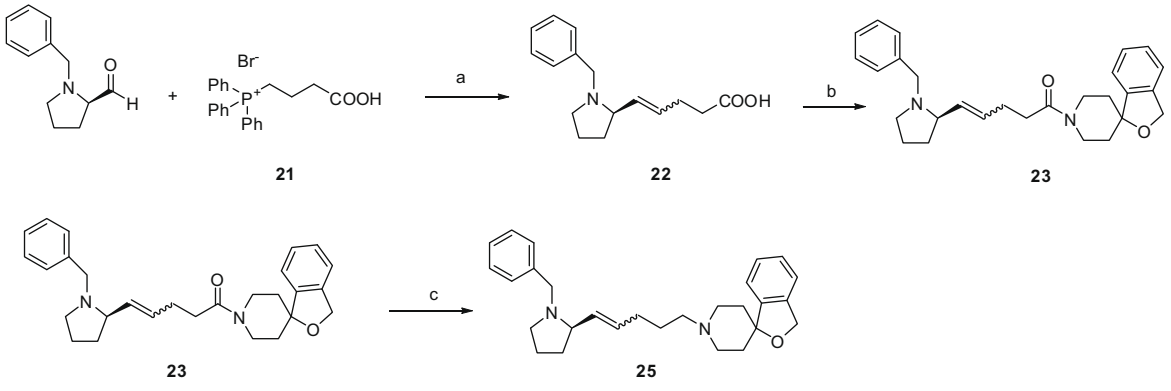

Scheme 3. Reagents and conditions: (a) NaH, DMSO, 77 °C 40 min, than *N*-Bn-D-Pro at 0 °C to rt, O.N.; (b) (**4**) DMF, HOBt, WSC, rt, O.N.; (c) THF, $(CH_3)_2S^* BH_3$, 0 °C to reflux O.N.

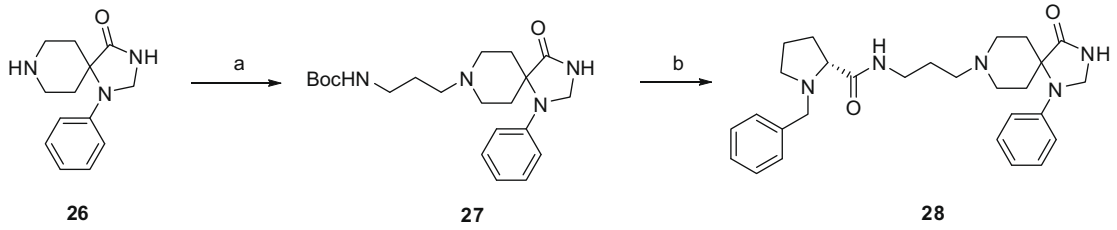

Scheme 4. Reagents and conditions: (a) DMF, BocNH-$(CH_2)_3$-Br, K_2CO_3, 60 °C, 1 h; (b) (i) TFA, 0 °C, 1 h; (ii) *N*-Bn-D-Pro, DMF, HOBt, WSC, 0 °C to rt, O.N.

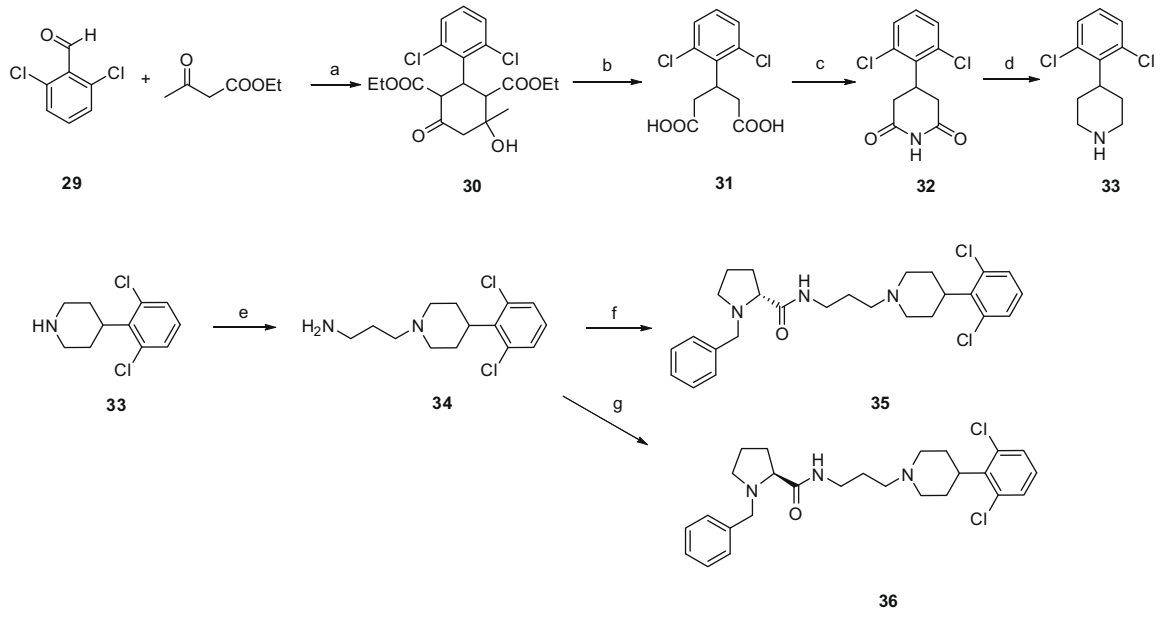

Scheme 5. Reagents and conditions: (a) EtOH, Pip, rt, O.N.; (b) NaOH 35%, EtOH, reflux, O.N.; (c) NH_4OH, 200 °C, 6 h; (d) $(CH_3)_2S^* BH_3$, THF, 0 °C to reflux O.N.; (e) DMF K_2CO_3, BocNH-$(CH_2)_2$-Br, 60 °C, O.N., then TFA; (f) DMF, HOBt, WSC, *N*-Bn-D-Pro, 0 °C to rt, O.N.; (g) DMF, HOBt, WSC, *N*-Bn-L-Pro, 0 °C to rt O.N.

The synthesis of the 4-(2,6-dichlorophenyl)-piperidine **33** starts from the reaction of 2,6-dichloro-benzaldehyde **29** with ethyl acetoacetate to give the diester **30**. Hydrolysis under basic conditions of **30** allowed us to obtain the corresponding diacid **31** that was treated with ammonia at 200 °C for 6 h to gave the immide **32**. Reduction using borane dimethyl sulfide complex of **32** gave the desired 4-(2,6-dichloro-phenyl)-piperidine **33** in moderate yield. The final compounds **35** and **36** were prepared using **33** following procedures reported in Scheme 2d (Scheme 5).

The compound **41** was prepared starting from the *tert*-butyloxycarbonyl protection of the commercially available 1-piperidin-4-yl-1,3-dihydro-benzoimidazol-2-one **37**. N3 ethylation of **38** with ethyl

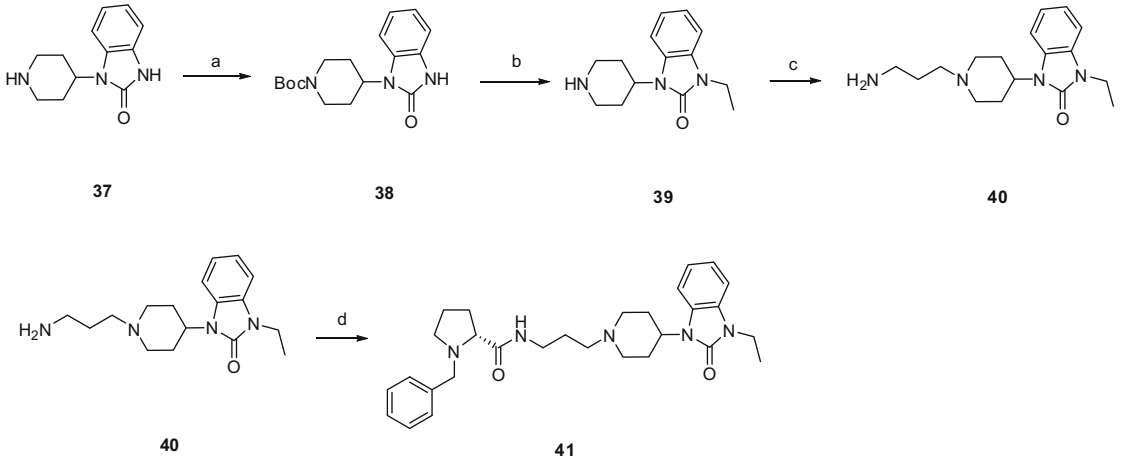

Scheme 6. Reagents and conditions: (a) CH_2Cl_2, $(Boc)_2O$, DMAP; (b) (i) DMF, EtBr, NaH, 0 °C to rt, 5 h; (ii) TFA, 1 h,rt; (c) (i) DMF, K_2CO_3, BocNH-$(CH_2)_3$-Br, 60 °C, 1 h; (ii) TFA, 1 h; (d) DMF, HOBt, *N*-Bn-D-Pro, 0 °C to rt, O.N.

bromide in presence of sodium hydride followed by TFA treatment gave compound **39**. The reaction of **39** with *N*-Boc-3-bromo-propyl amine followed by deprotection and acylation with *N*-Bn-D-Pro allowed us to obtain the final compound **41** (Scheme 6).

Compound **35** was selected as the most interesting molecule of this series. It was obtained with an overall yield of 21%. This value is similar to the overall yield of Comp **24** (25% in our laboratories[8], 31% in Banju laboratories[7]). On the contrary the overall yield of other NOP antagonists such as J-113397 and SB-612111 is much lower (approx. 1–2% in our laboratories). Moreover, the synthesis of the 2,6-dichlorophenyl-piperidine moiety of SB-612111 used for generating compound **35** has been performed avoiding the tedious, money and time consuming chromatographic purifications. In addition, the complete synthesis of compound **35** has been obtained in six steps while those of Comp **24** and of SB-612111 require 8 and 12 steps, respectively.

3. Results and discussion

The ability of the reference ligand, Comp **24**, and the novel molecules to bind to the NOP receptor was evaluated using CHO_{hNOP} cell membranes (Table 1). Comp **24** produced a concentration dependent inhibition of [^{3}H]N/OFQ binding with a pK_i value of 9.62. This result perfectly matches with that previously reported by Goto et al.[7] (pIC_{50} 9.57). The substitution of the *N*-benzyl D-Pro with D or L-Phe (compounds **9** and **10**) or Nphe (compound **11**) produced a profound (>100-fold) loss of NOP affinity suggesting a pivotal role of the *N*-benzyl D-Pro moiety for Comp **24** bioactivity. This result is not surprising since the simple inversion of Pro chirality was reported to generate an analogue 200-fold less potent than Comp **24**.[7]

Modifications of the amide bond obtained by N-methylation (compound **12**) or by replacement with a methyleneamino (compound **13**), an ester (compound **17**), a methyleneoxy (compound **20**), or an alkene bond (compound **25**), produced a drastic reduction in NOP receptor binding or, in the case of compound **25**, a complete loss of affinity. These results indicated that the amide bond represents a chemical feature crucial for the bioactivity of Comp 24. It is worthy of note, that an amide bond is a relatively uncommon chemical feature in non-peptide NOP ligands. However, this chemical bond is also present in the NOP receptor antagonist JTC-801 and its chemical modification (i.e., N-methylation and retro-inverso bond) was reported to be detrimental for binding affinity.[18] Thus, the amide bond might play a similar important role in both Comp 24 and JTC-801. In particular, according to the non-peptide NOP ligand pharmacophoric model proposed by Zaveri,[19] the amide bond may be part of the B-moiety that links and contributes to the maintainance of the correct spatial arrangement of the A-moiety (important for ligand affinity and selectivity) and the C-moiety (important for ligand efficacy).

Next, we considered replacement of the benzoisofurane group in position 4 of the Comp 24 piperidine scaffold with chemical moieties taken from the some position of other high affinity NOP receptor ligands. The substitution with 1-phenylimidazolidin-4-one, the chemical group of the NOP receptor agonist Ro 64-6198 (compound **28**), or with 1-ethylbenzoimidazol-2-one, the chemical group of the NOP receptor antagonist J-113397 (compound **41**), in position 4 generated inactive molecules. In contrast, the insertion of the piperidine scaffold of the 2,6-dichlorophenyl moiety (compound **35**), the pharmacophore of the NOP receptor antagonist SB-612111, in position 4 generated a molecule with high affinity for the NOP receptor (pK_i 9.14). In particular compound **35** is only threefold less potent than Comp 24. The results obtained with this limited series of chimeric compounds suggest that it is possible to combine pharmacophoric moieties taken from different NOP receptor ligands to generate novel biologically active molecules. In particular, the chemical groups benzoisofurane and 2,6-dichlorophenyl seem to contribute to NOP receptor binding in a very similar manner. This is corroborated by the finding that the substitution of D-Pro with L-Pro in the chimeric molecule compound **36** produced a 100-fold reduction in receptor affinity. This result is in agreement with compounds **22** and **23** of the Goto series.[7] Thus, D chirality of the Pro residue represents a crucial requirement for high affinity NOP receptor recognition for both Comp 24 and compound **35**.

Based on its high affinity for the NOP receptor, compound **35** was selected for further pharmacological characterization in vitro and in vivo. As shown in Figure 1 (top left panel) in CHO_{hNOP} cell membranes N/OFQ concentration dependently stimulated [^{35}S]GTPγS binding with pEC_{50} and E_{max} values of 8.91 and 10.93 ± 0.18 (stimulation factor), respectively. Over the concentration range of 1–100 nM, compound **35** was inactive per se but produced a rightward shift of the concentration response curve to N/OFQ in a parallel manner and without modifying the agonist maximal effect. Schild analysis of these data (Fig. 1 top right panel) is compatible with a competitive type of antagonism and a pA_2 value of 9.91 was derived. This potency value is close to that previously reported for Comp **24** by Goto et al. (pIC_{50} 9.82)[7] and by us (pA_2 9.98).[8] These results suggest that the benzoisofurane and 2,6-dichlorophenyl moieties of Comp **24** and compound **35** play a similar role not only in receptor binding but also in determining pharmacological activity that is, pure and competitive antagonism. This may be derived from the common ability of the spiro junction (Comp **24**) and of the 2,6-dichloro substitution (compound **35**) to favour an orthogonal spatial disposition between their piperidine and phenyl nuclei. Therefore, this conformational feature may likely be crucial for both NOP receptor binding and antagonist activity.

The pharmacological actions of compound **35** were further assessed at the hNOP receptor coupled to calcium signalling via the chimeric protein Gαqi5; this assay has been previously validated with a large panel of NOP receptor full and partial agonists and antagonists.[20] In CHO cells stably expressing the hNOP receptor and the Gαqi5 protein, N/OFQ produced a concentration dependent stimulation of intracellular calcium with a pEC_{50} of 9.24 and E_{max} of 198 ± 12% over the basal values. Compound **35** was inactive per se up to 10 μM while inhibiting the stimulatory effect of 10 nM N/OFQ in a concentration dependent manner. A pK_b value of 8.47 was derived from these experiments (Table 2). This potency value is approx threefold lower than that obtained with Comp **24** (pK_b 9.03).[8]

The competitive antagonist behaviour of compound **35** was confirmed at the native NOP receptor expressed in the mouse vas deferens. In this preparation, N/OFQ inhibited electrically evoked twitches in a concentration dependent manner with pEC_{50} and E_{max} values of 7.49 and −80 ± 2%, respectively (Fig. 1, right top panel). Compound **35** was inactive per se but caused a concentration dependent (10–1000 nM) and a parallel rightward shift of the concentration response curve to N/OFQ without modifying the agonist maximal effects. The relative Schild plot, depicted in Figure 1 right bottom panel, demonstrated a competitive type of antagonism with a pA_2 value of 8.00. This value of potency is close to that previously reported for Comp **24** that is, 8.24.[8] Similar results were obtained in other N/OFQ sensitive preparations such as the rat vas deferens and guinea pig ileum where compound **35** at 100 nM was inactive per se while antagonizing N/OFQ inhibitory actions with pK_b values of 8.06 and 8.84, respectively (Table 2).

Finally the selectivity of action of compound **35** over classical opioid receptors was assessed in animal tissues expressing native receptors and at recombinant human proteins. Compound **35** at 1 μM was inactive per se and did not modify the inhibitory effects

Table 1
Binding affinities at CHO_{hNOP} cell membranes of Comp 24 and related compounds

Compound	Structure	pK_i
Comp **24**	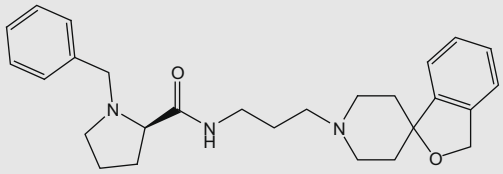	9.62 ± 0.07
9	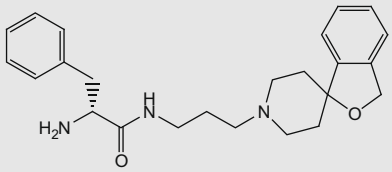	7.23 ± 0.19
10	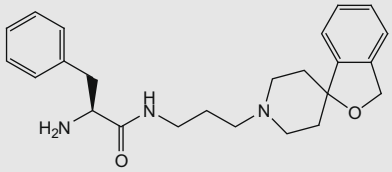	7.23 ± 0.05
11	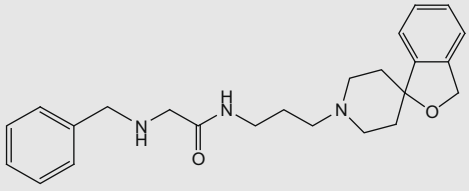	7.22 ± 0.08
12	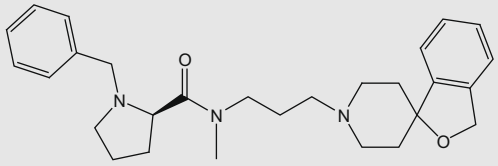	5.94 ± 0.28
13	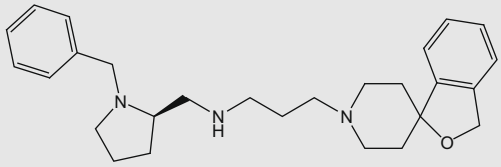	7.31 ± 0.06
17	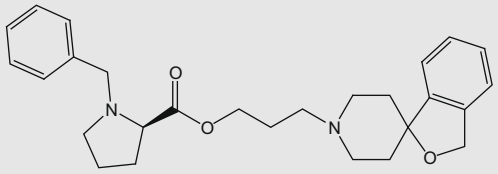	6.97 ± 0.02
20	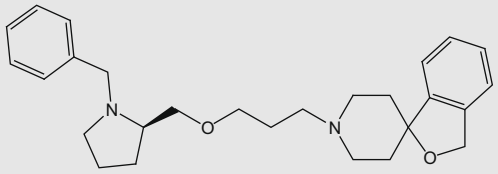	6.80 ± 0.80
25	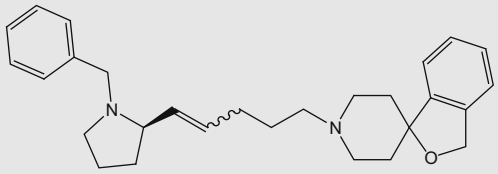	<5

(*continued on next page*)

Table 1 (*continued*)

Compound	Structure	pK_i
28	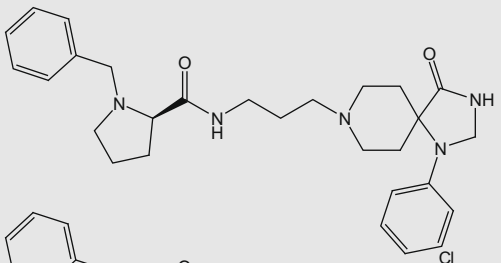	<5
35	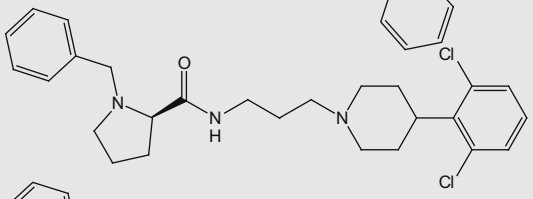	9.14 ± 0.05
36	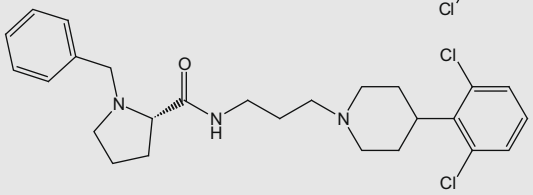	7.08 ± 0.02
41	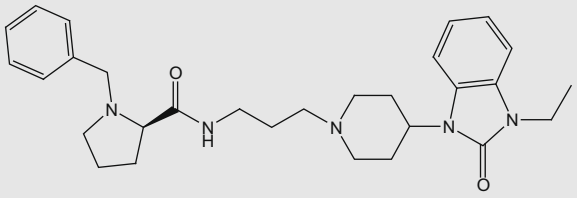	<5

Data are means ± sem of four separate experiments performed in duplicate.

elicited by the DOP selective agonist DPDPE in the mouse vas deferens (control pEC_{50} 8.38 ($CL_{95\%}$ 8.20–8.56), E_{max} −98 ± 1%; 1 μM compound **35** pEC_{50} 8.44 ($CL_{95\%}$ 8.26–8.62), E_{max} −98 ± 1%) or those produced by the MOP agonist dermorphin in the guinea pig ileum (control pEC_{50} 8.52 ($CL_{95\%}$ 8.35–8.69), E_{max} −90 ± 3%; 1 μM compound **35** pEC_{50} 8.44 ($CL_{95\%}$ 8.19–8.69), E_{max} −85 ± 5%). Results obtained with compound **35** and the universal opioid receptor antagonist naloxone in selectivity studies performed with receptor binding and calcium mobilization assays are summarized in Tables 3 and 4, respectively. Compound **35** up to 10 μM did not displace [^{3}H]DPN from DOP sites and showed very low affinity (less than 300-fold compared to NOP) at MOP and KOP sites (Table 3). In contrast, naloxone did not bind to the NOP receptor up to 10 μM, while it displaced [^{3}H]DPN at classical opioid receptors showing very high affinity for MOP and lower affinities for KOP and DOP (Table 3). Similar results were found in functional studies measuring calcium mobilization in CHO cells stably expressing the hNOP receptor or classical opioid receptors and the Gαqi5 protein (Table 4). Dermorphin, DPDPE and dynorphin A were used in these experiments as agonists for MOP, DOP and KOP receptors, respectively; they produced a concentration dependent stimulation of intracellular calcium with the following pEC_{50} values: 7.93 ($CL_{95\%}$ 7.67–8.19), 8.82 ($CL_{95\%}$ 8.43–9.21) and 8.47 ($CL_{95\%}$ 8.16–8.78). Naloxone inhibited the effects of these agonists with higher potency at MOP than KOP and DOP while being inactive against N/OFQ (Table 4). Thus, compound **35** was at least 300-fold less potent at classical opioid receptors than at the NOP receptor (Table 4).

These in vitro results demonstrated that compound **35** behaves as a pure, potent and competitive NOP receptor antagonist. Moreover selectivity studies indicated that the substitution of the benzoisofurane with the 2,6-dichlorophenyl moiety not only allows maintenance of high affinity and antagonist potency but also of high selectivity over classical opioid receptors.

Finally the pharmacological activity of compound **35** was assessed in vivo using the mouse tail withdrawal assay. In this test N/OFQ was reported to elicit opposite effects depending on the route of administration: the peptide induced pronociceptive actions when injected intracerebroventricularly (icv) while antinociceptive effects were reported after intrathecal (i.t.) injection (see for reviews[3,21] and for results obtained in our laboratories[22,23]). As shown in Figure 2 left panel, mice injected with saline displayed similar tail withdrawal latencies (≈6 s) over the time course of the experiment. N/OFQ 1 nmol given icv produced a clear but short lasting pronociceptive effect. Compound **35** at 10 mg/kg given intraperitoneally 30 min before icv injection, did not modify tail withdrawal latencies per se and did not affect the pronociceptive action of the peptide. When 1 nmol N/OFQ was given i.t., the peptide elicited a robust antinociceptive effect (Fig. 2 right panel). Again compound **35** at 10 mg/kg did not modify the effect of N/OFQ. Thus, in the mouse tail withdrawal assay compound **35** at 10 mg/kg was found inactive against the pronociceptive and antinociceptive effects of N/OFQ injected supraspinally and spinally, respectively. Under these same experimental conditions Comp 24 at 10 mg/kg significantly counteracted the actions of N/OFQ[8], while SB-612111 already at 1 mg/kg fully prevented the effects of the peptide.[24] Thus, despite a very similar in vitro pharmacological profile, the three NOP antagonists displayed very different in vivo potency that is, SB-612111 > Comp 24 ≫ compound **35**. Although the reasons for such variable in vivo potency are at present unknown, they might be due to

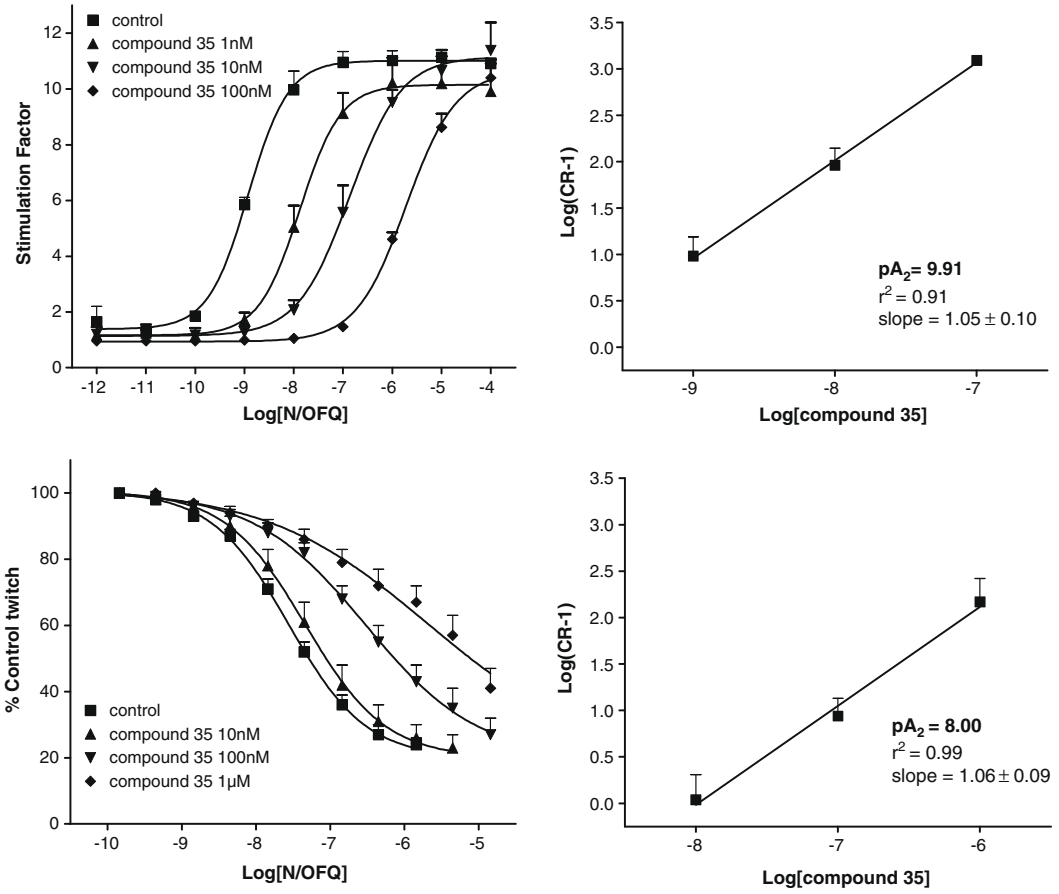

Figure 1. Concentration–response curve to N/OFQ in the absence and presence of increasing concentrations of compound **35** for [^{35}S]GTPγS binding to CHO_{hNOP} cell membranes (top left panel) and in electrically stimulated mouse vas deferens (bottom left panel). The corresponding Schild plots are shown in the right panels. Data are means ± SEM of four separate experiments.

Table 2
Compound **35** affinity/antagonist potency in various pharmacological assays

	CHO_{hNOP} cell membranes		$CHO_{hNOP/G\alpha qi5}$ cells	Electrically stimulated tissues		
	Receptor binding	[^{35}S]GTPγS binding	Ca^{2+} mobilization	Mouse vas deferens	Rat vas deferens	Guinea pig ileum
Compound **35**	9.14 (9.04–9.24)	9.91 (9.23–10.59)	8.47 (8.31–8.63)	8.00 (7.32–8.68)	8.06 (7.58–8.54)	8.84 (8.64–9.04)

Data are expressed as means ($CL_{95\%}$) of at least four separate experiments.

Table 3
Affinities of compound **35** and naloxone at NOP and classical opioid receptors expressed in CHO cell membranes

Receptor radioligand	NOP [^{3}H]N/OFQ	MOP [^{3}H]DPN	DOP [^{3}H]DPN	KOP [^{3}H]DPN
Naloxone	<6	9.25 (9.04–9.46)	7.67 (7.59–7.75)	8.35 (8.20–8.50)
Compound **35**	9.14 (9.04–9.24)	6.72 (6.47–6.97)	<6	6.50 (6.37–6.63)

Data are expressed as mean ($CL_{95\%}$) of four separate experiments. Naloxone data at classical opioid receptors are obtained from Vergura et al.[33]

Table 4
Antagonist potencies of compound **35** and naloxone evaluated in calcium mobilization experiments performed in CHO cells expressing NOP or classical opioid receptors and the $G\alpha_{qi5}$ protein

Receptor agonist	NOP N/OFQ 10 nM	MOP dermorphin 100 nM	DOP DPDPE 100 nM	KOP dynorphin A 100 nM
Naloxone	<6	9.09 (8.73–9.45)	7.32 (6.80–7.84)	7.14 (6.60–7.68)
Compound **35**	8.47 (8.31–8.63)	6.11 (5.92–6.30)	<6	<6

Data are expressed as mean ($CL_{95\%}$) of four separate experiments performed in duplicate.

marked differences in pharmacokinetics between the three molecules. Therefore the blending of Comp 24 and SB-612111 chemical moieties to generate compound **35** did not affect pharmacodynamics (i.e., receptor affinity, antagonist potency and selectivity of action) while it seems to have a detrimental effect on pharmacokinetics.

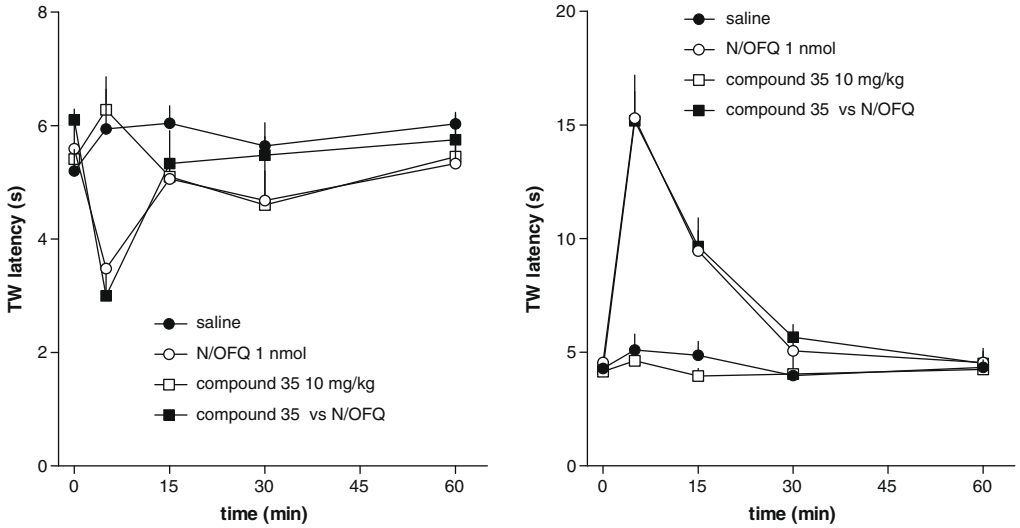

Figure 2. Mouse tail withdrawal assay. Effects of compound **35** (10 mg/kg ip, 30 min pre-treatment) on the pronociceptive or antinociceptive effects induced by 1 nmol N/OFQ injected icv (left panel) or i.t. (right panel). Data are mean ± SEM of four separate experiments.

4. Conclusions

The present study demonstrated that the *N*-benzyl D-Pro moiety as well as the amide bond of Comp 24 is essential for biological activity. In contrast the spirobenzoisofurane can be replaced with 2,6-dichlorophenyl moiety without significant loss of ligand potency, antagonist activity and selectivity of action. Thus by blending chemical moieties taken from known molecules (Comp 24 and SB-612111) we were able to identify compound **35** as a novel non-peptide selective NOP antagonist. While the in vitro pharmacological profile of compound **35** is similar to that of Comp 24 and SB-612111, the in vivo activities of these compounds are substantially different with the following order of antagonist potency SB-612111 > Comp 24 ≫ compound **35**. This limits the usefulness of compound **35** to in vitro investigations.

5. Experimental

5.1. Materials

Melting points (uncorrected) were measured with a Buchi-Tottoli apparatus, and ^{1}H, ^{13}C, and NMR spectra were recorded on a VARIAN400 MHz instrument unless otherwise noted. Chemical shifts are given in ppm (δ) relative to TMS and coupling constants are in hertz. MS analyses were performed on a ESI-Micromass ZMD 2000. Infrared spectra were recorded on a Perkin–Elmer FT-IR Spectum 100 spectrometer. Flash chromatography was carried out on a silica gel (Merck, 230–400 Mesh). Elemental analyses were performed at the analytical laboratories of the Department of Chemistry, University of Ferrara.

5.2. Synthetic procedure

5.2.1. 1′-Benzyl-spiro[isobenzofuran-1(3*H*),4′-piperidin]-3-one (2)

To a stirred solution of **1** (5 g, 25.38 mmol) in anhydrous THF at −78 °C and in argon atmosphere, *n*-BuLi (25.98 mL, 64.97 mmol) was added drop wise. The reaction was warmed at 0 °C for 1 h until a red-orange color appeared. At this time, *N*-benzyl-piperidone (10.68 mL, 57.61 mmol) was added and the reaction stirred at room temperature overnight. The reaction was checked by TLC (EtOAc/light petroleum, 3:2), quenched with HCl 3 N and the aqueous layer partitioned in chloroform and extracted three times with chloroform (30 mL each). The organic layer was dried and concentrated in vacuo to afford a yellow solid after crystallization with Et_2O (6.54 g, 22.345 mmol, yield 88%). mp = 210–215 °C. MS (ESI): $[MH]^+ = 294$. ^{1}H NMR ($CDCl_3$): δ 7.872 (td, 1H, $J = 8$, 0.9 Hz); 7.660 (dt, 1H, $J = 7.4$, 1.2 Hz); 7.51 (dt, 1H, $J = 7.4$, 0.8 Hz); 7.42 (td, 1H, $J = 7.6$, 0.7 Hz); 7.38–7.31 (m, 4H); 7.29–7.25 (m, 1H); 3.62 (s, 2H); 2.92 (dd, 2H, $J = 9$, 2.2 Hz); 2.56 (dt, 2H, $J = 12$, 2.4 Hz); 2.23 (dt, 2H, $J = 13.2$, 4.4 Hz); 1.71 (dd, 2H, $J = 14.4$, 2.4 Hz). ^{13}C NMR ($CDCl_3$): 168.80; 151.37; 135.09; 131.33 (2C); 130.36; 130.21; 129.53 (2C); 126.14 (2C); 124.80; 121.79; 81.56; 61.31; 48.92 (2C); 33.02 (2C).

5.2.2. 1′-Benzyl-spiro[isobenzofuran-1(3*H*),4′-piperidine] (3)

Under argon atmosphere 6.54 g (22.34 mmol) of compound **2** were suspended in anhydrous THF, the reaction mixture cooled at 0 °C and under vigorously stirring $(CH_3)_2S^{*}BH_3$ (4.30 mL, 44.68 mmol) was added drop wise. The reaction mixture was heated at reflux overnight. After this time the reaction was acidified (HCl 10%) until pH 2 and heated again at reflux for 4 h. The reaction was quenched with NaOH 2 N until pH 12, the THF was removed in vacuo and the aqueous layer extracted twice with EtOAc (30 mL each). The organic layer was dried, concentrated in vacuo and purified by flash chromatography (EtOAc/light petroleum, 1:1) to afford compound **3** in 55% yield. MS (ESI): $[MH]^+ = 280$. ^{1}H NMR ($CDCl_3$): δ 7.39–7.15 (m, 9H); 5.07 (s, 2H,); 3.60 (s, 2H); 2.85 (dd, 2H, $J = 10$, 2 Hz); 2.44 (dt, 2H, $J = 12$, 2.4 Hz); 2.01 (dt, 2H, $J = 13.2$, 4.4 Hz); 1.76 (dd, 2H, $J = 14.4$, 2.4 Hz). ^{13}C NMR ($CDCl_3$): 145.78; 138.98 (2C); 129.43 (2C); 128.28 (2C); 127.59; 127.38; 127.10; 121.10; 120.89; 84.81; 70.78; 63.54; 50.21 (2C); 36.64 (2C).

5.2.3. Spiro[isobenzofuran-1(3*H*),4′-piperidine] (4)

A solution of **3** (3.43 g, 12.29 mmol) in 200 mL of ethanol was hydrogenated in the Parr apparatus (50 psi) in the presence of 10% palladium on charcoal (0.1 g) for 48 h. Filtration of the catalyst through a Celite pad and solvent evaporation gave (**4**) (2.20 g, 11.64 mmol, yield 70%) as a colorless oil. MS (ESI): $[MH]^+ = 190$. ^{1}H NMR ($CDCl_3$): δ 7.31–7.28 (m, 2H); 7.23–7.21 (m, 2H); 5.79 (br, 1H); 5.06 (s, 2H); 3.40–3.87 (m, 2H); 2.75–2.65 (m, 2H); 2.37–2.28 (m, 2H); 1.83–1.81 (m, 2H).

5.2.4. 3-[Spiro[isobenzofuran-1(3*H*),4′-piperidin-1-yl]] propylamine (5)

To a stirred solution of **4** (2 g, 10.58 mmol) in DMF a solution of *N*-Boc-3-bromo-propyl-amine (2.99 g, 12.59 mmol) in 10 mL of DMF was added followed by addition of K_2CO_3 (2.92 g, 21.16 mmol); the reaction was warmed at 60 °C for 1 h. The reaction was concentrated and the residue was diluted with EtOAc and washed twice with NH_4Cl saturated solution (30 mL each) and brine (30 mL). The organic layer was dried and evaporated under reduced pressure. The crude material (3.45 g, 9.99 mmol) was treated with TFA at 0 °C for 1 h. NaOH 2 N was added until pH 12–14, the aqueous phase was extracted several times with EtOAc and the organic phases were combined, dried and evaporated under vacuum to give compound **5** (2.32 g, 9.417 mmol, 95% yield). MS (ESI): $[MH]^+ = 247$. ^1H NMR ($CDCl_3$): δ 7.27–7.24 (m, 2H); 7.20–7.14 (m, 2H); 5.06 (s, 2H); 2.89 (dd, 2H, $J = 9.4$, 2 Hz); 2.81 (t, 2H, $J = 6.8$ Hz); 2.50 (t, 2H, $J = 7.2$ Hz); 2.38 (t, 2H, $J = 12.4$ Hz); 2.23 (br, 2H); 1.98 (dt, 2H, $J = 12.4$, 4.4 Hz); 1.79–1.70 (m, 4H).

5.2.5. (D)-1-{3-[Spiro[isobenzofuran-1(3*H*),4′-piperidin-1-yl]-propylcarbamoyl}-2-phenyl-ethyl)-carbamic acid-*tert*-butyl estere (6)

To a stirred solution of Boc-D-Phe-OH (539 mg, 2.032 mmol) in DMF at 0 °C, HOBt (373 mg, 2.44 mmol) and WSC (467 mg, 2.44 mmol) were added and the reaction stirred for 10 min. After this time compound **5** (500 mg, 2.032 mmol) dissolved in DMF (20 mL) was added and the reaction mixture stirred for 24 h. The DMF was removed in vacuo and the product partitioned between EtOAc and $NaHCO_3$ 5%. The organic phase was dried, concentrated in vacuum and the crude product purified by flash chromatography (EtOAc/NH_4OH, 10:0.3) to give compound **6** in 30% yield. MS (ESI): $[MH]^+ = 494$. ^1H NMR ($CDCl_3$): δ 7.42 (br, 1H); 7.28–7.15 (m, 9H); 5.83 (br, 1H); 5.03 (s, 2H); 3.43 (s, 1H); 3.55–3.16 (m, 3H); 3.08–2.95 (m, 2H); 2.90–2.80 (m, 3H); 2.50–2.44 (m, 4H); 1.76–1.68 (m, 4H); 1.36 (s, 9H). ^{13}C NMR ($CDCl_3$): 173.02; 171.38; 144.70; 138.62; 136.946; 129.35 (2C); 128.63 (2C); 128.54; 127.83; 127.56; 126.82; 121.05 (2C); 83.92; 70.90; 60.41; 56.31; 50.498; 49.88; 39.06; 38.38; 35.82; 35.72; 28.29 (3C); 24.67. $[\alpha]_D^{20} = -8$ ($c = 0.1$ g/100 mL, chloroform).

5.2.6. (L)-1-{3-[Spiro[isobenzofuran-1(3*H*),4′-piperidin-1-yl]-propylcarbamoyl}-2-phenyl-ethyl)-carbamic acid-*tert*-butyl estere (7)

This product was obtained as reported for **6** using Boc-Phe-OH instead of Boc-D-Phe-OH. The crude product was purified by flash chromatography (EtOAc/NH_4OH, 10:0.3) to give compound **7** in 30% yield. MS (ESI): $[MH]^+ = 494$. ^1H NMR ($CDCl_3$): δ 7.42 (br, 1H); 7.28–7.15 (m, 9H); 5.83 (br, 1H); 5.03 (s, 2H); 3.43 (s, 1H); 3.55–3.16 (m, 3H); 3.08–2.95 (m, 2H); 2.90–2.80 (m, 3H); 2.50–2.44 (m, 4H); 1.76–1.68 (m, 4H); 1.36 (s, 9H). ^{13}C NMR ($CDCl_3$): 173.02; 171.38; 144.70; 138.62; 136.946; 129.35 (2C); 128.63 (2C); 128.54; 127.83; 127.56; 126.82; 121.05 (2C); 83.92; 70.90; 60.41; 56.31; 50.498; 49.88; 39.06; 38.38; 35.82; 35.72; 28.29 (3C); 24.67. $[\alpha]_D^{20} = +8$ ($c = 0.1$ g/100 mL, chloroform).

5.2.7. Benzyl-({3-[spiro[isobenzofuran-1(3*H*),4′-piperidin-1-yl]-propylcarbamoil}-methyl)-carbamic acid *tert*-butyl estere (8)

To stirred solution of (benzyl-*tert*-butoxycarbonyl-amino)acetic acid (200 mg, 0.754 mmol) in DMF, at 0 °C, HOBt (138 mg, 0.905 mmol) and WSC (173 mg, 0.905 mmol) were added and the reaction stirred for 10 min. After this time compound **5** (188 mg, 0.754 mmol) dissolved in DMF (20 mL) was added and the reaction mixture stirred for 24 h. The DMF was removed in vacuo and the product partitioned between EtOAc and $NaHCO_3$ 5%. The organic phase was dried, concentrated in vacuum and the crude product purified by flash chromatography (EtOAc/MeOH/NH_4OH, 9.5:0.5:0.3) to give compound **8** in 22% yield. MS (ESI): $[MH]^+ = 494$. ^1H NMR ($CDCl_3$): δ 7.31–7.18 (m, 9H); 5.05 (s, 2H); 4.58–4.43 (m, 6H); 3.82–3.76 (m, 4H); 3.46–3.32 (m, 4H); 2.98–2.65 (m, 4H); 2.38 (br, 1H); 1.45 (s, 9H). ^{13}C NMR ($CDCl_3$): 169.96; 156.34; 143.97; 138.51; 137.65; 128.68; 128.13; 128.00; 127.76; 127.46; 127.08; 121.14 (2C); 84.25; 80.79; 79.92; 71.13; 54.86; 51.67; 50.78; 50.28; 49.56; 36.96; 34.53; 28.40 (3C); 24.46; 14.25.

5.2.8. (D)-2-Amino-*N*-{3-[spiro[isobenzofuran-1(3*H*),4′-piperidin-1-yl]]-propyl}-3-phenyl-propyl-amide (9)

Compound **6** (160 mg, 0.324 mmol) was dissolved in TFA (5 mL) at room temperature for 1 h, after cooling at 0 °C the reaction was basified with NaOH 2 N until pH 13 and the aqueous layer was extracted three times with EtOAc (20 mL each). The solvent was evaporated under reduced pressure and the crude material was purified by flash chromatography (EtOAc/MeOH/NH_4OH, 9.5/0.5/0.3) to give compound **9** as oil in quantitative yield. MS (ESI): $[MH]^+ = 394$. ^1H NMR ($CDCl_3$): δ 7.27–7.19 (m, 9H); 5.06 (s, 2H); 3.61–3.20 (m, 6H); 2.98–2.65 (m, 4H); 2.54–2.38 (m, 5H); 1.80–1.73 (m, 5H). ^{13}C NMR ($CDCl_3$): 174.36; 145.72; 140.72; 138.88; 138.082; 129.40; 128.73; 127.73; 127.48; 126.83; 121.18; 120.80; 84.43; 70.89; 60.48; 57.11; 56.92; 50.371; 41.42; 38.48; 36.34; 25.89; 21.15; 14.27. $[\alpha]_D^{20} = +15$ (c = 0.2 g/100 mL, chloroform). Anal. ($C_{24}H_{31}N_3O_2$) C, H, N.

5.2.9. (L)-2-Amino-*N*-{3-[spiro[isobenzofuran-1(3*H*),4′-piperidin-1-yl]]-propyl}-3-phenyl-propyl-amide (10)

Compound **7** was treated as for obtaining **9** to give compound **10** in quantitative yield. MS (ESI): $[MH]^+ = 394$. ^1H NMR ($CDCl_3$): δ 7.27–7.19 (m, 9H); 5.06 (s, 2H); 3.61–3.20 (m, 6H); 2.98–2.65 (m, 4H); 2.54–2.38 (m, 5H); 1.80–1.73 (m, 5H). ^{13}C NMR ($CDCl_3$): 174.36; 145.72; 140.72; 138.88; 138.08; 129.40; 128.73; 127.77; 127.48; 126.83; 121.18; 120.80; 84.43; 70.89; 60.48; 57.11; 56.92; 50.37; 41.42; 38.48; 36.34; 25.89; 21.15; 14.27. $[\alpha]_D^{20} = -15$ ($c = 0.2$ g/100 mL, chloroform). Anal. ($C_{24}H_{31}N_3O_2$) C, H, N.

5.2.10. 2-Benzylamino-*N*-{3-[spiro[isobenzofuran-1(3*H*),4'-piperidin-1-yl]]-propyl}-acetamide (11)

Compound **8** was treated as for obtaining **9** to give **11** in quantitative yield. MS (ESI): $[MH]^+ = 394$. ^1H NMR ($CDCl_3$): δ 7.35–7.19 (m, 9H); 7.20–7.19 (m, 1H); 5.05 (s, 2H); 3.80 (s, 2H); 3.32–3.29 (m, 5H); 3.25–3.21 (m, 2H); 2.94–2.82 (m, 4H); 2.19–2.10 (m, 2H); 1.91–1.82 (m, 4H). ^{13}C NMR ($CDCl_3$): 173.72; 145.30; 140.09; 139.72; 129.68 (2C); 129.61 (2C); 129.24; 128.67; 128.55; 122.34; 121.68; 84.28; 71.90; 56.31; 54.06; 51.59; 50.92 (2C); 37.77; 35.85 (2C); 26.44. Anal. ($C_{24}H_{31}N_3O_2$) C, H, N.

5.2.11. (D)-1-Benzyl-pirrolidin-2-carboxilic acid {3-[spiro[isobenzofuran-1(3*H*),4′-piperidin-1-yl]]-propyl}-methyl-amide (12)

A solution of the Comp **24** (200 mg, 0.460 mmol) in DMF (10 mL) was added was added to a stirred suspension of sodium hydride 60% (20.276 mg, 0,5069 mmol) in DMF (5 mL) dropwise at 0 °C. The reaction mixture was left in the same conditions for half an hour, then a solution of methyl iodide (38 μl, 0.599 mmol) in DMF (1 mL) was added. After 24 h at room temperature, the reaction was monitored by TLC (EtOAc/MeOH/NH_3 9.5:0.5:0.3). The DMF was removed under vacuum and the residue was diluted with Brine (5 mL) and extracted thrice with EtOAc. The organic layers were combined, dried and evaporated under reduced pressure to give a crude product as a yellow oil. This was purified by flash chromatography to obtain compound **12** (53 mg, 0.118 mmol, yield 26%). MS (ESI): $[MH]^+ = 448$. ^1H NMR ($CDCl_3$): δ 7.80–7.25 (m, 9H); 5.07 (s, 2H); 3.78–3.29 (m, 10H); 2.95–2.87 (m, 4H); 2.56–2.12 (m,

6H); 2.06–1.69 (m, 6H). ^{13}C NMR ($CDCl_3$): 175.37; 171.47; 162.61; 141.82; 138.36; 138.25; 132.65; 129.390; 129.22; 128.70; 128.06; 127.54; 121.42; 81.22; 81.05; 71.47; 67.08; 66.69; 59.985; 58.04; 54.63; 45.77; 36.56; 36.25; 36.12; 31.45; 30.97; 24.18. Anal. ($C_{28}H_{37}N_3O_2$) C, H, N.

5.2.12. (1-Benzyl-pirrolidin-2-yl-methyl)-{3-[spiro[isobenzofuran-1(3*H*),4′-piperidin-1-yl]]-propyl}-amine (13)

In a two neck round bottom flask, under argon atmosphere, Comp 24 (150 mg, 0.346 mmol) was suspended in anhydrous THF (50 mL) and $(CH_3)_2S^*BH_3$ (100 μl, 1.038 mmol) was added drop wise. The reaction was heated at reflux overnight and monitored by TLC (EtOAc/light petroleum/NH_3 9:1:0.3). The mixture was cooled at 0 °C and acidified with HCl 10%. Then it was heated again at reflux and, after 4 h, it was cooled at 0 °C and basified with NaOH 2 N. THF was evaporated under reduced pressure and the remaining aqueous layer was extracted three times with EtOAc. The organic layers were combined, dried and evaporated under vacuum to obtain the crude product, which was purified by flash chromatography to give compound **13** (20 mg, 0.239 mmol, yield 69%). MS (ESI): $[MH]^+$ = 420. ^{1}H NMR ($CDCl_3$): δ 7.34–7.23 (m, 9H); 5.05 (s, 2H); 3.84–3.59 (m, 1H); 3.70–3.65 (m, 2H); 3.59 (m, 1H); 2.99–2.87 (m, 4H); 2.61–2.35 (m, 8H); 2.06–1.92 (m, 2H); 1.83–1.79 (m, 4H); 1.71–1.65 (m, 4H). ^{13}C NMR ($CDCl_3$): 145.18; 139.28; 138.99; 128.92; 128.59; 127.81; 127.49; 127.43; 121.23; 120.69; 84.31; 70.83; 62.87; 61.88; 59.69; 57.89; 55.14; 51.69; 50.99; 49.85; 49.74; 36.28; 36.11; 29.96; 29.06; 24.14; 23.29. Anal. ($C_{27}H_{37}N_3O$) C, H, N.

5.2.13. (3-Bromo-propyloxi)-*tert*-butyl-dimethyl-silane (14)

A mixture of 3-bromo-propanol (5 mL, 57.190 mmol), imidazole (11.68 g, 171.57 mmol) and TBDMS-Cl (11.206 g, 74.347 mmol) in anhydrous THF (100 mL) was stirred at room temperature for 24 h. The reaction was monitored by TLC (EtOAc/light petroleum 1:3). The solvent was removed under reduced pressure and the residue was diluted with water and extracted three times with DCM. The organic layers were combined, washed with Brine, dried and evaporated to obtain compound **14** in quantitative yield. ^{1}H NMR ($CDCl_3$): δ 3.73 (t, 2H, J = 2.8 Hz); 3.51 (t, 2H, J = 3.2 Hz); 2.07–1.99 (m, 2H); 0.89 (s, 9H); 0.06 (s, 6H).

5.2.14. 1-[3-(*tert*-Butyl-dimethyl-silan-yl-oxi)-propyl]-spiro[isobenzofuran-1(3*H*),4′-piperidine] (15)

To a stirred solution of **4** (1 g, 5.71 mmol) in DMF (50 mL) compound **14** (1.72 g, 6.8 mmol) and K_2CO_3 (1.58 g, 11.43 mmol) dissolved in DMF (10 mL) were added. The reaction was stirred and warmed at 60 °C for an hour and it was monitored by TLC (EtOAc/light petroleum/NH_3 5:1:0.3). The solvent was removed under vacuum and the residue was dissolved in EtOAc and washed twice with saturated NH_4Cl and once with Brine. The organic layer was dried and evaporated under reduced pressure to give the crude product as a red-orange oil. This was purified by flash chromatography to obtain compound **15** (1.93 g, 5.35 mmol, yield 94%). MS (ESI): $[MH]^+$ = 362. ^{1}H NMR ($CDCl_3$): δ 7.28–7.13 (m, 4H); 5.06 (s, 2H); 3.67 (t, 2H, J = 6 Hz); 2.91–2.83 (m, 2H); 2.53–2.36 (m, 4H); 1.99 (dt, 2H, J = 6, 4 Hz); 1.81–1.73 (m, 4H); 0.89 (s, 9H); 0.05 (s, 6H). ^{13}C NMR ($CDCl_3$): 145.77; 138.97; 127.60; 127.40; 121.08; 120.88; 84.82; 70.79 (2C); 61.68; 55.73; 50.30 (2C); 36.69 (2C); 30.32; 26.06 (3C); −5.29 (2C).

5.2.15. 3-{Spiro[isobenzofuran-1(3*H*),4′-piperidin-1-yl]}-propan-1-ol (16)

To a solution of compound **15** (1.930 g, 5.346 mmol) in anhydrous THF (35 mL), cooled at 0 °C, TBAF (5.06 g, 16.038 mmol) was added. The reaction was stirred at room temperature for 24 h and the solvent removed under vacuum. The residue was diluted with EtOAc and washed twice with water. The organic layer was dried and concentrated under reduced pressure to give the crude product, which was purified by flash chromatography to obtain compound **16** (1.239 g, 5.015 mmol, yield 94%). MS (ESI): $[MH]^+$ = 248. ^{1}H NMR ($CDCl_3$): δ 7.29–7.13 (m, 4H); 5.06 (s, 2H); 3.84 (t, 1H, J = 5.2 Hz); 3.61–3.60 (m, 1H); 3.08–3.01 (m, 2H); 2.72 (t, 1H, J = 5.6 Hz); 2.51–2.44 (m, 3H); 2.05–1.95 (m, 3H); 1.82–1.72 (m, 4H). ^{13}C NMR ($CDCl_3$): 145.20; 138.87; 127.78; 127.52; 121.14; 120.89; 84.46; 70.88; 64.64; 62.85; 59.16; 50.42; 36.55; 32.83; 27.16.

5.2.16. (D)-1-Benzyl-pirrolidin-2-carboxilic acid {3-[spiro[isobenzofuran-1(3*H*),4′-piperidin-1-yl]-propyl}estere (17)

To a solution of 1-benzyl-pirrolidin-2-carbossilic acid (264 mg, 1.288 mmol) in DMF, cooled at 0 °C, HOBt (236 mg, 1.546 mmol) and DCC (319 mg, 1.546 mmol) were added. After 10 min compound **16** (350 mg, 1.417 mmol) dissolved in DMF was added. The reaction mixture was stirred at room temperature for 24 h and monitored by TLC (EtOAc/light petroleum/NH_3 4:1:0.3). The solvent was evaporated under vacuum and the residue was basified with $NaHCO_3$ 5% and extracted with EtOAc. The organic layers were combined, dried and concentrated under reduced pressure to obtain the crude product, which was purified by flash chromatography to obtain compound **17** (170 mg, 0.392 mmol, yield 30%). MS (ESI): $[MH]^+$ = 435. ^{1}H NMR ($CDCl_3$): δ 7.31–7.23 (m, 9H); 5.04 (s, 2H); 4.12 (dt, 2H, J = 6.6, 2.4 Hz); 3.91 (d, 1H, J = 12.6 Hz); 3.57 (d, 1H, J = 12.8 Hz); 3.27–3.20 (m, 2H); 3.03–2.95 (m, 2H); 2.86–2.81 (m, 2H); 2.51–2.33 (m, 5H); 1.90–1.72 (m, 8H). ^{13}C NMR ($CDCl_3$): 174.21; 145.52; 138.85; 138.41; 129.177 (2C); 128.19 (2C); 127.61; 127.39; 127.09; 121.06; 120.83; 84.62; 70.76; 65.27; 63.10; 58.65; 55.29; 53.20; 50.16 (2C); 36.51 (2C); 29.38; 26.26; 23.03. $[\alpha]_D^{20}$ = +23 (c = 0.1 g/100 mL, Chloroform). Anal. ($C_{27}H_{34}N_2O_3$) C, H, N.

5.2.17. 1-(3-Chloro-propyl)-4-spiro[isobenzofuran-1(3*H*),4′-piperidine] (18)

In a two neck round bottom flask compound **16** (200 mg, 0.81 mmol) was dissolved in dry DCM (10 mL) and cooled at 0 °C, tosylchloride (170 mg, 0.89 mmol) and Et_3N (90 mg, 0.89 mmol) were added drop wise. The reaction was stirred at room temperature for 24 h and after evaporation, the crude material was dissolved in 20 mL of EtOAc. The organic phase was washed twice with $NaHCO_3$ saturated solution (20 mL each), the combined organic phases were concentrated to dryness and the product purified by flash chromatography (EtOAc/MeOH/NH_4OH, 9:1:0.3) to obtain compound **18** (85 mg, 0.320 mmol, yield 40%). MS (ESI): $[MH]^+$ = 266. ^{1}H NMR ($CDCl_3$): δ 7.27–7.14 (m, 4H); 5.05 (s, 2H); 3.61 (t, 2H, J = 6.6 Hz); 2.85–2.80 (m, 2H); 2.55 (t, 2H, J = 7.2 Hz); 2.40 (dt, 2H); 2.04–1.95 (m, 4H); 1.79–1.78 (m, 2H).

5.2.18. 1-[3-(1-Benzyl-pirrolidin-2-ylmetoxy)-propyl]-4-spiro-[isobenzofuran-1(3*H*),4′piperidine] (20)

To a stirred suspension of sodium hydride (14 mg, 0.34 mmol) in anhydrous THF at 0 °C, a solution of **19** (60 mg, 0.31 mmol) in THF was added. After 30 minutes, a catalytic amount of TBAI was added followed by drop wise addiction of compound **18** (85 mg, 0.31 mmol) dissolved in THF. After 24 h at room temperature, the reaction was heated at reflux for 12 h, the solvent was removed in vacuo, diluted with Et_2O and the resulting precipitate filtrated on Celite pad. The solvent was concentrated to dryness and the crude material purified by flash chromatography (EtOAc/MeOH/NH_4OH, 9.5:0.5:0.3) to give compound **20** in 56% yield. MS (ESI): $[MH]^+$ = 421. ^{1}H NMR ($CDCl_3$): δ 7.32–7.21 (m, 9H); 5.03 (s, 2H); 4.12 (dt, 2H, J = 6.6, 2.4 Hz); 3.91 (d, 1H, J = 12.6 Hz); 3.57 (d, 1H, J = 12.8 Hz); 3.45–3.21 (m, 2H); 3.27–3.20 (m, 2H); 3.03–2.95 (m, 1H); 2.86–2.81 (m, 2H); 2.51–2.33 (m, 5H); 1.90–1.72 (m, 8H).

^{13}C NMR ($CDCl_3$): 145.52; 138.85; 138.41; 129.17 (2C); 128.19 (2C); 127.61; 127.39; 127.09; 121.06; 120.83; 84.62; 74.34; 70.76; 65.27; 63.10; 58.65; 55.29; 53.20; 50.16 (2C); 36.51 (2C); 29.38; 26.26; 23.03. $[\alpha]_D^{20}$ = +21 (c = 0.2 g/100 mL, chloroform). Anal. ($C_{27}H_{36}N_2O_2$) C, H, N.

5.2.19. 5-(1-Benzyl-pirrolidin-2-yl)-pent-4-enoic acid (22)

In a two neck round bottom flask, under argon atmosphere, was placed NaH 60% (12.57 g, 64.31 mmol) and washed five times with anhydrous pentane (20 mL each). The resulting white solid was dried flushing argon and anhydrous DMSO (50 mL) was added; the mixture was heated at 77 °C for 40 min. At this time, the reaction was cooled at 0 °C and the (3-carboxy-propyl)-triphenyl-phosphonium bromide **21** (12.55 g, 29.23 mmol) dissolved in DMSO was added drop wise. When the reaction becomes a brown-red color, 1.105 g (5.85 mmol) of 1-benzyl-pirrolidine-2-carbaldheyde were added drop wise. The reaction was checked by TLC (EtOAc/MeOH/NH_4OH, 9:1:0.3), the DMSO was removed under vacuum and the crude material dissolved in EtOAc (60 mL) and washed with a 10% solution of citric acid (30 mL). The organic phases were dried and evaporated to dryness, the compound was purified by flash chromatography (EtOAc/MeOH/NH_4OH, 9:1:0.3) to give compound **22** (350 mg, 1.135 mmol, yield 23%). MS (ESI): $[MH]^+$ = 260. ^{1}H NMR (CD_3OD): δ 7.76–7.32 (m, 5H); 5.95–5.86 (m, 1H); 5.60–5.50 (m, 1H); 4.45–4.39 (m, 2H); 4.16–4.10 (m, 1H); 3.34–3.29 (m, 6H); 2.40–2.39 (m, 4H). ^{13}C NMR (CD_3OD): 177.93; 139.63; 132.54; 131.91; 131.02; 130.47; 124.63; 66.22; 57.71; 53.82; 50.47; 40.62; 35.48; 31.32; 25.01; 22.35. $[\alpha]_D^{20}$ = −7.14 (c = 0.21 g/100 mL, ethanol). IR: 3398.72; 2993.34; 1658.97; 1560.22; 1435.77; 1405.21; 1315.37; 1211.62; 1159.59; 1124.14; 1013.97; 952.12; 752.60; 701.61.

5.2.20. 5-(1-Benzyl-pirrolidin-2-yl)-1-[spiro[isobenzofuran-1(3*H*), 4′-piperidin-1-yl]]-pent-4-en-1-one (23)

Compound **22** (590 mg, 2.278 mmol) was dissolved in DMF (50 mL) and at 0 °C HOAt (372 mg, 2.773 mmol), WSC (524 mg, 2.733 mmol) and compound **4** (430 mg, 2.278 mmol) were added. After 12 h at room temperature, the solvent was removed by evaporation under reduced pressure and the residue diluted with EtOAc (50 mL); the organic layer washed with $NaHCO_3$ 5% (10 mL) and the aqueous phase extracted three times with EtOAc (30 mL each). The combined organic phases were dried and concentrated in vacuo. The crude product was purified by flash chromatography (EtOAc/light petroleum/NH_4OH, 1:1:0.3) to obtain compound **23** (783 mg, 1.822 mmol, yield 80%). MS (ESI): $[MH]^+$ = 431. ^{1}H NMR ($CDCl_3$): δ 7.2967.22 (m, 9H); 5.67–5.58 (m, 1H); 5.51–5.44 (m, 1H); 5.08 (s, 2H); 4.67–4.61 (m, 1H); 4.04–3.98 (m, 1H); 3.86–3.80 (m, 1H); 3.67 (t, 1H, J = 6.4 Hz); 3.57 (t, 1H, J = 6.4 Hz); 3.22–2.89 (m, 4H); 2.55–2.44 (m, 4H); 1.95–1.55 (m, 8H). ^{13}C NMR ($CDCl_3$): 170.73; 144.70; 139.43; 138.86; 133.47; 130.75; 129.11; 128.19; 127.97; 127.58; 126.85; 121.30; 120.69; 84.76; 71.03; 61.94; 58.52; 53.28; 44.99; 42.61; 38.73; 37.09; 36.19; 33.39; 31.40; 29.97; 23.84; 22.10. $[\alpha]_D^{20}$ = +18 (c = 0.1 g/100 mL, chloroform).

5.2.21. (D)-1-Benzyl-pirrolidin-2-carboxilic acid {3-[spiro[isobenzofuran-1(3*H*),4′-piperidin-1-yl]]-propyl}-amide (Comp 24)

To a stirred solution of *N*-Bn-D-Pro (860 mg, 3.496 mmol) in DMF (20 mL) cooled at 0 °C, HOBt (642 mg, 4.195 mmol), WSC (804 mg, 4.195 mmol) were added and the reaction stirred for 10 min. After this time compound **5** (716 mg, 3.496 mmol) dissolved in DMF (20 mL) was added and the reaction mixture was stirred for 24 h. The DMF was removed in vacuo and the product partitioned between EtOAc and $NaHCO_3$ 5%. The organic phase was dried, concentrated in vacuum and the crude product purified by flash chromatography (EtOAc/MeOH/NH_4OH, 9.5:0.5:0.3) to give Comp 24 in 37% yield. MS (ESI): $[MH]^+$ = 434. ^{1}H NMR ($CDCl_3$): δ 7.60 (br, 1H); 7.30–7.20 (m, 9H); 5.05 (s, 2H); 3.87 (d, 1H, J = 12.8 Hz); 3.48 (d, 1H, J = 12.8 Hz); 3.42–3.16 (m, 4H); 3.09–3.00 (m, 1H); 2.87–2.80 (m, 2H); 2.48–2.29 (m, 5H); 2.23–2.13 (m, 3H); 2.03–1.87 (m, 2H); 1.77–1.65 (m, 4H). ^{13}C NMR ($CDCl_3$): 174.62; 145.61; 138.94; 138.64; 128.81 (2C); 128.56 (2C); 127.62; 127.38 (2C); 121.10; 120.79; 84.69; 70.79; 67.61; 60.02; 56.76; 54.07; 50.54; 50.21; 37.67; 36.60 (2C); 30.78; 26.99; 24.09. $[\alpha]_D^{20}$ = +43 (c = 0.1 g/100 mL, chloroform). Anal. ($C_{27}H_{35}N_3O_2$) C, H, N.

5.2.22. 1-[5-(1-Benzyl-pirrolidin-2-yl)-pent-4-enyl]-spiro[isobenzofuran-1(3*H*),4′-piperidine] (25)

In a round-bottomed flask under argon atmosphere, to a stirred solution of **23** (140 mg, 0.325 mmol) in anhydrous THF (10 mL) cooled at 0 °C, was added drop wise to a solution of borane dimethylsulfide complex (0.094 mL, 0.977 mmol) dropwise. The solution was heated at reflux overnight, after this time, cooled at 0 °C and HCl 10% was added until pH 2. The resulting solution was stirred at reflux for 4 h, basified with NaOH 2 N and the solvent was removed under vacuum. The crude product was purified by flash chromatography (EtOAc/light petroleum/NH_4OH, 2:1:0.3) to give **25** (35 mg, 0.084 mmol, yield 26%). ^{1}H NMR ($CDCl_3$): δ 7.326–7.216 (m, 9H); 5.42–5.37 (m, 2H); 5.06 (s, 2H); 4.09 (t, 1H, J = 6.4 Hz); 3.77 (s, 1H); 3.67 (t, 1H, J = 6.4 Hz); 2.91–2.86 (m, 2H); 2.68–2.34 (m, 4H); 2.09–1.96 (m, 4H); 1.80–1.50 (m, 8H); 1.24–1.15 (m, 2H). ^{13}C NMR ($CDCl_3$): 145.70; 141.23; 138.93; 130.53; 130.06; 128.44; 128.19; 127.63; 127.43; 126.95; 121.09; 120.92; 84.77; 70.83; 64.34; 62.38; 59.00; 54.08; 50.27; 49.80; 36.60; 32.51; 30.40; 29.87; 27.88; 27.71; 26.48; 25.143. $[\alpha]_D^{20}$ = +1.67 (c = 0.31 g/100 mL, chloroform). Anal. ($C_{28}H_{36}N_2O$) C, H, N.

5.2.23. [3-(4-Oxo-1-phenyl-1,3,8-triaza-spiro[4.5]dec-8-yl)-propyl]-carbamic acid *tert*-butyl estere (27)

To a stirred solution of **26** (500 mg, 2.62 mmol) in DMF, was added *N*-Boc-3-bromo-propyl-amine (612 mg, 2.57 mmol) in 10 mL of DMF and K_2CO_3 (596 mg, 4.32 mmol), the reaction was warmed at 60 °C for 1 h. Most of the solvent was removed and the residue was diluted with EtOAc and washed twice with NH_4Cl saturated solution (30 mL each) and brine (30 mL). The organic layer was dried and evaporated under reduced pressure. The crude product was crystallized from Et_2O to give the final compound (535 mg, 1.38 mmol, yield 64%). mp = 163–165 °C. MS (ESI): $[MH]^+$ = 389. ^{1}H NMR ($CDCl_3$): δ 7.31–7.23 (m, 3H); 6.90–6.84 (m, 2H); 5.38 (br, 2H); 4.73 (s, 2H); 3.23–3.19 (m, 2H); 2.82–2.45 (m, 8H); 1.75–1.66 (m, 4H); 1.41 (s, 9H). ^{13}C NMR ($CDCl_3$): 178.14; 156.20; 143.21; 129.37 (2C); 119.02 (2C); 115.50 (2C); 79.00; 59.50; 59.38; 56.98; 49.84 (2C); 40.16; 29.31; 28.55 (3C); 26.91.

5.2.24. Acid-(D)-1-benzyl-pirrolidin-2-carboxilic-[3-(4-oxo-1-fenyl-1,3,8-triaza-spiro[4.5]dec-8-yl)-propyl]-amide (28)

Compound **27** (535 mg, 1.37 mmol) was treated with TFA (5 mL) at 0 °C for 1 h. NaOH 2 N was added until pH 12–14, the aqueous phase was extracted several times with EtOAc and the organic phases were combined, dried and evaporated under vacuum to give the free amine (395 mg, 1.37 mmol) in 100% yield. This product was condensed with *N*-Bn-D-Pro in a similar manner as reported for Comp **24**. The crude product was purified by flash chromatography (EtOAc/MeOH/NH_4OH, 9.5:0.5:0.3) to give **28** in 56% yield. MS (ESI): $[MH]^+$ = 476. ^{1}H NMR ($CDCl_3$): δ 7.94–7.83 (m, 2H); 7.35–6.86 (m, 10H); 4.72 (s, 2H); 3.84 (d, 1H, J = 13 Hz); 3.51 (d, 1H, J = 13 Hz); 3.27–3.19 (m, 3H); 3.07–2.81 (m, 6H); 2.76–2.47 (m, 2H); 2.36–1.66 (m, 10H). ^{13}C NMR ($CDCl_3$): 178.00; 175.06; 143.32; 138.80; 129.52 (2C); 128.91 (2C); 128.74 (2C); 127.54; 125.82; 119.61; 116.19 (2C); 115.30; 67.58; 60.17; 59.59; 56.04; 54.33; 49.86; 37.55; 30.98; 29.90; 29.34; 27.22;

24.37. $[\alpha]_D^{20}$ = +24 (c = 0.1 g/100 mL, chloroform). Anal. ($C_{28}H_{37}N_5O_2$) C, H, N.

5.2.25. 2-(2,6-Dichloro-phenyl)-4-hydroxy-4-methyl-6-oxo-cyclohexane-1,3-dicarboxylic acid diethyl ester (30)

Compound **29** (5 g, 28.57 mmol) and ethyl aceto-acetate (7.22 mL, 57.14 mmol) were dissolved in 20 mL of ethanol 96%. At this stirred solution was added piperidine (0.5 mL) and the reaction mixture was stirred at room temperature overnight.

The solvent was removed under reduced pressure and the product was crystallized from Et_2O to give compound **30** with a quantitative yield. mp = 112–115 °C. MS (ESI): $[MH]^+$ = 418. ^{1}H NMR ($CDCl_3$): δ 12.50 (s, 1H); 7.28–7.18 (m, 2H); 7.05 (t, 1H, 8 Hz); 5.01 (d, 1H, J = 11 Hz); 4.05–3.83 (m, 5H); 3.10 (d, 1H, J = 11.4 Hz); 2.48 (s, 2H); 1.32 (s, 3H); 0.98 (t, 3H, 7.4 Hz); 0.85 (t, 3H, 7 Hz). ^{13}C NMR ($CDCl_3$): 174.77; 171.11; 170.52; 138.03; 137.03; 134.28; 130.16; 128.04; 127.90; 98.09; 69.35; 61.36; 60.29; 50.85; 41.72; 38.28; 28.05; 13.83; 13.39.

5.2.26. 3-(2,6-Dichloro-phenyl)-pentane-dioic acid (31)

Compound **30** (7 g, 16.79 mmol) dissolved in ethanol 96% (55 mL), NaOH 35% (40.75 mL) and of water (16.3 mL) were added. The reaction mixture was stirred at reflux for 3 h. The solvent was removed under reduced pressure, the resulting aqueous layer was acidified at 0 °C with HCl 20% and extracted with ethyl acetate. The organic layers were combined, dried and evaporated under vacuum to obtain the crude product, which was crystallized from ethyl ether to give **31** (4.026 g, 14.53 mmol, yield 87%). mp = 153–155 °C. MS (ESI): $[MH]^+$ = 278. ^{1}H NMR ($CDCl_3$): δ 12.20 (s, 2H); 7.41 (t, 2H, J = 8 Hz); 7.23 (t, 1H, J = 8 Hz); 3.43–3.32 (m, 1H); 2.92–2.70 (m, 4H). IR: 2918.07; 1713.09; 1560.58; 1438.02; 1310.02; 1226.35; 1202.58; 1085.05; 903.48; 779.13.

5.2.27. 4-(2,6-Dichloro-phenyl)-piperidin-2,6-dione (32)

Compound **31** (4.026 g, 15.60 mmol) was dissolved in NH_4OH (40 mL). The solvent was evaporated under vacuum and the solid residue was heated at 200 °C for 6 h. At the crude product was added DCM (150 mL) and was washed twice with Na_2CO_3 0.1 M. The organic layer was dried and concentrated in vacuum to obtain a crude product, which was crystallized from ethyl ether to give **32** with a quantitative yield. mp = 155–157 °C. MS (ESI): $[MH]^+$ = 259. ^{1}H NMR ($CDCl_3$): δ 8.20 (br, 1H); 7.36–7.13 (m); 4.43–4.30 (m, 1H); 3.60 (dd, 2H, J = 18, 13.5 Hz); 2.69 (dd, 2H, J = 17.7, 4.6 Hz). IR: 3208.19; 3078.49; 2921.50; 2385.98; 2342.76; 1696.60; 1560.07; 1437.89; 1361.16; 1271.72; 1150.48; 1079.12; 770.20; 731.23.

5.2.28. 4-(2,6-Dichloro-phenyl)-piperidine (33)

Compound **32** (4 g, 15.5 mmol) was suspended, under argon atmosphere, in anhydrous THF (150 mL) and $(CH_3)_2S^*BH_3$ (14.9 mL, 155 mmol) added at 0 °C under stirring. The reaction was heated at reflux overnight. The solution was cooled at 0 °C, HCl 10% (66.6 mL) was added until pH of the solution was strongly acidic and the solution was left at reflux for 4 h. The reaction mixture was cooled again at 0 °C, basified with NaOH 2 N and monitored by TLC (EtOAc/light petroleum 3:2). The THF was evaporated under vacuum and the aqueous layer was extracted with ethyl acetate. The organic layers were combined, dried and concentrated under vacuum to obtain the crude product, which was crystallized with ethyl ether to give **33** (1.23 g, 5.348 mmol, yield 35%). mp = 210–215 °C. MS (ESI): $[MH]^+$ = 231. ^{1}H NMR ($CDCl_3$): δ 9.77 (br, 1H); 7.28–7.25 (m, 2H); 7.089 (t, 1H, J = 8 Hz); 3.78–3.72 (m, 1H); 3.67–3.64 (m, 2H); 3.13–3.02 (m, 4H); 1.82–1.79 (m, 2H). ^{13}C NMR ($CDCl_3$): 137.08; 135.21; 130.67; 128.65 (2C); 44.73 (2C); 38.30 (2C); 24.80 (2C).

5.2.29. 3-[4-(2,6-Dichloro-phenyl)-piperidin-1-yl]-propylamine (34)

To a stirred solution of **33** (284 mg, 1.236 mmol) in DMF (5 mL), *N*-Boc-3-bromo-propyl-amine (350 mg, 1.471 mmol) and K_2CO_3 (341.77 mg, 2.473 mmol) were added. The reaction mixture was stirred at 60 °C for 1 h and than evaporated under vacuum, the residue was dissolved in EtOAc and washed twice with a saturated solution of NH_4Cl and once with Brine. The organic layer was dried and concentrated under reduced pressure to obtain the product as a red-orange oil. This crude product was then purified by flash chromatography (EtOAc/light petroleum/NH_4OH 5:1:0.3) (yield 94%). At the product so obtained (1.163 mmol), cooled at 0 °C, was added drop wise 1 mL of TFA. The reaction was monitored by TLC (EtOAc/light petroleum 5:1) and after about 1 h was cooled at 0 °C and basified with NaOH 2 N. The aqueous layer was extracted three times with EtOAc and the organic layers were combined, dried and evaporated under vacuum to give compound **34** with a quantitative yield. MS (ESI): $[MH]^+$ = 288. ^{1}H NMR ($CDCl_3$): δ 7.25–7.00 (m, 3H); 3.53–3.46 (m, 1H); 3.36 (br, 2H); 3.116 (dd, 2H, J = 9.6, 4 Hz); 2.90 (t, 2H, J = 6.8 Hz); 2.67–2.56 (m, 2H); 2.50 (t, 2H, J = 6.8 Hz); 2.05 (dt, 2H, J = 10, 2.4 Hz); 1.75 (t, 2H, J = 6.4 Hz); 1.58 (d, 2H, J = 12.4 Hz).

5.2.30. (D)-1-Benzyl-pirrolidin-2-carbossilic acid {3-[4-(2,6-dichloro-phenyl)-piperidin-1-yl]-propyl}-amide (35)

N-Bn-D-Pro and compound **34** were condensed in the same experimental condition as for Comp 24 yielding **35** (48 mg, 0.101 mmol, yield 65%). MS (ESI): $[MH]^+$ = 475. ^{1}H NMR ($CDCl_3$): δ 7.56–7.52 (br, 1H); 7.35–7.24 (m, 7H); 7.03 (t, 1H, J = 8 Hz); 3.86 (d, 1H, J = 13.2 Hz); 3.50 (d, 1H, J = 13.2 Hz); 3.28–3.17 (m, 2H); 3.07–3.03 (m, 3H); 2.69–2.64 (m, 2H); 2.47–2.34 (m, 3H); 2.27–2.19 (m, 2H); 2.06–2.01 (m, 2H); 1.92–1.90 (m, 2H); 1.75–1.72 (m, 4H); 1.56 (d, J = 12.8 Hz). ^{13}C NMR ($CDCl_3$): 174.71; 138.67; 130.41; 128.76 (2C); 128.57 (2C); 127.78 (2C); 127.35 (2C); 67.52; 59.95 (2C); 56.41; 54.64; 54.10; 40.57; 37.43 (2C); 30.78 (2C); 27.64; 26.80; 24.14 (2C). $[\alpha]_D^{20}$ = +27 (c = 0.1 g/100 mL, chloroform). Anal. ($C_{26}H_{33}Cl_2N_3O$) C, H, N, Cl.

5.2.31. (L)-1-Benzyl-pirrolidin-2-carboxilic acid {3-[4-(2,6-dichloro-phenyl)-piperidin-1-yl]-propyl}-amide (36)

N-Bn-Pro and compound **34** were condensed in the same experimental condition as for Comp 24. yielding **36** (48 mg, 0.101 mmol, yield 35%). MS (ESI): $[MH]^+$ = 475. ^{1}H NMR ($CDCl_3$): δ 7.53 (br, 1H); 7.33–7.25 (m, 7H); 7.03 (t, 1H, J = 8 Hz); 3.86 (d, 1H, J = 13.2 Hz); 3.50 (d, 1H, J = 13.2 Hz); 3.30–3.17 (m, 3H); 3.07–3.03 (m, 2H); 2.67–2.64 (m, 2H); 2.42–2.32 (m, 3H); 2.24–2.19 (m, 2H); 2.07–2.01 (m, 3H); 1.88–1.85 (m, 2H); 1.78–1.67 (m, 3H); 1.57–1.54 (m, 2H). ^{13}C NMR ($CDCl_3$): 174.69; 138.69; 130.40; 128.73 (2C); 128.57 (2C); 127.74 (2C); 127.35 (2C); 67.53; 59.95 (2C); 56.51; 54.68; 54.09; 40.64; 37.47 (2C); 30.78 (2C); 27.74; 26.86; 24.14 (2C). $[\alpha]_D^{20}$ = −27 (c = 0.1 g/100 mL, chloroform). Anal. ($C_{26}H_{33}Cl_2N_3O$) C, H, N, Cl.

5.2.32. 4-(2-Oxo-2,3-dihydro-benzoimidazol-1-yl)-piperidine-1-carboxylic acid *tert*-butyl ester (38)

To a stirred solution of compound **37** (1 g, 4.60 mmol) in DCM (50 mL) at 0 °C, a catalytical amount of DMAP and $(Boc)_2O$ (1.57 g, 6.9 mmol) were added. After 6 h at room temperature, water (100 mL) was added and the organic layer washed with citric acid 10% (10 mL × 3), $NaHCO_3$ saturated solution (10 mL × 3) and brine (10 mL × 3). The organic phase was dried and concentrated in vacuo to give compound **38** in quantitative yield pure enough to be used in the next step without further purification.

5.2.33. 1-Ethyl-3-piperidin-4-yl-1,3-dihydro-benzoimidazol-2-one (39)

To a suspension of sodium hydride (92 mg, 3.79 mmol) in anhydrous DMF (5 mL), compound **38** was added dropwise at 0 °C. After

30 minutes, ethyl bromide (413 mg, 3.79 mmol) was added, and the reaction mixture was allowed to stir at room temperature overnight. The DMF was removed in vacuo and the salts were dissolved in water, the aqueous layer was extracted with EtOAc (25 mL × 3), dried and concentrated in vacuo. The crude material was dissolved in 5 mL of TFA and stirred for 1 h; after this time, the TFA was evaporated and the solution was basified with NaOH 20% until pH 12. The aqueous layer was extracted twice with EtOAc (30 mL each), concentrated to dryness and purified by flash chromatography using EtOAc/light petroleum/NH_4OH: 2:1:0.3 as eluent to give 0.84 g of desired compound (yield 75%). MS (ESI): $[MH]^+$ = 246.3 ^1H NMR ($CDCl_3$): δ 7.25 (m, 1H); 7.07–7.00 (m, 3H); 4.43 (m, 1H); 3.98–3.87 (q, 2H, J = 6 Hz); 3.22 (br s, 2H); 2.79 (dt, 2H, J = 15.6 Hz, J = 2.4 Hz); 2.37–2.30 (dq, 2H, J = 8.4 Hz, J = 4.2 Hz); 1.85 (bs, 2H); 1.32 (t, 3H, J = 7.4 Hz).

5.2.34. 1-[1-(3-Amino-propyl)-piperidin-4-yl]-3-ethyl-1,3-dihydro-benzoimidazol-2-one (40)

To a stirred solution of **39** (92 mg, 0.375 mmol) in DMF (5 mL), *N*-Boc-3-bromo-propyl-amine (106 mg, 0.447 mmol) and K_2CO_3 (103 mg, 0.750 mmol) were added. After 1 h at 60 °C, most of the solvent was removed and the residue diluted with EtOAc and washed twice with NH_4Cl saturated solution (30 mL each) and brine (30 mL). The organic layer was dried and evaporated under reduced pressure. The crude material was treated at 0 °C with TFA (5 mL) for 1 h and then treated with NaOH 2 N until pH 12–14. The aqueous phase was extracted several times with EtOAc and the organic phases were combined, dried and evaporated under vacuum to give compound **40** in 80% yield. The product was enough pure to be used in the next step without further purification.

5.2.35. 1-Benzyl-pyrrolidine-2-carboxylic acid {3-[4-(3-ethyl-2-oxo-2,3-dihydro-benzoimidazol-1-yl)-piperidin-1-yl]-propyl}-amide (41)

N-Bn-D-Pro and compound **40** were condensed in the same experimental condition as for Comp 24 yielding **41** in 24% yield after purification by flash chromatography (EtOAc/MeOH/NH_4OH, 9.5:0.5:0.3). MS (ESI): $[MH]^+$ = 490. ^1H NMR ($CDCl_3$): δ 7.58–7.52 (m, 1H); 7.29–7.25 (m, 5H); 7.04–7.01 (m, 4H); 4.58–4.42 (m, 1H); 3.92 (q, 2H, J = 7.2 Hz); 3.866–3.560 (dd, a–b sistem, 2H, J = 13 Hz); 3.24–3.09 (m, 5H); 2.59–2.19 (m, 9H); 1.87–1.72 (m, 7H); 1.315 (t, 3H, J = 7.2 Hz). ^{13}C NMR ($CDCl_3$): 175.07; 153.40; 138.58; 129.14; 128.71; 128.586; 127.87; 127.39; 121.06; 120.98; 109.80; 107.67; 67.41; 59.95; 55.44; 54.17; 53.00; 52.92; 49.83; 36.93; 35.95; 30.77; 28.11; 26.36; 24.13; 13.62. Anal. ($C_{29}H_{39}N_5O_2$) C, H, N.

5.3. Cell culture and cell membrane preparation

CHO_{hNOP} cells were cultured in DMEM and Hams F-12 (1:1) supplemented with 5% foetal calf serum, penicillin (100 IU/mL), Streptomycin (100 μg/mL) and Fungizone (2.5 μg/mL). Stock cultures were further supplemented with geneticin (G418, 200 μg/mL) and Hygromycin B (200 μg/mL) as described previously.[25] CHO cell lines stably expressing the human MOP, DOP, KOP and NOP receptors and the C-terminally modified $G\alpha_{qi5}$[26] were generated as described previously[8] and maintained in Dulbecco Minimum Essential Medium (DMEM) and Hams F-12 (1:1) supplemented with 10% fetal bovine serum, 2 mM L-glutamine, 200 μg/mL Geneticin and 100 μg/mL Hygromicin B. Cells were cultured at 37 °C in 5% carbon dioxide humidified air, and used when confluent.

For binding experiments membranes were prepared from freshly harvested cell suspensions in Tris–HCl (50 mM), Mg^{++} (5 mM) pH 7.4 ([^{3}H]N/OFQ binding experiments) or in Tris–HCl (50 mM), EGTA (0.2 mM) pH 7.4 ([^{35}S]GTPγS binding experiments) via homogenisation and centrifugation at 13,500 rpm for 10 min at 4 °C. The final protein concentration was determined according to Lowry.[27]

5.4. Receptor binding

[^{3}H]N/OFQ binding experiments. 5 μg of CHO_{hNOP} homogenate protein was incubated in 0.5 mL volumes of Tris-HCl (50 mM) buffer supplemented with 10 μM peptidase inhibitors (amastatin, bestatin, captopril and phosphoramidon), 0.5% bovine serum albumin (BSA), increasing concentrations of compounds under study and approximately 200 pM [^{3}H]-N/OFQ. Total radiolabel bound was ≪10%. Non-specific binding was determined in the presence of 1 μM unlabeled N/OFQ. In all experiments Comp 24 was included as a reference ligand. Reactions were incubated for 1 h at room temperature and terminated by vacuum filtration (Brandel Harvester) through Whatman GF/B filters soaked at 0.5% polyethylenimine (PEI). Radioactivity was determined after 8 h extraction in scintillation cocktail. [^{3}H]-Diprenorphine binding experiments. 50 μg (CHO_{hMOP}), 25 μg (CHO_{hDOP}) and 40 μg (CHO_{hKOP}) membrane protein were incubated in 0.5 ml buffer containing Tris-HCl (50 mM) pH 7.4, BSA (0.5%), ∼0.7 nM [^{3}H]Diprenorphine and increasing concentrations of naloxone and compound **35**. Non-specific binding was determined in the presence of 10 μM naloxone. Reactions were incubated at room temperature for 1 h, harvesting and determination of radioactivity were as for [^{3}H]N/OFQ binding.

5.5. [^{35}S]GTPγS binding

20 μg of CHO_{hNOP} membranes were incubated in 0.5 mL buffer containing Tris–HCl (50 mM), EGTA (0.2 mM) $MgCl_2$ (1 mM), NaCl (100 mM), bacitracin (0.15 mM) peptidase inhibitors (as above), GDP (100 μM) and approximately 150 pM [^{35}S]GTPγS. Compound **35** was pre-incubated for 15 min at 30 °C. Non-specific binding was determined in the presence of unlabeled 10 μM GTPγS. The reaction was incubated for 1 h with increasing concentration of N/OFQ at 30 °C with gentle shaking and terminated by filtration through Whatman GF/B filters using a Brandel Harvester. PEI was not used.

5.6. Calcium mobilization experiments

CHO_{hMOP}, CHO_{hDOP}, CHO_{hKOP} and CHO_{hNOP} stably expressing the $G\alpha_{qi5}$ protein were seeded at a density of 40,000 cells/well into 96-well black, clear-bottom plates. After 24 h incubation the cells were loaded with medium supplemented with 2.5 mM of probenecid, 3 μM of the calcium sensitive fluorescent dye Fluo-4 AM and 0.01% pluronic acid, for 30 min at 37 °C. Afterwards, the loading solution was aspirated and 100 μL/well of assay buffer: Hank's Balanced Salt Solution (HBSS) supplemented with 20 mM HEPES, 2.5 mM probenecid and 500 μM Brilliant Black (Aldrich) was added. Stock solutions (1 mM) of ligands were prepared in distilled water and stored at −20 °C. Serial dilutions of ligands for experimental use were made in HBSS/HEPES (20 mM) buffer (containing 0.02% BSA fraction V). After placing both plates (cell culture and compound plate) into the FlexStation II (Molecular Device, Union City, CA), fluorescence changes were measured at room temperature. On-line additions were carried out in a volume of 50 μL/well.

5.7. Electrically stimulated isolated tissues

Tissues were taken from male Swiss mice (30–35 g), albino guinea pigs (300–350 g) and Sprague-Dawley rats (300–350 g). The mouse and the rat vas deferens and the guinea pig ileum were prepared as previously described.[28] Tissues were continuously stimulated through two platinum ring electrodes with supramaximal

rectangular pulses of 1 ms duration and 0.05 Hz frequency. The electrically evoked contractions (twitches) were measured isotonically with a strain gauge transducer (Basile 7006, UgoBasile s.r.l., Varese, Italy) and recorded with the PC based acquisition system Power Lab (ADInstrument, USA).

Following an equilibration period of 60 min, the contractions induced by electrical field stimulation were stable. At this time, cumulative concentration–response curves to N/OFQ were performed (0.5 log unit steps) in the absence or presence of compound **35** (15 min pre-incubation time). For selectivity studies, in some experiments the DOP selective agonist DPDPE was used in the mouse vas deferens and the MOP selective agonist dermorphin was used in the guinea pig ileum.

5.8. Mouse tail withdrawal assay

Male Swiss albino mice weighing 25–30 g were used. Animals were handled according to guidelines published in the European Communities Council directives (86/609/EEC) and Italian national regulations (D.L. 116/92). They were housed in 425 × 266 × 155-mm cages (Techniplast, Milan, Italy), fifteen animals/cage, under standard conditions (22 °C, 55% humidity, 12-h light/dark cycle, light on at 7:00 am) with food (MIL, standard diet; Morini, Reggio Emilia, Italy) and water ad libitum for at least 5 days before experiments began. Each mouse was used only once. Icv (2 μl/mouse) or i.t (5 μl/mouse) injections were given according to the procedure described by Laursen and Belknap[29] and Hylden and Wilcox[30], respectively.

All experiments were started at 10:00 am and performed according to the procedure described previously in detail.[22] Briefly, the mice were placed in a holder and the distal half of the tail was immersed in water at 48 °C. Withdrawal latency time was measured by an experienced observer blind to drug treatment. A cut-off time of 20 s was chosen to avoid tissue damage. For each experiment sixteen mice were used by randomly assigning four animals to each treatment group. The experiment was repeated four times; therefore, each experimental point shown in Figure 2 is the mean of the results obtained in 16 mice. Tail-withdrawal latency was determined immediately before and 5, 15, 30, and 60 min after icv or i.t. injection of vehicle (saline) or N/OFQ (1 nmol). Compound **35** (10 mg/kg) or its vehicle (2% DMSO and 10% encapsin) were given i.p. 30 min before icv injection. Increased and decreased tail withdrawal latencies compared with baseline indicated antinociceptive and pronociceptive effects, respectively.

5.9. Data analysis and terminology

All data are expressed as means ± standard error of the mean (sem) of *n* experiments. For potency values confidence limits 95% were indicated. Data have been analyzed statistically using one-way ANOVA followed by Dunnett's test for multiple comparisons or the Student's t test. In competition binding studies (Tables 2 and 3), the log concentration of competitor producing 50% inhibition of specific binding (pIC_{50}) was corrected for the competing mass of radiolabel according to Cheng and Prusoff[31] to yield pK_i values. K_D values for [^{3}H]N/OFQ in CHO_{hNOP} was 83 pM and for [^{3}H]diprenorphine in MOP, DOP and KOP were 125, 323, and 134 pM, respectively.

[^{35}S]GTPγS data are expressed as a stimulation factor that is, the ratio between agonist-stimulated [^{35}S]GTPγS specific (minus NSB) binding and basal specific binding. Calcium mobilization data are expressed as fluorescence intensity units (FIU) in percent over the baseline. Isolated tissue data are expressed as percent of the twitch response to electrical field stimulation.

Agonist potencies are given as pEC_{50} = the negative logarithm to base 10 of the molar concentration of an agonist that produces 50% of the maximal possible effect. Antagonist potencies have been evaluated (i) using pA_2 derived from the classical Schild protocol in [^{35}S]GTPγS binding and mouse vas deferens experiments (Fig. 1 and Table 2), (ii) using pK_b derived from the Gaddum Schild equation:

$$K_b = ((CR - 1)/[\text{antagonist}])$$

assuming a slope value equal to unity, where CR indicate the ratio between agonist potency in the presence and in the absence of the antagonist, in rat vas deferens and guinea pig ileum experiments (Table 2). Finally, (iii) using pK_b values derived from the following equation:[32]

$$K_b = IC_{50}/([2 + ([A]/EC_{50})^n]^{1/n} - 1$$

where IC_{50} is the concentration of antagonist that produces 50% inhibition of the agonist response, [*A*] is the concentration of the agonist, EC_{50} is the concentration of agonist producing a 50% maximal response and *n* is the Hill coefficient of the concentration response curve to the agonist in inhibition response experiments measuring calcium mobilization (Tables 2 and 4).

Acknowledgments

This work was supported by funds from the University of Ferrara (FAR grants to SS and GC) and the Italian Ministry of the University (PRIN and FIRB grants to RG).

Supplementary data

Supplementary data associated with this article can be found, in the online version, at doi:10.1016/j.bmc.2009.05.068.

References and notes

1. Meunier, J. C.; Mollereau, C.; Toll, L.; Suaudeau, C.; Moisand, C.; Alvinerie, P.; Butour, J. L.; Guillemot, J. C.; Ferrara, P.; Monserrat, B.; Mazarguil, H.; Vassart, G.; Parmentier, M.; Costentin, J. *Nature* **1995**, *377*, 532.
2. Reinscheid, R. K.; Nothacker, H. P.; Bourson, A.; Ardati, A.; Henningsen, R. A.; Bunzow, J. R.; Grandy, D. K.; Langen, H.; Monsma, F. J., Jr.; Civelli, O. *Science* **1995**, *270*, 792.
3. Lambert, D. G. *Nat. Rev. Drug Disc.* **2008**, *7*, 694.
4. Jenck, F.; Wichmann, J.; Dautzenberg, F. M.; Moreau, J. L.; Ouagazzal, A. M.; Martin, J. R.; Lundstrom, K.; Cesura, A. M.; Poli, S. M.; Roever, S.; Kolczewski, S.; Adam, G.; Kilpatrick, G. *Proc. Natl. Acad. Sci. U.S.A.* **2000**, *97*, 4938.
5. Ozaki, S.; Kawamoto, H.; Itoh, Y.; Miyaji, M.; Azuma, T.; Ichikawa, D.; Nambu, H.; Iguchi, T.; Iwasawa, Y.; Ohta, H. *Eur. J. Pharmacol.* **2000**, *402*, 45.
6. Zaratin, P. F.; Petrone, G.; Sbacchi, M.; Garnier, M.; Fossati, C.; Petrillo, P.; Ronzoni, S.; Giardina, G. A.; Scheideler, M. A. *J. Pharmacol. Exp. Ther.* **2004**, *308*, 454.
7. Goto, Y.; Arai-Otsuki, S.; Tachibana, Y.; Ichikawa, D.; Ozaki, S.; Takahashi, H.; Iwasawa, Y.; Okamoto, O.; Okuda, S.; Ohta, H.; Sagara, T. *J. Med. Chem.* **2006**, *49*, 847.
8. Fischetti, C.; Camarda, V.; Rizzi, A.; Pela', M.; Trapella, C.; Guerrini, R.; McDonald, J.; Lambert, D. G.; Salvadori, S.; Regoli, D.; Calo, G. *Eur. J. Pharmacol.* **2009**, *614*, 50.
9. Guerrini, R.; Calo, G.; Bigoni, R.; Rizzi, A.; Varani, K.; Toth, G.; Gessi, S.; Hashiba, E.; Hashimoto, Y.; Lambert, D. G.; Borea, P. A.; Tomatis, R.; Salvadori, S.; Regoli, D. *J. Med. Chem.* **2000**, *43*, 2805.
10. Guerrini, R.; Calo, G.; Lambert, D. G.; Carra, G.; Arduin, M.; Barnes, T. A.; McDonald, J.; Rizzi, D.; Trapella, C.; Marzola, E.; Rowbotham, D. J.; Regoli, D.; Salvadori, S. *J. Med. Chem.* **2005**, *48*, 1421.
11. Neises, B.; Steglich, W. *Angew. Chem., Int. Ed. Engl.* **1978**, *17*, 522.
12. Sudau, A.; Muench, W.; Bats, J. W.; Nubbemeyer, U. *Eur. J. Org. Chem.* **2002**, *2002*, 3304.
13. Blackburn, L.; Kanno, H.; Taylor, R. J. K. *Tetrahedron Lett.* **2003**, *44*, 115.
14. Wadsworth, W. S.; Emmons, W. D. *J. Am. Chem. Soc.* **1961**, *83*, 1733.
15. Cremonesi, G.; Dalla Croce, P.; Fontana, F.; Forni, A.; La Rosa, C. *Tetrahedron: Asymmetry* **2007**, *18*, 1667.
16. Corey, E. J.; Chaykovsky, M. *J. Org. Chem.* **1962**, *84*, 866.
17. Corey, H. S.; McCormick, J. R. D.; Swensen, W. E. *J. Org. Chem.* **1964**, *86*, 1884.
18. Shinkai, H.; Ito, T.; Iida, T.; Kitao, Y.; Yamada, H.; Uchida, I. *J. Med. Chem.* **2000**, *43*, 4667.
19. Zaveri, N.; Jiang, F.; Olsen, C.; Polgar, W.; Toll, L. *Aaps J.* **2005**, *7*, E345.
20. Camarda, V.; Fischetti, C.; Anzellotti, N.; Molinari, P.; Ambrosio, C.; Kostenis, E.; Regoli, D.; Trapella, C.; Guerrini, R.; Salvadori, S.; Calo, G. *Naunyn-Schmiedebergs Arch. Pharmacol.* **2009**, *379*, 599.

21. Zeilhofer, H. U.; Calo, G. *J. Pharmacol. Exp. Ther.* **2003**, *306*, 423.
22. Calo, G.; Rizzi, A.; Marzola, G.; Guerrini, R.; Salvadori, S.; Beani, L.; Regoli, D.; Bianchi, C. *Br. J. Pharmacol.* **1998**, *125*, 373.
23. Nazzaro, C.; Rizzi, A.; Salvadori, S.; Guerrini, R.; Regoli, D.; Zeilhofer, H. U.; Calo, G. *Peptides* **2007**, *28*, 663.
24. Rizzi, A.; Gavioli, E. C.; Marzola, G.; Spagnolo, B.; Zucchini, S.; Ciccocioppo, R.; Trapella, C.; Regoli, D.; Calo, G. *J. Pharmacol. Exp. Ther.* **2007**, *321*, 968.
25. McDonald, J.; Calo, G.; Guerrini, R.; Lambert, D. G. *Naunyn-Schmiedeberg's Arch. Pharmacol.* **2003**, *367*, 183.
26. Coward, P.; Chan, S. D.; Wada, H. G.; Humphries, G. M.; Conklin, B. R. *Anal. Biochem.* **1999**, *270*, 242.
27. Lowry, O. H.; Rosenbrough, N. J.; Farr, A. L.; Randall, R. J. *J. Biol. Chem.* **1951**, *193*, 265.
28. Bigoni, R.; Giuliani, S.; Calo, G.; Rizzi, A.; Guerrini, R.; Salvadori, S.; Regoli, D.; Maggi, C. A. *Naunyn-Schmiedeberg's Arch. Pharmacol.* **1999**, *359*, 160.
29. Laursen, S. E.; Belknap, J. K. *J. Pharmacol. Methods* **1986**, *16*, 355.
30. Hylden, J. L.; Wilcox, G. L. *Eur. J. Pharmacol.* **1980**, *17*, 313.
31. Cheng, Y.; Prusoff, W. H. *Biochem. Pharmacol.* **1973**, *22*, 3099.
32. Kenakin, T. *A Pharmacology Primer*; Elsevier Academic Press: San Diego, 2004.
33. Vergura, R.; Valenti, E.; Hebbes, C. P.; Gavioli, E. C.; Spagnolo, B.; McDonald, J.; Lambert, D. G.; Balboni, G.; Salvadori, S.; Regoli, D.; Calo, G. *Peptides* **2006**, *27*, 3322.

European Journal of Pharmacology 614 (2009) 50–57

Contents lists available at ScienceDirect

European Journal of Pharmacology

journal homepage: www.elsevier.com/locate/ejphar

Neuropharmacology and Analgesia

Pharmacological characterization of the nociceptin/orphanin FQ receptor non peptide antagonist Compound 24

Carmela Fischetti [a,b,c], Valeria Camarda [a,b], Anna Rizzi [a,b], Michela Pelà [d], Claudio Trapella [d], Remo Guerrini [d], John McDonald [c], David G. Lambert [c], Severo Salvadori [c], Domenico Regoli [a,b], Girolamo Calo' [a,b,*]

[a] Department Experimental and Clinical Medicine, Section of Pharmacology and Neuroscience Center, University of Ferrara, Ferrara, Italy
[b] National Institute of Neuroscience, Ferrara, Italy
[c] Department of Cardiovascular Sciences (Pharmacology and Therapeutics Group), Division of Anaesthesia, Critical Care and Pain Management, University of Leicester, Leicester Royal Infirmary, Leicester, LE1 5WW, UK
[d] Department of Pharmaceutical Sciences and Biotechnology Center, University of Ferrara, Ferrara, Italy

ARTICLE INFO

Article history:
Received 12 December 2008
Received in revised form 16 April 2009
Accepted 29 April 2009
Available online 12 May 2009

Keywords:
Nociceptin/orphanin FQ
NOP receptor
Compound 24
Calcium mobilization
N/OFQ sensitive tissues
Mouse tail withdrawal assay

ABSTRACT

Compound 24, 1-benzyl-N-{3-[spiroisobenzofuran-1(3H),4′-piperidin-1-yl]propyl} pyrrolidine-2-carboxamide was recently identified as a nociceptin/orphanin FQ (N/OFQ) peptide receptor (NOP) ligand. In this study, the *in vitro* and *in vivo* pharmacological profiles of Compound 24 were investigated. *In vitro* studies were performed measuring receptor and [^{35}S]GTPγS binding and calcium mobilization in cells expressing the recombinant NOP receptor as well as using N/OFQ sensitive tissues. *In vivo* studies were conducted using the tail withdrawal assay in mice. Compound 24 produced a concentration-dependent displacement of [^{3}H]N/OFQ binding to CHO_{hNOP} cell membranes showing high affinity (pK_i 9.62) and selectivity (1000 fold) over classical opioid receptors. Compound 24 antagonized with high potency the following *in vitro* effects of N/OFQ: stimulation of [^{35}S]GTPγS binding in CHO_{hNOP} cell membranes (pA_2 9.98), calcium mobilization in CHO_{hNOP} cells expressing the $G\alpha_{qi5}$ chimeric protein (pK_B 8.73), inhibition of electrically evoked twitches in the mouse (pA_2 8.44) and rat (pK_B 8.28) vas deferens, and in the guinea pig ileum (pK_B 9.12). In electrically stimulated tissues, Compound 24 up to 1 μM did not modify the effects of classical opioid receptor agonists. Finally *in vivo*, in the mouse tail withdrawal assay, Compound 24 at 10 mg/kg antagonized the pronociceptive and antinociceptive effects of 1 nmol N/OFQ given supraspinally and spinally, respectively. Under the same experimental conditions Compound 24 did not affect the antinociceptive action of 3 nmol endomorphin-1 injected intrathecally. The present study demonstrated that Compound 24 is a pure, competitive, and highly potent non-peptide NOP receptor selective antagonist.

1. Introduction

Nociceptin/orphanin FQ (N/OFQ) (Meunier et al., 1995; Reinscheid et al., 1995) modulates several different biological functions via selective activation of the N/OFQ peptide (NOP) receptor (Lambert, 2008). There are numerous studies describing the central and peripheral actions of N/OFQ and selective NOP agonists. In contrast, relatively few studies are available regarding the effects of selective NOP receptor antagonists. This is mainly due to the fact that only few such molecules are described in the literature (Chiou et al., 2007; Lambert, 2008). Moreover not all the described NOP receptor antagonists are commercially available. Nevertheless, there is convincing evidence that blockade of NOP receptors may be beneficial in some conditions or pathological states. For instance, peptide ([Nphe^1]N/OFQ(1-13)-NH_2 (Calo et al., 2000) and UFP-101 (Calo et al., 2002b)) and non peptide (J-113397 (Ozaki et al., 2000) and SB-612111 (Zaratin et al., 2004)) NOP antagonists were demonstrated to evoke antidepressant like actions in rodents (Gavioli and Calo, 2006; Gavioli et al., 2003, 2004; Redrobe et al., 2002; Rizzi et al., 2007). Interestingly and corroborating antagonist studies $NOP^{-/-}$ mice displayed an antidepressant-like phenotype (Gavioli et al., 2003). Moreover, in a rather elegant series of studies, it has been demonstrated that the endogenous N/OFQ–NOP receptor signalling inhibits motor behaviour and that NOP receptor antagonists (UFP-101, J-113397, and Trap-101 (Trapella et al., 2006)) produce beneficial effects in rodent models of Parkinson's disease (Marti et al., 2004a,b, 2005, 2007; Viaro et al., 2008). This indication has also been confirmed in non-human primates (Viaro et al., 2008; Visanji et al., 2008). Very recent findings indicated that plasma N/OFQ levels in sepsis were higher in patients who died within 30 days (Williams et al., 2008) and this parallels the preclinical observation that the NOP receptor antagonist UFP-101

Abbreviations: N/OFQ, Nociceptin/orphanin FQ; NOP, N/OFQ peptide receptor; Compound 24, 1-benzyl-N-{3-[spiroisobenzofuran-1(3H),4′-piperidin-1-yl]propyl} pyrrolidine-2-carboxamide; CHO, Chinese hamster ovary; DPN, diprenorphine; DPDPE, [D-Pen^2,D-Pen^5]enkephalin; BSA, bovine serum albumin; HBSS, Hank's Balanced Salt Solution; encapsin, hydroxypropyl-beta-cyclodextrin: AUC, area under the curve.

* Corresponding author. Via Fossato di Mortara 19, 44100 Ferrara, Italy. Tel.: +39 0532 455 221; fax: +39 0532 455 205.
E-mail address: g.calo@unife.it (G. Calo').

0014-2999/$ – see front matter © 2009 Elsevier B.V. All rights reserved.
doi:10.1016/j.ejphar.2009.04.054

reduces animal mortality in a rat model of sepsis (Carvalho et al., 2008). To be fully validated and firmly attributed to the NOP receptor antagonist class of drugs, these emerging indications should be confirmed in future studies using several chemically unrelated molecules.

A novel NOP receptor non-peptide antagonist, 1-benzyl-N-{3-[spiroisobenzofuran-1(3H),4′-piperidin-1-yl]propyl} pyrrolidine-2-carboxamide, has been recently identified by Banyu investigators and named Compound 24 (Goto et al., 2006). The synthesis of this novel ligand is relatively easy and the overall yield relatively high (25% in our laboratory, 31% in Goto et al. (2006)). This is particularly true when compared to the synthesis of other non peptide NOP antagonists such as J-113397 and SB-612111 whose synthesis is very difficult and of low overall yield (≈1% for both molecules in our laboratories, C. Trapella personal communication).

Thus, the aim of the present study was the synthesis and detailed investigation of the pharmacological profile of Compound 24. The novel ligand was investigated *in vitro* in receptor binding and [^{35}S]GTPγS experiments performed in CHO_{hNOP} cell membranes, in calcium mobilization experiments performed in CHO_{hNOP} cells expressing the $G\alpha_{qi5}$ protein, and in N/OFQ sensitive isolated tissues. Finally, the *in vivo* actions of Compound 24 were assessed in mice using the tail withdrawal assay.

2. Materials and methods

2.1. Cell culture and membrane preparation

CHO_{hNOP} cells were cultured in Dulbecco Minimum Essential Medium (DMEM) and Ham F-12 (1:1) supplemented with 5% foetal calf serum, penicillin (100 IU/ml), Streptomycin (100 μg/ml) and Fungizone (2.5 μg/ml). Stock cultures were further supplemented with geneticin (G418, 200 μg/ml) and Hygromycin B (200 μg/ml) as described previously (McDonald et al., 2003). CHO_{hmu}, CHO_{hdelta}, CHO_{hkappa} and CHO_{hNOP} stably expressing the $G\alpha_{qi5}$ protein were generated as previously described (Camarda et al., 2009) and maintained in DMEM and Ham F-12 (1:1) supplemented with 10% fetal bovine serum, 2 mM L-Glutamine, 200 μg/ml Geneticin, 100 μg/ml Hygromycin B. Cells were cultured at 37 °C in 5% carbon dioxide humidified air, and used when confluent. For binding experiments membranes were prepared from freshly harvested cell suspensions in Tris–HCl (50 mM), Mg^{2+} (5 mM) pH 7.4 ([^{3}H]N/OFQ binding experiments) or in Tris–HCl (50 mM), EGTA (0.2 mM) pH 7.4 ([^{35}S]GTPγS binding experiments) via homogenisation and centrifugation at 13,500 rpm for 10 min at 4 °C. The final protein concentration was determined according to Lowry et al. (1951).

2.2. Receptor binding experiments

2.2.1. [Leucyl-^{3}H]N/OFQ binding

5 μg of CHO_{hNOP} homogenate protein was incubated in 0.5 ml volumes of Tris–HCl (50 mM) buffer supplemented with 10 μM peptidase inhibitors (amastatin, bestatin, captopril and phosphoramidon), 0.5% bovine serum albumin (BSA), increasing concentrations of Compound 24 and approximately 200 pM [^{3}H]–N/OFQ. Total radiolabel bound was <<10%. Non-specific binding was determined in the presence of 1 μM unlabelled N/OFQ. In all experiments N/OFQ was included as a reference ligand. Reactions were incubated for 1 h at room temperature and terminated by vacuum filtration (Brandel Harvester) through Whatman GF/B filters soaked in 0.5% polyethylenimine. Radioactivity was determined after 8 h extraction in scintillation cocktail.

2.2.2. [^{3}H]-Diprenorphine binding

50 μg (CHO_{hmu}), 25 μg (CHO_{hdelta}) and 40 μg (CHO_{hkappa}) membrane protein were incubated in 0.5 ml buffer containing Tris–HCl (50 mM) pH 7.4, BSA (0.5%), ~0.7 nM [^{3}H]-Diprenorphine and increasing concentrations of naloxone and Compound 24. Non-specific binding was determined in the presence of 10 μM naloxone. Reactions were incubated at room temperature for 1 h. Harvesting and determination of radioactivity were as for [leucyl-^{3}H]N/OFQ binding.

2.3. [^{35}S]GTPγS binding experiments

20 μg of CHO_{hNOP} membranes were incubated in 0.5 ml buffer containing Tris–HCl (50 mM), EGTA (0.2 mM) $MgCl_2$ (1 mM), NaCl (100 mM), bacitracin (0.15 mM) peptidase inhibitors (as above), GDP (100 μM) and approximately 150 pM [^{35}S]GTPγS (McDonald et al., 2003). Compound 24 was pre-incubated for 15 min at 30 °C. Non-specific binding was determined in the presence of 10 μM unlabelled GTPγS. The reaction was incubated for 1 h at 30 °C with gentle shaking and terminated by filtration through Whatman GF/B filters using a Brandel Harvester.

2.4. Calcium mobilization experiments

CHO_{hmu}, CHO_{hdelta}, CHO_{hkappa} and CHO_{hNOP} stably expressing the $G\alpha_{qi5}$ protein were seeded at a density of 40,000 cells/well into 96-well black, clear-bottom plates. After 24 h incubation the cells were loaded with medium supplemented with 2.5 mM probenecid, 3 μM of the calcium sensitive fluorescent dye Fluo-4 AM and 0.01% pluronic acid, for 30 min at 37 °C. Afterwards the loading solution was aspirated and 100 μl/well of assay buffer: Hank's Balanced Salt Solution (HBSS) supplemented with 20 mM HEPES, 2.5 mM probenecid and 500 μM Brilliant Black (Aldrich) was added. Stock solutions (1 mM) of ligands were made in distilled water and stored at −20 °C. Serial dilutions of ligands for experimental use were made in HBSS/HEPES (20 mM) buffer (containing 0.02% BSA fraction V). After placing both plates (cell culture and compound plate) into the FlexStation II (Molecular Device, Union City, CA 94587, US), fluorescence changes were measured at room temperature. On-line additions were carried out in a volume of 50 μl/well.

2.5. Electrically stimulated isolated tissue experiments

Tissues were taken from male Swiss mice (30–35 g), albino guinea pigs (300–350 g) and Sprague-Dawley rats (300–350 g). The mouse and rat vas deferens and the guinea pig ileum were prepared as previously described (Bigoni et al., 1999; Calo et al., 1996). Tissues were suspended in 5 ml organ baths containing heated Krebs solution oxygenated with 95% O_2 and 5% CO_2. The bath temperature was set at 33 °C for mouse vas deferens and 37 °C for rat vas deferens and guinea pig ileum. Tissues were continuously stimulated through two platinum ring electrodes with supramaximal rectangular pulses of 1 ms duration and 0.05 Hz frequency. A resting tension of 0.3, 1 and 1.5 g was applied to the mouse and rat vas deferens, and guinea pig ileum, respectively. The electrically evoked contractions (twitches) were measured isotonically with a strain gauge transducer (Basile 7006, UgoBasile s.r.l., Varese, Italy) and recorded with the PC based acquisition system Power Lab (ADInstrument, USA).

Following an equilibration period of 60 min, the contractions induced by electrical field stimulation were stable. At this time, cumulative concentration-response curves to N/OFQ were performed (0.5 log unit steps) in the absence or presence of Compound 24 (15 min pre-incubation time). For selectivity studies, in some experiments the delta selective agonist DPDPE was used in the mouse vas deferens while in others the mu selective agonist Dermorphin was used in the guinea pig ileum.

2.6. Tail withdrawal assay

Male Swiss albino mice weighing 25–30 g were used. Animals were handled according to guidelines published in the European Communities Council directives (86/609/EEC) and Italian national regulations

Table 1
Affinities of Compound 24 and naloxone at NOP and classical opioid receptors expressed in CHO cell membranes.

Receptor	NOP	Mu	Delta	Kappa
Radioligand	[^{3}H]N/OFQ	[^{3}H]DPN	[^{3}H]DPN	[^{3}H]DPN
Naloxone[a]	<6	9.25 (9.04–9.46)	7.67 (7.59–7.75)	8.35 (8.20–8.50)
Compound 24	9.62 (9.47–9.77)	6.72 (6.43–6.97)	<6	6.47 (6.20–6.74)

[a] Naloxone affinities at classical opioid receptors are from Vergura et al. (2006). Data are mean ($CL_{95\%}$) of 3 separate experiments.

(D.L. 116/92). They were housed in 425×266×155-mm cages (Techniplast, Milan, Italy), fifteen animals/cage, under standard conditions (22 °C, 55% humidity, 12-h light/dark cycle, light on at 7:00 am) with food (MIL, standard diet; Morini, Reggio Emilia, Italy) and water *ad libitum* for at least 5 days before experiments began. Each mouse was used only once. I.c.v. (2 µl/mouse) or i.t (5 µl/mouse) injections were given according to the procedure described by Laursen and Belknap (1986) and Hylden and Wilcox (1980), respectively.

All experiments were started at 10:00 am and performed according to the procedure described previously in detail (Calo et al., 1998). Briefly, the mice were placed in a holder and the distal half of the tail was immersed in water at 48 °C. Withdrawal latency time was measured by an experienced observer blind to drug treatment. A cut-off time of 20 s was chosen to avoid tissue damage. For each experiment sixteen mice were used by randomly assigning four animals to each treatment group. The experiment was repeated four times; therefore, each experimental point shown in Figs. 5 and 6 is the mean of the results obtained in 16 mice. Tail-withdrawal latency was determined immediately before and 5, 15, 30, and 60 min after i.c.v. or i.t. injection of vehicle (saline) or N/OFQ (1 nmol) or endomorphin-1 (3 nmol, only i.t.). Compound 24 (10 mg/kg) or its vehicle (2% DMSO and 10% encapsin) were given i.p. 30 min before N/OFQ or endomorphin-1 administration. Increased and decreased tail withdrawal latencies compared with baseline indicated antinociceptive and pronociceptive effects, respectively.

2.7. Drugs

The peptides used in this study were prepared and purified as previously described (Guerrini et al., 1997). [D-Pen^2,D-Pen^5]enkephalin (DPDPE) and endomorphin-1 were purchased from NeoMPS (Strasbourg, France). Compound 24 was synthesized in house following the procedures described in detail by Goto et al. (2006) with little modification. The structure and purity (>99%) of Compound 24 was confirmed by HPLC, mass spectrometry, proton and carbon NMR and polarimetry.

All tissues culture media and supplements were from Invitrogen (Paisley, UK). [^{35}S]GTPγS (1250 Ci/mmol) and [^{3}H]DPN were from Perkin Elmer Life Sciences and [^{3}H]N/OFQ (75–133 Ci/mmol) from Amersham Biosciences. All other reagents were from Sigma Chemical Co. (Poole, U.K.) or E. Merck (Darmstadt, Germany) and were of the highest purity available.

For *in vitro* experiments Compound 24 was solubilized in dimethyl sulfoxide at a final concentration of 10 mM, and the successive dilutions were made in saline, whereas the other compounds were solubilized distilled water; stock solutions were kept at −20 °C until use. For *in vivo* studies, Compound 24 was dissolved in 2% DMSO and 10% encapsin (hydroxypropyl-beta-cyclodextrin) just before performing the experiment.

2.8. Data analysis and terminology

All data are expressed as means ± standard error of the mean (S.E.M.) of *n* experiments. For potency values 95% confidence limits were indicated. Data have been analyzed statistically using one-way ANOVA followed by Dunnett's test for multiple comparisons. Receptor binding data (Table 1) are expressed as pK_i derived from the Cheng and Prusoff (Cheng and Prusoff, 1973) equation:

$$pK_i = IC_{50}/(1 + ([R]/K_d))$$

where [*R*] is the concentration of the radiolabel and K_d is the radiolabel affinity for the receptor under investigation. The [^{3}H]N/OFQ K_d was 83 pM while those of [^{3}H]diprenorphine were 125, 323, and 134 pM at mu, delta, and kappa, respectively.

[^{35}S]GTPγS data are expressed as a stimulation factor i.e., the ratio between agonist-stimulated [^{35}S]GTPγS specific (minus NSB) binding and basal specific binding. Calcium mobilization data are expressed as fluorescence intensity units (FIU) in percent over the baseline. Isolated tissue data are expressed as percent of the twitch induced by electrical field stimulation.

Agonist potencies are given as pEC_{50} = the negative logarithm to base 10 of the molar concentration of an agonist that produces 50% of the maximal possible effect. Concentration response curve to agonists were fitted with the following equation:

$$\text{Effect} = \text{baseline} + (\text{Emax} - \text{baseline}) \div (1 + 10\text{^}((\text{LogEC}_{50} - X)\text{*HillSlope}))$$

where *X* is the agonist concentration.

Antagonist potencies have been calculated in different ways. In [^{35}S]GTPγS binding (Fig. 1) and mouse vas deferens (Fig. 3) pA_2 values were derived from the classical Schild protocol. For rat vas deferens

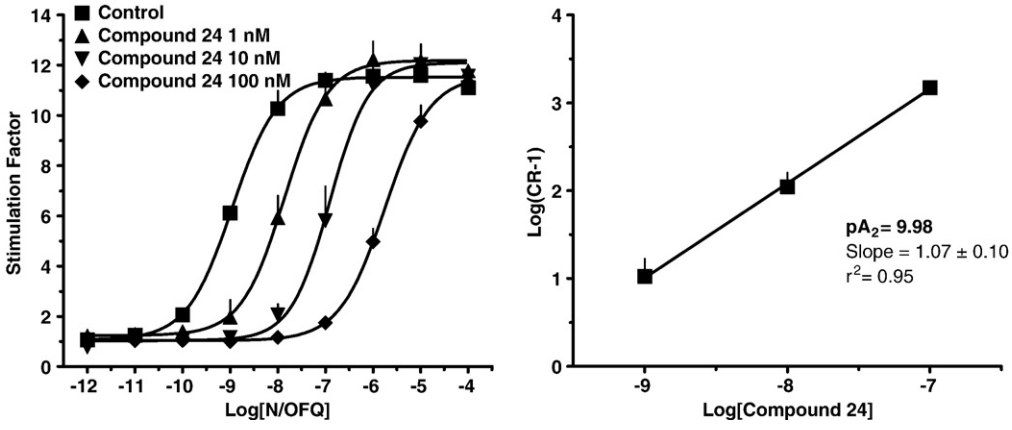

Fig. 1. Left panel: concentration response curves to N/OFQ obtained in the absence (control) and presence of increasing concentrations of Compound 24 (1–100 nM) in the [^{35}S]GTPγS binding assay performed on CHO_{hNOP} cell membranes. The relative Schild Plot is shown in the right panel. Data are mean ± S.E.M. of 4 separate experiments.

and guinea pig ileum experiments (Fig. 4) pK_B values were derived from the Gaddum Schild equation:

$$K_B = ((CR - 1) / [antagonist])$$

assuming a slope value equal to unity, where CR indicate the ratio between agonist potency in the presence and absence of antagonist. For calcium mobilization experiments pK_B values were derived from inhibition response curves (Table 2) using the following equation:

$$K_B = IC_{50} / \left(\left[2 + ([A] / EC_{50})^n \right]^{1/n} - 1 \right)$$

where IC_{50} is the concentration of antagonist that produces 50% inhibition of the agonist response, [*A*] is the concentration of agonist, EC_{50} is the concentration of agonist producing a 50% maximal response and n is the Hill coefficient of the concentration response curve to the agonist (Kenakin, 2004). In addition the pK_B for Compound 24 evaluated at different concentrations against the concentration response curve to N/OFQ (Fig. 2) was calculated using the following equation:

$$K_B = [antagonist] / (slope - 1)$$

where slope is calculated from a double-reciprocal plot of equieffective concentrations of agonist in the absence and presence of antagonist (Kenakin, 2004).

For *in vivo* studies, raw data from tail withdrawal experiments were converted to the area under the time versus tail withdrawal latency curve (AUC min/s). AUC data for the time interval (0–15 and 0–30 min for i.c.v. and i.t. studies, respectively) was calculated and used for statistical analysis.

3. Results

3.1. Receptor binding

In receptor binding experiments performed on CHO_{hNOP} cell membranes Compound 24 displaced [^{3}H]N/OFQ in a concentration dependent manner showing subnanomolar affinity (pK_i 9.62, Table 1). Under the same experimental conditions, Compound 24 did not bind the delta receptor and showed low affinities for mu and kappa sites (pK_i 6.72 and 6.47, respectively). In contrast, the universal opioid receptor ligand naloxone did not bind the NOP receptor while showed the expected rack order of affinity at classical opioid receptors i.e., mu (pK_i 9.25)>kappa (pK_i 8.35)>delta (pK_i 7.67) (Table 1).

3.2. [^{35}S]GTPγS binding

In CHO_{hNOP} cell membranes N/OFQ stimulated [^{35}S]GTPγS binding in a concentration-dependent manner with a pEC_{50} value of 8.95 ± 0.05 and E_{max} of 11.71 ± 0.37 (Fig. 1, left panel). The antagonistic properties of Compound 24 were evaluated over the 1–100 nM concentration range, in order to obtain data for a Schild analysis. Compound 24 up to 10 μM did not elicit any stimulation of [^{35}S]GTPγS binding in CHO_{hNOP} cell membranes, however it produced a concentration dependent and parallel shift of the concentration response curve to N/OFQ without modifying the maximal effects induced by the agonist (Fig. 1, left panel). Schild analysis of the data (Fig. 1, right panel) demonstrated a linear ($r^2 = 0.95$) plot with a slope not significantly different from unity. The extrapolated pA_2 value was 9.98.

Table 2
Antagonist potencies of Compound 24 and naloxone evaluated in calcium mobilization experiments performed in CHO cells expressing NOP or classical opioid receptors and the $G\alpha_{qi5}$ protein.

Receptor	NOP	Mu	Delta	Kappa
Agonist	N/OFQ 10 nM	Dermorphin 100 nM	DPDPE 100 nM	Dynorphin A 100 nM
Naloxone	<6	9.09 (8.73–9.45)	7.32 (6.11–8.53)	7.14 (6.60–7.68)
Compound 24	9.03 (8.83–9.23)	<6	<6	<6

Data are mean ($CL_{95\%}$) of 4 separate experiments.

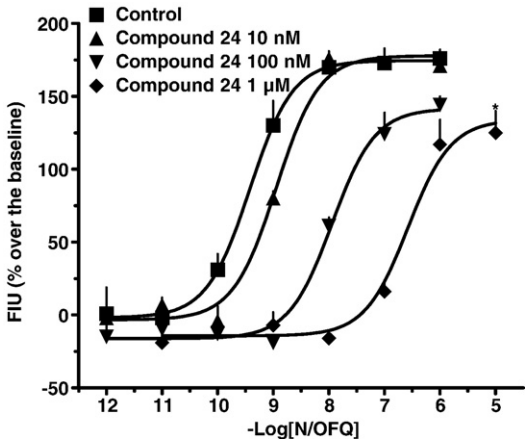

Fig. 2. Concentration response curves to N/OFQ obtained in the absence (control) and presence of increasing concentrations of Compound 24 (10 nM–1 μM) in the calcium mobilization assay performed on CHO_{hNOP} cells stably expressing the $G\alpha_{qi5}$ protein. Data are mean ± S.E.M. of 4 separate experiments performed in duplicate. *$p<0.05$ versus control according to ANOVA followed by Dunnett's test.

3.3. Calcium mobilization

In CHO_{hNOP} cells stably expressing the $G\alpha_{qi5}$ chimeric protein N/OFQ evoked a concentration dependent stimulation of calcium release (pEC_{50} 9.24 ($CL_{95\%}$ 9.10–9.38)). Compound 24 was inactive per se but in the range 0.01 nM–10 μM concentration-dependently inhibited calcium mobilization induced by 10 nM N/OFQ with a pK_B value of 9.03 ± 0.20 (Table 2). Naloxone was inactive up to 1 μM. To assess the selectively of action of Compound 24 similar experiments were performed in CHO cells stably expressing $G\alpha_{qi5}$ and classical opioid receptors. Dermorphin, DPDPE and Dynorphin A were used in these experiments as agonists for mu, delta and kappa receptors, respectively. They produced a concentration dependent stimulation of calcium with the following values of pEC_{50} and E_{max}:Dermorphin 7.93 ($CL_{95\%}$ 7.67–8.19), 196 ± 9%; DPDPE 8.82 ($CL_{95\%}$ 8.43–9.21), 130 ± 10%; Dynorphin A 8.47 ($CL_{95\%}$ 8.16–8.78) 174 ± 14%. Naloxone inhibited the effects of these agonists showing higher potency at mu (pK_B 9.09) than kappa (pK_B 7.14) and delta (pK_B 7.32) (Table 2). In contrast Compound 24 was inactive up to 1 μM against DPDPE, Dynorphin A, and Dermorphin (Table 2).

To investigate the type of antagonism produced by Compound 24 in calcium mobilization experiments a Schild analysis has been performed by testing this molecule at various concentrations (0.01, 0.1 and 1 μM) against the concentration-response curve to N/OFQ. As shown in Fig. 2, Compound 24 produced a rightward shift of the concentration-response curve to N/OFQ in a concentration dependent manner. However, the maximal effects elicited by N/OFQ appear to be slightly but significantly reduced by Compound 24. A pK_B value of 8.73 was derived from these experiments. It is worthy of mention that this value is close to that obtained in inhibition response experiments (9.03).

3.4. Electrically stimulated isolated tissue

Compound 24 was assessed against N/OFQ in the electrically stimulated mouse and rat vas deferens and guinea pig ileum. In the

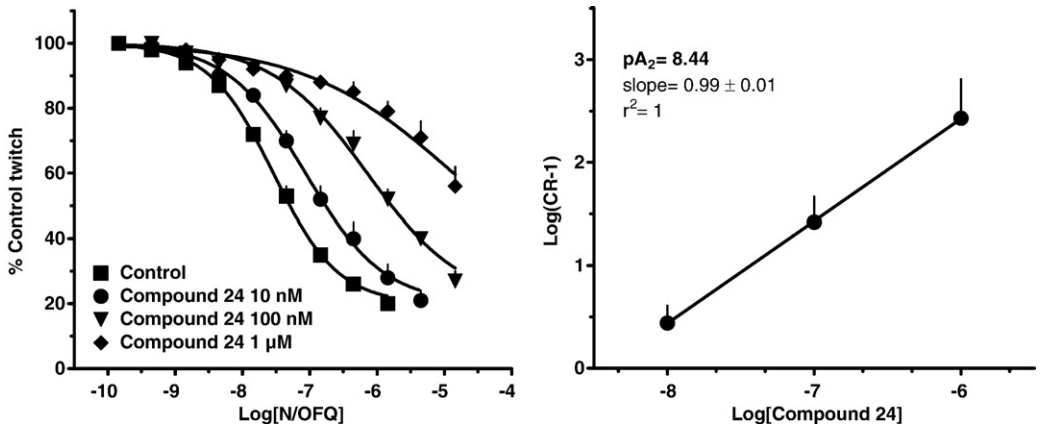

Fig. 3. Left panel: concentration response curves to N/OFQ obtained in the absence (control) and presence of increasing concentrations of Compound 24 (10 nM–1 μM) in the electrically stimulated mouse vas deferens. The relative Schild Plot is shown in the right panel. Data are mean ± S.E.M. of 4 separate experiments.

mouse vas deferens N/OFQ inhibited the twitch response to electrical field stimulation in a concentration dependent manner (pEC_{50} value 7.46, Fig. 3 left panel). Compound 24, tested over the concentration range 10 nM–1 μM, did not modify *per se* the electrically-induced twitches, but displaced to the right the concentration response curve to N/OFQ in a concentration dependent manner. Curves obtained in the presence of Compound 24 were parallel to the control (Fig. 3, left panel) with no modification of the agonist maximal effect (this parameter could not be estimated in the presence of Compound 24 1 μM because the concentration response curve to N/OFQ was still incomplete at 10 μM concentration of peptide). The corresponding Schild plot was linear ($r^2 = 1.00$) with a slope not significantly different from unity, yielding a pA_2 value of 8.44 (Fig. 3, right panel).

In the rat vas deferens and in guinea pig ileum Compound 24 was tested at the single concentration of 100 nM against the effects of N/OFQ. In both preparations the concentration response curves to N/OFQ obtained in the absence and presence of Compound 24 were parallel and reached similar maximal effects. The estimated pK_B values were 8.28 ± 0.12 and 9.12 ± 0.19 in the rat vas deferens (Fig. 4, left panel) and guinea pig ileum (Fig. 4, right panel), respectively. In these preparations, Compound 24 up to 1 μM was *per se* inactive.

Finally, Compound 24 at 1 μM did not modify the inhibitory effects of DPDPE in the mouse vas deferens (control: pEC_{50} (95% confidence limit) 8.38 (8.20–8.56), E_{max}, 98 ± 1%; 1 μM Compound 24: pEC_{50} 8.30 (7.80–8.80), E_{max}, 99 ± 1%) or those evoked by Dermorphin in the guinea pig ileum (control: pEC_{50} 8.52 (8.35–8.69), E_{max}, 98 ± 3%; 1 μM Compound 24: pEC_{50}, 8.51 (8.35–8.67), E_{max}, 95 ± 3%).

3.5. Tail withdrawal assay

In tail withdrawal experiments, mice injected with vehicle (either i.c.v. or i.t.) displayed tail withdrawal latencies of approximately 5 s that were stable over the time course of the experiment (Fig. 5). In line with previous studies, N/OFQ (1 nmol) applied i.c.v. significantly reduced tail withdrawal latency with a maximal effect (about 50% reduction in tail withdrawal latency) obtained at 5 min ($AUC_{[0-15\ min]}$ vehicle 77 ± 5; 1 nmol of N/OFQ 51 ± 3, $p<0.05$). The i.p. administration of Compound 24 up to 10 mg/kg did not modify, *per se*, tail withdrawal latencies ($AUC_{[0-15\ min]}$, 80 ± 7) but prevented the pronociceptive effects of the natural peptide ($AUC_{[0-15\ min]}$, 66 ± 5) (Fig. 5, left panel). On the other hand Compound 24 at 1 mg/kg did not modify the pronociceptive effect of i.c.v. N/OFQ (data not shown).

When the same dose of N/OFQ was administered i.t., a statistically significant antinociceptive effect was recorded ($AUC_{[0-30\ min]}$ vehicle, 165 ± 14; 1 nmol N/OFQ 346 ± 25, $p<0.05$) (Fig. 5, right panel). This antinociceptive effect was reduced by Compound 24 at 10 mg/kg ($AUC_{[0-30\ min]}$, 226 ± 25) (Fig. 5, right panel) but not at 1 mg/kg (data not shown).

In a separate set of experiments performed under the same experimental conditions, the selective mu receptor agonist endomorphin-1 produced after i.t. injection a clear antinociceptive effect ($AUC_{[0-30\ min]}$

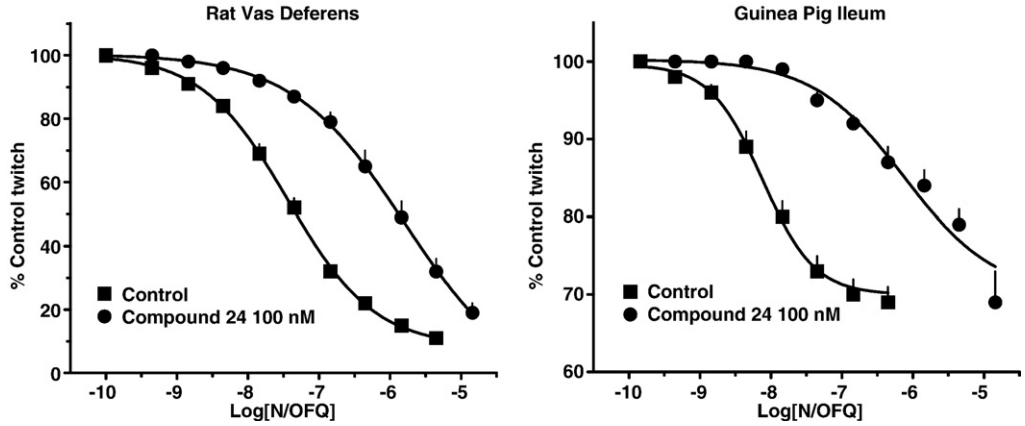

Fig. 4. Concentration response curves to N/OFQ obtained in the absence (control) and presence of 100 nM Compound 24 in the electrically stimulated rat vas deferens (left panel) and guinea pig ileum (right panel). Data are mean ± S.E.M. of 4 separate experiments.

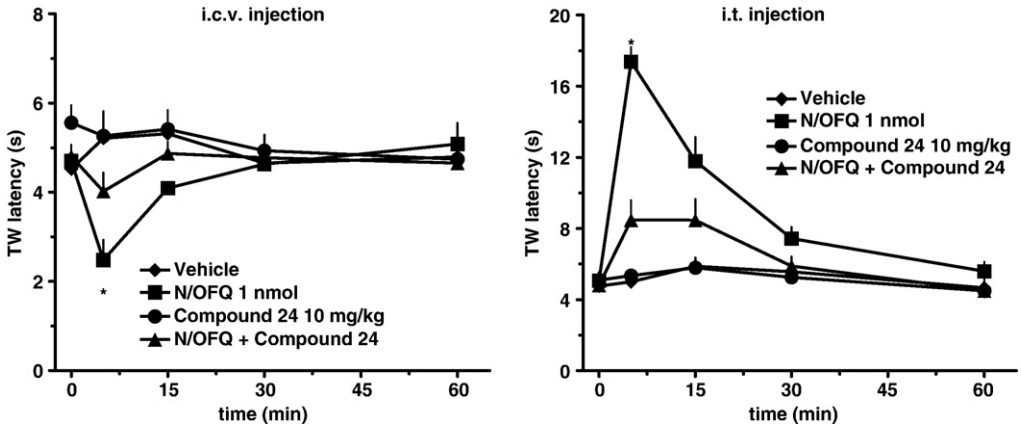

Fig. 5. Mouse tail withdrawal assay. Effects of Compound 24 (10 mg/kg i.p., 30 min pre-treatment) on the pronociceptive or antinociceptive effects induced by 1 nmol N/OFQ injected i.c.v. (left panel) or i.t. (right panel). Data are mean ± S.E.M. of 4 separate experiments.*$p<0.05$ versus vehicle according to ANOVA followed by the Dunnett's test.

vehicle, 152 ± 18; 3 nmol endomorphin-1 395 ± 31, $p<0.05$) (Fig. 6). Ten mg/kg of Compound 24 did not produce any effect per se ($AUC_{[0-30\ min]}$, 184 ± 17) and did not affect the antinociceptive effects elicited by endomorphin-1 ($AUC_{[0-30\ min]}$, 352 ± 35) (Fig. 6).

4. Discussion

The present study extend previous findings (Goto et al., 2006) demonstrating that Compound 24 binds with high affinity the NOP receptor and behaves as a pure and potent NOP receptor antagonist showing high selectivity over classical opioid receptor. These pharmacological features of Compound 24 were consistently observed in various assays and preparations expressing the human recombinant as well as the animal native receptors. In addition, the NOP selective antagonist properties of Compound 24 have been confirmed *in vivo* in mice subjected to the tail withdrawal assay. Therefore Compound 24 represents a valuable research tool that should be included in the class of selective NOP receptor antagonists and used in future target validations studies.

In receptor binding studies Compound 24 displayed very high affinity for the NOP receptor; in fact, the pK_i value calculated from the present experiments (9.62) is virtually superimposable to that previously reported by Goto et al. (2006) (pIC_{50} 9.57). These values of affinity are similar to that reported for SB-612111 and higher than that of J-113397 (Ozaki et al., 2000; Spagnolo et al., 2007; Zaratin et al., 2004). In functional studies performed on the human recombinant receptor ([^{35}S]GTPγS binding and calcium mobilization assays) and on animal native receptors from various species (mouse, rat, guinea pig) Compound 24 consistently behaved as a pure NOP receptor antagonist showing, in line with receptor binding studies, high values of potency (range 8.28–9.12). The only result which was out of this range is that obtained in [^{35}S]GTPγS binding studies where Compound 24 displayed a pA_2 of 9.98. However, this result, which is again superimposable to that obtained by Goto et al. (2006)(pIC_{50} 9.82), is expected on the basis of what we have observed with several NOP receptor antagonists, including the peptides [Nphe^1]N/OFQ(1–13)NH_2 and UFP-101 (Calo et al., 2002a, 2005), and the non peptides J-113397, Trap-101, and SB-612111 (Spagnolo et al., 2007; Trapella et al., 2006), that consistently showed, in this particular assay, values of potency approx 10 fold higher than in the other tests. As previously suggested (Spagnolo et al., 2007), this might be due to the higher receptor accessibility in membranes (where the [^{35}S]GTPγS binding assay is performed) than in whole cells or tissue preparations (where the other assays are performed). Despite this minor difference, very similar antagonist potency values were obtained in the different assays for Compound 24 demonstrating the recombinant and native as well as species-specific NOP receptors are similarly sensitive to this antagonist. This also applies to the NOP receptors expressed in rat periaqueductal gray slices (Yan-Yu and Chiou, 2008) and sympathetic neurons (Ruiz-Velasco et al., 2008) although no quantitative data were reported in these latter studies. The consistency of Compound 24 potency values among preparations and species corroborates previous findings obtained with peptide (Calo et al., 2000, 2002a,b, 2005) and non peptide (Bigoni et al., 2000; Ozaki et al., 2000; Spagnolo et al., 2007; Trapella et al., 2006; Zaratin et al., 2004) NOP antagonists and enable the following rank order of antagonist potency to be proposed: Compound 24 (≈8.5) = SB-612111 (≈8.5) > J-113397 (≈8.0) > UFP-101 (≈7.5) = Trap-101 (≈7.5) > [Nphe^1]N/OFQ(1–13)NH_2 (≈6.5) as NOP receptor fingerprint.

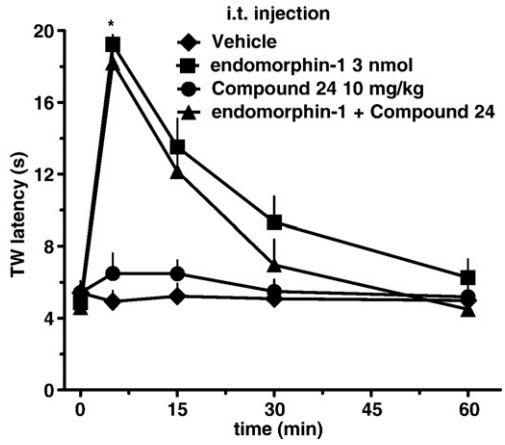

Fig. 6. Mouse tail withdrawal assay. Effects of Compound 24 (10 mg/kg i.p., 30 min pre-treatment) on the antinociceptive effects induced by 3 nmol emdomophin-1 injected i.t. Data are mean ± S.E.M. of 4 separate experiments. *$p<0.05$ versus vehicle according to ANOVA followed by the Dunnett's test.

With respect to the type of antagonism exerted by Compound 24, results obtained in the [^{35}S]GTPγS binding and mouse vas deferens assay by performing concentration response curve to N/OFQ in the presence of increasing concentrations of antagonist are clearly compatible with a competitive type of interaction between Compound 24 and N/OFQ. Similar results were obtained by testing Compound 24 in the calcium mobilization assay where a rightward displacement of the concentration response curve to N/OFQ was recorded in response to increasing concentration of antagonist. However in these experiments Compound 24 at the highest concentrations tested produced a slight but statistically significant reduction of N/OFQ maximal effect. This apparent insurmountable antagonism behaviour can be attributed to i) the transient nature of the calcium response that may not allow equilibrium between agonist–antagonist competition to be

reached thus generating depression of the agonist response in the presence of high concentrations of antagonist (Kenakin, 2004), ii) lack of stirring in the 96 well plate which is another source of hemiequilibrium conditions (Kenakin, 2004), iii) a combination of the two factors. The observation that a truly competitive antagonist produces a reduction of agonist maximal effects in calcium mobilization assay is not uncommon. For instance, the urotensin-II receptor antagonists urantide and UFP-803 competitively antagonized the contractile effects of urotensin-II in the rat aorta bioassay while depressed maximal responses to the agonist in calcium experiments performed on cells expressing the rat recombinant urotensin-II receptor (Camarda et al., 2006). On this basis, we propose to classify Compound 24 as a competitive NOP receptor antagonist.

Selectivity of action along with high affinity/potency and pure antagonist activity is another important feature of a valuable research tool. This property of Compound 24 has been evaluated in three sets of experiments over classical opioid receptors. In receptor binding studies Compound 24 displayed approximately 1000 fold selectivity over classical opioid receptors. A superimposable value of selectivity was found in functional studies performed measuring calcium mobilization in cells expressing the $G\alpha_{qi5}$ chimeric protein. Finally at least 300 fold selectivity of Compound 24 for NOP over mu and delta receptors was obtained in bioassay experiments. These data confirm the impressive selectivity profile of Compound 24 reported by Goto et al. (2006). Thus, in terms of selectivity over classical opioid receptor Compound 24 seems to be similar to SB-612111 (Spagnolo et al., 2007; Zaratin et al., 2004) and UFP-101 (Calo et al., 2002b) and certainly more selective then J-113397 (Ozaki et al., 2000; Spagnolo et al., 2007) for which NOP independent effects were reported *in vivo* (Koizumi et al., 2004). However more comprehensive selectivity studies are needed against a large panel of receptors and ion channels to firmly classifying Compound 24 as a highly selective NOP receptor antagonist.

Collectively, these *in vitro* data confirm and extend previous findings (Goto et al., 2006) demonstrating that Compound 24 is a pure, competitive, selective and potent NOP receptor antagonist. This excellent *in vitro* pharmacological profile is associated with good brain penetration after peripheral administration (Goto et al., 2006). Indeed, Compound 24 was reported to be active *in vivo* in mice where at 10 mg/kg it prevented the inhibitory effects on locomotor activity of a non peptide NOP agonist (Goto et al., 2006). Here we assessed the *in vivo* effects of Compound 24 in the mouse tail withdrawal assay. N/OFQ has been repeatedly demonstrated to exert in rodents pronociceptive and antinociceptive effects following supraspinal and spinal injection, respectively (Zeilhofer and Calo, 2003). The present results i.e., pronociceptive and antinociceptive response to 1 nmol N/OFQ given i.c.v. and i.t., are therefore in line with the literature. Both of these *in vivo* actions of N/OFQ are due to selective NOP receptor activation as consistently demonstrated by knockout (Nazzaro et al., 2007; Nishi et al., 1997) and receptor antagonist (UFP-101 (Calo et al., 2002b; Nazzaro et al., 2007), J-113397 (Ozaki et al., 2000; Ueda et al., 2000), SB-612111 (Rizzi et al., 2007; Zaratin et al., 2004)) studies. In line with these findings, Compound 24 at 10 mg/kg antagonised both the pronociceptive and antinociceptive effects evoked by N/OFQ when given spinally and supraspinally, respectively. Moreover, in line with *in vitro* findings, the antagonist action of Compound 24 *in vivo* is selective for the NOP receptor as demonstrated by the lack of effect of this molecule against the antinociceptive effects elicited by spinal injection of the mu selective agonist endomorphin-1. These results demonstrated, on the one hand, that Compound 24 is an effective and selective antagonist at NOP receptors regulating pain transmission *in vivo* and, on the other, that the effects of N/OFQ on pain transmission are exclusively due to NOP receptor activation. Interestingly, Compound 24 at 10 mg/kg counteracted rather than fully prevented the effects of 1 nmol N/OFQ. Under the same experimental conditions SB-612111 completely blocked the actions of the same dose of N/OFQ at ten fold lower doses (i.e., 1 mg/kg) (Rizzi et al., 2007). Therefore SB-612111 appeared to be more potent than Compound 24 *in vivo* in the mouse tail withdrawal assay. Since the *in vitro* potency of the two antagonists is similar (see above), it can be proposed that *in vivo* potency differences may derive from better pharmacokinetic properties of SB-612111 than Compound 24. However, this is merely speculation that required rigorous experimental validation. Finally, the systemic administration of Compound 24 at pharmacologically active doses did not modify per se tail withdrawal latencies. Again this is in line with previous findings obtained with both receptor antagonists (Ozaki et al., 2000; Rizzi et al., 2007; Ueda et al., 2000; Zaratin et al., 2004) and mice knockout for the NOP receptor gene (Nazzaro et al., 2007; Nishi et al., 1997), and indicates that the endogenous N/OFQ-NOP receptor system is not activated by the mild and acute stimulus employed for evoking the nociceptive response in this assay. However the endogenous N/OFQergic signalling can be activated using more intense and prolonged nociceptive stimuli such as formalin. In fact in the mouse formalin assay the spinal antinociceptive action of endogenous N/OFQ seems to prevail on the supraspinal pronociceptive effect as indicated by the pronociceptive phenotype of NOP knockout mice (Depner et al., 2003; Rizzi et al., 2006) (recently confirmed in the acetic acid-induced writhing test by Rizzi et al. (2008)) and by the pronociceptive effects elicited by NOP antagonists e.g. systemic J-113397 (Rizzi et al., 2006).

In conclusion the present study demonstrated that Compound 24 is a pure, competitive, selective and potent NOP receptor antagonist. The NOP antagonist properties of Compound 24 were demonstrated in a large panel of *in vitro* assays and *in vivo* in the mouse tail withdrawal assay. Based on its pharmacological profile Compound 24 should be included (together with J-113397, SB-612111 and UFP-101) in the list of potent and selective NOP receptor antagonists to be tested in future target validation studies for firmly defining their therapeutic potential as innovative drugs for treating depression, Parkinson's disease and possibly sepsis.

Acknowledgements

We would like to thank Prof. E. Kostenis (Institute for Pharmaceutical Biology, Bonn, Germany) for supplying the plasmid encoding for $G\alpha_{qi5}$ protein and Prof T. Costa and his collaborators Dr P Molinari and C Ambrosio (Istututo Superiore di Sanità, Rome, Italy) for generating CHO cells stably expressing the $G\alpha_{qi5}$ chimeric protein. This work was supported by funds from the University of Ferrara (FAR grant to SS and GC) and the Italian Ministry of University (PRIN 2006 grant to DR and RG, FIRB 2004 grant to RG).

References

Bigoni, R., Giuliani, S., Calo, G., Rizzi, A., Guerrini, R., Salvadori, S., Regoli, D., Maggi, C.A., 1999. Characterization of nociceptin receptors in the periphery: in vitro and in vivo studies. Naunyn-Schmiedebergs Arch. Pharmacol. 359, 160–167.

Bigoni, R., Calo, G., Rizzi, A., Guerrini, R., De Risi, C., Hashimoto, Y., Hashiba, E., Lambert, D.G., Regoli, D., 2000. In vitro characterization of J-113397, a non-peptide nociceptin/orphanin FQ receptor antagonist. Naunyn-Schmiedebergs Arch. Pharmacol. 361, 565–568.

Calo, G., Guerrini, R., Bigoni, R., Rizzi, A., Marzola, G., Okawa, H., Bianchi, C., Lambert, D.G., Salvadori, S., Regoli, D., 2000. Characterization of [Nphe(1)]nociceptin(1-13)NH(2), a new selective nociceptin receptor antagonist. Br. J. Pharmacol. 129, 1183–1193.

Calo, G., Rizzi, A., Bogoni, G., Neugebauer, V., Salvadori, S., Guerrini, R., Bianchi, C., Regoli, D., 1996. The mouse vas deferens: a pharmacological preparation sensitive to nociceptin. Eur. J. Pharmacol. 311, R3–5.

Calo, G., Rizzi, A., Marzola, G., Guerrini, R., Salvadori, S., Beani, L., Regoli, D., Bianchi, C., 1998. Pharmacological characterization of the nociceptin receptor mediating hyperalgesia in the mouse tail withdrawal assay. Br. J. Pharmacol. 125, 373–378.

Calo, G., Rizzi, A., Bigoni, R., Guerrini, R., Salvadori, S., Regoli, D., 2002a. Pharmacological profile of nociceptin/orphanin FQ receptors. Clin. Exp. Pharmacol. Physiol. 29, 223–228.

Calo, G., Rizzi, A., Rizzi, D., Bigoni, R., Guerrini, R., Marzola, G., Marti, M., McDonald, J., Morari, M., Lambert, D.G., Salvadori, S., Regoli, D., 2002b. [Nphe1,Arg14,Lys15] nociceptin-NH2, a novel potent and selective antagonist of the nociceptin/orphanin FQ receptor. Br. J. Pharmacol. 136, 303–311.

Calo, G., Guerrini, R., Rizzi, A., Salvadori, S., Burmeister, M., Kapusta, D.R., Lambert, D.G., Regoli, D., 2005. UFP-101, a peptide antagonist selective for the nociceptin/orphanin FQ receptor. CNS Drug Rev. 11, 97–112.

Camarda, V., Spagnol, M., Song, W., Vergura, R., Roth, A.L., Thompson, J.P., Rowbotham, D.J., Guerrini, R., Marzola, E., Salvadori, S., Cavanni, P., Regoli, D., Douglas, S.A., Lambert, D.G., Calo, G., 2006. In vitro and in vivo pharmacological characterization of the novel UT receptor ligand [Pen(5),DTrp(7),Dab(8)]urotensin II(4-11) (UFP-803). Br. J. Pharmacol. 147, 92–100.

Camarda, V., Fischetti, C., Molinari, P., Ambrosio, C., Kostenis, E., Regoli, D., Guerrini, R., Salvadori, S., Calo, G., 2009. Pharmacological characterization of nociceptin/orphanin FQ receptors coupled with calcium signaling via the chimeric protein Galphaqi5. Naunyn Schmiedebergs Arch Pharmacol. 379, 599–607.

Carvalho, D., Petronilho, F., Vuolo, F., Machado, R.A., Constantino, L., Guerrini, R., Calo, G., Gavioli, E.C., Streck, E.L., Dal-Pizzol, F., 2008. The nociceptin/orphanin FQ-NOP receptor antagonist effects on an animal model of sepsis. Intensive Care Med. 34, 2284–2290.

Cheng, Y., Prusoff, W.H., 1973. Relationship between the inhibition constant (K1) and the concentration of inhibitor which causes 50 percent inhibition (I50) of an enzymatic reaction. Biochem. Pharmacol. 22, 3099–3108.

Chiou, L.C., Liao, Y.Y., Fan, P.C., Kuo, P.H., Wang, C.H., Riemer, C., Prinssen, E.P., 2007. Nociceptin/orphanin FQ peptide receptors: pharmacology and clinical implications. Curr. Drug Targets 8, 117–135.

Depner, U.B., Reinscheid, R.K., Takeshima, H., Brune, K., Zeilhofer, H.U., 2003. Normal sensitivity to acute pain, but increased inflammatory hyperalgesia in mice lacking the nociceptin precursor polypeptide or the nociceptin receptor. Eur. J. Neurosci. 17, 2381–2387.

Gavioli, E.C., Calo, G., 2006. Antidepressant- and anxiolytic-like effects of nociceptin/orphanin FQ receptor ligands. Naunyn-Schmiedebergs Arch. Pharmacol. 372, 319–330.

Gavioli, E.C., Marzola, G., Guerrini, R., Bertorelli, R., Zucchini, S., De Lima, T.C., Rae, G.A., Salvadori, S., Regoli, D., Calo, G., 2003. Blockade of nociceptin/orphanin FQ-NOP receptor signalling produces antidepressant-like effects: pharmacological and genetic evidences from the mouse forced swimming test. Eur. J. Neurosci. 17, 1987–1990.

Gavioli, E.C., Vaughan, C.W., Marzola, G., Guerrini, R., Mitchell, V.A., Zucchini, S., De Lima, T.C., Rae, G.A., Salvadori, S., Regoli, D., Calo, G., 2004. Antidepressant-like effects of the nociceptin/orphanin FQ receptor antagonist UFP-101: new evidence from rats and mice. Naunyn-Schmiedebergs Arch. Pharmacol. 369, 547–553.

Goto, Y., Arai-Otsuki, S., Tachibana, Y., Ichikawa, D., Ozaki, S., Takahashi, H., Iwasawa, Y., Okamoto, O., Okuda, S., Ohta, H., Sagara, T., 2006. Identification of a novel spiropiperidine opioid receptor-like 1 antagonist class by a focused library approach featuring 3D-pharmacophore similarity. J. Med. Chem. 49, 847–849.

Guerrini, R., Calo, G., Rizzi, A., Bianchi, C., Lazarus, L.H., Salvadori, S., Temussi, P.A., Regoli, D., 1997. Address and message sequences for the nociceptin receptor: a structure-activity study of nociceptin-(1-13)-peptide amide. J. Med. Chem. 40, 1789–1793.

Hylden, J.L., Wilcox, G.L., 1980. Intrathecal morphine in mice: a new technique. Eur. J. Pharmacol. 17, 313–316.

Kenakin, T., 2004. A Pharmacology Primer. Elsevier Academic Press, San Diego.

Koizumi, M., Sakoori, K., Midorikawa, N., Murphy, N.P., 2004. The NOP (ORL1) receptor antagonist Compound B stimulates mesolimbic dopamine release and is rewarding in mice by a non-NOP-receptor-mediated mechanism. Br. J. Pharmacol. 143, 53–62.

Lambert, D.G., 2008. The nociceptin/orphanin FQ receptor: a target with broad therapeutic potential. Nat. Rev. Drug Discov. 7, 694–710.

Laursen, S.E., Belknap, J.K., 1986. Intracerebroventricular injections in mice. Some. methodological refinements. J. Pharmacol. Methods 16, 355–357.

Lowry, O.H., Rosenbrough, N.J., Farr, A.L., Randall, R.J., 1951. Protein measurement with the Folin phenol reagent. J. Biol. Chem. 193, 265–275.

Marti, M., Mela, F., Guerrini, R., Calo, G., Bianchi, C., Morari, M., 2004a. Blockade of nociceptin/orphanin FQ transmission in rat substantia nigra reverses haloperidol-induced akinesia and normalizes nigral glutamate release. J. Neurochem. 91, 1501–1504.

Marti, M., Mela, F., Veronesi, C., Guerrini, R., Salvadori, S., Federici, M., Mercuri, N.B., Rizzi, A., Franchi, G., Beani, L., Bianchi, C., Morari, M., 2004b. Blockade of nociceptin/orphanin FQ receptor signaling in rat substantia nigra pars reticulata stimulates nigrostriatal dopaminergic transmission and motor behavior. J. Neurosci. 24, 6659–6666.

Marti, M., Mela, F., Fantin, M., Zucchini, S., Brown, J.M., Witta, J., Di Benedetto, M., Buzas, B., Reinscheid, R.K., Salvadori, S., Guerrini, R., Romualdi, P., Candeletti, S., Simonato, M., Cox, B.M., Morari, M., 2005. Blockade of nociceptin/orphanin FQ transmission attenuates symptoms and neurodegeneration associated with Parkinson's disease. J. Neurosci. 25, 9591–9601.

Marti, M., Trapella, C., Viaro, R., Morari, M., 2007. The nociceptin/orphanin FQ receptor antagonist J-113397 and L-DOPA additively attenuate experimental parkinsonism through overinhibition of the nigrothalamic pathway. J. Neurosci. 27, 1297–1307.

McDonald, J., Calo, G., Guerrini, R., Lambert, D.G., 2003. UFP-101, a high affinity antagonist for the nociceptin/orphanin FQ receptor: radioligand and GTPgamma (35)S binding studies. Naunyn-Schmiedebergs Arch. Pharmacol. 367, 183–187.

Meunier, J.C., Mollereau, C., Toll, L., Suaudeau, C., Moisand, C., Alvinerie, P., Butour, J.L., Guillemot, J.C., Ferrara, P., Monserrat, B., Mazarguil, H., Vassart, G., Parmentier, M., Costentin, J., 1995. Isolation and structure of the endogenous agonist of opioid receptor-like ORL1 receptor. Nature 377, 532–535.

Nazzaro, C., Rizzi, A., Salvadori, S., Guerrini, R., Regoli, D., Zeilhofer, H.U., Calo, G., 2007. UFP-101 antagonizes the spinal antinociceptive effects of nociceptin/orphanin FQ: behavioral and electrophysiological studies in mice. Peptides 28, 663–669.

Nishi, M., Houtani, T., Noda, Y., Mamiya, T., Sato, K., Doi, T., Kuno, J., Takeshima, H., Nukada, T., Nabeshima, T., Yamashita, T., Noda, T., Sugimoto, T., 1997. Unrestrained nociceptive response and disregulation of hearing ability in mice lacking the nociceptin/orphaninFQ receptor. EMBO J. 16, 1858–1864.

Ozaki, S., Kawamoto, H., Itoh, Y., Miyaji, M., Azuma, T., Ichikawa, D., Nambu, H., Iguchi, T., Iwasawa, Y., Ohta, H., 2000. In vitro and in vivo pharmacological characterization of J-113397, a potent and selective non-peptidyl ORL1 receptor antagonist. Eur. J. Pharmacol. 402, 45–53.

Redrobe, J.P., Calo, G., Regoli, D., Quirion, R., 2002. Nociceptin receptor antagonists display antidepressant-like properties in the mouse forced swimming test. Naunyn-Schmiedebergs Arch. Pharmacol. 365, 164–167.

Reinscheid, R.K., Nothacker, H.P., Bourson, A., Ardati, A., Henningsen, R.A., Bunzow, J.R., Grandy, D.K., Langen, H., Monsma Jr., F.J., Civelli, O., 1995. Orphanin FQ: a neuropeptide that activates an opioidlike G protein-coupled receptor. Science 270, 792–794.

Rizzi, A., Nazzaro, C., Marzola, G., Zucchini, S., Trapella, C., Guerrini, R., Zeilhofer, H.U., Regoli, D., Calo, G., 2006. Endogenous nociceptin/orphanin FQ signalling produces opposite spinal antinociceptive and supraspinal pronociceptive effects in the mouse formalin test: pharmacological and genetic evidences. Pain 124, 100–108.

Rizzi, A., Gavioli, E.C., Marzola, G., Spagnolo, B., Zucchini, S., Ciccocioppo, R., Trapella, C., Regoli, D., Calo, G., 2007. Pharmacological characterization of the nociceptin/orphanin FQ receptor antagonist SB–612111 [(-)-cis-1-methyl-7-[[4-(2,6-dichlorophenyl)piperidin-1-yl]methyl]-6,7,8,9-tetrahydro-5H-benzocycloheptен-5-ol]: in vivo studies. J. Pharmacol. Exp. Ther. 321, 968–974.

Rizzi, A., Marzola, G., Guerrini, R., Salvadori, S., Regoli, D., Calo, G., 2008. Antinociceptive effects of nociceptin/orphanin FQ receptor agonists in the mouse writhing test in: Society of Neuroscience Abstract 269.215 Washington, DC, USA. November, 15–19.

Ruiz-Velasco, V., Trapella, C., Calo, G., Margas, W., 2008. Pharmacology of constitutively active NOP opioid receptors heterologously expressed in rat sympathetic neurons, in: Society for Neuroscience, Abstract 533.9. Washington, DC, USA. November, 15–19.

Spagnolo, B., Carra, G., Fantin, M., Fischetti, C., Hebbes, C., McDonald, J., Barnes, T.A., Rizzi, A., Trapella, C., Fanton, G., Morari, M., Lambert, D.G., Regoli, D., Calo, G., 2007. Pharmacological characterization of the nociceptin/orphanin FQ receptor antagonist SB-612111 [(−)-cis-1-Methyl-7-[[4-(2,6-dichlorophenyl)piperidin-1-yl]methyl]-6,7,8,9-tetrahydro-5H-benzocyclohepten-5-ol]: in vitro studies. J. Pharmacol. Exp. Ther. 321, 961–967.

Trapella, C., Guerrini, R., Piccagli, L., Calo, G., Carra, G., Spagnolo, B., Rubini, S., Fanton, G., Hebbes, C., McDonald, J., Lambert, D.G., Regoli, D., Salvadori, S., 2006. Identification of an achiral analogue of J-113397 as potent nociceptin/orphanin FQ receptor antagonist. Bioorg. Med. Chem. 14, 692–704.

Ueda, H., Inoue, M., Takeshima, H., Iwasawa, Y., 2000. Enhanced spinal nociceptin receptor expression develops morphine tolerance and dependence. J. Neurosci. 20, 7640–7647.

Vergura, R., Valenti, E., Hebbes, C.P., Gavioli, E.C., Spagnolo, B., McDonald, J., Lambert, D.G., Balboni, G., Salvadori, S., Regoli, D., Calo, G., 2006. Dmt-Tic-NH-CH2-Bid (UFP-502), a potent DOP receptor agonist: in vitro and in vivo studies. Peptides 27, 3322–3330.

Viaro, R., Sanchez-Pernaute, R., Marti, M., Trapella, C., Isacson, O., Morari, M., 2008. Nociceptin/orphanin FQ receptor blockade attenuates MPTP-induced Parkinsonism. Neurobiol. Dis. 30, 430–438.

Visanji, N.P., de Bie, R.M., Johnston, T.H., McCreary, A.C., Brotchie, J.M., Fox, S.H., 2008. The nociceptin/orphanin FQ (NOP) receptor antagonist J-113397 enhances the effects of levodopa in the MPTP-lesioned nonhuman primate model of Parkinson's disease. Mov Disord. 23, 1922–1925.

Williams, J.P., Thompson, J.P., Young, S.P., Gold, S.J., McDonald, J., Rowbotham, D.J., Lambert, D.G., 2008. Nociceptin and urotensin-II concentrations in critically ill patients with sepsis. Br. J. Anaesth. 100, 810–814.

Yan-Yu, L., Chiou, L.C., 2008. Effect of compound 24, a novel nociceptin/orphanin FQ (NOP) receptor antagonist, on NOP receptor-mediated k+ channel activation in rat periaqueductal gray slices. Society for Neuroscience, Abstract 826.14 Washington, DC, USA. November, 15–19.

Zaratin, P.F., Petrone, G., Sbacchi, M., Garnier, M., Fossati, C., Petrillo, P., Ronzoni, S., Giardina, G.A., Scheideler, M.A., 2004. Modification of nociception and morphine tolerance by the selective opiate receptor-like orphan receptor antagonist (−)-cis-1-methyl-7-[[4-(2,6-dichlorophenyl)piperidin-1-yl]methyl]-6,7,8,9- tetrahydro-5H-benzocyclohepten-5-ol (SB-612111). J. Pharmacol. Exp. Ther. 308, 454–461.

Zeilhofer, H.U., Calo, G., 2003. Nociceptin/orphanin FQ and its receptor-potential targets for pain therapy? J. Pharmacol. Exp. Ther. 306, 423–429.

Peptides 31 (2010) 1194–1204

Contents lists available at ScienceDirect

Peptides

journal homepage: www.elsevier.com/locate/peptides

Pharmacological profile and antiparkinsonian properties of the novel nociceptin/orphanin FQ receptor antagonist 1-[1-cyclooctylmethyl-5-(1-hydroxy-1-methyl-ethyl)-1,2,3,6-tetrahydro-pyridin-4-yl]-3-ethyl-1,3-dihydro-benzoimidazol-2-one (GF-4)

Mattia Volta[a,b], Matteo Marti[a,b], John McDonald[d], Stefano Molinari[a,b], Valeria Camarda[a,b], Michela Pelà[c], Claudio Trapella[c], Michele Morari[a,b,*]

[a] Department of Experimental and Clinical Medicine, Section of Pharmacology, University of Ferrara, Ferrara Italy
[b] Neuroscience Center and National Institute of Neuroscience, University of Ferrara, Ferrara Italy
[c] Department of Pharmaceutical Sciences and Biotechnology Center, University of Ferrara, Ferrara Italy
[d] Department of Cardiovascular Sciences, University of Leicester, Leicester Royal Infirmary, Leicester, UK

ARTICLE INFO

Article history:
Received 21 January 2010
Received in revised form 10 March 2010
Accepted 10 March 2010
Available online 20 March 2010

Keywords:
6-Hydroxydopamine
Microdialysis
Nociceptin/orphanin FQ
NOP receptor knock-out
Parkinson's disease
GF-4

ABSTRACT

In this study we provided a pharmacological characterization of the recently synthesized nociceptin/orphanin FQ (N/OFQ) peptide receptor (NOP) antagonist 1-[1-Cyclooctylmethyl-5-(1-hydroxy-1-methyl-ethyl)-1,2,3,6-tetrahydro-pyridin-4-yl]-3-ethyl-1,3-dihydro-benzoimidazol-2-one (GF-4) and investigated its antiparkinsonian properties. GF-4 inhibited N/OFQ binding to CHO_{hNOP} cell membranes (pK_i 7.46), and antagonized N/OFQ effects in a calcium mobilization assay and electrically stimulated isolated tissues (pK_B 7.27–7.82), showing a ~5-fold selectivity over classical opioid receptors. In vivo, GF-4 dually modulated stepping activity in wild-type mice, causing facilitation in the 0.01–10 mg/kg dose range and inhibition at 30 mg/kg. These effects were mediated by NOP receptors since GF-4 was ineffective in NOP receptor knock-out mice. Antiparkinsonian properties of GF-4 were investigated in 6-hydroxydopamine hemilesioned rats. GF-4 ameliorated akinesia, bradykinesia and overall gait ability in the 0.1–10 mg/kg dose range, but inhibited motor activity at 30 mg/kg. To investigate the circuitry underlying motor facilitating and inhibitory effects of GF-4, microdialysis coupled to behavioral testing (akinesia test) was performed. An anti-akinetic dose of GF-4 (1 mg/kg) reduced glutamate (GLU) and enhanced GABA release in SNr, while the pro-akinetic dose of GF-4 (30 mg/kg) evoked opposite effects. Moreover, the anti-akinetic dose of GF-4 reduced GABA and increased GLU release in ventro-medial thalamus, the pro-akinetic dose decreasing GABA without affecting GLU release in this area. We conclude that GF-4 is an effective NOP receptor antagonist able to attenuate parkinsonian-like symptoms in vivo via inhibition of the nigro-thalamic pathway.

1. Introduction

The neuropeptide nociceptin/orphanin FQ (N/OFQ; [27,34]) is the endogenous ligand of the N/OFQ peptide (NOP) receptor and participates in the regulation of a number of central biological processes such as pain perception, food intake, learning, anxiety, reward and locomotion [16]. Although most interest is focused on therapeutic applications of NOP receptor agonists, evidence that NOP receptor antagonists may also be useful in some pathological conditions such as depression [33] and Parkinson's disease (PD; [21,22]) has been presented. The NOP receptor is particularly expressed in substantia nigra (SN) where dopamine (DA) neurons degenerating in PD are located [21,28]. Interestingly, N/OFQ has been shown to inhibit the activity of DA neurons in SN compacta

Abbreviations: 6-OHDA, 6-hydroxydopamine; AP, antero-posterior; CHO, Chinese hamster ovary; DA, dopamine; DOP, delta opioid peptide; GLU, glutamate; J-113397, 1-[(3R,4R)-1-cyclooctylmethyl-3-hydroxymethyl-4-piperidyl]-3-ethyl-1,3-dihydro-2H-benzoimidazole-2-one; KOP, kappa opioid peptide; ML, medio-lateral; MOP, mu opioid peptide; N/OFQ, nociceptin/orphanin FQ; NOP, nociceptin/orphanin FQ peptide; PD, Parkinson's disease; SNc, substantia nigra pars compacta; SNr, substantia nigra pars reticulata; Trap-101, 1-[1-(cyclooctylmethyl)-1,2,3,6-tetrahydro-5-(hydroxymethyl)-4-pyridinyl]-3-ethyl-1,3-dihydro-2H-benzimidazol-2-one; VD, ventro-dorsal; VMTh, ventro-medial thalamus.

* Corresponding author at: Department of Experimental and Clinical Medicine, Section of Pharmacology, University of Ferrara, via Fossato di Mortara 17-19, 44100 Ferrara, Italy. Tel.: +39 0532 455210; fax: +39 0532 455205.
E-mail address: m.morari@unife.it (M. Morari).

0196-9781/$ – see front matter © 2010 Elsevier Inc. All rights reserved.
doi:10.1016/j.peptides.2010.03.015

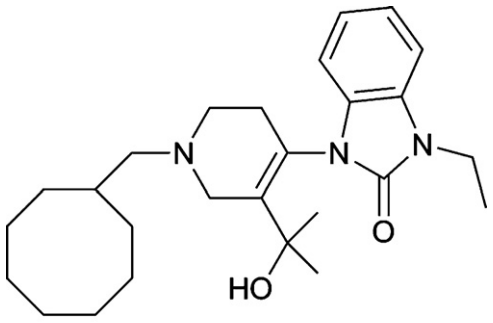

GF-4

Fig. 1. Structure of 1-[1-cyclooctylmethyl-5-(1-hydroxy-1-methyl-ethyl)-1,2,3,6-tetrahydro-pyridin-4-yl]-3-ethyl-1,3-dihydro-benzoimidazol-2-one (GF-4).

(SNc) at the same doses required to inhibit locomotion [19]. Conversely, DA loss is associated with increased N/OFQ expression and release [2,8,21] suggesting that DA tonically inhibits N/OFQ transmission. This inhibitory relationship appears relevant for PD since NOP receptor antagonists such as the peptide UFP-101 [4] and the nonpeptide J-113397 [30] alleviated akinesia/bradykinesia in haloperidol-treated or 6-hydroxydopamine (6-OHDA) hemilesioned rats [20–22]. Moreover, J-113397 attenuated motor deficits in MPTP-treated mice and nonhuman primates [40,42]. In order to develop novel nonpeptide NOP receptor antagonists, we considered to modify the structure of the reference compound, J-113397, first obtaining Trap-101 [39]. In vitro, Trap-101 was found slightly (~3-fold) less potent than but as selective (>100-fold) as J-113397 (racemic mixture) for NOP versus the classical opioid receptors. In vivo, Trap-101 promoted motor activity in 6-OHDA hemilesioned rats and potentiated the antiparkinsonian action of L-DOPA [23]. Moreover, consistently with results obtained with J-113397, it inhibited glutamate (GLU) release and enhanced GABA release in SNr, while reducing GABA release in ventro-medial thalamus (VMTh; [21,23]). Based on these findings, we modified Trap-101 structure and introduced two methyl groups in the hydroxymethyl function at the carbon 3 of the piperidine ring, thus obtaining GF-4 (Fig. 1).

In the present study we investigated in vitro pharmacological properties of GF-4 using receptor binding assays (in CHO_{hNOP} cell membranes), calcium mobilization assays (in CHO_{hNOP}-$G\alpha_{qi5}$ cells) and electrically stimulated isolated tissues (mouse and rat vas deferens). In vivo selectivity of GF-4 was studied in NOP receptor knock-out mice ($NOP^{-/-}$). The antiparkinsonian potential of GF-4 was investigated in 6-OHDA hemilesioned rats through a battery of previously validated behavioral tests: the bar, drag and rotarod tests [21–23,40]. Finally, to unravel the circuitry involved in motor actions of GF-4, GABA and GLU release was monitored in the lesioned SNr and ipsilateral VMTh in animals subjected to microdialysis and simultaneously performing the bar test.

2. Materials and methods

Animals employed in this study (see below) were kept under regular lighting conditions (12 h dark/light cycle) with free access to food and water. Adequate measures were taken to minimize animal pain and discomfort. This study was compliant with the European Council Directive of 24 November 1986 (86/609/EEC) and approved by the Ethical Committee of the University of Ferrara and Italian Ministry of Health (licence no. 194-2008-B).

2.1. In vitro studies

2.1.1. Cell culture and membrane preparation

Chinese Hamster Ovary cells (CHO) stably expressing the human NOP receptor (CHO_{hNOP}) were cultured in medium consisting of Dulbecco's MEM/HAM'S F-12 (50/50) supplemented with 5% foetal calf serum (FCS), penicillin (100 IU/ml), streptomycin (100 μg/ml), fungizone (2.5 μg/ml), geneticin (G418; 200 μg/ml) and hygromycin B (200 mg/ml) as described previously [25]. CHO cell stocks expressing the human delta opioid peptide (DOP; CHO_{DOP}), the mu opioid peptide (MOP; CHO_{MOP}), or the kappa opioid peptide (KOP; CHO_{KOP}) receptors were maintained in Ham F12 containing 10% FCS, 100 IU/ml penicillin, 100 μg/ml streptomycin and 400 μg/ml G418. Cell cultures were kept at 37 °C in 5% CO_2 humidified air. In all cases experimental cultures were free from selection agents (hygromycin B, G418). Cells were sub-cultured with trypsin/EDTA and used for experimentation once confluent (3–4 days).

CHO cell lines stably co-expressing NOP receptors and the C-terminally modified $G\alpha_{qi5}$ were generated as described in [3]. CHO cell lines co-expressing MOP, DOP or KOP and $G\alpha_{qi5}$ were obtained in similar way, as described in [9].

Membranes were prepared from freshly harvested cell suspensions in Tris–HCl (50 mM), Mg^{++} (5 mM) pH 7.4 via homogenization and centrifugation at 13,500 rpm for 10 min at 4 °C. The final protein concentration was determined according to [17].

2.1.2. Receptor binding experiments

[Leucyl-^{3}H]N/OFQ binding: 5 μg of CHO_{hNOP} homogenate protein was incubated in 0.5 ml of Tris–HCl (50 mM) buffer supplemented with 10 μM peptidase inhibitors (amastatin, bestatin, captopril and phosphoramidon), 0.5% bovine serum albumin (BSA), increasing concentrations of competing ligands and approximately 200 pM [^{3}H]N/OFQ. Total radiolabel bound was <10%. Non-specific binding was determined in the presence of 1 μM unlabelled N/OFQ. In all experiments, N/OFQ was included as a reference ligand. Reactions were incubated for 1 h at room temperature and terminated by vacuum filtration (Brandel Harvester) through Whatman GF/B filters soaked in 0.5% polyethylenimine. Radioactivity was determined after 8 h extraction in scintillation cocktail. [^{3}H]Diprenorphine binding: 50 μg CHO_{hMOP}, 25 μg CHO_{hDOP} and 40 μg CHO_{hKOP} membrane protein were incubated in 0.5 ml buffer containing Tris–HCl (50 mM) pH 7.4, BSA (0.5%), ~0.7 nM [^{3}H]Diprenorphine and increasing concentrations of competing ligands. Non-specific binding was determined in the presence of 10 μM naloxone. Reactions were incubated at room temperature for 1 h. Harvesting and determination of radioactivity were as for [Leucyl-^{3}H]N/OFQ binding.

2.1.3. Calcium mobilization experiments

CHO_{hMOP}, CHO_{hDOP}, CHO_{hKOP} and CHO_{hNOP} stably expressing the $G\alpha_{qi5}$ protein were seeded at a density of 40,000 cells/well into 96-well black, clear-bottom plates. After 24 h incubation, the cells were loaded with medium supplemented with 2.5 mM probenecid, 3 μM of the calcium sensitive fluorescent dye Fluo-4 AM and 0.01% pluronic acid, for 30 min at 37 °C. Afterwards the loading solution was aspirated and 100 μl/well of assay buffer Hank's Balanced Salt Solution (HBSS) supplemented with 20 mM HEPES, 2.5 mM probenecid and 500 μM Brilliant Black (Aldrich) was added. Serial dilutions of ligands for experimental use were made in HBSS/HEPES (20 mM) buffer (containing 0.02% BSA fraction V). After placing both plates (cell culture and compound plate) into the FlexStation II (Molecular Device, Union City, CA 94587, US), fluorescence changes were measured at room temperature. On-line additions were carried out in a volume of 50 μl/well.

2.1.4. Electrically stimulated isolated tissues

Tissues were taken from male Swiss mice (30–35 g) and Sprague–Dawley rats (300–350 g). The mouse and rat vas deferens were prepared as previously described [1]. Tissues were suspended in 5 ml organ baths containing heated Krebs solution (composition

in mM: NaCl 118.5, KCl 4.7, KH_2PO_4 1.2, $NaHCO_3$ 25, glucose 10 and $CaCl_2$ 2.5 for mouse and 1.8 for rat tissues) oxygenated with 95% O_2 and 5% CO_2. The bath temperature was set at 33 °C for mouse vas deferens and 37 °C for rat vas deferens. Tissues were continuously stimulated through two platinum ring electrodes with supramaximal rectangular pulses of 1 ms duration and 0.05 Hz frequency. A resting tension of 0.3 and 1 g was applied to the mouse and rat vas deferens, respectively. The electrically evoked contractions (twitches) were measured isotonically with a strain gauge transducer (Basile 7006, Ugo Basile s.r.l., Varese, Italy) and recorded with the PC based acquisition system Power Lab (ADInstrument, USA).

Following an equilibration period of 60 min, the contractions induced by electrical field stimulation were stable. At this time, cumulative concentration–response curves to N/OFQ were performed (0.5 log unit steps) in the absence or presence of the antagonist under investigation (15 min pre-incubation time).

2.2. In vivo studies

2.2.1. Naïve mice

To investigate the in vivo specificity of GF-4, motor activity was evaluated in CD1/C57BL6J/129 $NOP^{+/+}$ and $NOP^{-/-}$ mice (25–30 g; 12–15 weeks old; [21]) by means of the drag test. This test measures the ability of the animal to balance its body posture with forelimbs in response to an externally imposed dynamic stimulus (dragging backwards; [21]), and is a modification of the 'wheelbarrow test' [36]. It gives information regarding the time to initiate (akinesia) and execute (bradykinesia) a movement. The animal was gently lifted from the tail allowing the forepaws to rest on the table, and dragged backwards at a constant speed (about 20 cm/s) for a fixed distance (100 cm). The number of steps made with each paw was recorded by two distinct observers.

2.2.2. 6-OHDA hemilesioned rats

2.2.2.1. 6-OHDA lesion. Unilateral lesion of DA neurons [21] was induced in isoflurane-anesthetized male Sprague–Dawley rats (150 g; Harlan Italy; S. Pietro al Natisone, Italy). Eight micrograms of 6-OHDA (in 4 μl of saline containing 0.02% ascorbic acid) were stereotaxically injected according to the following coordinates from bregma: AP = −4.4 mm, ML = −1.2 mm, VD = −7.8 below dura [32]. The rotational model was used to select the rats which had been successfully lesioned. Two weeks after surgery, rats were injected with amphetamine (5 mg/kg i.p., dissolved in saline) and only those rats performing >7 ipsilateral turns/min were enrolled in the study. This behavior has been associated with >95% loss of striatal extracellular DA levels and tyrosine-positive terminals [22]. Experiments were performed 6–8 weeks after lesion.

2.2.2.2. Behavioral analysis. Motor activity was evaluated in 6-OHDA hemilesioned rats by means of three behavioral tests specific for different motor abilities, as previously described [21,22]: the bar, drag and rotarod test. The three tests were repeated in a fixed sequence (bar, drag and rotarod) before and after drug injection (starting at 15 and at 70 min after treatment). Animals were trained for approximately 10 days to the specific motor tasks until their performance became reproducible.

2.2.2.3. Bar test. Originally developed to quantify morphine-induced catalepsy [15], this test measures the ability of the animal to respond to an externally imposed static posture.

The rat was placed gently on a table and forepaws were placed alternatively on blocks of increasing heights (3, 6 and 9 cm). The time (in s) that each paw spent on the block (i.e. the immobility time) was recorded (cut-off time of 20 s).

2.2.2.4. Drag test. This test was performed as described above (in mice).

2.2.2.5. Rotarod test. The fixed-speed rotarod test [35] measures different motor parameters such as motor coordination, gait ability, balance, muscle tone and motivation to run. It was employed according to a previously described protocol [19]. Briefly, rats were tested in a control session at four increasing speeds (15, 20, 25 and 30 rpm; 180 s each), causing a progressive decrement of performance to ~40% of the maximal response (i.e. the experimental cut-off time).

2.2.2.6. Microdialysis. Two microdialysis probes (1 mm dialyzing membrane, AN69, Hospal, Bologna, Italy) were implanted in the lesioned SNr (AP −5.5, ML −2.2, VD −8.3) and ipsilateral VMTh (AP −2.3, ML −1.4, VD −7.4) of isoflurane-anesthetized hemiparkinsonian rats. Twenty-four hours after implantation, probes were perfused (3 μl/min) with a modified Ringer solution (in nM: $CaCl_2$ 1.2; KCl 2.7; NaCl 148 and $MgCl_2$ 0.85) and sample collection (every 15 min) started after a 6–7 h wash-out period. GF-4 was administered systemically (i.p.) and GLU and GABA levels were monitored for 90 min. At the end of the experiments rats were killed and probe location verified by microscopic examination.

2.2.2.7. Behavioral testing during microdialysis. To correlate changes of amino acid dialysate levels with motor activity, rats undergoing microdialysis were challenged in the bar test [20,22] every 15 min. The bar test was performed essentially as described above. Rat forepaws were placed alternatively on blocks of increasing heights (3, 6 and 9 cm) and the immobility time was recorded (cut-off time of 20 s).

2.2.2.8. Amino acid analysis. GLU and GABA levels in the dialysate were measured by HPLC coupled to fluorometric detection [22]. Briefly, 40 μl samples were pipetted into glass microvials and placed in a thermostated (4 °C) Triathlon autosampler (Spark Holland, Emmen, The Netherlands). Thirty-five μl of *o*-phthaldialdehyde/mercaptoethanol reagent were added to each sample, and 60 μl of the mixture injected onto a Chromsep analytical column (3 mm inner diameter, 10 cm length; Chrompack, Middelburg, The Netherlands). The column was eluted at a flow rate of 0.48 ml/min (Beckman 125 pump; Beckman Instruments, Fullerton, CA, USA) with a mobile phase containing 0.1 M sodium acetate, 10% methanol and 2.5% tetrahydrofuran (pH 6.5). GLU and GABA were detected by means of a Jasco fluorescence spectrophotometer FP-2020 Plus (Jasco, Tokyo, Japan). GLU and GABA retention times were 3.5 ± 0.2 and 18 ± 0.5 min, respectively. The limit of detection was about 1 nM for GLU and 0.5 nM for GABA.

2.3. Data presentation, statistical analysis and terminology

For in vitro experiments data are expressed as means ± standard error of the mean (SEM) of *n* experiments. For potency values 95% confidence limits were indicated. Receptor binding data are expressed as pK_i derived from the Cheng and Prusoff [5] equation:

$$pK_i = \frac{IC_{50}}{1 + ([R]/K_d)}$$

where [*R*] is the concentration of the radiolabel and K_d is the radiolabel affinity for the receptor under investigation. The K_d of [^{3}H]N/OFQ at NOP receptors was 83 pM while those of [^{3}H]Diprenorphine at MOP, DOP, and KOP receptors were 125, 323, and 134 pM, respectively [13].

Calcium mobilization data are expressed as fluorescence intensity units (FIUs) in percent over the baseline. Isolated tissues data

are expressed as percent of the twitch induced by electrical field stimulation.

Agonist potencies are given as pEC_{50} = the negative logarithm to base 10 of the molar concentration of an agonist that produces 50% of the maximal possible effect. Concentration response curves to agonists were fitted with the following equation:

$$\text{Effect} = \frac{\text{baseline} + (E_{max} - \text{baseline})}{(1 + 10((\log EC_{50} - X) \times \text{HillSlope})}$$

where X is the agonist concentration.

For isolated tissues experiments antagonist potencies were derived from the Gaddum Schild equation:

$$K_B = \frac{CR - 1}{[\text{antagonist}]}$$

assuming a slope value equal to unity, where CR indicates the ratio between agonist potency in the presence and the absence of antagonist. For calcium mobilization experiments, pK_B values were derived from inhibition response curves using the following equation:

$$K_B = \frac{IC_{50}}{(2 + ([A]/EC_{50})^{1/n} - 1}$$

where IC_{50} is the concentration of antagonist that produces 50% inhibition of the agonist response, [A] is the concentration of agonist, EC_{50} is the concentration of agonist producing a 50% maximal response and n is the Hill coefficient of the concentration response curve to the agonist [12].

For in vivo experiments, motor performance has been calculated as time spent on bar or on rod (in s) and number of steps (drag test) and expressed as percent of the control session. In microdialysis studies, GLU and GABA release has been expressed as percentage ± SEM of basal values (calculated as mean of the two samples before the treatment).

Statistical analysis has been performed on percent data by two-way repeated measure (RM) analysis of variance (ANOVA). In case ANOVA yielded to a significant F score, *post hoc* analysis has been performed by contrast analysis to determine group differences. In case a significant time x treatment interaction was found, the sequentially rejective Bonferroni's test was used (implemented on excel spreadsheet) to determine specific differences (i.e. at the single time point level) between groups. P values <0.05 were considered to be statistically significant.

2.4. Materials

Amphetamine and 6-OHDA were purchased from Sigma Chemical Company (St. Louis, MO, USA). GF-4 (1-[1-cyclooctylmethyl-5-(1-hydroxy-1-methyl-ethyl)-1,2,3,6-tetrahydropyridin-4-yl]-3-ethyl-1,3-dihydro-benzoimidazol-2-one) was synthesized in our laboratories by modification of the last step of the Trap-101 (1-[1-(cyclooctylmethyl)-1,2,3,6-tetrahydro-5-(hydroxymethyl)-4-pyridinyl]-3-ethyl-1,3-dihydro-2H-benzimidazol-2-one) synthesis [39]. In particular, methyl magnesium bromide was used instead of lithyumaluminiumhydride to produce the tertiary alcohol. The peptides used in this study were prepared and purified as previously described [11]. [D-Pen^{2,5}]enkephalin (DPDPE) was purchased from NeoMPS (Strasbourg, France). All tissues culture media and supplements were from Invitrogen (Paisley, UK). [^{3}H]Diprenorphine was from Perkin-Elmer Life Sciences and [^{3}H]N/OFQ (75–133 Ci mmol^{-1}) from Amersham Biosciences. All other reagents were from Sigma Chemical Company or Merck (Darmstadt, Germany) and were of the highest purity available. For in vitro experiments, stocks solutions (10 mM) of J-113397 (1-[(3R,4R)-1-cyclooctylmethyl-3-hydroxymethyl-4-piperidyl]-3-ethyl-1,3-dihydro-2H-benzimidazol-2-one), Trap-101 and GF-4 were made in dimethyl sulfoxide, and final concentrations reached with saline; the other compounds were solubilized in distilled water. Stock solutions were kept at −20 °C until use.

For in vivo experiments drugs were freshly dissolved in isoosmotic saline solution just prior to use. GF-4 was vortexed and sonicated until fully dissolved.

3. Results

3.1. In vitro studies

3.1.1. Receptor binding assay

In receptor binding experiments performed on CHO_{hNOP} cell membranes, GF-4 displaced [^{3}H]N/OFQ in a concentration-dependent manner showing affinity in the nanomolar range (pK_i 7.46, K_i 34.7 nM; Table 1). In parallel experiments, the nonpeptide antagonists J-113397 and Trap-101 displayed pK_i values of 8.58 (K_i 2.6 nM) and 8.36 (K_i 4.4 nM). Under the same experimental conditions, GF-4 showed lower affinities for MOP (pK_i 6.78, K_i 166.0 nM) and KOP (pK_i 6.84 and K_i 144.5 nM) receptors and did not bind to the DOP receptor (Table 1).

3.1.2. Calcium mobilization assay

In CHO_{hNOP} cells stably expressing the $G\alpha_{qi5}$ chimeric protein, N/OFQ evoked a concentration-dependent stimulation of calcium release displaying high potency (pEC_{50} 9.24; $CL_{95\%}$ 9.10–9.38) and efficacy (~200% over the basal values; Fig. 2A).

J-113397, Trap-101 and GF-4 did not evoke calcium release up to 10 μM. Inhibition response experiments were then performed by challenging increasing concentrations of J-113397, Trap-101 and GF-4 (10 pM-10 μM) against a fixed concentration of N/OFQ (10 nM), close to its EC_{80}. As shown in Fig. 2B-D, J-113397, Trap-101 and GF-4 were able to inhibit in a concentration-dependent manner the stimulatory effect of N/OFQ, showing similar pK_B values of 7.88, 7.93 and 7.27, respectively (see also Table 2; J-113397 data not shown).

To assess the in vitro selectivity of GF-4, similar experiments were performed in CHO cells stably expressing $G\alpha_{qi5}$ and classical opioid receptors (Fig. 3). Dermorphin, DPDPE and Dynorphin A were used as agonists for MOP, DOP and KOP receptors, respectively. They evoked concentration-dependent calcium rise with the following pEC_{50} and E_{max} values: Dermorphin 7.93 ($CL_{95\%}$ 7.67–8.19), 196 ± 9%; DPDPE 8.82 ($CL_{95\%}$ 8.43–9.21), 130 ± 10%; Dynorphin A 8.47 ($CL_{95\%}$ 8.16–8.78) 174 ± 14%. GF-4, inactive up to 10 μM against DPDPE and Dynorphin A, inhibited the effect of

Table 1
Receptor binding profile of GF-4 to human recombinant NOP, MOP, DOP, and KOP receptors expressed in CHO cells. Data are mean ($CL_{95\%}$) of three separate experiments.

	pK_i values ($CL_{95\%}$)			
	CHO_{hNOP} N/OFQ	CHO_{hMOP} Endomorphin-1	CHO_{hDOP} Naltrindole	CHO_{hKOP} Norbinaltorphimine
Standard ligand	9.27 (9.07–9.47)	8.41 (8.15–8.67)	9.46 (9.12–9.80)	9.93 (9.8–10.06)
GF-4	7.46 (7.09–7.83)	6.78 (6.57–6.99)	<6	6.84 (6.52–7.16)

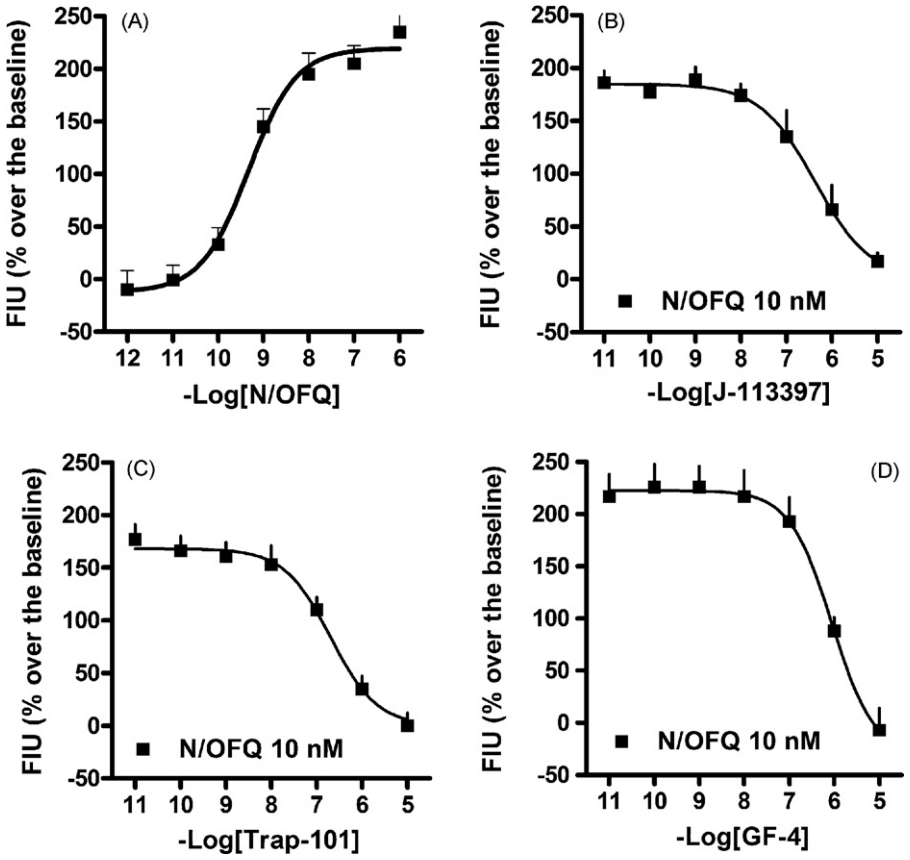

Fig. 2. GF-4 inhibited N/OFQ-induced calcium mobilization. Concentration–response curve to N/OFQ in calcium mobilization experiments performed in CHO_{hNOP} cells stably expressing the $G\alpha_{qi5}$ protein (A). N/OFQ effect was expressed as percent over the baseline. Inhibition experiments obtained by challenging 10 nM N/OFQ with increasing concentrations of J-113397 (B), Trap-101 (C) and GF-4 (D). Data are means ± SEM of four separate experiments performed in duplicate.

Table 2
Antagonist potencies (pK_B values) of naloxone, Trap-101 and GF-4 evaluated in calcium mobilization experiments performed in CHO cells expressing NOP or classical opioid receptors (MOP, DOP and KOP) and the $G\alpha_{qi5}$ protein. Data are mean ($CL_{95\%}$) of 4 separate experiments.

	NOP N/OFQ 10 nM	MOP Dermorphin 100 nM	DOP DPDPE 100 nM	KOP Dynorphin A 100 nM
Naloxone	<6	9.09 (8.73–9.45)	7.32 (6.11–8.53)	7.14 (6.60–7.68)
Trap-101	7.93 (7.25–8.61)	6.24 (5.90–6.58)	<6	<6
GF-4	7.27 (6.69–7.85)	6.48 (6.07–6.89)	<6	<6

Dermorphin with pK_B value of 6.48. In parallel experiments, Trap-101 inhibited the effect of Dermorphin with a similar potency value (pK_B 6.24; Fig. 3, Table 2). Naloxone was inactive up to 10 μM against N/OFQ and inhibited the effects of the classical opioid receptor agonists with higher potency at MOP (pK_B 9.09) than KOP (pK_B 7.14) or DOP (pK_B 7.32) receptors (Table 2).

3.1.3. Electrically stimulated isolated tissues

J-113397, Trap-101 and GF-4 were assessed against N/OFQ in the electrically stimulated mouse and rat vas deferens. N/OFQ inhibited the twitch response to electrical field stimulation in a concentration-dependent manner in both the mouse (pEC_{50} 7.55, E_{max} 76 ± 2%; Fig. 4A–C) and rat (pEC_{50} 7.51, E_{max} 78 ± 2%; Fig. 4D–F) vas deferens. The NOP receptor antagonists did not modify the electrically induced twitch response up to 1 μM. When tested at 100 nM, they produced a rightward shift of the concentration–response curve to N/OFQ without significantly affecting the maximal agonist response both in the mouse and rat vas deferens. The pK_B values for J-113397, Trap-101 and GF-4 were 8.13, 7.46 and 7.82 in the mouse (Fig. 4; Table 3) and 7.37, 7.53 and 7.30 in the rat (Fig. 4; Table 3), respectively.

3.2. In vivo studies

3.2.1. Effects of GF-4 on motor activity in naïve mice

To investigate the in vivo selectivity of GF-4, $NOP^{+/+}$ and $NOP^{-/-}$ mice were challenged in the drag test (Fig. 5). Basal motor activity in naïve mice was similar at the left (23.1 ± 0.9 steps) and right (22.2 ± 0.8 steps) paw so data were pooled together. GF-4 given i.p. dually modulated motor activity in $NOP^{+/+}$ mice, facilitating stepping activity in the 0.01–10 mg/kg dose range and inhibiting it at 30 mg/kg. The facilitation induced by the 0.01 mg/kg dose was only

Table 3
Antagonist potencies (pK_B values) of J-113397, Trap-101 and GF-4 against N/OFQ in the electrically stimulated mouse and rat vas deferens.

	Electrically stimulated tissues	
	Mouse vas deferens pK_B	Rat vas deferens pK_B
J-113397	8.13 (7.69–8.57)	7.37 (6.88–7.86)
Trap-101	7.46 (6.97–7.92)	7.53 (6.73–8.33)
GF-4	7.82 (7.61–8.03)	7.30 (6.58–8.02)

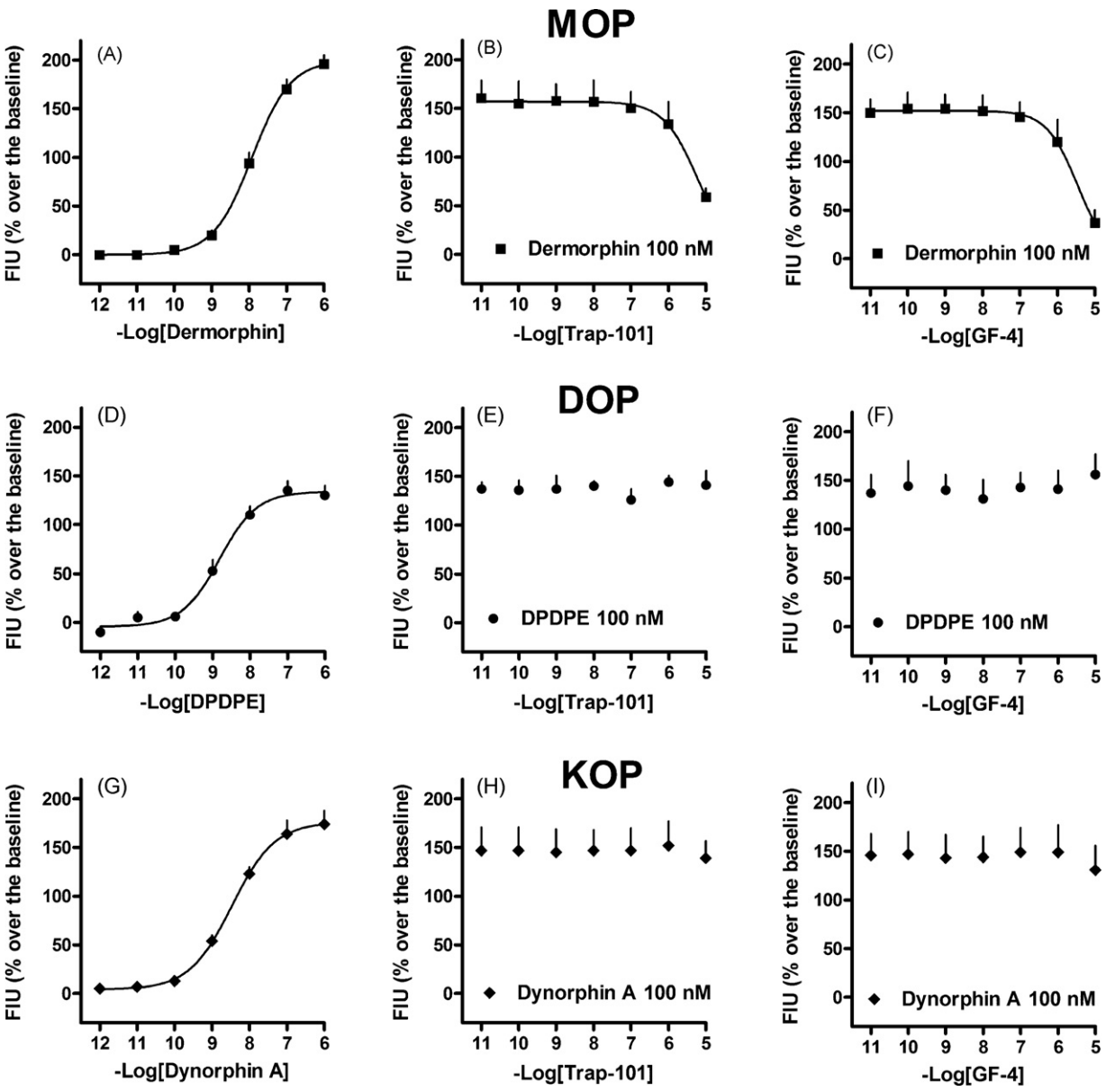

Fig. 3. High concentrations of GF-4 inhibited calcium mobilization induced by MOP but not DOP or KOP receptors. Inhibition experiments obtained by challenging 100 nM Dermorphin (A–C), DPDPE (D–F) and Dynorphin A (G–I) with increasing concentrations of Trap-101 and GF-4 in the calcium mobilization assay performed in CHO cells expressing the classical opioid receptors (CHO_{hMOP}; CHO_{hKOP}; CHO_{hDOP}) and the $G\alpha_{qi5}$ protein. Data are mean ± SEM of four separate experiments performed in duplicate.

detected 15 min after injection. The effects of higher doses were longer lasting and detected up to 90 min after injection. GF-4, tested only at high doses (10 and 30 mg/kg), was ineffective in $NOP^{-/-}$ mice.

3.2.2. *Effects of GF-4 on motor activity in 6-OHDA hemilesioned rats*

To investigate whether GF-4 has antiparkinsonian potential, GF-4 was administered systemically (i.p.) to 6-OHDA hemilesioned rats and motor activity evaluated by the bar, drag and rotarod tests (Fig. 6). 6-OHDA lesioning produced motor asymmetry mostly affecting the paw contralateral to the 6-OHDA injection side. Indeed, the immobility time (bar test, in s) and the number of steps (drag test) were 27.6 ± 3.9 and 11.4 ± 0.7 at the ipsilateral paw, and 37.7 ± 3.5 and 3.8 ± 0.6 at the contralateral one. Overall rotarod performance (0–55 rpm range) of 6-OHDA hemilesioned rats (537 ± 112.5 s) was also reduced compared to sham-operated animals (1176 ± 64 s; [23])

In the bar test (Fig. 6A), GF-4 (0.1–30 mg/kg) dually affected the immobility time at the contralateral paw 15 min after injection, reducing it at 1 and 10 mg/kg and increasing it at 30 mg/kg. After 70 min from administration, only motor facilitation induced by the 1 mg/kg dose was detected. GF-4 also affected the immobility time at the ipsilateral paw, causing a short-lasting increase at 30 mg/kg. In the drag test (Fig. 6B), GF-4 produced a long lasting increase in stepping activity at the contralateral paw in the 0.1–10 mg/kg dose range and a long lasting reduction at 30 mg/kg. GF-4 also elevated stepping activity at the ipsilateral paw at 10 mg/kg and reduced it at 30 mg/kg. Finally, GF-4 dually modulated rotarod performance (Fig. 6C), causing improvement at 1 and 10 mg/kg and inhibition at 30 mg/kg.

3.2.3. *Effects of GF-4 on nigral and thalamic amino acid levels in 6-OHDA hemilesioned rats*

To investigate the neuronal circuitry underlying motor actions of GF-4, microdialysis was performed in rats undergoing the bar

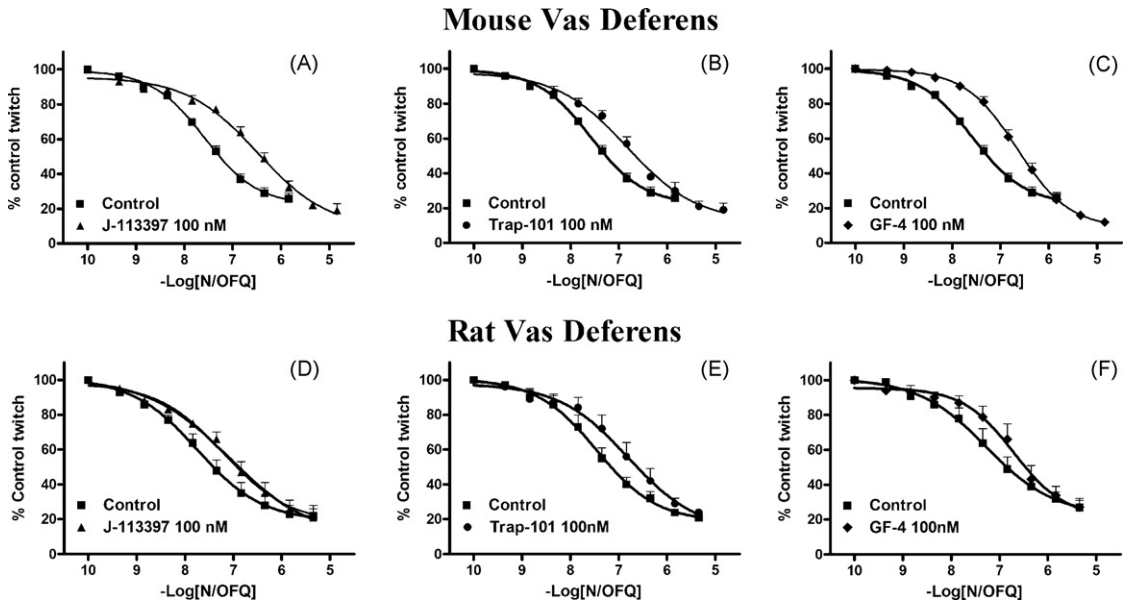

Fig. 4. GF-4 counteracted N/OFQ inhibition of the electrically induced contraction in mouse and rat vas deferens. Concentration–response curves to N/OFQ, obtained in the absence and presence of 100 nM J-113397, Trap-101 and GF-4, in the electrically stimulated mouse (A–C) and rat (D–F) vas deferens. Values are means ± SEM of four separate experiments.

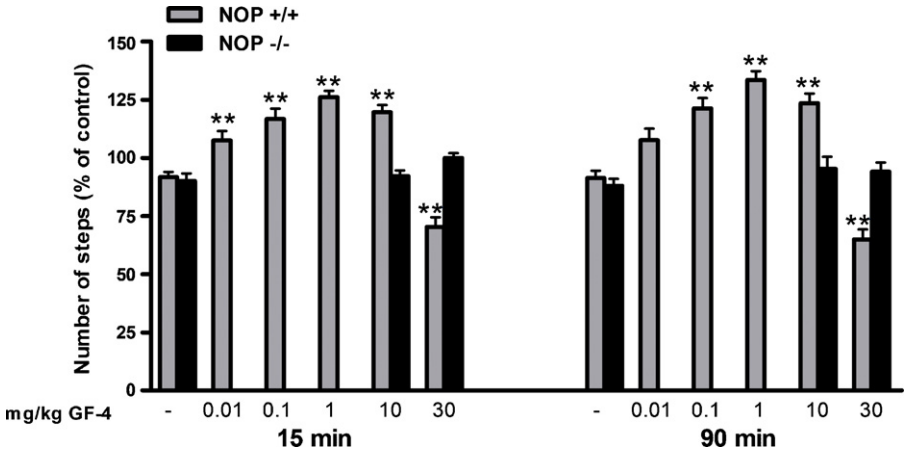

Fig. 5. GF-4 dually modulated motor activity in naïve NOP$^{+/+}$ mice, being ineffective in NOP$^{-/-}$ mice. GF-4 was administered systemically (i.p.) and motor activity evaluated in the drag test. Each experiment consisted of three different sessions: a control session followed by two other sessions performed 15 and 90 min after saline or GF-4 administration (see Section 2). Data are expressed as percentages of motor activity in the control session and are means ± SEM of 6–9 determinations per group. Basal motor activity values in the drag test are given in text (Section 3.2.1). Statistical analysis was performed by RM-ANOVA followed by contrast analysis and the sequentially rejective Bonferroni's test. $p^{**} < 0.01$ significantly different from saline.

test. GF-4 was administered systemically (i.p.) at low (1 mg/kg), motor facilitating, and high (30 mg/kg), motor inhibitory, doses. Amino acid release was monitored in SNr and ipsilateral VMTh simultaneously with behavioral testing. GF-4 (1 mg/kg) caused long lasting reduction of immobility time at the contralateral (Fig. 7A) but not ipsilateral (Fig. 7B) forepaw in the bar test. The higher dose of GF-4 (30 mg/kg) had the opposite effect, namely an increase in the time spent on the blocks with both the contralateral (Fig. 7A) and ipsilateral (Fig. 7B) paws. The percentage increase was greater at the ipsilateral paw possibly due to lower immobility time (i.e. less akinesia) compared to the contralateral one.

The anti-akinetic dose of GF-4 (1 mg/kg) increased GABA release (Fig. 8A) and reduced GLU release (Fig. 8B) in SNr while the pro-akinetic dose (30 mg/kg) had opposite effects. Finally, the anti-akinetic dose of GF-4 reduced GABA release (Fig. 8C) and increased GLU release (Fig. 8D) in VMTh while the pro-akinetic dose elevated GABA release but did not affect GLU release in this area.

4. Discussion

GF-4 is a novel NOP receptor antagonist generated from the Trap-101 structure. In vitro, GF-4 antagonized N/OFQ actions at human recombinant and rodent native NOP receptors in a concentration-dependent and competitive manner (pK_B 7.27–7.88) without exerting primary effects. The affinity at recombinant NOP receptors (~35 nM, pK_i 7.45) is ~100-fold lower than those of the most potent nonpeptide NOP receptor antagonists thus described, namely Compound 24 (0.27 nM; [10]) and SB-612111 (0.33 nM; [43]), ~10-fold lower than that of J-113397 and Trap-101 (see also [30,38,43]) and closer to that of JTC-801 (8.2 nM [37]; 30.8 nM [43]). In vitro potency values in recombinant and native preparations are in line with this rank order, although the differences are less pronounced. For instance, in calcium mobilization assay, GF-4 was ~57-fold less potent than Compound 24 [9] and ~5-fold less potent than Trap-101. In the mouse vas deferens, GF-4 was

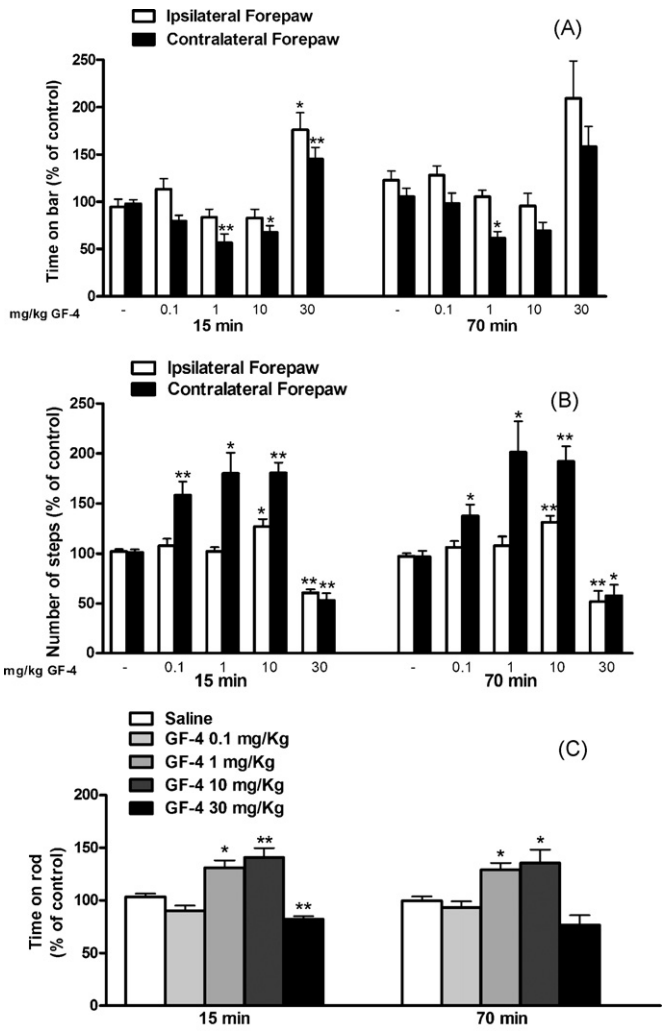

Fig. 6. GF-4 attenuated motor deficits in 6-OHDA hemilesioned rats. GF-4 (0.1–30 mg/kg) was administered systemically (i.p.) and motor activity evaluated in the bar (A), drag (B) and rotarod (C) tests. Each experiment consisted of three different sessions: a control session followed by two other sessions performed 15 and 70 min after saline or GF-4 administration (see Section 2). Data are expressed as percentages of motor activity in the control session and are means ± SEM of 6–8 determinations per group. Basal motor activity values in the bar, drag and rotarod tests are given in text (Section 3.2.2). Statistical analysis was performed by RM-ANOVA followed by contrast analysis and the sequentially rejective Bonferroni's test. $^{*}p < 0.05$ and $^{**}p < 0.01$ significantly different from saline.

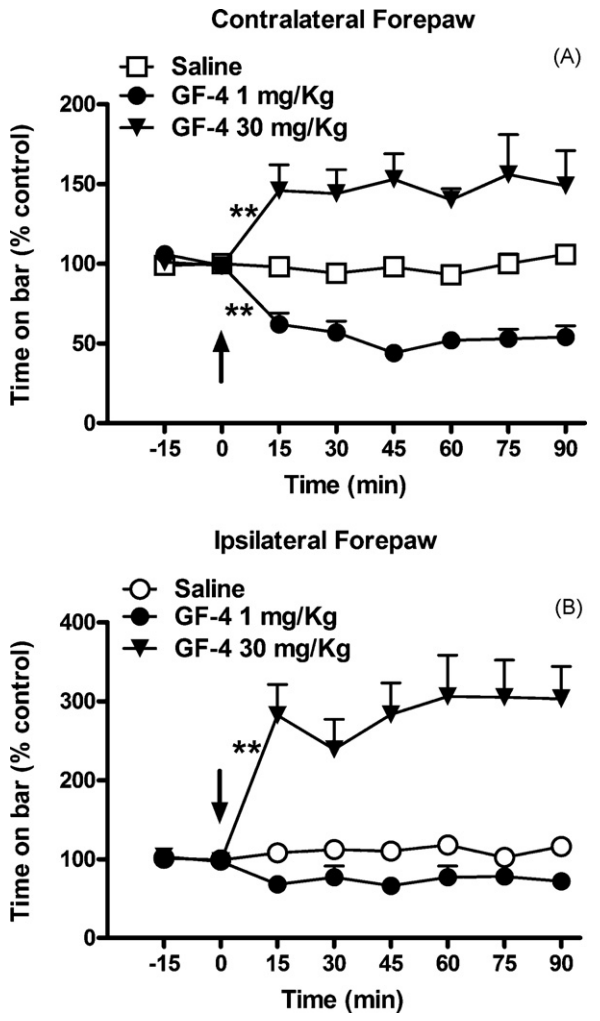

Fig. 7. Systemic GF-4 modulated akinesia in animals undergoing microdialysis. Hemiparkinsonian rats implanted in SNr and VMTh were challenged in the bar test (described in Section 2) following systemic administration (i.p., arrow) of saline ($n = 7$) or GF-4. Both motor facilitating (1 mg/kg; $n = 8$) and inhibitory (30 mg/kg; $n = 8$) doses of GF-4 were administered. Akinesia was evaluated at the contralateral and ipsilateral forepaws every 15 min for up to 90 min. Data are expressed as mean percentages ± SEM of baseline motor activity. Basal activity levels at the ipsilateral and contralateral forepaw were 8.5 ± 0.4 and 39.8 ± 1.4 s, respectively. Statistical analysis was performed by RM-ANOVA followed by contrast analysis. $^{**}p < 0.01$, significantly different from saline.

only ~5-fold less potent than SB-612111 [38] and Compound 24 [9], and ~2-fold less potent than J-113397. In this preparation, GF-4 was found ~2-fold more potent than Trap-101 (see also [39]) while in the rat vas deferens the reverse was true, Trap-101 being more potent than GF-4. Since no species differences with respect to responsiveness to NOP receptor ligands have been observed in these preparations, it is likely that these slight discrepancies in potency are due to experimental variability. Therefore, Trap-101 and GF-4 can be considered equipotent in isolated tissues. Original binding and functional experiments in recombinant systems [30] revealed that J-113397 is at least 350-fold selective over MOP and >1000-fold selective over DOP and KOP receptors. More recent studies [38,43], confirmed the high selectivity over DOP receptors but found the selectivity over KOP (30-fold) and, particularly, MOP (~10–15-fold) receptors to be much lower than previously reported. Introduction of a double bond in the J-113397 molecule (i.e. elimination of chirality) did not change selectivity as shown by a comparative study between J-113397 and Trap-101 [39]. Conversely, the introduction of a tertiary alcohol function had dramatic effects, since selectivity over MOP receptors dropped from ~49-fold (Trap-101) to ~6-fold (GF-4). This finding questions about the usefulness of GF-4 in in vitro experiments. However, despite its poor in vitro selectivity, GF-4 was selective for NOP receptors in mice in vivo up to 30 mg/kg. Interestingly, as previously shown for J-113397 [40] and Trap-101 [23], GF-4 was able to exert dual control over stepping activity, namely facilitation at low doses and inhibition at high ones, through blockade of NOP receptors. In fact, no motor changes were observed in $NOP^{-/-}$ mice following administration of high doses of GF-4. No major differences in efficacy were found among J-113397, Trap-101 and GF-4. Nevertheless, these compounds showed different potencies and ranges of activity. Thus, facilitation was observed in the 0.1–1 mg/kg dose range for J-113397 [40], in the 1–10 mg/kg dose range for Trap-101 [23] and in the 0.01–10 mg/kg dose range for GF-4. Despite the lowering of threshold for motor facilitation, GF-4 inhibited motor activity in the same range of doses as J-113397 (10 mg/kg) and Trap-101 (30 mg/kg). Thus, structural changes widened the motor facilitating dose range without changing the threshold for motor inhibition.

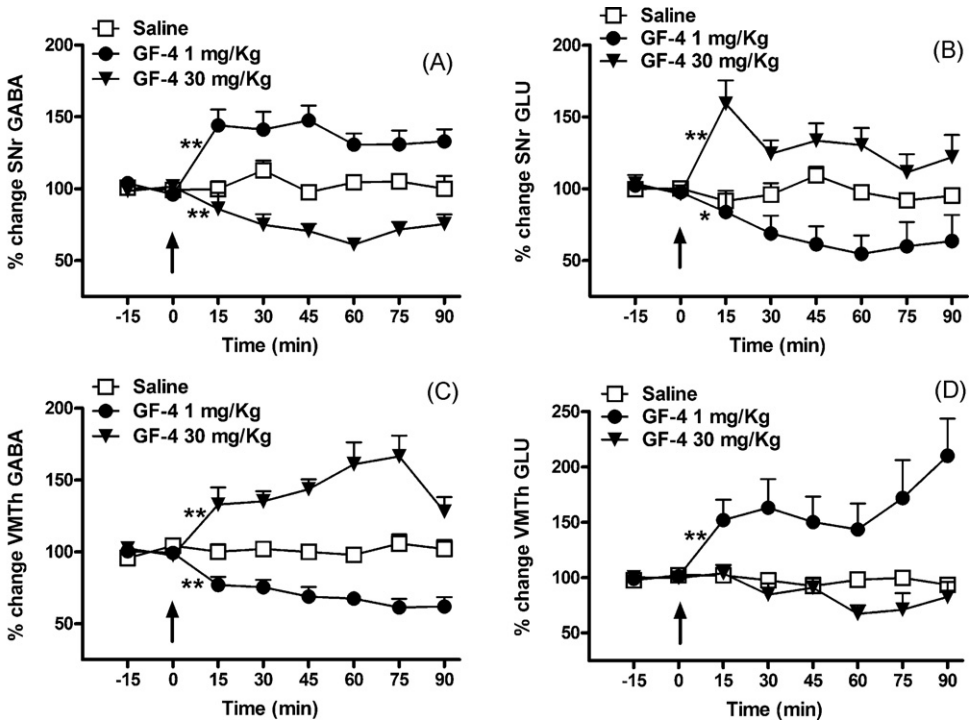

Fig. 8. Systemic GF-4 modulated GLU and GABA release in SNr and ipsilateral VMTh. Two microdialysis probes were implanted in the lesioned SNr and ipsilateral VMTh of hemiparkinsonian rats, and GABA (A and C) and GLU (B and D) release monitored while rats were undergoing the bar test (see Fig. 7). Rats were treated systemically (i.p., arrow) with saline ($n = 6$) or motor facilitating (1 mg/kg; $n = 7$) and inhibitory (30 mg/kg; $n = 8$) doses of GF-4. Data are expressed as mean percentages ± SEM of pre-treatment (basal) values. Basal GLU and GABA levels (nM) in the dialysate from the lesioned SNr were, respectively: 80.9 ± 28.7, 3.2 ± 0.8 (saline); 85.1 ± 23.7, 5.7 ± 0.6 (GF-4 1 mg/kg); 32.8 ± 8.2, 4.4 ± 0.3 (GF-4 30 mg/kg). Basal GLU and GABA levels (nM) in the dialysate from the ipsilateral VMTh were, respectively: 71.5 ± 19.9, 19.2 ± 0.7 (saline); 53.7 ± 6.1, 26.3 ± 1.7 (GF-4 1 mg/kg); 92.2 ± 13.7, 19.2 ± 0.7 (GF-4 30 mg/kg). Statistical analysis was performed by RM-ANOVA followed by contrast analysis. $^{*}p < 0.05$ and $^{**}p < 0.01$ significantly different from saline.

It is possible these changes may be related to pharmacokinetic reasons, such as greater brain penetrability or resistance to metabolic degradation.

Consistent with that found in mice, GF-4 was found more potent than expected on the basis of the in vitro data in 6-OHDA hemilesioned rats. Previous studies in this model showed that NOP receptor antagonists such as the peptide UFP-101 and the nonpeptides J-113397 and Trap-101 [21–23] mimicked the effects of L-DOPA and attenuated parkinsonian-like motor impairment. In these studies, J-113397 promoted motor activity in the 0.1–3 mg/kg dose range, being ~10 times more potent than Trap-101 (1–30 mg/kg; [21–23]), and caused motor inhibition at 30 mg/kg [40]. The dose response curve to GF-4 thus overlaps that to J-113397, with the difference that highest potency was observed in the drag and not bar test, as for J-113397. This difference may rely on experimental reasons since rats treated with J-113397 showed a slightly greater immobility time at the contralateral paw (~50 s; [21,22]) than rats treated with Trap-101 (~44 s) or GF-4 (~37 s), although no difference was observed in basal stepping activity at the contralateral paw between groups (~2–3 steps). Alternatively, this difference may reflect a different ability of J-113397 and GF-4 to discriminate between NOP receptors modulating akinesia (bar test) rather than bradykinesia (drag test).

Previous microdialysis studies carried out with a number of peptide ([Nphe^{1}]N/OFQ(1-13)-NH_2; UFP-101) and nonpeptide (J-113397, Trap-101) NOP receptor antagonists, given systemically or perfused into SNr, have pointed out that NOP receptor blockade in SNr caused inhibition of GLU release. This effect was observed in naïve [18], haloperidol-treated [20,21] and 6-OHDA hemilesioned [21–23] rats. Inhibition of GLU release in parkinsonian animals correlated with attenuation of akinesia, suggesting that normalization of pathologically elevated nigral GLU transmission is the mechanism underlying the antiparkinsonian action of NOP receptor antagonists [19,21,22]. Nevertheless, the finding that J-113397, Trap-101 and, now, GF-4 also elevated GABA release in SNr simultaneously reducing GABA release in ipsilateral VMTh suggests that their antiparkinsonian action is the results of a combined reduction of excitatory GLU inputs and enhancement of inhibitory GABA inputs upon nigro-thalamic GABA neurons. Reduction of GABA influence over thalamic filter is expected to cause thalamic disinhibition [7], i.e. increased activity of thalamocortical pathways leading to increased motor cortical output. The novel finding that the anti-akinetic dose of GF-4 elevated GLU release in VMTh, confirms this view. Indeed, the main source of GLU release in VMTh is represented by cortico-thalamic projections [26] and an increase in thalamic GLU release may lead to motor activation [14]. Alternatively, increased GLU release may arise from disinhibition of GLU nerve terminals from an inhibitory intrathalamic GABAergic tone (possibly mediated by $GABA_B$ receptors; [29]). The failure of 30 mg/kg GF-4 to affect GLU release in spite of increasing GABA release may be related to the saturation of inhibitory presynaptic GABA receptors caused by tonic activity of nigro-thalamic neurons. Thus, further increases in nigro-thalamic activity and GABA release would not cause GLU release inhibition.

The neurobiological mechanisms underlying the dual action of NOP receptor antagonists on motor activity and neurotransmitter release in SNr and VMTh are presently under investigation. *Different* populations of NOP receptors located along functional opposing motor pathways, in the same or different brain areas, may be affected at different doses of GF-4. The different sensitivity to GF-4 may rely on receptor saturation by endogenous N/OFQ, affinity for GF-4 (splice variants of the NOP receptors have been

reported [6,31]) or relevance of the targeted pathway in motor behavior. Alternatively, an ingravescent blockade of a *single* population of NOP receptors may trigger biochemical/neurochemical events leading to an initial motor facilitation (low antagonist doses) followed by inhibition (higher antagonist doses). Based on the findings that: (i) the motor inhibition induced by high doses of J-113397 (10 mg/kg) in MPTP-treated mice was reversed into facilitation by the D_2/D_3 receptor antagonist raclopride [41], and (ii) NOP receptor antagonists elevate striatal DA release [19] we put forward the hypothesis that high doses of NOP receptor antagonist inhibit movement via stimulation of D_2 receptors [41]. To which extent this holds true also in 6-OHDA rats, i.e. rats bearing almost complete destruction of the nigro-striatal DA projection, it remains to be established.

5. Concluding remarks

GF-4 is a Trap-101 derivative obtained by introducing two methyl groups in the hydroxymethyl function at the position 3 of the piperidine nucleus. Such chemical modification did not alter the pharmacological activity of the compound (a pure and competitive NOP receptor antagonist) but slightly reduced its potency at recombinant NOP receptors and, more dramatically, in vitro selectivity over classical opioid receptors. Nevertheless, GF-4 was NOP receptor selective in vivo, replicating the antiparkinsonian effect and neurochemical changes typical of its parent compounds, and being as potent as J-113397. Further studies are needed to elucidate whether the in vivo gain in potency is due to greater metabolic stability, possibly to greater resistance to cytochrome oxidation [24] as predicted on the basis of the structural changes made [39]. The present data offer new insights into the structural requirements for optimal antagonist activity at NOP receptors and selectivity over classical opioid receptors. Moreover, they confirm that NOP receptor antagonists are able to attenuate parkinsonian-like symptoms via re-setting of GLU and GABA inputs upon nigro-thalamic GABA projection neurons [21–23].

Acknowledgements

Supported by University of Ferrara (FAR 2008) and Italian Ministry of University (FIRB Internazionalizzazione no. RBIN047W33) grants to M Morari.

References

[1] Bigoni R, Giuliani S, Calò G, Rizzi A, Guerrini R, Salvadori S, et al. Characterization of nociceptin receptors in the periphery: in vitro and in vivo studies. Naunyn Schmiedebergs Arch Pharmacol 1999;359:160–7.
[2] Brown JM, Gouty S, Iyer V, Rosenberger J, Cox BM. Differential protection against MPTP or metamphetamine toxicity in dopamine neurons by deletion of ppN/OFQ expression. J Neurochem 2006;98:495–505.
[3] Camarda V, Fischetti C, Anzellotti N, Molinari P, Ambrosio C, Kostenis E, et al. Pharmacological profile of NOP receptors coupled with calcium signaling via the chimeric protein $G\alpha_{qi5}$. Naunyn Schmiedebergs Arch Pharmacol 2009;379:599–607.
[4] Calò G, Rizzi A, Rizzi D, Bigoni R, Guerrini R, Marzola G, et al. [Nphe1,Arg14,Lys15]nociceptin-NH2, a novel potent and selective antagonist of the nociceptin/orphanin FQ receptor. Br J Pharmacol 2002;136:303–11.
[5] Cheng Y, Prusoff WH. Relationship between the inhibition constant (K1) and the concentration of inhibitor which causes 50 per cent inhibition (I50) of an enzymatic reaction. Biochem Pharmacol 1973;22:3099–108.
[6] Currò D, Yoo JH, Anderson M, Song I, Del Valle J, Owyang C. Molecular cloning of the orphanin FQ receptor gene and differential tissue expression of splice variants in rat. Gene 2001;266:139–45.
[7] Deniau JM, Chevalier G. Disinhibition as a basic process in the expression of striatal functions. II. The striato-nigral influence on thalamocortical cells of the ventromedial thalamic nucleus. Brain Res 1985;334:227–33.
[8] Di Benedetto M, Cavina C, D'Addario C, Leoni G, Candeletti S, Cox BM, et al. Alterations of N/OFQ and NOP receptor gene expression in the substantia nigra and caudate putamen of MPP^+ and 6-OHDA lesioned rats. Neuropharmacology 2009;56:761–7.
[9] Fischetti C, Camarda V, Rizzi A, Pelà M, Trapella C, Guerrini R, et al. Pharmacological characterization of the nociceptin/orphanin FQ receptor nonpeptide antagonist Compound 24. Eur J Pharmacol 2009;614:50–7.
[10] Goto Y, Arai-Otsuki S, Tachibana Y, Ichikawa D, Ozaki S, Takahashi H, et al. Identification of a novel spiropiperidine opioid receptor-like 1 antagonist class by a focused library approach featuring 3D-pharmacophore similarity. J Med Chem 2006;49:847–9.
[11] Guerrini R, Calò G, Rizzi A, Bianchi C, Lazarus LH, Salvadori S, et al. Address and message sequences for the nociceptin receptor: a structure-activity study of nociceptin-(1-13)-peptide amide. J Med Chem 1997;40:1789–93.
[12] Kenakin T. A pharmacology primer. San Diego: Elsevier Academic; 2004.
[13] Kitayama M, Barnes TA, Carra G, Calò G, Guerrini R, Rowbotham DJ, et al. Pharmacological profile of the cyclic nociceptin/orphanin FQ analogues c[Cys10,14]N/OFQ(1-14)NH2 and c[Nphe1,Cys10,14]N/OFQ(1-14)NH2. Naunyn Schmiedebergs Arch Pharmacol 2003;368:528–37.
[14] Klockgether T, Turski L, Schwarz M, Sontag KH. Motor actions of excitatory amino acids and their antagonists within the rat ventromedial thalamic nucleus. Brain Res 1986;399:1–9.
[15] Kuschinsky K, Hornykiewicz O. Morphine catalepsy in the rat: relation to striatal dopamine metabolism. Eur J Pharmacol 1972;19:119–22.
[16] Lambert DG. The nociceptin/orphanin FQ receptor: a target with broad therapeutic potential. Nat Rev Drug Discov 2008;7:694–710.
[17] Lowry OH, Rosebrough NJ, Farr AL, Randall RJ. Protein measurement with the Folin phenol reagent. J Biol Chem 1951;193:265–75.
[18] Marti M, Guerrini R, Beani L, Bianchi C, Morari M. Nociceptin/orphanin FQ receptors modulate glutamate extracellular levels in the substantia nigra pars reticulata. A microdialysis study in the awake freely moving rat. Neuroscience 2002;112:153–60.
[19] Marti M, Mela F, Veronesi C, Guerrini R, Salvadori S, Federici M, et al. Blockade of nociceptin/orphanin FQ receptor signaling in rat substantia nigra pars reticulate stimulates nigrostriatal dopaminergic transmission and motor behavior. J Neurosci 2004;24:6659–66.
[20] Marti M, Mela F, Guerrini R, Calò G, Bianchi C, Morari M. Blockade of nociceptin/orphanin FQ transmission in rat substantia nigra reverses haloperidol-induced akinesia and normalizes nigral glutamate release. J Neurochem 2004;91:1501–4.
[21] Marti M, Mela F, Fantin M, Witta J, Di Benedetto M, Buzas B, et al. Blockade of nociceptin/orphanin FQ transmission attenuates symptoms and neurodegeneration associated with Parkinson's disease. J Neurosci 2005;95:9591–601.
[22] Marti M, Trapella C, Viaro R, Morari M. The nociceptin/orphanin FQ receptor antagonist J-113397 and L-DOPA additively attenuate experimental Parkinsonism through overinhibition of the nigrothalamic pathway. J Neurosci 2007;27:1297–307.
[23] Marti M, Trapella C, Morari M. The novel nociceptin/orphanin FQ receptor antagonist Trap-101 alleviates experimental parkinsonism through inhibition of the nigro-thalamic pathway: positive interaction with L-DOPA. J Neurochem 2008;107:1683–96.
[24] McClanahan RH, Huitric AC, Pearson PG, Desper JC, Nelson SD. Evidence for a cyotchrome P-450 catalyzed allylic rearrangement with double bond topomerization. J Am Chem Soc 1988;110:1979–81.
[25] McDonald J, Calò G, Guerrini R, Lambert DG. UFP-101, a high affinity antagonist for the nociceptin/orphanin FQ receptor: radioligand and GTPgamma(35)S binding studies. Naunyn Schmiedebergs Arch Pharmacol 2003;367:183–7.
[26] McFarland NR, Haber SN. Thalamic relay nuclei of the basal ganglia form both reciprocal and nonreciprocal cortical connections, linking multiple frontal cortical areas. J Neurosci 2002;22:8117–32.
[27] Meunier JC, Mollereau C, Toll L, Suaudeau C, Moisand C, Alvinerie P, et al. Isolation and structure of the endogenous agonist of opioid receptor-like ORL1 receptor. Nature 1995;377:532–5.
[28] Norton CS, Neal CR, Kumar S, Akil H, Watson SJ. Nociceptin/orphanin FQ and opioid receptor-like receptor mRNA expression in dopamine systems. J Comp Neurol 2002;444:358–68.
[29] Nyitrai G, Szàrics E, Kovàcs I, Kékesi KA, Juhàsz G, Kardos J. Effect of CGP 36742 on the extracellular level of neurotransmitter amino acids in the thalamus. Neurochem Int 1999;34:391–8.
[30] Ozaki S, Kawamoto H, Itoh Y, Miyagi M, Azuma T, Ichikawa D, et al. In vitro and in vivo pharmacological characterization of J-113397, a potent and selective non-peptidyl ORL1 receptor antagonist. Eur J Pharmacol 2000;402:45–53.
[31] Pan YX, Xu J, Wan BL, Zuckerman A, Pasternak GW. Identification and differential regional expression of KOR-3/ORL-1 gene splice variants in mouse brain. FEBS Lett 1998;435:65–8.
[32] Paxinos G, Watson C. The rat brain in stereotaxic coordinates. Sydney: Academic Press; 1982.
[33] Redrobe JP, Calò G, Regoli D, Quirion R. Nociceptin receptor antagonists display antidepressant-like properties in the mouse forced swimming test. Naunyn Schmiedebergs Arch Pharmacol 2002;365:164–7.
[34] Reinscheid RK, Nothacker HP, Bourson A, Ardati A, Henningsen RA, Bunzow JR, et al. Orphanin FQ: a neuropeptide that activates an opioid-like G protein-coupled receptor. Science 1995;270:792–4.
[35] Rozas G, Guerra MJ, Labandeira-Garcia JL. An automated rotarod method for quantitative drug-free evaluation of overall motor deficits in rat models of parkinsonism. Brain Res Brain Res Protoc 1997;2:75–84.

[36] Schallert T, De Ryck M, Whishaw IQ, Ramirez VD, Teitelbaum P. Excessive bracing reactions and their control by atropine and L-DOPA in an animal analog of parkinsonism. Exp Neurol 1979;64:33–43.
[37] Shinkai H, Ito T, Iida T, Kitao Y, Yamada H, Uchida I. 4-Aminoquinolines: novel nociceptin antagonists with analgesic activity. J Med Chem 2000;43:4667–77.
[38] Spagnolo B, Carrà G, Fantin M, Fischetti C, Hebbes C, McDonald J, et al. Pharmacological characterization of the nociceptin/orphanin FQ receptor antagonist SB-612111 [(−)-*cis*-1-methyl-7-[[4-(2,6-dichlorophenyl)piperidin-1-yl]methyl]-6,7,8,9-tetrahydro-5H-benzocyclohepten-5-ol]: in vitro studies. J Pharmacol Exp Ther 2007;321:961–7.
[39] Trapella C, Guerrini R, Piccagli L, Calò G, Carrà G, Spagnolo B, et al. Identification of an achiral analogue of J-113397 as potent nociceptin/orphanin FQ receptor antagonist. Bioorg Med Chem 2006;14:692–704.
[40] Viaro R, Sanchez-Pernaute R, Marti M, Trapella C, Isacson O, Morari M. Nociceptin/orphanin FQ receptor blockade attenuates MPTP-induced parkinsonism. Neurobiol Dis 2008;30:430–8.
[41] Viaro R, Marti M, Morari M. Dual motor response to L-DOPA and nociceptin/orphanin FQ receptor antagonists in 1-methyl-4-phenyl-1,2,5,6-tetrahydropyridine (MPTP) treated mice: paradoxical inhibition is relieved by D(2)/D(3) receptor blockade. Exp Neurol; doi:10.1016/j.expneurol.2010.01.014.
[42] Visanji NP, de Bie RM, Johnston TH, McCreary AC, Brotchie JM, Fox SH. The nociceptin/orphanin FQ (NOP) receptor antagonist J-113397 enhances the effects of levodopa in the MPTP-lesioned nonhuman primate model of Parkinson's disease. Mov Disord 2008;23:1922–5.
[43] Zaratin PF, Petrone G, Sbacchi M, Garnier M, Fossati C, Petrillo P, et al. Modification of nociceptin and morphine tolerance by the selective opiate receptor-like orphan receptor antagonist (−)-*cis*-1-methyl-7-[[4-(2,6-dichlorophenyl)piperidin-1-yl]methyl]-6,7,8,9-tetrahydro-5H-benzocyclohepten-5-ol (SB-612111). J Pharmacol Exp Ther 2004;308:454–61.

Peptides 31 (2010) 915–925

Contents lists available at ScienceDirect

Peptides

journal homepage: www.elsevier.com/locate/peptides

Further studies on the pharmacological profile of the neuropeptide S receptor antagonist SHA 68

Chiara Ruzza[a], Anna Rizzi[a], Claudio Trapella[b], Michela Pela'[b], Valeria Camarda[a], Valentina Ruggieri[c], Monica Filaferro[c], Carlo Cifani[d], Rainer K. Reinscheid[e], Giovanni Vitale[c], Roberto Ciccocioppo[d], Severo Salvadori[b], Remo Guerrini[b], Girolamo Calo'[a,*]

[a] Department of Experimental and Clinical Medicine, Section of Pharmacology and Neuroscience Center and National Institute of Neuroscience, University of Ferrara, via Fossato di Mortara 19, 44100 Ferrara, Italy
[b] Department of Pharmaceutical Sciences and Biotechnology Center, University of Ferrara, via Fossato di Mortara 19, 44100 Ferrara, Italy
[c] Department of Biomedical Sciences-Section of Pharmacology, University of Modena and Reggio Emilia, Via G. Campi 287, I-41100 Modena, Italy
[d] Department of Pharmacological Sciences and Experimental Medicine, University of Camerino, Via Madonna delle Carceri, Camerino, Italy
[e] Department of Pharmaceutical Sciences, University of California Irvine, 2214 Natural Sciences I, Irvine, CA 92697, USA

ARTICLE INFO

Article history:
Received 18 January 2010
Received in revised form 12 February 2010
Accepted 12 February 2010
Available online 19 February 2010

Keywords:
Neuropeptide S
NPS receptor
SHA 68
Calcium assay
In vivo studies

ABSTRACT

Neuropeptide S (NPS) regulates various biological functions by selectively activating the NPS receptor (NPSR). Previous studies demonstrated that the non-peptide molecule SHA 68 acts as a selective NPSR antagonist. In the present study the pharmacological profile of SHA 68 has been further investigated in vitro and in vivo. In cells expressing the mouse NPSR SHA 68 was inactive per se up to 10 μM while it antagonized NPS-stimulated calcium mobilization in a competitive manner showing a pA_2 value of 8.06. In the 10–50 mg/kg range of doses, SHA 68 counteracted the stimulant effects elicited by NPS, but not those of caffeine, in mouse locomotor activity experiments. In the mouse righting reflex assay SHA 68 fully prevented the arousal-promoting action of the peptide. The anxiolytic-like effects of NPS were slightly reduced by SHA 68 in the mouse open field, fully prevented in the rat elevated plus maze and partially antagonized in the rat defensive burying paradigm. Finally, SHA 68 was found poorly active in antagonizing the NPS inhibitory effect on palatable food intake in rats. In all assays SHA 68 did not produce any effect per se. In conclusion, the present study demonstrated that SHA 68 behaves as a selective NPSR antagonist that can be used to characterize the in vivo actions of NPS. However the usefulness of this research tool is limited by its poor pharmacokinetic properties.

1. Introduction

Neuropeptide S (NPS, human sequence SFRNGVGTGMKKTSFQRAK) is the endogenous ligand of the 7TM receptor NPSR [39,45]. In cells expressing the recombinant NPSR, NPS displayed high affinity and stimulated calcium mobilization and cAMP accumulation suggesting Gq and Gs coupling for the NPSR [35,45]. In vitro, in brain tissue preparations, NPS has been reported to control neuronal electrophysiological properties [19,25] and neurotransmitter release [34]. In vivo, in rodents, NPS has been shown to control several biological functions including wakefulness [6,37,45], locomotor activity [8,15,30,37,41,45], stress and anxiety [22,30,37,44,45], food intake and gastrointestinal functions [3,9,11,17,41], memory processes [18,19,25,27], drug abuse [2,7,24,30], and nociception [23]. To deeply investigate these NPS-sensitive biological functions and to identify the therapeutic potential of drugs interacting with NPSR, potent and selective ligands are required (for a recent review in this field see [16]).

SHA 68, i.e. the racemic mixture (9R/S)-3-oxo-1,1-diphenyl-tetrahydro-oxazolo[3,4-a]pyrazine-7-carboxylic acid 4-fluoro-benzylamide has been identified by Takeda researchers [12] and characterized pharmacologically in vitro and in vivo by Okamura et al. [28]. In radioligand ([^{125}I][Tyr^{10}]NPS) binding experiments performed in HEK293$_{hNPSR}$ cells SHA 68 displayed high affinity (pKi 7.3). In calcium mobilization experiments SHA 68 was inactive per se while antagonizing NPS stimulatory effects in a concentration-dependent and competitive manner. Similar high pA_2 values were obtained with SHA 68 at Ile107 (7.6) and Asn107 (7.8) hNPSR isoforms expressed in HEK293 cells. SHA 68 appeared to be selective for NPSR since it did not affect signaling at 14 unrelated G-protein-coupled receptors [28]. In vivo in mice SHA 68 reached pharmacologically relevant levels in plasma and brain after i.p. administration. Despite this, SHA 68 (50 mg/kg i.p.) was only able to partially counteract NPS-induced stimulation

* Corresponding author. Tel.: +39 0532 455 221; fax: +39 0532 455 205.
E-mail address: g.calo@unife.it (G. Calo').

0196-9781/$ – see front matter © 2010 Elsevier Inc. All rights reserved.
doi:10.1016/j.peptides.2010.02.012

of locomotor activity [28]. In a separate study [19], bilateral intra-amygdala administrations of SHA 68 exerted functionally opposing responses compared to NPS: in fact the peptide induced anxiolytic-like effects in the open field test while anxiogenic-like effects were measured in response to SHA 68. Finally, NPS treatment attenuated MK-801-induced vacuolization in the rat retrosplenial cortex and this protective effect of NPS could be blocked by systemic administration of SHA 68 [29].

In the present study the pharmacological profile of SHA 68 was further investigated in vitro in calcium mobilization experiments performed on HEK293 cells expressing the mouse NPSR and in vivo in a rather large panel of assays sensitive to NPS including locomotor activity (LA), righting reflex (RR) and open field behavior (OF) in mice, and elevated plus maze (EPM), defensive burying (DB) and palatable food intake (PFI) paradigms in rats.

2. Materials and methods

2.1. Cell culture and calcium mobilization experiments

$HEK293_{mNPSR}$ were generated as previously described [35] and maintained in DMEM medium supplemented with 10% fetal bovine serum, 2 mM L-glutamine, hygromycin B (100 mg/l), and cultured at 37 °C in 5% CO_2 humidified air. $HEK293_{mNPSR}$ cells were seeded at a density of 50,000 cells/well into poly-D-lysine coated 96-well black, clear-bottom plates.

The following day, the cells were incubated with medium supplemented with 2.5 mM probenecid, 3 μM of the calcium sensitive fluorescent dye Fluo-4 AM and 0.01% pluronic acid, for 30 min at 37 °C. After that time the loading solution was aspirated and 100 μl/well of assay buffer (Hank's Balanced Salt Solution; HBSS) supplemented with 20 mM 4-(2-hydroxyethyl)-1-piperazineethanesulfonic acid (HEPES), 2.5 mM probenecid and 500 μM Brilliant Black (Aldrich) was added. Concentrated solutions (1 mM) of NPS were made in bidistilled water and kept at −20 °C. SHA 68 was dissolved in 10% Tween 80 solution in saline. Serial dilutions were carried out in HBSS/HEPES (20 mM) buffer (containing 0.02% bovine serum albumin fraction V). After placing both plates (cell culture and master plate) into the fluorometric imaging plate reader FlexStation II (Molecular Devices, Sunnyvale, CA), fluorescence changes were measured. On-line additions were carried out in a volume of 50 μl/well. To facilitate drug diffusion into the wells in antagonist type experiments, the present studies were performed at 37 °C and three cycles of mixing (25 μl from each well moved up and down 3 times) were performed immediately after antagonist injection to the wells. Inhibition response curves were determined against the stimulatory effect of 30 nM NPS. SHA 68 was injected into the wells 24 min before adding NPS.

2.2. Animals

All experimental procedures adopted for in vivo studies complied with the standards of the European Communities Council directives (86/609/EEC) and national regulations (D.L. 116/92). Male Swiss mice (30–38 g, Morini RE, Italy) and male Wistar rats (200 g for DB and EPM studies and 300 g for PFI studies, Charles River MI, Italy) were used. They were housed in Plexiglas® cages (Tecniplast, MN, Italy), under standard conditions (22 °C, 55% humidity, 12 h light–dark cycle, lights on 7.00 am) with food (mice: MIL, standard diet Morini RE, Italy, rats: 4RF, Mucedola, Settimo Milanese, MI, Italy) and water *ad libitum* for at least 5 days before experiments began. Each animal was used only once, with the exception of PFI studies. NPS was given intracerebroventricularly (i.c.v.), while SHA 68 was injected intraperitoneally (i.p.) 10 min before NPS. In mice, i.c.v. injections (2 μl per mouse) were given under light (just sufficient to produce a loss of the righting reflex) isoflurane anesthesia, into the left ventricle according to the procedure described by [21] and routinely adopted in our laboratory [36]. For i.c.v. injections in rats, stainless-steel guide cannula (23 ga) (Plastic One, Roanoke, VA, USA) were stereotaxically implanted in the right lateral ventricle, to a depth of 0.5 mm above the ventricle (coordinates were taken from the rat brain atlas [32] and adjusted for the animal body weight), under ketamine plus xylazine anesthesia (115 + 2 mg/kg i.p.; Farmaceutici Gellini, Aprilia, Italy and Bayer, Milan, Italy, respectively) and fixed in place with acrylic dental cement and one skull screw. A removable plug was kept in place except during the drug injections. In rats i.c.v. injections were in a volume of 5 μl. After the end of the experiment, rats were i.c.v. injected with 5 μl of Evans Blue and sacrificed under anesthesia. The correct placement of the cannula was ascertained by inspection of dye diffusion in the right lateral ventricle. All procedures were randomized across test groups.

2.3. Mouse locomotor activity

Experiments were performed during the light cycle (between 09.00 and 13.00) according to [15]. Naïve mice were treated i.c.v. 5 min before the beginning of the test and LA was recorded for 60 min. For these experiments the ANY-maze video tracking system was used (Ugo Basile, application version 4.52c Beta). Mice were positioned in a square plastic cage (40 cm × 40 cm), one mouse per cage. Four mice were monitored in parallel. Mouse horizontal activity was monitored by a camera while vertical activity was measured by an infrared beam array. The parameters measured were cumulative distance traveled (total distance in m that the animal traveled during the test), immobility time (the animal is considered immobile when 90% of it remains in the same place for a minimum of 2.5 s), and the number of rearings (the number of beam breaks due to vertical movements). Previous studies performed under the present experimental conditions demonstrated that NPS-stimulated LA in a dose-dependent manner [15]; from these studies the dose of 0.1 nmol was selected as the lower dose inducing statistically significant effects. SHA 68 (10 and 50 mg/kg, i.p.) was administered 10 min before NPS (0.1 nmol, i.c.v.). In a separate series of experiments, to investigate the selectivity of action of SHA 68, the NPSR antagonist (at 50 mg/kg, 10 min pretreatment) was tested against the stimulatory effect of caffeine (20 mg/kg, i.p.). Caffeine was administered 5 min before recording LA.

2.4. Mouse righting reflex recovery

This assay was performed according to the procedures previously described in detail [37]. Briefly, mice were given an i.p. injection of diazepam (15 mg/kg). When the animals lost the RR, they were placed in a plastic cage and the time was recorded by an expert observer blind to drug treatments. Animals were judged to have regained the RR response when they could right themselves three times within 30 s. Sleep time is defined as the amount of time between the loss and regaining of the RR and was rounded to the nearest minute. Previous studies performed under the present experimental conditions demonstrated that NPS facilitated RR recovery in a dose-dependent manner [37]; from these studies the dose 0.1 nmol was selected as the lower dose inducing statistically significant effects. SHA 68 (10 and 50 mg/kg, i.p.) was administered 10 min before NPS, and the peptide was given i.c.v. (0.1 nmol) 5 min before the injection of diazepam. In a separate series of experiments in order to investigate in detail the possible effects of the NPSR antagonist on benzodiazepine-induced sleep, SHA 68 (50 mg/kg, i.p.) was injected 10 min before the administration of different doses (5, 10, and 15 mg/kg) of diazepam.

2.5. Mouse open field

Mice were moved to the testing room to acclimate the day before the test. This assay was performed using the ANY-maze video tracking system (Ugo Basile, application version 4.52c Beta). Briefly the mouse was placed in a square plastic cage (40 cm × 40 cm) and ambulatory behavior was monitored for 10 min. The central zone of the open field was defined as the central 20 cm × 20 cm square. Horizontal activity was monitored by a camera. Four mice were monitored in parallel in each experiment. The parameters measured were the number of entries in the central zone and the time spent by the animal in the central area of the field. An entry in the central zone occurred when the entire area of the animal was in the central square and the time in the central zone is defined as the amount of time in seconds that the animal spent in the central square. In the first series of experiments the dose response curve to NPS (0.01, 0.1 and 1 nmol) was evaluated. In these experiments NPS was given i.c.v. 15 min before starting the test. From these studies the dose of 0.1 nmol was selected as the lower dose inducing statistically significant effects. In the second series of experiments, the effects of SHA 68 per se and vs NPS 0.1 nmol was evaluated. In these experiments SHA 68 (50 mg/kg, i.p.) was administered 10 min before NPS, and the peptide was given i.c.v. (0.1 nmol) 15 min before starting the test.

2.6. Rat elevated plus maze

The rat EPM assay was carried out as previously described [43]. The rat EPM consisted of two open arms and two enclosed arms each measuring 55 cm × 10 cm, with black wooden floors, emanating from a common central platform (10 cm × 10 cm) to form a plus shape. The open arms were bounded by 1 cm high ledges on the sides, but there were no ledges at the ends of the arms. The closed arms had 40 cm high transparent Plexiglas walls. The maze was elevated 80 cm above the ground. The rats were brought to the room in a clear plastic neutral box measuring 32 cm × 22 cm × 11 cm. Five days after surgery, each animal was treated with saline or increasing doses of NPS (0.1–10 nmol, i.c.v.) and submitted to the EPM 15 min thereafter. For antagonism experiments, SHA 68 (25–50 mg/kg, i.p.) or its vehicle was administered 10 min before NPS. Caffeine (20 mg/kg, i.p.) and diazepam (1.5 mg/kg, i.p.), injected 30 min before the assay, were used in parallel experiments as standard anxiogenic and anxiolytic drug, respectively. The animal was placed in the center of the maze (central platform = arena) facing an open arm and its behavior recorded by an expert group of experimenters, unaware of the treatments, for a period of 5 min. At the end of each test, the animal was removed and the maze floor was thoroughly cleaned. The time spent in open arms and the number of open arm entries (defined as the movements of all four paws from one arm to another) were recorded [33].

2.7. Rat defensive burying

This assay was performed according to the procedures previously described in details [44]. A rectangular Plexiglas burying apparatus consisting of an acrylic cage (27 cm × 38 cm × 38 cm), with the floor covered with fine sawdust, was used. A continuously electrified probe consisting of wires wrapped around a wooden dowel was positioned in the apparatus so that it protruded 10.3 cm into the chamber and was 7.5 cm from the bottom of the chamber. Contact with the probe produced a shock of 1 mA. Bedding in the chamber was approximately 5.0 cm in depth. After recovery from surgery, animals were habituated (three to four cagemates together) to the apparatus, in the absence of the shock probe, for 1 min each day for 4 consecutive days. On the fifth day, rats were tested individually for 15 min with the electrified probe in place. The height of bedding behind the probe was measured before testing and at the end of each 30 min test period and was expressed as the height of bedding above the 5.0 cm of bedding already placed in the chamber. Fresh bedding was placed in the apparatus before testing each animal. Behavior during the 30 min test period was recorded and later scored by two independent observers unaware of the treatments. Behaviors measured were height of buried bedding, duration of burying behavior, and duration of immobility/freezing over the entire test period. In particular, the cumulative time of burying behavior has been suggested to reflect the rat anxiety levels in a specific manner [42]. Previous studies performed under the present experimental conditions demonstrated that NPS produced anxiolytic-like effects in this assay in a dose-dependent manner [44]; from these studies the dose of 1 nmol was selected as the lower dose inducing statistically significant effects. Rats were treated and submitted to the test following the same experimental procedures described for EPM experiments.

2.8. Rat palatable food intake

Experiments began 1 week after surgery and were performed during the light phase of the light/dark cycle. Before the beginning of the experiments, animals received i.c.v. injections of saline to habituate them to the drug administration procedure. Palatable food was prepared by mixing powdered normal dehydrated food pellets, sweet condensed milk (Argenti Srl, Ponte Felcino, Perugia, Italy) and water in the respective percent ratio: 50%, 33% and 17%. To habituate animals to palatable food consumption, a group of freely fed rats ($n = 8$) received 4 palatable 1-h food meals. Three-day intervals were allowed between palatable food presentations. Once stable palatable food intake was established according to a within subject design, animals were treated with SHA 68 (25 and 50 mg/kg, i.p.) or its vehicle 10 min before the i.c.v. injection of NPS or saline. Normal food chow was removed from the animal cages immediately before drug treatment and was returned to them at the end of the experiment. Drug treatments were performed at intervals of 3–4 days. Palatable food intake was measured at 15, 30 and 60 min by weighing the food cups and taking into account spillage. Water was offered in graduated drinking tubes, and its intake was recorded at the same time as food intake. Food and water intakes were expressed as g/kg to correct for the influence of body weight differences.

2.9. Drugs and reagents

NPS was synthesized according to published methods [38] using Fmoc/tBu chemistry with a SYRO XP multiple peptide synthesizer (MultiSyntech, Witten Germany). Crude peptides were purified by preparative reversed-phase HPLC and the purity checked by analytical HPLC and mass spectrometry using a matrix-assisted laser desorption ionization time of flight (Bruker BioScience, Billerica, MA, US) and an ESI Micromass ZMD-2000 mass spectrometer (Waters Corporation, Milford, MA, US). SHA 68 was synthesized using the procedures described by Okamura et al. [28]. All other reagents, including caffeine and diazepam, were purchased from Sigma Chemical Co (St Louis, MO, USA). The vehicle used for injecting NPS was saline. For in vivo studies, SHA 68 was dissolved in saline containing 10% cremophor EL (Sigma) and 3 and 1 ml/kg were injected i.p. in mice and rats, respectively.

2.10. Terminology and statistical analysis

The pharmacological terminology adopted in this paper is consistent with IUPHAR recommendations [26]. In vitro data were expressed as mean ± sem of at least four independent experiments

made in duplicate. Maximum change in fluorescence, expressed in percent of baseline fluorescence, was used to determine agonist response. Non-linear regression analysis using GraphPad Prism software (v.4.0) allowed logistic iterative fitting of the resultant responses and the calculation of agonist potencies and maximal effects. Agonist potencies are given as pEC_{50} (the negative logarithm to base 10 of the molar concentration of an agonist that produces 50% of the maximal possible effect). SHA 68 antagonist properties were first evaluated in inhibition experiments; the antagonist potency was expressed as pK_B derived from the following equation:

$$K_B = \frac{IC_{50}}{(2 + ([A]/EC_{50})^n)^{1/n} - 1}$$

where IC_{50} is the concentration of antagonist that produces 50% inhibition of the agonist response, [*A*] is the concentration of agonist, EC_{50} is the concentration of agonist producing a 50% maximal response and *n* is the Hill coefficient of the concentration response curve to the agonist [20]. Moreover to investigate the type of antagonism exerted by SHA 68 at NPSR the classical Schild protocol was performed; in this case the antagonist potency was expressed as pA_2.

In vivo data are expressed as mean ± sem of *n* animals. Data were analyzed using Students' *t*-test, one-way ANOVA followed by the Dunnett's post hoc test, or two-way ANOVA followed by the Bonferroni post hoc test as specified in figure legends. Differences were considered statistically significant when $p < 0.05$.

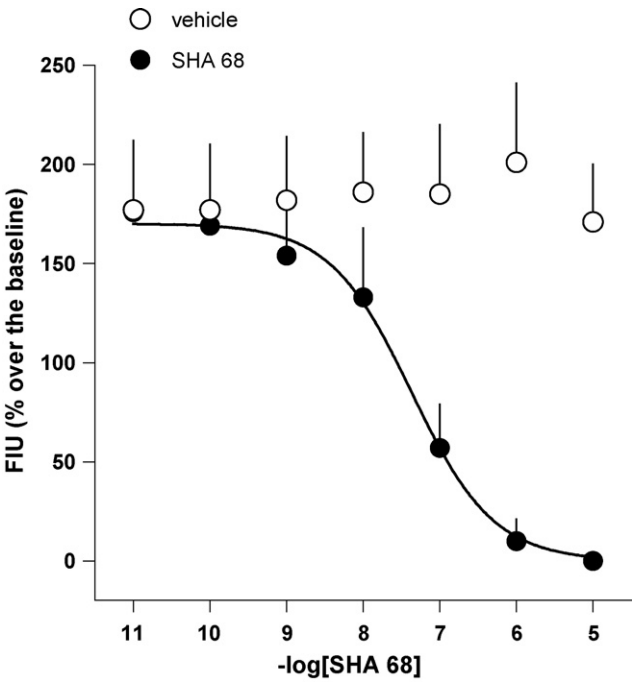

Fig. 1. Calcium mobilization assay performed on $HEK293_{mNPSR}$ cells. Inhibition–response curve to SHA 68 against the stimulatory effect of NPS 30 nM. Data are mean ± sem of 4 separate experiments made in duplicate.

3. Results

3.1. Calcium mobilization assay

In the calcium mobilization assay performed on $HEK293_{mNPSR}$ cells, NPS increased the intracellular calcium concentrations in a concentration-dependent manner with pEC_{50} and E_{max} values of 8.30 and 236 ± 15% over the basal values, respectively. Inhibition response curve to SHA 68 (0.01 nM–10 μM) were performed against the stimulatory effect of 30 nM NPS, approximately corresponding to the EC_{80} value for the agonist. As shown in Fig. 1, SHA 68 concentration-dependently inhibited 30 nM NPS stimulatory effects with a pIC_{50} value of 7.37. A pK_B value of 7.74 ($CL_{95\%}$ 7.44–8.04) was derived for SHA 68 from these experiments.

In order to investigate the nature of the antagonist action exerted by SHA 68 the classical Schild analysis was performed. As depicted in Fig. 2 left panel, SHA 68 in the range of 10–1000 nM did not produce any effect per se but displaced the concentration response curve to NPS to the right in a concentration-dependent and parallel manner. A slight but significant depression of NPS E_{max} was recorded in the presence of the highest concentrations of antagonist (i.e. 100 and 1000 nM). The corresponding Schild plot, which was linear ($r^2 = 0.97$) with a slope of 1.00 ± 0.18, is shown in the right panel of Fig. 2. The extrapolated pA_2 value was 8.06.

3.2. Mouse locomotor activity

As shown in Fig. 3 and in line with previous findings [37], NPS injected i.c.v. at 0.1 nmol evoked a stimulatory effect on mouse LA by increasing cumulative distance traveled by the animals and their number of rearings, and reducing the total immobility time, in a statistically significant manner. SHA 68 at 50 mg/kg did not modify per se the animal behavior (Fig. 3). When challenged with NPS, SHA 68 at 10 mg/kg displayed a trend toward inhibition of the stimulatory effects evoked by the peptide. Statistically significant effects were obtained with SHA 68 50 mg/kg (Fig. 3) although the antagonist did not fully prevented the effects elicited by the peptide.

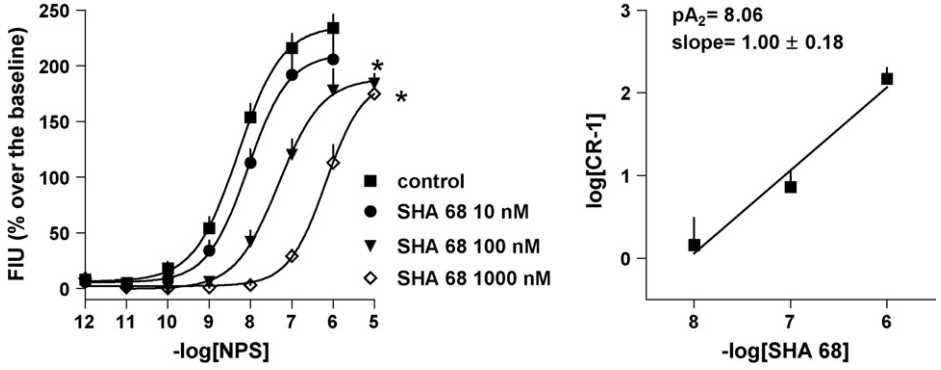

Fig. 2. Calcium mobilization assay performed on $HEK293_{mNPSR}$ cells. The left panel shows the concentration–response curve to NPS obtained in the absence (control) and in presence of increasing concentrations of SHA 68 (10–1000 nM). The corresponding Schild plot is shown in the right panel. Data are mean ± sem of 4 separate experiments made in duplicate. *$p < 0.05$ vs control, according to ANOVA followed by Dunnett's test for multiple comparisons.

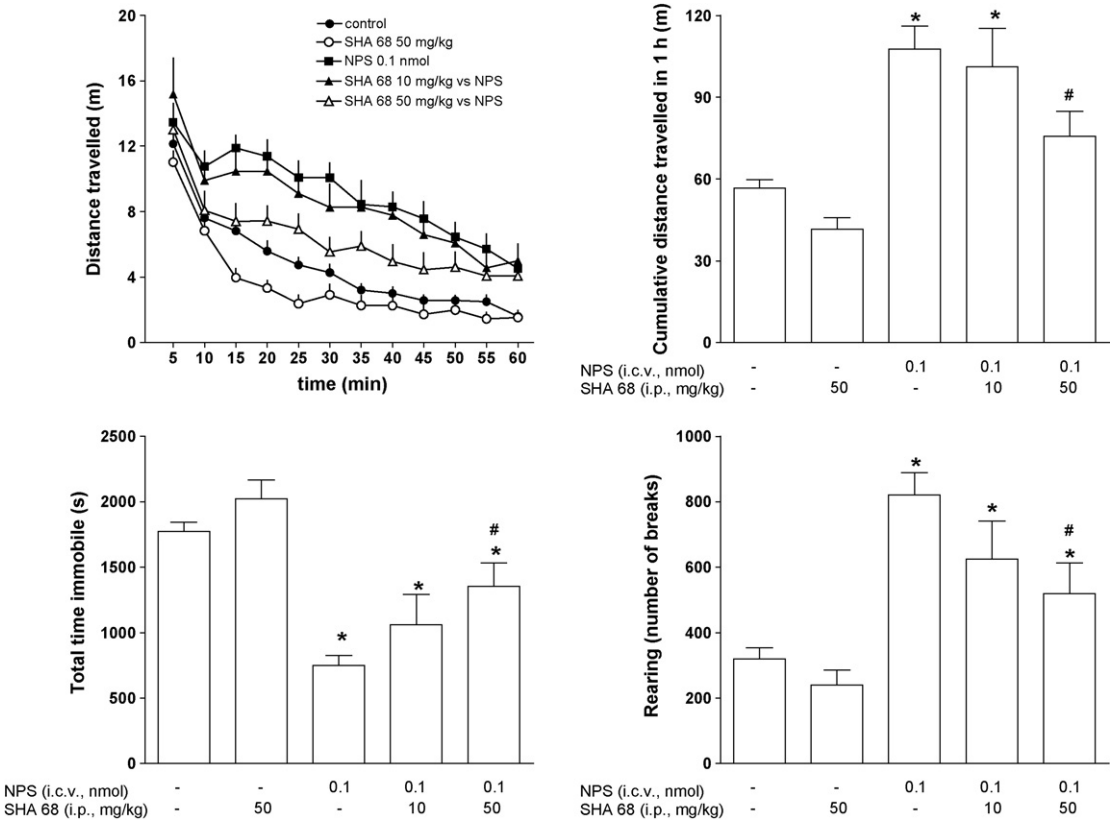

Fig. 3. Effects of NPS and SHA 68 on mouse locomotor activity. Time course of the distance traveled is shown in the top left panel, while the other panels display the cumulative effects exerted by the peptide and SHA 68 on distance traveled (top right panel), total time immobile (bottom left panel), and number of rearings (bottom right panel) over the 60 min observation period. Data are mean ± sem of 4 separate experiments (total 16 mice per group). $^{*}p < 0.05$ vs control, $^{\#}p < 0.05$ vs NPS 0.1 nmol according to two-way ANOVA followed by the Bonferroni test for multiple comparisons.

In order to investigate the in vivo selectivity of action of SHA 68, the NPSR antagonist was tested against the effect of caffeine in LA experiments. Caffeine at 20 mg/kg evoked a clear stimulatory effect on mouse locomotor activity by increasing cumulative distance traveled by the animals and reducing the total time immobile, in a statistically significant manner. SHA 68 at 50 mg/kg did not affect the stimulatory effects of caffeine (Fig. 4).

3.3. Mouse righting reflex recovery

As shown in Fig. 5 and in line with previous findings [6,37], i.p. injection of diazepam at the hypnotic dose of 15 mg/kg produced loss of the RR in all treated mice and approximately 100 min were needed to regain this reflex. NPS injected i.c.v. at 0.1 nmol reduced both the percent of animals responding to diazepam below 75% and their sleep time to approximately 50 min. The administration of SHA 68 (10 and 50 mg/kg) did not significantly modify the hypnotic effect of diazepam either in terms of percent of animals losing the RR or duration of their sleep time (Fig. 5). When SHA 68 (10 mg/kg) was co-administered with 0.1 nmol NPS, it prevented the NPS-mediated reduction in the percent of mice responding to diazepam but did not modify their sleep time. On the contrary, SHA 68 50 mg/kg fully prevented the arousal promoting effect of NPS; in fact results obtained in mice treated with NPS plus SHA 68 50 mg/kg were superimposable to those of vehicle-treated animals (Fig. 5).

In order to investigate the possible effects of the NPSR antagonist on the hypnotic action of diazepam, a separate series of experiments were performed by testing SHA 68 50 mg/kg against different doses of the benzodiazepine. As shown in Fig. 6, 5 mg/kg diazepam was inactive in the RR paradigm. At 10 mg/kg the benzodiazepine produced loss of the RR in 70% of the treated mice and approximately 25 min were needed to regain the reflex. Diazepam at 15 mg/kg produced loss of the RR in all treated mice and their sleep time was approximately 110 min. At 50 mg/kg SHA 68 did not modify the dose response curve to diazepam; in fact superimposable results were obtained in animals treated with saline or SHA 68 both in terms of percent of animals losing the RR and regarding their sleep time (Fig. 6).

3.4. Mouse open field

In a first series of experiments the dose response curve to NPS was assessed in mice subjected to the open field assay. Mice treated with saline spent on average 18 s in the central zone and made 14 entries over the 10 min observation period (Fig. 7). Supraspinal administration of NPS (0.01–1 nmol) increased in a dose-dependent and statistically significant manner the number of entries into the central zone and the time spent by the animals in this area of the field (Fig. 7). From these experiments the NPS dose of 0.1 nmol was selected to be challenged with SHA 68. As shown in Fig. 8, SHA 68 50 mg/kg did not significantly modify per se the behavior of mice subjected to the OF assay. Moreover, SHA 68 50 mg/kg only counteracted the effects elicited by NPS on time in the central area but not on the number of entries (Fig. 8).

3.5. Rat elevated plus maze

In the elevated plus maze test, rats injected with saline spent approximately 20% of the time in the open arms and made on average 3 entries into open arms (Fig. 9). Under the same experimental conditions caffeine (20 mg/kg, i.p.) evoked clear anxiogenic-like effects, reducing in a statistically significant manner both the time

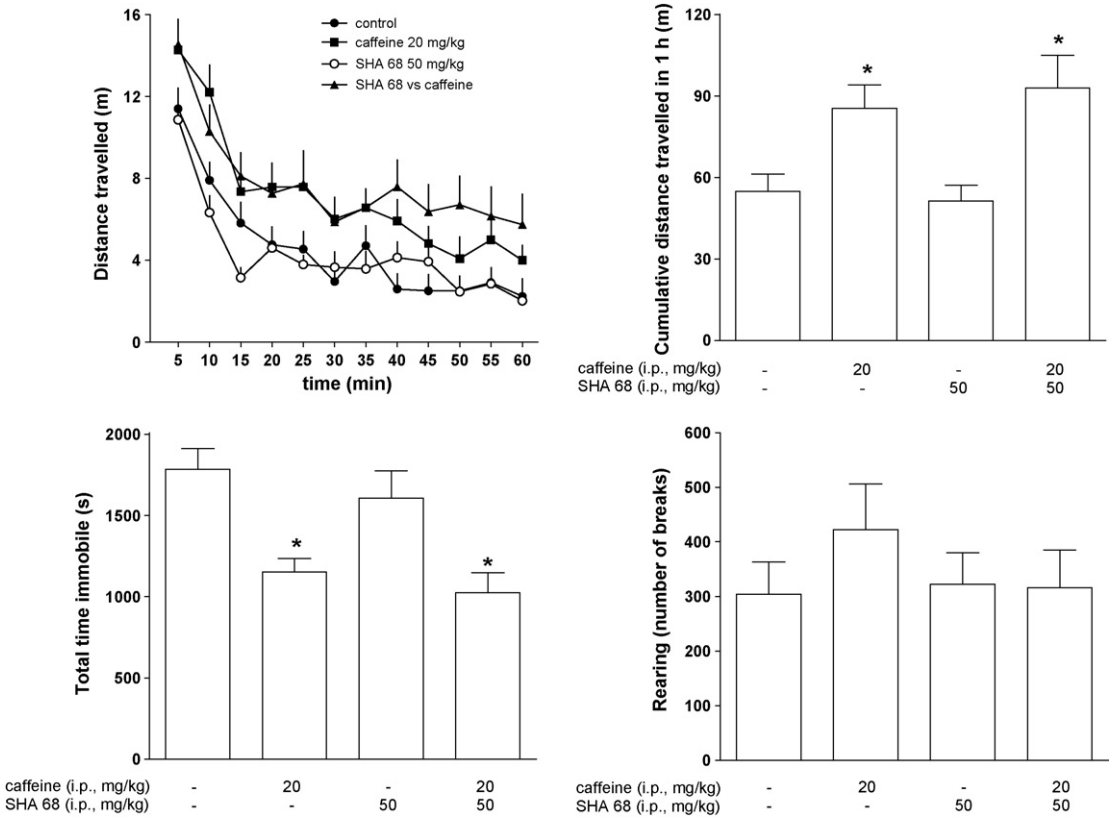

Fig. 4. Effects of caffeine and SHA 68 on mouse locomotor activity. Time course of the distance traveled is shown in the top left panel, while the other panels display the cumulative effects exerted by caffeine and SHA 68 on distance traveled (top right panel), total time immobile (bottom left panel), and number of rearings (bottom right panel) over the 60 min observation period. Data are mean ± sem of 4 separate experiments (total 16 mice per group). *$p < 0.05$ vs control, according to two-way ANOVA followed by the Bonferroni test for multiple comparisons.

spent and number of entries in the open arms (data not shown). On the contrary, diazepam (1.5 mg/kg, i.p.) elicited opposite effects by increasing in a statistically significant manner both parameters (data not shown). Similar to diazepam, the administration of NPS dose-dependently increased these behavioral parameters (Fig. 9). The peptide was inactive at 0.1 nmol while both at 1 and 10 nmol it produced statistically significant anxiolytic-like effects (Fig. 9). From these experiments the NPS dose of 1 nmol was selected to be challenged with SHA 68. SHA 68 at 50 mg/kg did not significantly modify per se animal behavior in the elevated plus maze (Fig. 10). However, in the range 25–50 mg/kg the compound antagonized the action of 1 nmol NPS. The time spent and the number of entries in the open arms of animals treated with NPS 1 nmol + SHA 68 at 50 mg/kg were similar to those of rats treated with vehicle (Fig. 10).

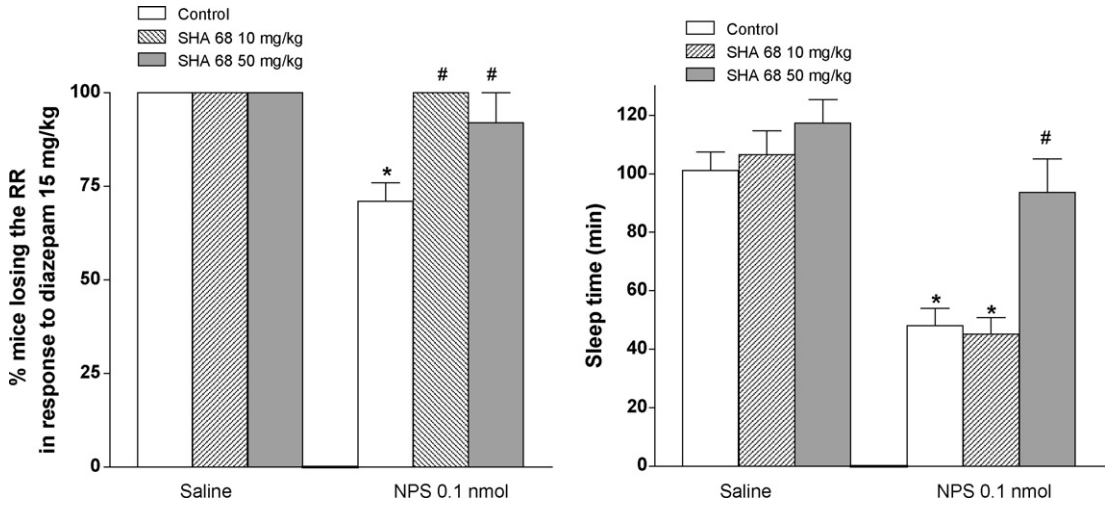

Fig. 5. Recovery of righting reflex in mice. Effects of NPS and SHA 68 on the percent of animals losing of the righting reflex in response to diazepam 15 mg/kg i.p. (left panel) and on their sleep time (right panel). Sleep time is defined as the amount of time between the loss and regaining of the righting reflex. Data are mean ± sem of 4 separate experiments (total 16 mice per group). *$p < 0.05$ vs control, #$p < 0.05$ vs NPS 0.1 nmol according to two-way ANOVA followed by the Bonferroni test for multiple comparisons.

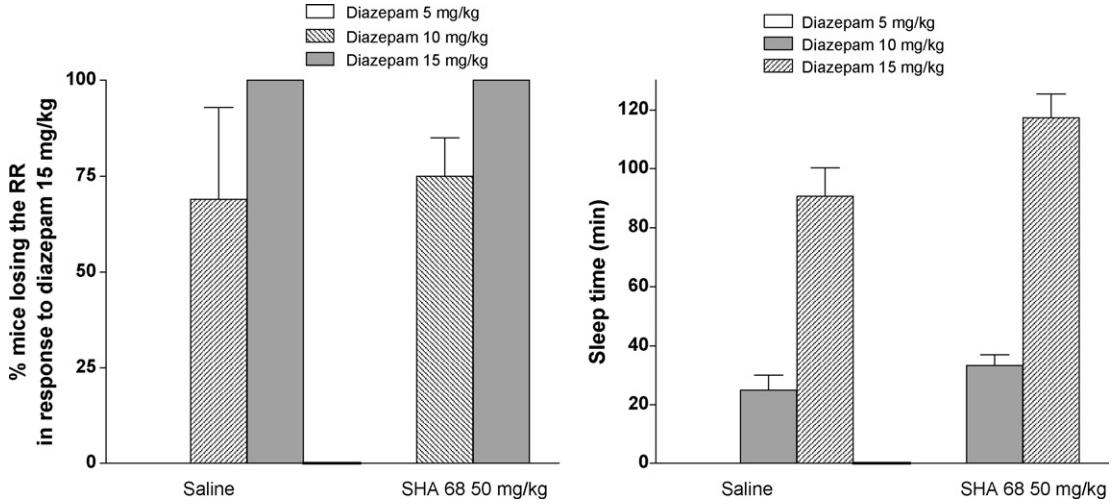

Fig. 6. Recovery of righting reflex in mice. Effect of i.p. injection of SHA 68 (50 mg/kg) on the percent of animals losing their righting reflex (left panel) and on their sleep time (right panel) in response to diazepam 5, 10, and 15 mg/kg i.p. Sleep time is defined as the amount of time between the loss and regaining of the righting reflex. Data are mean ± sem of 4 separate experiments (total 16 mice per group).

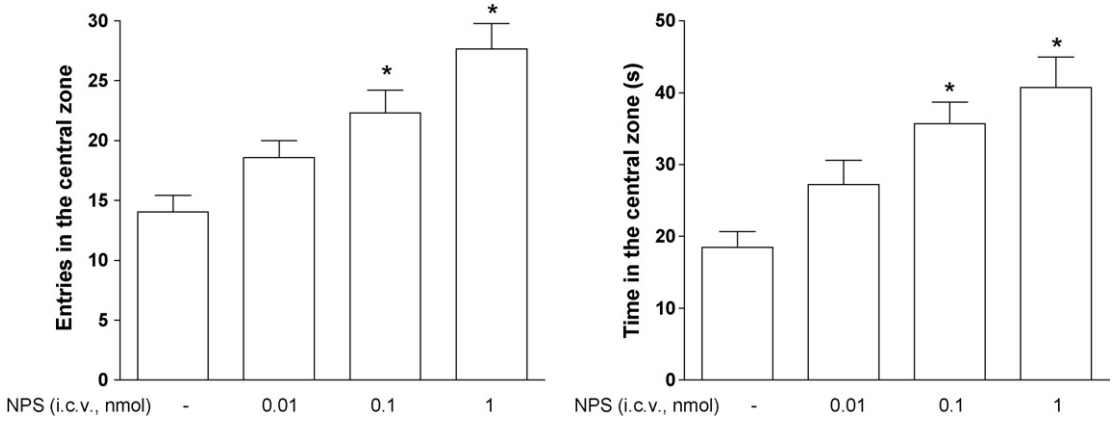

Fig. 7. Open field assay in mice. Dose–response effects of NPS (0.01–1 nmol) on the number of entries in the central zone (left panel) and the time spent in this are of the field (right panel). Data are mean ± sem of 5 separate experiments (total 20 mice per group). $^{*}p < 0.05$ vs control, according to ANOVA followed by Dunnett's test for multiple comparisons.

3.6. Rat defensive burying

In the DB assay, control rats spent about 60 s in covering the probe with bedding material (burying behavior) in response to the shocks with an average height of buried bedding of 5.6 cm; moreover they displayed immobility/freezing behavior for approximately 600 s (Fig. 11). In line with previous findings [44], 1 nmol NPS produced a statistically significant decrease of all these behav-

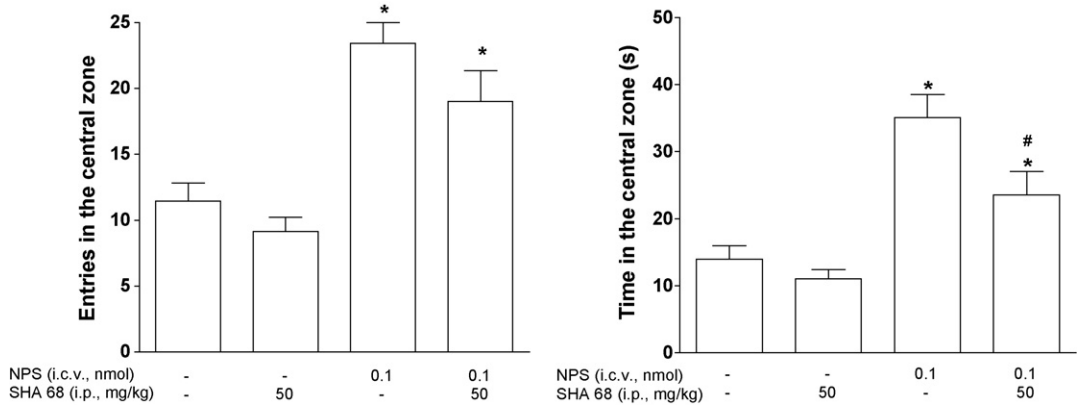

Fig. 8. Open field assay in mice. Effects of NPS and SHA 68 on the number of entries in the central zone (left panel) and the time spent in this are of the field (right panel). Data are mean ± sem of 5 separate experiments (total 20 mice per group). $^{*}p < 0.05$ vs control, $^{\#}p < 0.05$ vs NPS 0.1 nmol according to two-way ANOVA followed by the Bonferroni test for multiple comparisons.

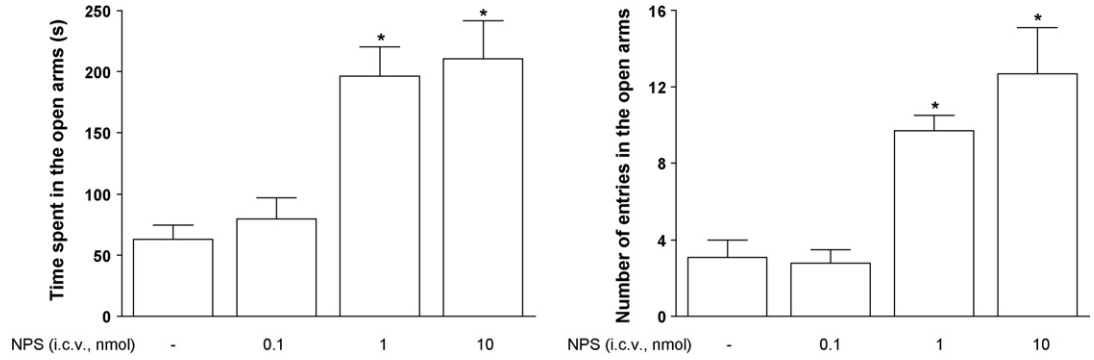

Fig. 9. Elevated plus maze in rats. Dose–response effects of NPS (0.1–10 nmol) on the time spent in the open arms (left panel) and the number of entries into open arms (right panel). Data are mean ± sem of 8–10 rats per group. $^{*}p < 0.05$ vs control, according to ANOVA followed by Dunnett's test for multiple comparisons.

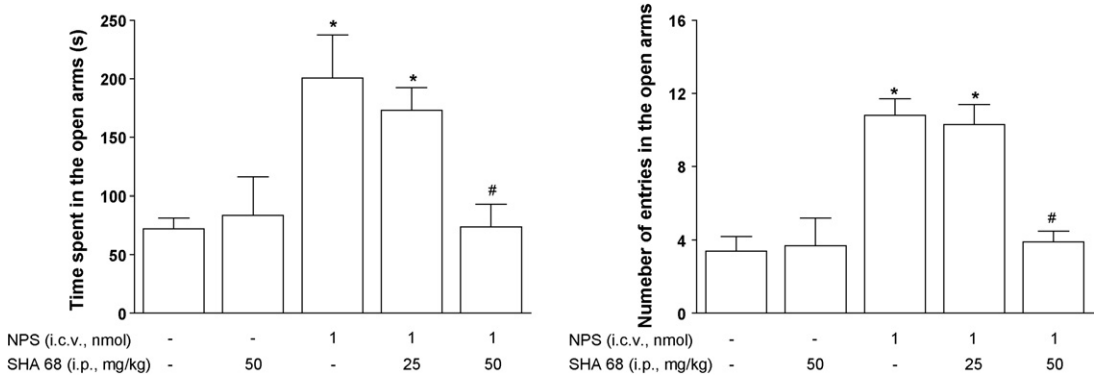

Fig. 10. Elevated plus maze in rats. Effects of NPS and SHA 68 on the time spent in the open arms (left panel) and the number of entries into open arms (right panel). Data are mean ± sem of 8–10 rats per group. $^{*}p < 0.05$ vs control, $^{\#}p < 0.05$ vs NPS 0.1 nmol according to two-way ANOVA followed by the Bonferroni test for multiple comparisons.

ioral parameters, thus promoting anxiolytic-like effects (Fig. 11). SHA 68 (50 mg/kg) did not produce any effect per se however, in the dose range 25–50 mg/kg, it counteracted the action of 1 nmol NPS. At the higher dose tested (i.e. 50 mg/kg) the antagonist fully prevented the effect of the peptide on immobility/freezing behavior while only partially counteracted those on burying behavior and height of buried bedding (Fig. 11).

3.7. Rat palatable food intake

As shown in Fig. 12 left panel, vehicle-treated rats consumed approximately 30 g/kg of palatable food over the time course of the experiments. In line with previous findings [11], i.c.v. injection of 1 nmol NPS produced a significant and profound decrease of food consumption (Fig. 12, right panel). SHA 68 (25 and 50 mg/kg) per se did not affect palatable food intake (Fig. 12, left panel). The NPSR antagonist only slightly counteracted the anorectic action of NPS producing statistically significant effect at 50 mg/kg (Fig. 12, right panel).

4. Discussion

In the present study the in vitro and in vivo pharmacological profile of the NPSR ligand SHA 68 was investigated. Our findings confirmed and extended previous results [28] demonstrating that SHA 68 behaves in vitro as a pure and potent NPSR antagonist. In vivo, in mice and rats, SHA 68 was investigated in a panel of assays sensitive to the stimulatory and arousal promoting (LA and RR [37,45]), anxiolytic-like (OF, EPM, and DB [44,45]) and anorectic (PFI [11]) actions of NPS. Depending on the assay, SHA 68 displayed different effectiveness: it fully blocked NPS effects in the RR and EPM assay, partially counteracted the actions of the peptide in the LA and DB assay, was barely active in the OF and PFI assay. The reasons for this different pattern of action of SHA 68 are not known but they may likely be attributed to its poor pharmacokinetic profile [28].

In $HEK293_{mNPSR}$ cells SHA 68 behaved as a pure antagonist. Similar high values of potency were obtained in inhibition curve experiments (pK_B 7.74) and by performing the classical Schild protocol (pA_2 8.06). Results obtained in the latter assay are however not compatible with a simple competitive interaction between SHA 68 and NPS since the antagonist at the highest concentration tested produced a slight but significant depression of NPS maximal effects. However, the following considerations suggest that the depression of NPS E_{max} caused by SHA 68 in the calcium mobilization assay probably derives from hemiequilibrium conditions rather than from a real insurmountable type of antagonism. In fact in a pilot series of experiments performed at room temperature and without three cycles of mixing, SHA 68 caused, in a concentration-dependent manner, a profound depression of NPS maximal effects (down to less than 50% E_{max}). This depression of E_{max} was strongly reduced even if not completely eliminated (see Fig. 2) by performing the experiments at 37 °C and introducing three cycles of mixing. Similar results were obtained investigating the NPSR antagonist properties of the NPS-related peptide [^{t}Bu-D-Gly^{5}]NPS [14]. Thus, the fact that antagonist-induced depression of agonist maximal effects is highly sensitive to procedures which facilitate drug diffusion (i.e. increase in temperature and cycles of mixing) strongly suggests that this phenomenon is due to hemiequilibrium conditions due to lack of stirring [20] and not to a real insurmountable type of antagonism.

The value of SHA 68 potency at mouse NPSR obtained in the present study is superimposable to those measured at human NPSR isoforms Asn107 (pA_2 7.77) and Ile107 (pA_2 7.55) [28]

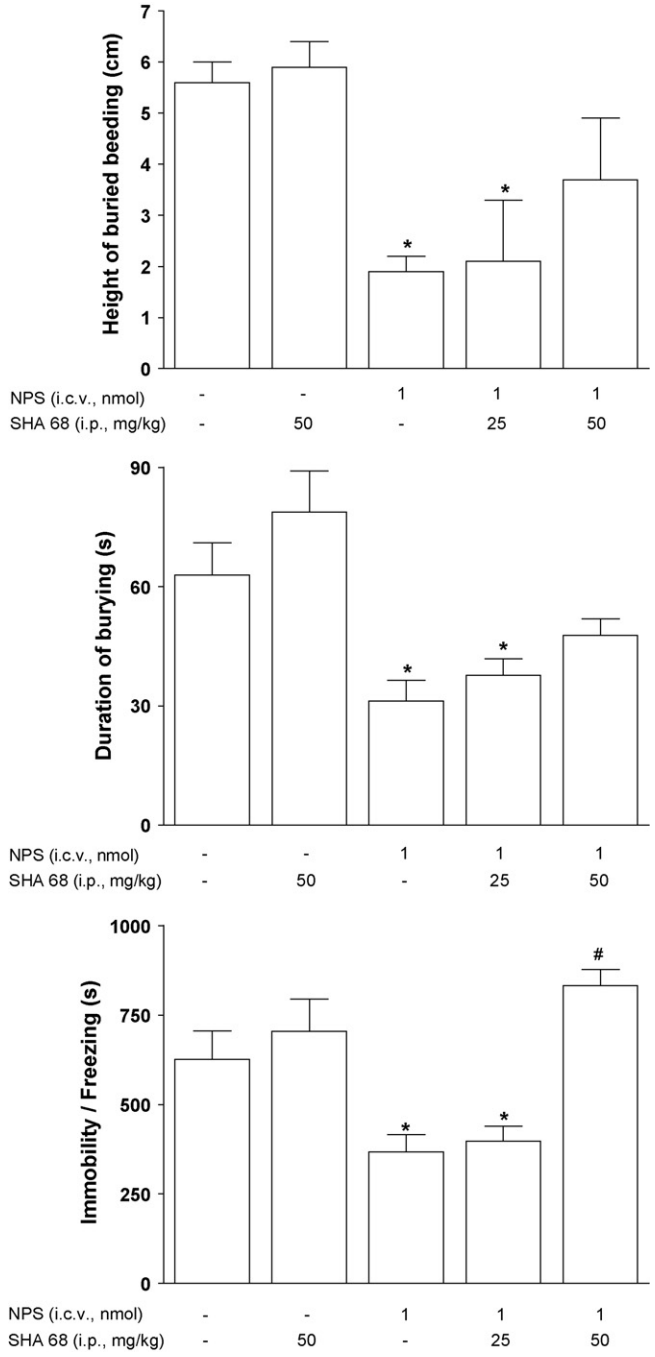

Fig. 11. Defensive burying test in rats. Effects of NPS and SHA 68 on the height of buried bedding (top panel), the duration of burying (middle panel), and the immobility/freezing behavior (bottom panel). Data are mean ± sem of 8 rats per group. $^{*}p < 0.05$ vs control, $^{\#}p < 0.05$ vs NPS 0.1 nmol according to two-way ANOVA followed by the Bonferroni test for multiple comparisons.

indicating that this NPSR ligand does not discriminate between NPSR species-specific proteins and isoforms. This is in contrast to findings for NPS [4,35] and NPS-related peptides [5] that displayed significantly higher agonist potencies at hNPSR Ile107 and mNPSR (that contains Ile at position 107) than at the hNPSR Asn107 isoform. It would be interesting in future studies to analyze and compare the pharmacological profile of NPSR peptide antagonists (i.e. [D-Cys(^{t}Bu)^{5}]NPS [6], [D-Val^{5}]NPS [15], [^{t}Bu-D-Gly^{5}]NPS [14]) and non-peptide agonists (that are not yet described in the literature) at NPSR species-specific proteins and isoforms. Such studies may help to identify the specific binding site(s) recognized by peptide and non-peptide ligands able of block or activate NPSR, and thus facilitate molecular modeling studies and the rational design of novel potent NPSR ligands.

In vivo SHA 68 was first challenged against the LA stimulatory effect of NPS. This action of NPS has been independently replicated in several different laboratories (see for a review [16]). Data obtained in LA experiments with SHA 68 are virtually superimposable to those previously published by Okamura et al. [28] and recently confirmed by Shaw and Gehlert [40]. SHA 68 at the higher dose tested (50 mg/kg) was inactive per se and only partially counteracted the stimulatory effect elicited by the supraspinal injection of NPS. The absence of a full block of NPS effects despite the relatively high dose of antagonist used may likely be linked to the poor pharmacokinetic properties of this molecule, in particular its very high lipophilicity [28] that may reduce the ability of this molecule to reach its target. Recent findings obtained by industrial investigators corroborate this view [40]. In fact, ex vivo binding studies demonstrated that only approximately 50% of [^{125}I]NPS binding to brain sections is inhibited by treating mice with SHA 68 50 mg/kg. The results obtained with the peptide NPSR antagonist [D-Val^{5}]NPS that fully blocked NPS stimulatory effects but being per se inactive [15] parallel those of SHA 68. Thus findings obtained from different laboratories using chemically unrelated molecules demonstrated that the stimulatory effect of NPS on LA is solely due to NPSR activation. This has been recently confirmed by knockout studies that demonstrated that NPS can stimulate LA in NPSR(+/+) but not in NPSR(−/−) mice [10]. In line with in vitro findings (SHA 68 does not affect signaling at 14 unrelated G-protein-coupled receptors [28]), the present in vivo results confirmed that SHA 68 antagonist properties are selective for the NPSR since the stimulatory effect of caffeine on LA was not affected by this molecule.

As mentioned in Section 1 the supraspinal administration of NPS elicits a robust arousal-promoting action in rodents [16]. SHA 68 was able to fully prevent this NPS effect in the mouse RR assay. This implies that NPSR regulating arousal might be more accessible to the antagonist than those stimulating LA. This result parallels previous data obtained under the same experimental conditions using the NPSR antagonist [D-Cys(^{t}Bu)^{5}]NPS and investigating the phenotype of NPSR(−/−) mice [6]. [D-Cys(^{t}Bu)^{5}]NPS blocked the arousal promoting effect of NPS and NPS elicited its stimulatory effects in NPSR(+/+) but not in NPSR(−/−) mice [6]. In addition, NPSR(+/+) and NPSR(−/−) animals were similarly sensitive to the hypnotic effect of diazepam and the peptide NPSR antagonist did not modify per se the effect of the benzodiazepine. This latter result has been confirmed and extended in the present study by challenging SHA 68 vs increasing doses of diazepam. Thus collectively these results demonstrated that (i) NPSR activation is involved in the arousal-promoting action of NPS, and (ii) endogenous NPSR is not tonically activated under the present experimental conditions. Obviously this does not preclude the possibility that the endogenous NPS/NPSR system might be important for controlling circadian sleep/wakefulness cycles. In fact, NPSR(−/−) mice displayed reduced late peak wheel running (an index of activity of the internal clock) compared to NPSR(+/+) mice [10] and, more importantly, the functional hNPSR polymorphism Ile107 has been associated with delayed average bedtime in humans [13].

In line with previous findings [19,22,37,44,45] the present data confirmed that the supraspinal injection of NPS elicited dose-dependent anxiolytic-like actions in rodents. In fact, NPS increased the time spent in and the number of entries into the central area of the OF in mice, the time spent in and the number of entries into open arms in the rat EPM, and reduced the duration of burying, immobility, and height of buried bedding in the rat DB assay. These actions of NPS were differently affected by SHA 68. This molecule slightly and non-significantly reduced the effects of the peptide in the mouse OF, fully prevented the anxiolytic-like actions of NPS

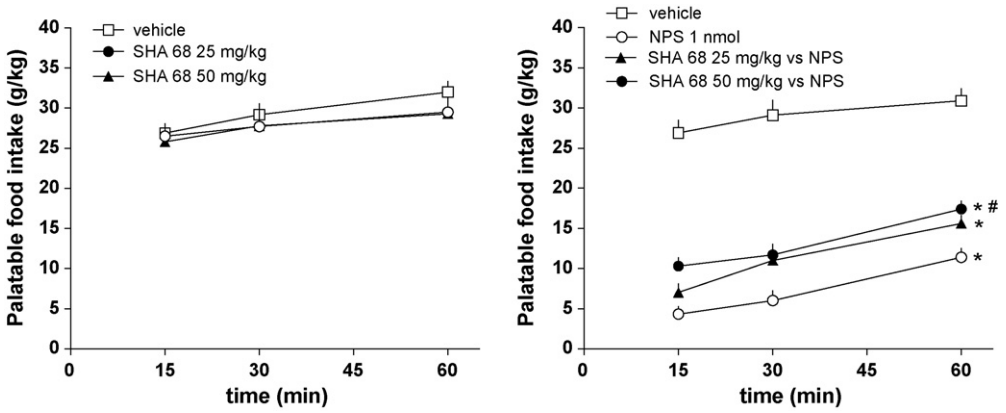

Fig. 12. Palatable food intake in rats. Effects of SHA 68 alone (left panel) and in combination with NPS (right panel) on palatable food intake. Data are mean ± sem of 8 rats per group. $^{*}p < 0.05$ vs control, $^{\#}p < 0.05$ vs NPS 0.1 nmol according to two-way ANOVA followed by the Bonferroni test for multiple comparisons.

in the rat EPM, and partially (but significantly) counteracted the effects of the peptide in the rat DB. The reasons for these differences in SHA 68 effectiveness are not completely known, however they may likely be attributed to the pharmacokinetic rather than pharmacodynamic properties of this molecule. Although the present data are not fully consistent, they still support the hypothesis that the anxiolytic-like actions evoked by NPS in rodents are due to the selective activation of the NPSR protein. This proposal should be however confirmed in future studies with the use of chemically unrelated peptide and non-peptide NPSR selective antagonists. It is worthy of note that SHA 68 did not produce any effect per se in the OF, EPM, and DB tests. These assays and experimental conditions are able to detect anxiogenic-like actions of drugs as demonstrated at least in the EPM (present study) and DB [44] with the use of caffeine. Thus, based on these results and consideration we should propose that endogenous NPS signaling does not tonically control anxiety levels. However the opposite is suggested by the following findings: (i) the intra-amygdala administration of SHA 68 in mice subjected to the open field test reduced the number of entries and the time spent by the animal in the central area (i.e. elicited an anxiogenic-like response) [19], (ii) NPSR(−/−) mice display increased levels of anxiety-like behaviors in the OF, EPM, and light dark box assays [10]. However the genetic background of these mice (129S6/SvEvTac) is known to generate highly anxious animals and this may represent a bias for this type of behavioral experiments. Collectively these latter findings may suggest that the lack of anxiogenic effects of SHA 68 given systemically may derive from an incomplete occupation of brain NPSR controlling fear and anxiety levels which are most probably located in the amygdala [19,25,31]. Clearly further studies performed with different NPSR selective antagonists and the generation of NPSR(−/−) and possibly ppNPS(−/−) mice backcrossed on genetic backgrounds suitable for behavioral investigations are needed before drawing firm conclusions on the role of the endogenous NPS/NPSR system in the control of fear and anxiety.

It is known that NPS inhibits food intake (see for a review of the available evidence [16]) and it has been recently shown that NPS exerts a robust inhibitory effect on palatable food intake in rats probably acting on neurons located in the paraventricular nucleus of the hypothalamus [11]. Therefore the effects of SHA 68 have been also investigated in the PFI assay in rats. NPS given i.c.v. at 1 nmol produced a profound inhibition of PFI. SHA 68 at 25 and 50 mg/kg did not modify food intake per se and only slightly counteracted the anorectic action of the peptide. These findings might be interpreted either assuming that SHA 68 after systemic administration is not able to reach in sufficient concentrations the NPSR regulating palatable food intake or, alternatively, that this biological action of NPS is due to a mechanism different from NPSR activation. In this context it is worthy of mention that the peptide NPSR antagonist [D-Cys(^{t}Bu)^{5}]NPS has been reported to fully prevent the inhibitory effect of NPS on PFI [11]; thus, this finding makes the former hypothesis more likely.

In conclusion, this study confirmed and extended previous findings demonstrating that the bicyclic piperazine derivative SHA 68 behaves as a selective NPSR antagonist in vitro and in vivo. However the usefulness of this research tool is limited by its poor pharmacokinetic properties. This may likely be one reason for the variable effectiveness of SHA 68 in the different NPS-sensitive assays examined in the present study. Nevertheless SHA 68 can be successfully used as a template for the identification of non-peptide NPSR selective antagonists characterized by better pharmacokinetic features. These kind of molecules should be used together with the available NPSR peptide ligands [16] and genetic models [1] for performing detailed target validation studies that will hopefully allow to firmly identify the therapeutic potential of innovative drugs acting at NPSR.

Acknowledgements

This work was supported by funds from the University of Ferrara (FAR grant to GC and SS), the Italian Ministry of University (PRIN grant to RC, SS, and GC), the Compagnia San Paolo Foundation (NPSNP grant to RC and GC) and the National Institute of Mental Health (MH-71313 grant to RKR).

References

[1] Allen IC, Pace AJ, Jania LA, Ledford JG, Latour AM, Snouwaert JN, et al. Expression and function of NPSR1/GPRA in the lung before and after induction of asthma-like disease. Am J Physiol Lung Cell Mol Physiol 2006;291:L1005–17.
[2] Badia-Elder NE, Henderson AN, Bertholomey ML, Dodge NC, Stewart RB. The effects of neuropeptide S on ethanol drinking and other related behaviors in alcohol-preferring and -nonpreferring rats. Alcohol Clin Exp Res 2008;32:1380–7.
[3] Beck B, Fernette B, Stricker-Krongrad A. Peptide S is a novel potent inhibitor of voluntary and fast-induced food intake in rats. Biochem Biophys Res Commun 2005;332:859–65.
[4] Bernier V, Stocco R, Bogusky MJ, Joyce JG, Parachoniak C, Grenier K, et al. Structure-function relationships in the neuropeptide S receptor: molecular consequences of the asthma-associated mutation N107I. J Biol Chem 2006;281:24704–12.
[5] Calo G, Camarda V, Ruzza C, Rizzi A, Salvadori S, Guerrini R, et al. Pharmacological profile of murine and human neuropeptide S receptors. Washington, DC, US: Society for Neuroscience; 2008. p. 826.9/D40.
[6] Camarda V, Rizzi A, Ruzza C, Zucchini S, Marzola G, Marzola E, et al. In vitro and in vivo pharmacological characterization of the neuropeptides S receptor antagonist [D-Cys(tBu)5]NPS. J Pharmacol Exp Ther 2009;328:549–55.

[7] Cannella N, Economidou D, Kallupi M, Stopponi S, Heilig M, Massi M, et al. Persistent increase of alcohol-seeking evoked by neuropeptide S: an effect mediated by the hypothalamic hypocretin system. Neuropsychopharmacology 2009;34:2125–34.
[8] Castro AA, Moretti M, Casagrande TS, Martinello C, Petronilho F, Sterckert AV, et al. Neuropeptide S produces hyperlocomotion and prevents oxidative stress damage in the mouse brain: a comparative study with amphetamine and diazepam. Pharmacol Biochem Behav 2009;91:636–42.
[9] Cline MA, Godlove DC, Nandar W, Bowden CN, Prall BC. Anorexigenic effects of central neuropeptide S involve the hypothalamus in chicks (Gallus gallus). Comp Biochem Physiol A Mol Integr Physiol 2007;148:657–63.
[10] Duangdao DM, Clark SD, Okamura N, Reinscheid RK. Behavioral phenotyping of neuropeptide S receptor knockout mice. Behav Brain Res 2009;205:1–9.
[11] Fedeli A, Barconi S, Economidou D, Cannella N, Kallupi M, Guerrini R, et al. The paraventricular nucleus of the hypothalamus is a neuroanatomical substrate for the inhibition of palatable food intake by neuropeptide S. Eur J Neurosci 2009;30:1594–602.
[12] Fukatzu K, Nakayama Y, Tarui N, Mori M, Matsumoto H, Kurasawa O, et al. Bicyclic piperazine compound and use thereof. Takeda Pharmaceuticals; 2004. PCT/JP04/12683.
[13] Gottlieb DJ, O'Connor GT, Wilk JB. Genome-wide association of sleep and circadian phenotypes. BMC Med Genet 2007;8:S9.
[14] Guerrini R, Camarda V, Trapella C, Calo' G, Rizzi A, Ruzza C, et al. Further studies at neuropeptide S position 5: discovery of novel neuropeptide S receptor antagonists. J Med Chem 2009;52:4068–71.
[15] Guerrini R, Camarda V, Trapella C, Calo G, Rizzi A, Ruzza C, et al. Synthesis and biological activity of human neuropeptide S analogues modified in position 5: identification of potent and pure neuropeptide S receptor antagonists. J Med Chem 2009;52:524–9.
[16] Guerrini R, Salvadori S, Rizzi A, Regoli D, Calo G. Neurobiology, pharmacology and medicinal chemistry of neuropeptide S and its receptor. Med Res Rev 2010; in press.
[17] Han RW, Chang M, Pheng YL, Qiao LY, Yin XQ, Li W, et al. Central neuropeptide S inhibits distal colonic transit through activation of central neuropeptide S receptor in mice. Peptides 2009;30:1313–7.
[18] Han RW, Yin XQ, Chang M, Peng YL, Li W, Wang R. Neuropeptide S facilitates spatial memory and mitigates spatial memory impairment induced by N-methyl-D-aspartate receptor antagonist in mice. Neurosci Lett 2009;455:74–7.
[19] Jungling K, Seidenbecher T, Sosulina L, Lesting J, Sangha S, Clark SD, et al. Neuropeptide S-mediated control of fear expression and extinction: role of intercalated GABAergic neurons in the amygdala. Neuron 2008;59:298–310.
[20] Kenakin T. A pharmacology primer. San Diego: Elsevier Academic Press; 2004.
[21] Laursen SE, Belknap JK. Intracerebroventricular injections in mice. Some methodological refinements. J Pharmacol Methods 1986;16:355–7.
[22] Leonard SK, Dwyer JM, Sukoff Rizzo SJ, Platt B, Logue SF, Neal SJ, et al. Pharmacology of neuropeptide S in mice: therapeutic relevance to anxiety disorders. Psychopharmacology (Berl) 2008;197:601–11.
[23] Li W, Chang M, Peng YL, Gao YH, Zhang JN, Han RW, et al. Neuropeptide S produces antinociceptive effect at the supraspinal level in mice. Regul Pept 2009;156:90–5.
[24] Li W, Gao YH, Chang M, Peng YL, Yao J, Han RW, et al. Neuropeptide S inhibits the acquisition and the expression of conditioned place preference to morphine in mice. Peptides 2009;30:234–40.
[25] Meis S, Bergado-Acosta JR, Yanagawa Y, Obata K, Stork O, Munsch T. Identification of a neuropeptide S responsive circuitry shaping amygdala activity via the endopiriform nucleus. PLoS ONE 2008;3:e2695.
[26] Neubig RR, Spedding M, Kenakin T, Christopoulos A. International Union of Pharmacology Committee on Receptor Nomenclature and Drug Classification. XXXVIII. Update on terms and symbols in quantitative pharmacology. Pharmacol Rev 2003;55:597–606.
[27] Okamura N, Duangdao DM, Reinscheid RK. Neuropeptide S enhances long-term memory formation. Washington, DC: Society for Neuroscience; 2008. p. 193.2/UU17.
[28] Okamura N, Habay SA, Zeng J, Chamberlin AR, Reinscheid RK. Synthesis and pharmacological in vitro and in vivo profile of 3-oxo-1,1-diphenyl-tetrahydro-oxazolo[3,4-a]pyrazine-7-carboxylic acid 4-fluoro-benzylamide (SHA 68), a selective antagonist of the neuropeptide S receptor. J Pharmacol Exp Ther 2008;325:893–901.
[29] Okamura N, Reinscheid RK, Ohgake S, Iyo M, Hashimoto K. Neuropeptide S attenuates neuropathological, neurochemical and behavioral changes induced by the NMDA receptor antagonist MK-801. Neuropharmacology 2010;58:166–72.
[30] Paneda C, Huitron-Resendiz S, Frago LM, Chowen JA, Picetti R, de Lecea L, et al. Neuropeptide S reinstates cocaine-seeking behavior and increases locomotor activity through corticotropin-releasing factor receptor 1 in mice. J Neurosci 2009;29:4155–61.
[31] Pape HC, Jungling K, Seidenbecher T, Lesting J, Reinscheid RK. Neuropeptide S: a transmitter system in the brain regulating fear and anxiety. Neuropharmacology 2010;58:29–34.
[32] Paxinos G, Watson C. The rat brain stereotaxic coordinates. New York: Academic Press; 1997.
[33] Pellow S, Chopin P, File SE, Briley M. Validation of open:closed arm entries in an elevated plus-maze as a measure of anxiety in the rat. J Neurosci Methods 1985;14:149–67.
[34] Raiteri L, Luccini E, Romei C, Salvadori S, Calo G. Neuropeptide S selectively inhibits the release of 5-HT and noradrenaline from mouse frontal cortex nerve endings. Br J Pharmacol 2009;157:474–81.
[35] Reinscheid RK, Xu YL, Okamura N, Zeng J, Chung S, Pai R, et al. Pharmacological characterization of human and murine neuropeptide S receptor variants. J Pharmacol Exp Ther 2005;315:1338–45.
[36] Rizzi A, Bigoni R, Marzola G, Guerrini R, Salvadori S, Regoli D, et al. Characterization of the locomotor activity-inhibiting effect of nociceptin/orphanin FQ in mice. Naunyn Schmiedebergs Arch Pharmacol 2001;363:161–5.
[37] Rizzi A, Vergura R, Marzola G, Ruzza C, Guerrini R, Salvadori S, et al. Neuropeptide S is a stimulatory anxiolytic agent: a behavioural study in mice. Br J Pharmacol 2008;154:471–9.
[38] Roth AL, Marzola E, Rizzi A, Arduin M, Trapella C, Corti C, et al. Structure-activity studies on neuropeptide S: identification of the amino acid residues crucial for receptor activation. J Biol Chem 2006;281:20809–16.
[39] Sato S, Shintani Y, Miyajima N, Yoshimura K. Novel G-protein coupled receptor protein and DNA thereof. WO 02/31145 A1; 2002.
[40] Shaw JL, Gehlert DR. Evaluation of the central occupancy and locomotor effects of the NPSR antagonist, SHA 68. Chicago, IL: Society for Neuroscience; 2009. p. 418.11/C38.
[41] Smith KL, Patterson M, Dhillo WS, Patel SR, Semjonous NM, Gardiner JV, et al. Neuropeptide S stimulates the hypothalamo-pituitary-adrenal axis and inhibits food intake. Endocrinology 2006;147:3510–8.
[42] Treit D, Pinel JP, Fibiger HC. Conditioned defensive burying: a new paradigm for the study of anxiolytic agents. Pharmacol Biochem Behav 1981;15:619–26.
[43] Vitale G, Arletti R, Ruggieri V, Cifani C, Massi M. Anxiolytic-like effects of nociceptin/orphanin FQ in the elevated plus maze and in the conditioned defensive burying test in rats. Peptides 2006;27:2193–200.
[44] Vitale G, Filaferro M, Ruggieri V, Pennella S, Frigeri C, Rizzi A, et al. Anxiolytic-like effect of neuropeptide S in the rat defensive burying. Peptides 2008;29:2286–91.
[45] Xu YL, Reinscheid RK, Huitron-Resendiz S, Clark SD, Wang Z, Lin SH, et al. Neuropeptide S: a neuropeptide promoting arousal and anxiolytic-like effects. Neuron 2004;43:487–97.

Tetrahedron: *Asymmetry* 21 (2010) 255–274

Contents lists available at ScienceDirect

Tetrahedron: *Asymmetry*

journal homepage: www.elsevier.com/locate/tetasy

Tetrahedron: *Asymmetry* report number 122

Mastering chiral substituted 2-oxopiperazines

Carmela De Risi *, Michela Pelà, Gian Piero Pollini *, Claudio Trapella, Vinicio Zanirato

Dipartimento di Scienze Farmaceutiche, Via Fossato di Mortara 19, 44121 Ferrara, Italy

ARTICLE INFO

Article history:
Received 18 January 2010
Accepted 11 February 2010

ABSTRACT

Stereoselective routes for the preparation of chiral 2-oxopiperazines, important structures widely found in naturally occurring substances and pharmaceutically relevant compounds, are studied.

Contents

1. Introduction

The piperazine moiety is an important pharmacophore which is found in a large number of biologically active molecules. Piperazines and their keto analogues are amongst the most important scaffolds in today's drug discovery industries.

Due to the high number of positive hits encountered in biological screens with this heterocycle and its congeners, the piperazine moiety is widely recognized as a 'privileged scaffold' in medicinal chemistry.[1,2]

Moreover, piperazine ring systems are the key structural elements in a vast array of natural products as well as being a large class of biologically active compounds. Examples include indinavir **1**, an HIV-protease inhibitor,[3] glivec **2**, a potent antiproliferative agent,[4] several compounds acting at receptors in the CNS such as arylpiperazines, powerful 5-HT_1 ligands,[5–7] lemonomycin **3**,[8,9] ecteinascidin 743 **4**,[10] TAN-1251A **5**,[11] and dragmacidins B and C **6**–**7**[12] (Fig. 1).

On the other hand, the related 2-oxopiperazine nucleus is a common structural feature of a number of natural compounds such as pseudotheonamides A_1 and A_2 **8**–**9**,[13,14] (−)-A agelastatin A **10**,[15–17] marcfortine B **11**,[18] the Phakellin group **12**–**14**,[19–21] and guadinomine C_2 **15**,[22] which are shown in Figure 2.

Furthermore, it is well known that 2-oxopiperazine derivatives have been used as peptidomimetic moieties for the discovery of novel, bioactive small molecules. Thus, the conversion of peptides into conformationally restricted peptide analogues is a generally accepted and widely used approach to design nonpeptide ligands that target protein receptors.

Excellent examples of peptidomimetic drugs discovered using a 2-oxopiperazine template that conformationally mimics the dipeptide moiety include constrained substance P analogues,[23] farnesyltransferase (FTase)[24] and protein geranylgeranyltransferase-I (PGGTase-I)[25] inhibitors, compounds with dual farnesyltransferase/geranylgeranyltransferase-I inhibitory activity,[26] elastase,[27] factor Xa,[28] renin[29–31] and BACE1[32] inhibitors, melanocortin receptors (MCRs) agonists,[33] fibrinogen glycoprotein IIb–IIIa,[34,35] and neuropeptide S (NPS) receptor[36,37] antagonists.

Recently, an interesting review covering the importance of α-ketoheterocycles in the discovery of potent enzyme inhibitors has been published.[38]

* Corresponding authors. Tel.: +39 0532 455922; fax: +39 0532 455953 (C.D.R.); tel.: +39 0532 455924; fax: +39 0532 455953 (G.P.P.).
E-mail addresses: drc@unife.it (C. De Risi), pol@unife.it (G.P. Pollini).

0957-4166/$ - see front matter © 2010 Elsevier Ltd. All rights reserved.
doi:10.1016/j.tetasy.2010.02.008

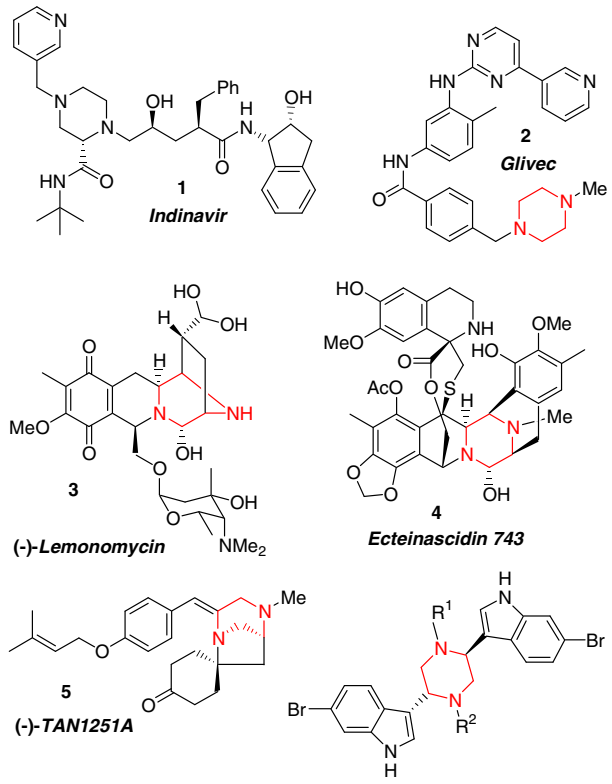

Figure 1.

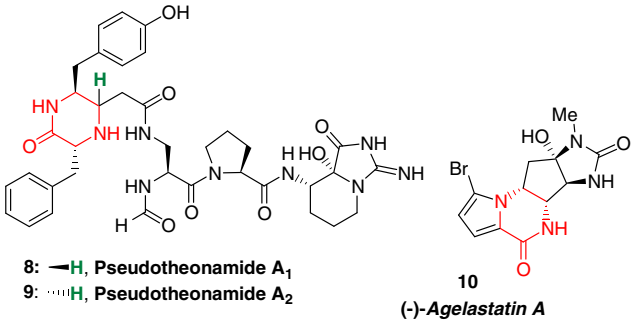

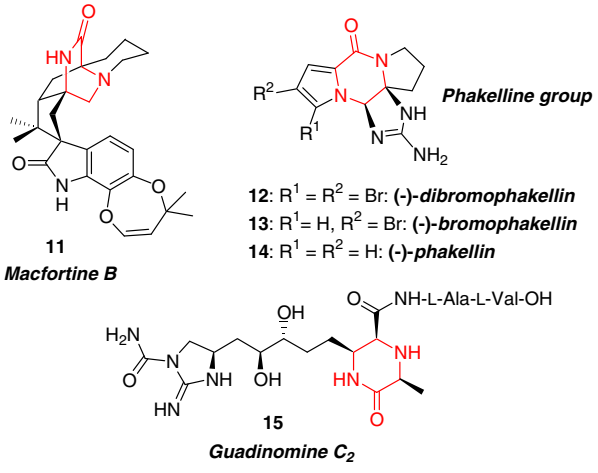

Figure 2.

Furthermore, the role of piperazines and diketopiperazines as efficient chiral ligands in enantioselective catalysis has been also examined.[39]

Therefore, it is not surprising that there is a plethora of different synthetic methods that allow for the fast and efficient assembly of these heterocyclic systems. All these methodologies have been collected in three excellent reviews.[40–42]

Although the syntheses of piperazine derivatives have been known for almost a century, the chiral syntheses of 2-oxopiperazines have rarely been reported and still remain a daunting challenge to organic chemists.

Chiral piperazines and related piperazinones are only now beginning to make their mark as useful therapeutics. Therefore, the search for efficient routes toward these compounds with substitution at different ring positions are of crucial and particular significance in view of the importance of substituted piperazine ring systems in medicinal chemistry and drug discovery.

The most interesting methods for the introduction of high diversity around the piperazine scaffold is likely represented by multicomponent reactions (MCRs) that seem to be particularly well suited to assemble ketopiperazines.[43] However, it is not suited to control the stereospecificity with regard to the carbons in the piperazine template, thus generating mixtures of stereoisomers.[44]

The need for viable routes to this class of compounds is well illustrated by praziquantel, a well-known effective antihelminthic drug used worldwide in the treatment of schistosomiasis. The (*S*)-(+)-enantiomer is inactive and harmless, while the (*R*)-(−)-enantiomer **16** is active (Fig. 3).[45]

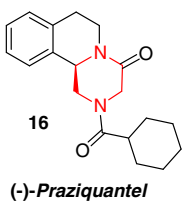

Figure 3.

The aim of this report is to focus on stereoselective routes to chiral 2-oxopiperazine derivatives with substitution at various ring positions. In the majority of cases, in the absence of an asymmetric synthesis strategy, the final stereochemistry is dependant on the starting material's configuration.

The different strategies developed to obtain chiral 2-piperazinones have been organized into sections according to the C–N bond formation in the ring-forming reaction, a similar classification previously used by Dinsmore and Beshore.[41]

When more than one bond is required for the assembly of the piperazinone ring system, usually a two-step sequence involving an initial intermolecular reaction followed by the intramolecular ring-forming step, the latter has been considered in the classification.

Section 2 has been dedicated to synthetic strategies proceeding via the formation of the N_1–C_2 linkage, while Section 3 deals with C_3–N_4 bond-forming reactions. Cyclization at N_4–C_5 is discussed in Section 4, which has been organized into sub-sections (4.1–4.4) depending on the different strategies used to prepare the piperazine ring. Finally, C_6–N_1 bond construction has been covered in Section 5.

Moreover, the positions of the substituents introduced through the different methodologies for originating the chirality are also emphasized.

For the sake of clarity, red and blue colors, respectively, have been used to show the formed carbon–nitrogen bond and the attacking nitrogen atom.

2. Cyclization at N_1–C_2

The intramolecular reaction between an amino group and an ester has been widely used to prepare 2-piperazinones. Several of these methods are based on a ring-forming coupling reaction of a primary amine with a doubly activated substrate. In almost all these processes, the substituent on the amine reactant is destined to be the amide substituent in the derived piperazinone.

Yamashita et al.[46,47] have developed a simple way to obtain chiral 1,3-disubstituted 2-oxopiperazines by acid-catalyzed lactamization of easily accessible 3,6-diaza-1,8-octanedioic acids of general structure **19**, linear *N*,*N*′-ethylene-bridged bis-α-amino acids, in turn prepared by reacting two enantiomerically pure amino acids **17** and **18**, and 1,2-dibromoethane (Scheme 1).

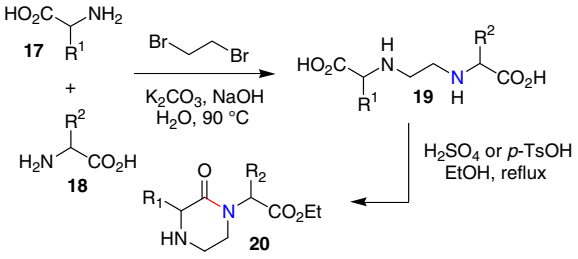

Scheme 1.

Acid-promoted cyclization of **19** proceeded with concomitant esterification to give piperazinones **20**, which have been eventually used to obtain constrained mimics of Met- and Leu-Enkephalin,[46] biologically relevant pseudotetrapeptides[47] and dermorphin analogues.[48]

The use of two different amino acids furnished a mixture of 2-oxopiperazines which could be separated by chromatography. However, Yamashita's approach is particularly suited for the preparation of 2-oxopiperazine derivatives composed of two identical amino acids, thus by-passing the tedious purification step.

As shown in Scheme 2, the ethylene-bridged compounds **21** and **22**, obtained from D-tryptophan and L-phenylalanine, respectively,[49,25] represent linear precursors of 2-oxopiperazines **23** and **24**, which have been used to obtain constrained mimics of the growth hormone secretagogue NN703[49] and PGGTase-I inhibitors,[25] respectively.

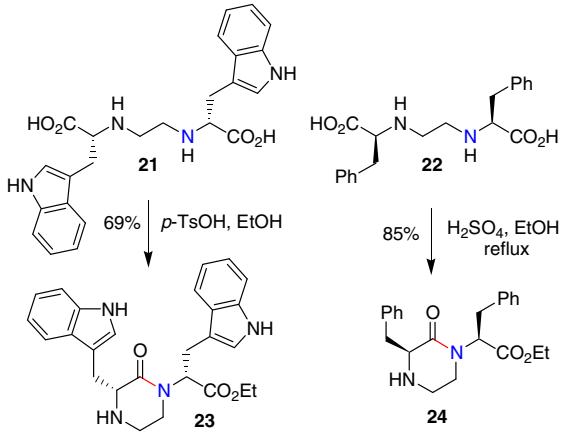

Scheme 2.

Further studies in this area, allowed Goodman et al.[50] to establish a convenient route to the piperazinone ring structure through the reductive amination of α-amino aldehyde **25** with glycine methyl ester followed by reaction of the released secondary amine **26** with *Z*-L-serine-β-lactone (Vederas lactone) **27** (Scheme 3).

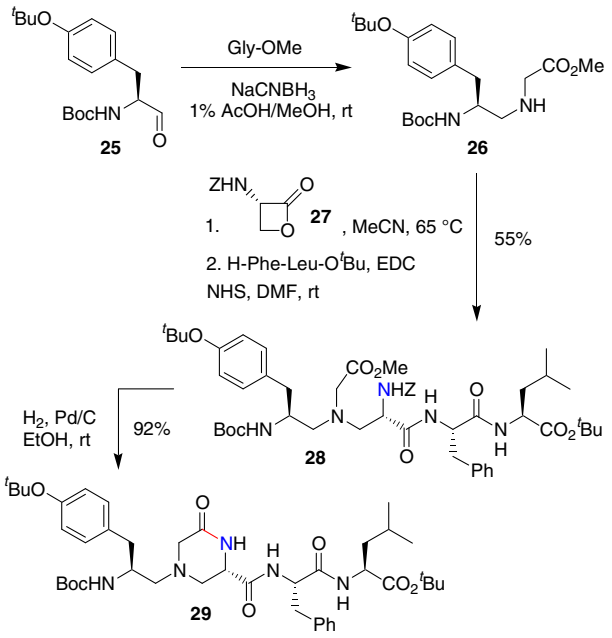

Scheme 3.

Subsequent coupling with H-Phe-Leu-O^{t}Bu by standard peptide chemistry produced the linear precursor **28** which underwent concomitant hydrogenolysis of the *Z* group and cyclization to give the 4,6-disubstituted piperazin-2-one derivative **29**. This was eventually converted to an enkephalin analogue by TFA-mediated removal of the remaining protecting groups.

Later, the same authors reported the solid-phase synthesis of a series of piperazinone-derived Leu-enkephalin analogues,[51] the key step being represented by the reaction of Wang resin-bound *N*-(4-*tert*-butyloxy-phenethyl)-glycine **30** with Boc-L-serine-β-lactone **31** (Scheme 4). The released carboxylic acid was reacted with diverse monosubstituted benzylamine derivatives in the presence of a BOP reagent to produce resin-bound tertiary amides **32**. Subsequent treatment with 5% H_2O in TFA-promoted sequential cleavage, deprotection, and cyclization to yield 4,6-disubstituted piperazin-2-ones **33**.

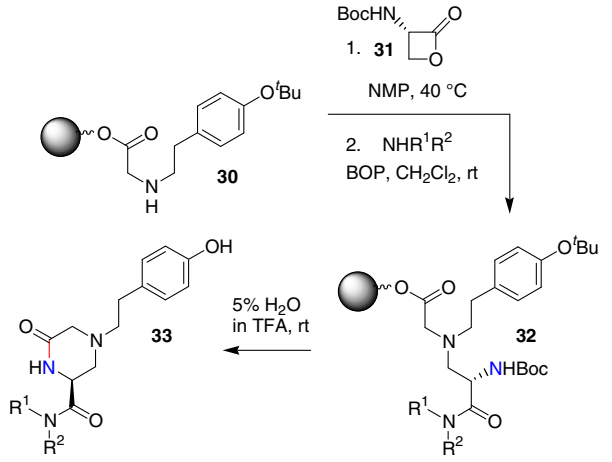

Scheme 4.

Notably, the same synthetic sequence has been successfully applied to obtain the enantiomeric 2-oxopiperazines using Boc-D-serine-β-lactone as the counterpart of **30**.

Hansen et al.[49] reported the synthesis of a constrained mimic of the C-terminal D-phenylalanine group of NN703, namely (3*R*)-3-benzyl-2-piperazinone **37**. Thus, Boc-glycinal **34** was converted via reductive alkylation with D-phenylalanine methyl ester into secondary amine **35** (Scheme 5). Deprotection with TFA followed by cyclization of the intermediate amine **36** with potassium carbonate in methanol at room temperature produced the 3-substituted piperazin-2-one **37**.

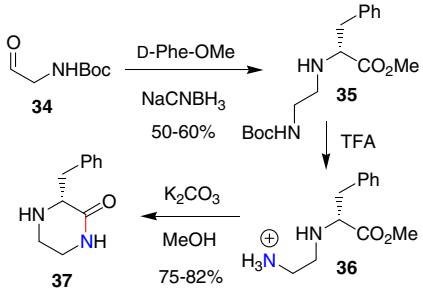

Scheme 5.

2-Oxopiperazine derivatives have been often designed as mimics of β- and γ-turn conformationally constrained peptides.

In order to obtain 2-oxopiperazines as new γ-turn mimics,[52,53] epimeric mixtures of cyanomethyleneamino pseudopeptides **38** were reacted with amino acid derivatives to give the C-backbone branched pseudopeptides **39** (Scheme 6). Notably, neither racemization at the inserted amino acid nor epimerization at the stereogenic centers of **38** were observed during this step. Heating of **39** at 100 °C in toluene afforded diastereomeric 1,3,5-trisubstituted 2-oxopiperazines **40**, which were eventually resolved by flash chromatography.

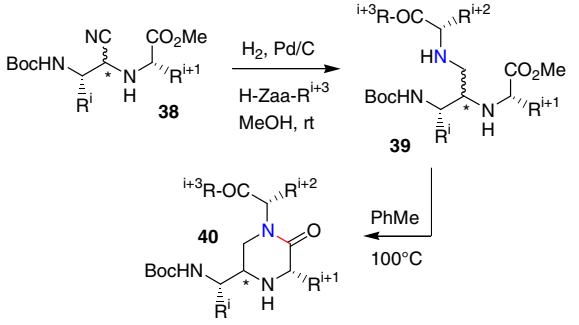

Scheme 6.

Recently, Piarulli et al.[54] have developed an easy entry to both enantiomers of *N*-Boc-5-oxo-piperazine-2-carboxylic acid (PCA), in order to evaluate their role as inducers of turn structures when inserted into tetrapeptide sequences. Thus, the primary alcohol **41** obtained by reductive amination of L-serine methyl ester with ethyl glyoxylate underwent Mitsunobu reaction using a solution of hydrazoic acid in toluene to give azide **42** (Scheme 7). Other methodologies are unsuitable, causing the elimination and formation of the corresponding dehydroalanine derivative as the major reaction product. Catalytic hydrogenation of **42** and concurrent cyclization of the resulting primary amine produced (*S*)-methyl 5-oxo-piperazine-2-carboxylate **43**, which was converted into (*S*)-*N*-Boc-5-oxo-piperazine-2-carboxylic acid **44** by one-pot hydrolysis and *N*-Boc protection. The (*R*)-enantiomer was similarly obtained using D-serine methyl ester as the starting material.

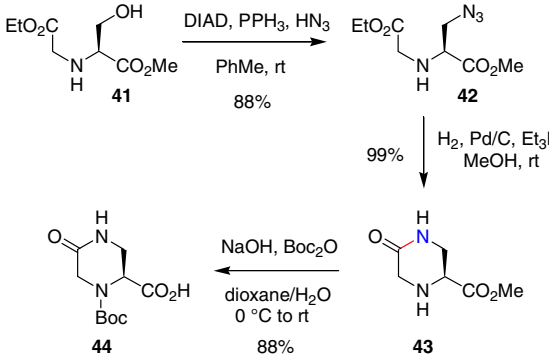

Scheme 7.

Ketopiperazines represent valuable platforms for the development of new synthetic methodologies entailing the N_1–C_2 bond-forming reaction.

Giannis et al.[55] reported the use of *N*-*Z*-D-glucosamine **45** as the common starting material for the synthesis of diastereomeric 3,6-disubstituted piperazin-2-ones **49** and **53** (Scheme 8).

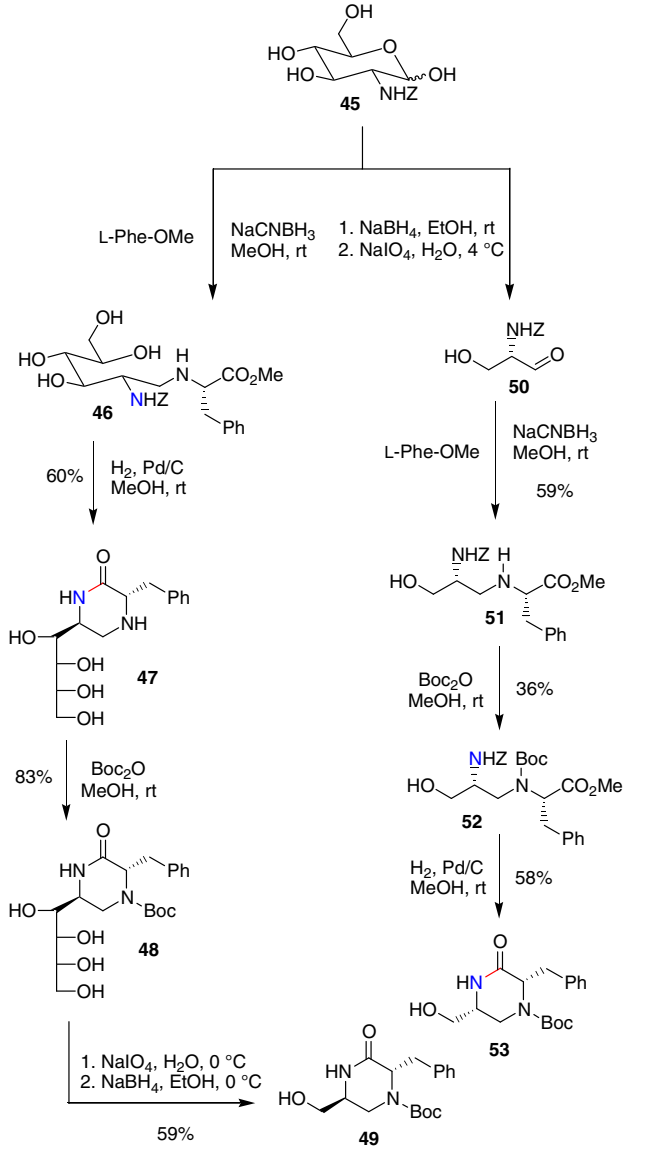

Scheme 8.

Thus, the reductive amination of **45** with L-phenylalanine methyl ester gave the intermediate **46**, which was cyclized to **47** by hydrogenolytic removal of the *Z*-protecting group. Subsequent *N*-Boc protection, oxidative cleavage of the polyol moiety of intermediate **48** and rapid reduction of the corresponding aldehyde yielded the piperazinone derivative **49** without detectable racemization.

The synthesis of diastereomeric piperazinone **53** required the conversion of *N*-*Z*-D-glucosamine **45** into *N*-*Z*-L-serinal **50**, followed by reductive amination with L-phenylalanine methyl ester to yield diamine **51**. Protection of the secondary amino group as the corresponding *tert*-butoxycarbonyl derivative produced compound **52** which took part in the catalytic hydrogenation leading to the concomitant removal of the *Z*-protecting group and spontaneous cyclization.

Later, the same authors used *N*-*Z*-D-glucosamine **45** as the starting point for the synthesis of either 6-substituted piperazin-2-one **56** or 3,6-disubstituted piperazin-2-ones **60** and **61** (Scheme 9).[56]

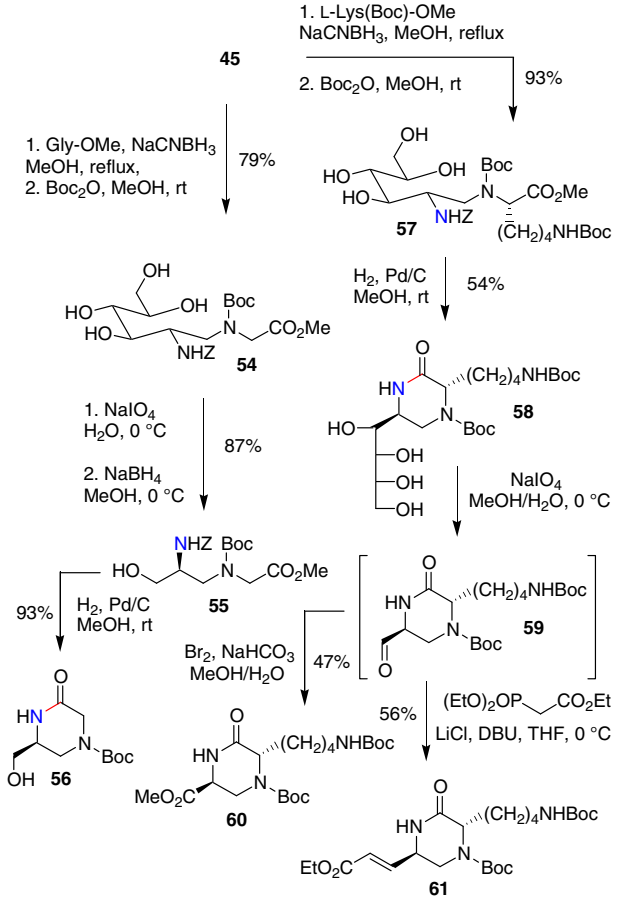

Scheme 9.

Thus, the secondary amine **54** was prepared by the reductive amination of **45** with glycine methyl ester and subsequent derivatization, with the introduction of the *tert*-butoxycarbonyl-protecting group being crucial for the final cyclization step. An oxidative cleavage/reduction sequence performed on **54** yielded the amino alcohol **55**, which underwent the well-established deprotection/cyclization protocol leading to **56**.

Analogously, the secondary amine **57**, generated by the amination of **45** with L-ε-Boc-lysine methyl ester followed by Boc protection, was cyclized to compound **58** after the removal of the *Z* group. Oxidative cleavage of the polyol side chain produced the aldehyde **59**, which was used directly to obtain methyl ester **60** and the vinylogous derivative **61**.

A highly efficient triflate alkylation has been used by Jacobsen[57,58] as the key step in the synthesis of enantiomeric *trans*-3,5-dimethylpiperazin-2-ones, which represent suitable precursors of *trans*-2,6-dimethylpiperazines.

As outlined in Scheme 10, the dibenzylamide **62**, obtained from Boc-L-alanine, was subjected to TFA-promoted deprotection and borane–methyl sulfide reduction to give the diamine **63** in high ee (>98%).[57] Its reaction with methyl (*R*)-2-[(trifluoromethylsulfonyl)oxy]propionate proceeded uneventfully with inversion of configuration to produce a 94% yield of the ester **64**. Hydrogenolytic monodebenzylation and subsequent acid-catalyzed cyclization provided 3,5-disubstituted piperazin-2-one **65** in 81% yield.

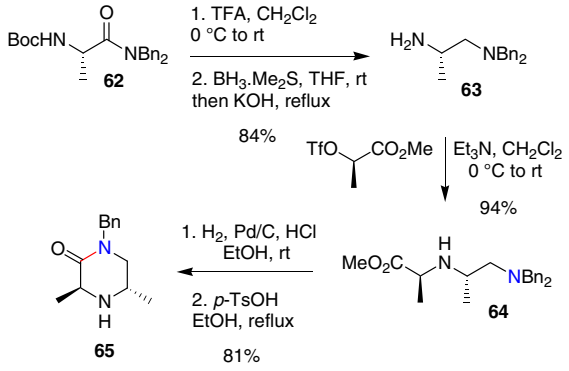

Scheme 10.

The corresponding enantiomer has been similarly obtained using Boc-D-alanine and methyl (*S*)-2-[(trifluoromethylsulfonyl)-oxy]propionate.[58]

This chemistry has also been applied to the enantioselective synthesis of (*R*)-3,5,5-trimethylpiperazin-2-one **69**.[57] The starting point was the diamine **67** in turn obtained by tritylation of 1,2-diamino-2-methylpropane **66**. Reaction of **67** with methyl (*S*)-2-[(trifluoromethylsulfonyl)oxy]propionate produced the intermediate **68** which was converted by a one-pot deprotection/cyclization sequence to the piperazinone **69** (Scheme 11).

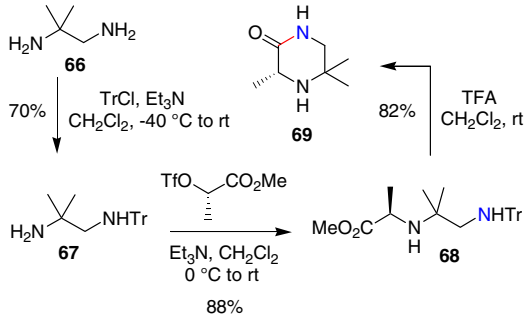

Scheme 11.

Similarly, the corresponding enantiomer was prepared using methyl (*R*)-2-[(trifluoromethanesulfonyl)oxy]propionate as the alkylating agent.

A three-component process involving the one-step condensation of alkenyl, aryl, or heteroaryl boronic acids with 1,2-diamines and glyoxylic acid has been introduced for the direct synthesis of piperazinones.[43] The organoboronic acids act as both reactants and catalysts in the cyclization of the intermediate amino acid adducts.

The effectiveness of this approach has been illustrated by the reaction between secondary 1,2-diamine **70**, heteroaryl boronic acid **71**, and glyoxylic acid in acetonitrile at 80 °C leading to 2-piperazinone **72** in 65% yield and 40% de (Scheme 12).

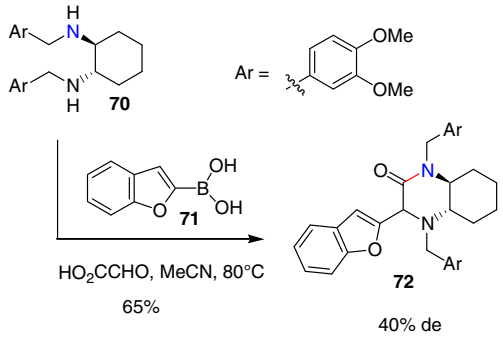

Scheme 12.

Unfortunately, the stereochemistry of the major isomer of **72** could not be determined since the authors did not provide any data.

Figueroa-Peréz et al.[59] described the solid-phase synthesis of 3,6-disubstituted 2-oxopiperazines featuring three rapid and efficient steps, namely: (1) reductive alkylation of a resin-bound α-amino acid with a freshly prepared *N*-protected-α-amino aldehyde; (2) N-deprotection; and (3) cyclitive cleavage of the acyclic resin-bound amine precursor to give the target compounds.

As outlined in Scheme 13, Fmoc-L-phenylalaninal **73**, easily obtained by oxidation of the corresponding commercially available Fmoc-L-phenylalaninol with a polymer-bound diacetoxybromite, was mixed with a suspension of the Wang resin-bound *O*-^{t}Bu-tyrosine **74** in trimethylorthoformiate (TMOF) and the resulting imine reduced in situ by adding an excess of $Na(AcO)_3BH$ to yield the intermediate amine **75**. N-Deprotection and subsequent cyclization gave the piperazin-2-one derivative **76** with very high purity (96%).

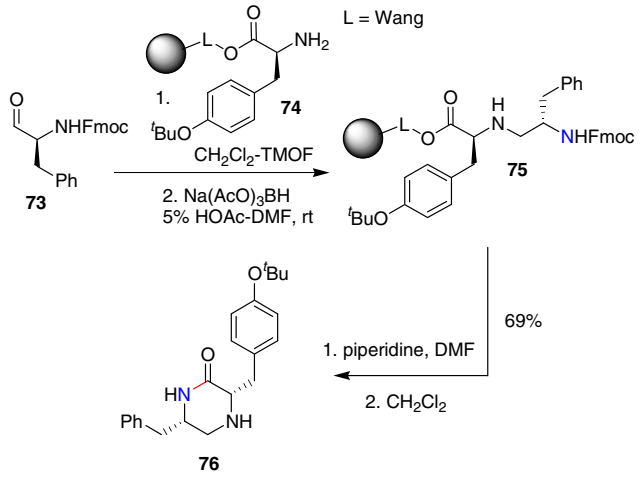

Scheme 13.

Similar results were obtained using Merrifield resin-bound *O*-^{t}Bu-tyrosine and Boc-L-phenylalaninal as convenient starting materials.

Dinsmore et al.[60] discovered a novel approach to the synthesis of piperazin-2-one derivatives entailing on a one-pot, tandem reductive amination–transamidation–cyclization reaction (Scheme 14).

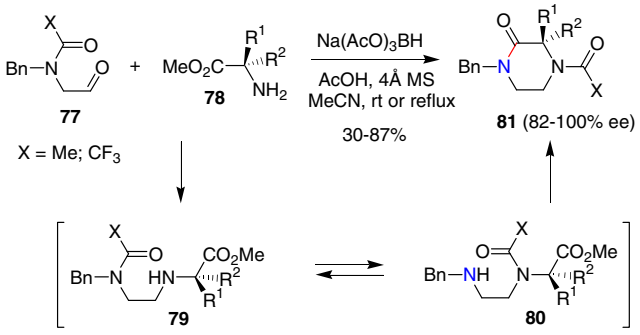

Scheme 14.

Thus, the reductive amination of an *N*-(2-oxoethylamide) **77** with α-amino esters **78** produced the secondary amines **79** which are prone to give amides **80** by an intramolecular *N*,*N*′-acyl transfer. Their subsequent intramolecular cyclization led to piperazin-2-ones **81**.

The wide availability of natural and unnatural α-amino acids makes this approach very effective for the synthesis of 2-oxopiperazine derivatives bearing variable substituents at C-3.

This methodology has been successfully applied to the synthesis of the conformationally restricted FTase inhibitor **86**,[60] as shown in Scheme 15.

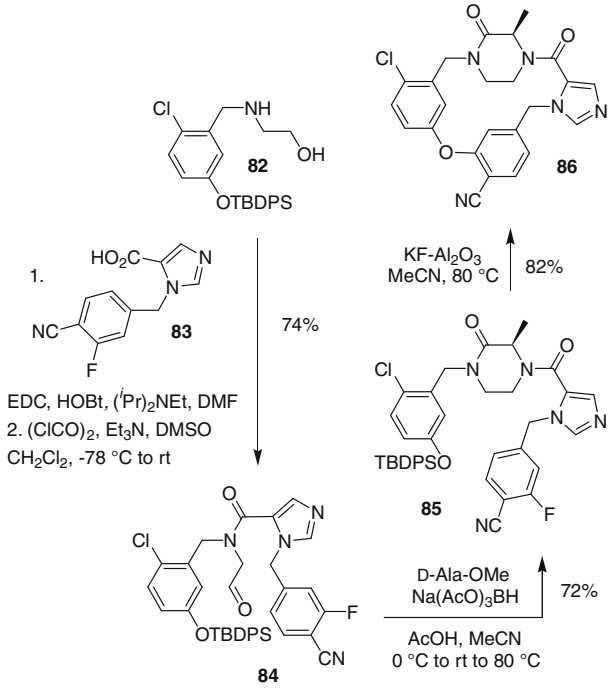

Scheme 15.

The amino alcohol **82**, readily prepared from 4-chloro-3-methylphenol by standard chemistry, was transformed into the key aldehyde **84** by reaction with the acid **83** and Swern oxidation of the primary alcohol moiety. Subsequent reductive amination with D-alanine methyl ester gave piperazin-2-one **85**, which underwent tandem deprotection-macrocyclization in the presence of KF on alumina in refluxing acetonitrile, provided the target FTase inhibitor **86**.

The 3-substituted piperazin-2-one **89**[27] has been conveniently prepared by starting from compound **87** obtained in rather low yield (33%) by the alkylation of L-isoleucine *tert*-butyl ester with *N*-(*tert*-butoxycarbonyl)-2-chloroethylamine. The TFA-promoted deprotection furnished the linear precursor **88**, which was cyclized to the δ-lactam **89** by treatment with DCC and pyridine (Scheme 16).

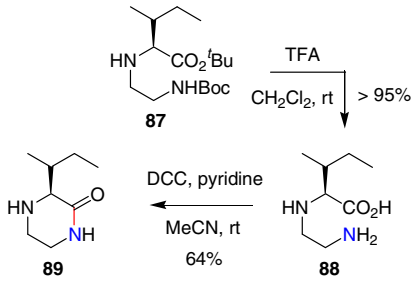

Scheme 16.

Although this approach could be extended using different N-protection, the presence of electron-withdrawing groups (e.g., *p*-toluenesulfonyl) on the primary amine of the cyclization precursor severely hampers lactam formation in sufficiently high yield.

The reactivity of α-amino esters toward 1,2-cyclic sulfamidates has been successfully used to open a flexible entry to piperazin-2-one derivatives bearing substituents at various positions (Scheme 17).[61] Thus, the use of the L-phenylalanine-derived 1,2-sulfamidate **90** as a prototype in the reaction with *N*-tosyl glycine ethyl ester gave a 84% yield of the differently protected 6-substituted piperazin-2-one **92** via the intermediate **91**.

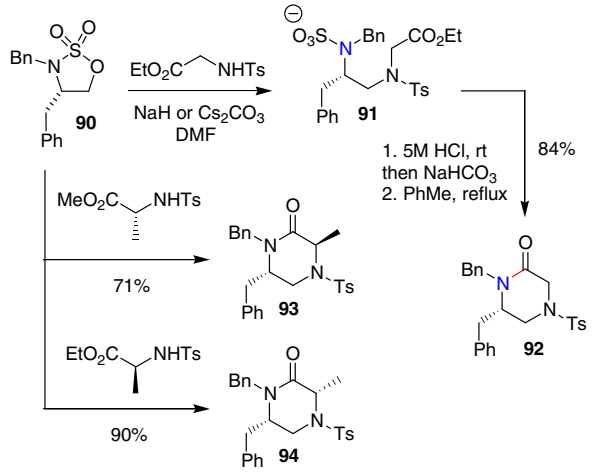

Scheme 17.

The reaction of **90** with *N*-tosyl-α-amino esters derived from D- and L-alanine, respectively, exclusively gave the corresponding *trans*- and *cis*-3,6-disubstituted piperazin-2-ones **93** and **94**, thus demonstrating the stability of epimerizable substrates in the conditions used in this approach.

However, some problems were encountered in the reaction of **90** with L-proline ethyl ester, as shown in Scheme 18.

Thus, the initial adduct **95** underwent slow and very inefficient thermal lactamization in refluxing xylene producing **96** without epimerization at C(8a), while a fast and essentially quantitative lactamization was achieved using NaOMe in MeOH giving rise to **96** as a 1:1 mixture of diastereomers at C(8a). However, the latter could be obtained as a single diastereomer in 50% yield performing the final ring-closure step in the presence of catalytic sodium cyanide.

Analogously, when ethyl L-pyroglutamate was employed as the counterpart of **90**, the bicyclic adduct **97** could be isolated as a single diastereomer in 63% overall yield.

Garner's aldehyde **98** has been utilized as the source of the C-6 stereogenic center for 6-substituted 2-oxopiperazines.[62]

The synthetic sequence involved the reductive amination with ethyl *N*-benzylglycine to give **99** followed by the one-pot removal

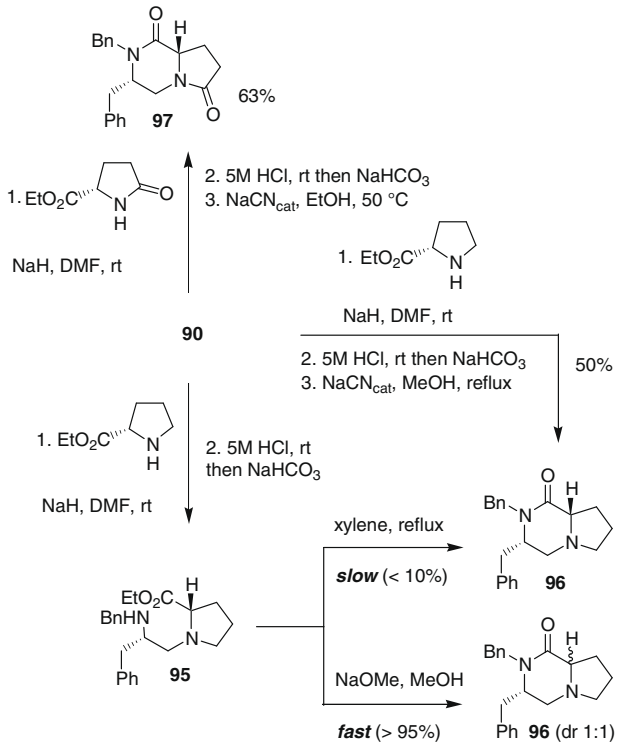

Scheme 18.

of the *N*-Boc-protecting group and cyclization by treatment with hydrochloric acid in refluxing methanol furnishing the chiral 2-oxopiperazine **100** in an excellent yield. The latter could be converted into chiral 1-aryl-6-hydroxymethyl-2-oxopiperazine **101** (Scheme 19).

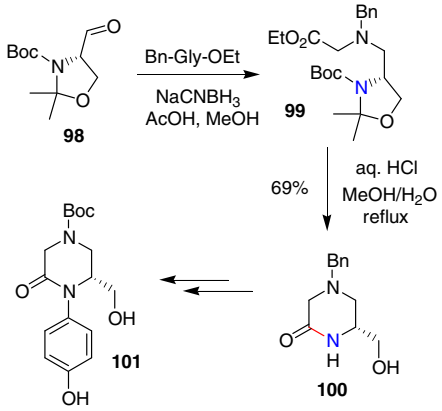

Scheme 19.

A simple entry to 3-substituted piperazin-2-one **103**[63] was based on the use of optically active nitroester **102**, easily obtained through an intermolecular Michael reaction between *N*-benzyl-L-aspartic acid dimethyl ester and nitroethylene (Scheme 20). Catalytic reduction of the nitro group and intramolecular cyclization of the intermediate primary amine provided 2-oxopiperazine **103**.

An appropriate choice of the starting α-amino ester allowed the preparation of chiral non-racemic piperazin-2-ones bearing variable substituents at the 3-position of the heterocyclic nucleus.

Furthermore, this chemistry is also suitable for the synthesis of heterocyclic scaffolds bearing amino- and hydroxy-substituted side chains at the 4-nitrogen atom.

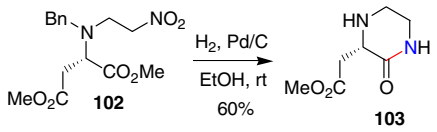

Scheme 20.

Orthogonally protected enantiomerically pure 2-oxopiperazine building blocks for peptidomimetic combinatorial chemistry have been prepared starting from accessible chiral α-amino aldehydes bearing α-Boc and ω-Alloc or *Z* orthogonal protecting groups.[64,65] A representative application of this approach is depicted in Scheme 21.

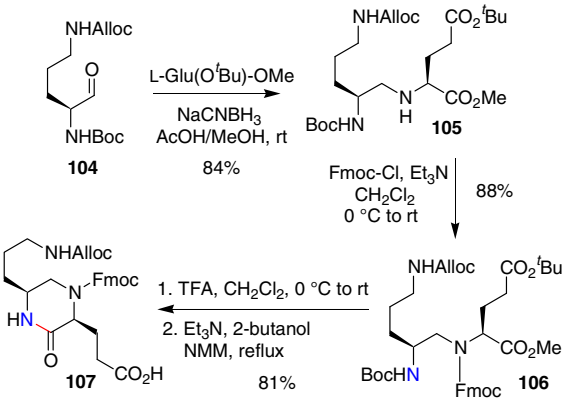

Scheme 21.

Sequential reductive alkylation of the α-amino aldehyde **104** derived from L-ornithine with L-Glu(O^{t}Bu)-OMe and Fmoc protection of the resulting dipeptide **105** furnished the linear precursor **106**, which was deprotected and cyclized to the corresponding 3,6-disubstituted 2-oxopiperazine derivative **107** by standard chemistry.

Interestingly, the chemistry involved is general and applicable for the preparation of a diverse library of scaffolds, controlling chirality, arm position and length as well as the nature of functional moieties at the arms for further diversification in three independent directions.

A recent paper described a convenient way to assemble 3-substituted-6-phenylpiperazin-2-ones via a two-step procedure involving an initial alkylation of 2-bromoacetophenone with an α-amino ester followed by a one-pot reductive amination and cyclization step.[66]

As shown in Scheme 22, the β-ketoamine **108** obtained by the reaction of L-alanine methyl ester with 2-bromoacetophenone underwent reductive amination with benzylamine and cyclization to produce piperazinone **109** as a 1:1 mixture of diastereomers, with no epimerization at C-3 being observed.

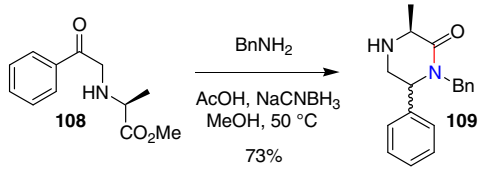

Scheme 22.

An N_1–C_2 bond-forming reaction between an amino group and an amide moiety was the featuring step in the solid-phase synthesis of ketopiperazines bearing up to four points of diversity.[67] The starting point was the sulfonamide resin **110** possessing a 2,4-dimethoxybenzyl arylhydrazine (DMBAH) linker.

As illustrated in Scheme 23 for a selected example, alkylation of **110** with *N*-Dde L-phenylalaninol **111** under Mitsunobu conditions gave **112** which was subsequently N-deprotected to produce the resin-bound secondary amine **113**. Acylation with 2-naphthoyl chloride and hydrazine-promoted N-deprotection yielded amino derivative **114** which took part in a cyclitive cleavage furnishing 3,4,6-trisubstituted 2-oxopiperazine **115** by sequential treatment with TFA and copper(II)/pyridine.

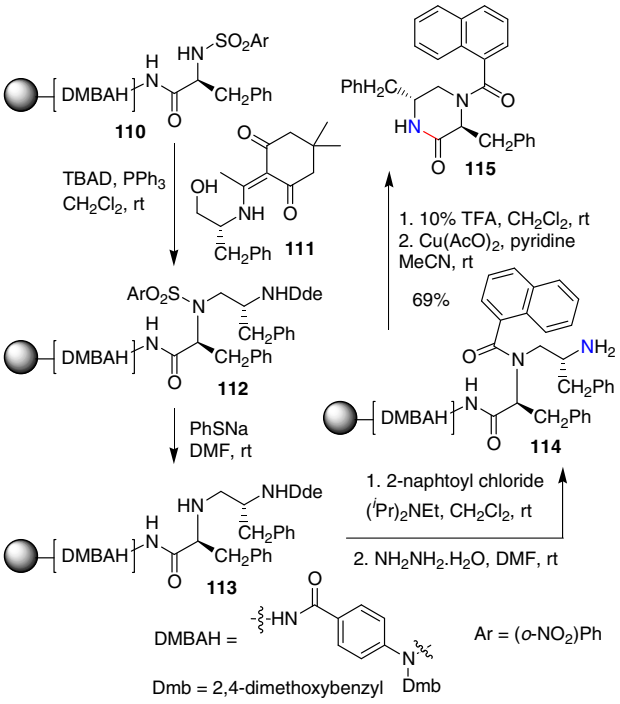

Scheme 23.

3. Cyclization at C_3–N_4

As already noted, the cyclization of a linear peptide dimer deriving from two different amino acids produces a mixture of 2-oxopiperazines, requiring a further separation step.[46,47] Thus, the development of convenient and easy methods for generating such compounds from two different amino acids represents a major aim with regard to the synthesis of chiral piperazinones.

A convenient method for generating piperazinones from two different amino acids involved the reductive alkylation of Boc-glycinal **34** with peptide **116** followed by acylation with chloroacetic anhydride to produce the intermediate acylated derivative **117** (Scheme 24).[49] After removal of the Boc-protecting group with TFA, cyclization of the derived **118** occurred smoothly simply by adjusting the pH to neutral, yielding the 1-substituted piperazin-2-one **119**, which could be then elongated by ordinary peptide couplings to give a NN703 analogue.

A simple piperazinone could be considered as a versatile and useful synthon for the enantioselective synthesis of more substituted piperazinones through diastereoselective alkylation.

A general synthetic pathway involving piperazinone assembly via C_3–N_4 cyclization followed by a stereoselective alkylation step has been widely used for the preparation of chiral disubstituted 2-oxopiperazines incorporating a large diversity of substituents at the 3-position.

The asymmetric synthesis of 1,3-disubstituted 2-oxopiperazines has been achieved by the stereoselective alkylation of a suit-

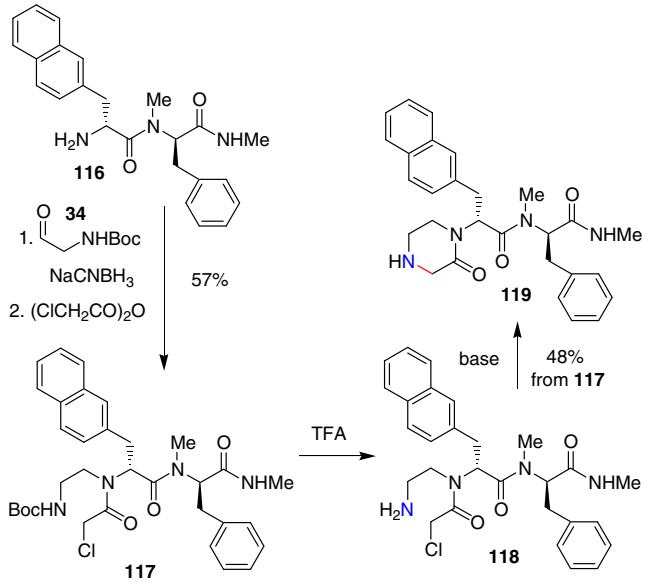

Scheme 24.

able 2-oxopiperazine using a non-racemic α-substituted β-amino alcohol as a chiral inductor, in turn assembled from L-phenylglycinol,[68,69] L-leucine methyl ester,[70] or *O*-benzyl-L-serine methyl ester,[71] whose nitrogen atom is part of the heterocyclic nucleus.

As shown in Scheme 25, the DCC-promoted condensation of L-phenylglycinol **120** and L-leucine methyl ester with Boc glycine gave amides **121** and **122**,[68–70] which were submitted to a reduction/protection sequence leading to silyl ethers **123** and **124**.

Selective condensation with bromoacetic acid furnished the intermediate bromomethylacylated derivatives **125** and **126**, which were subsequently cyclized to the piperazinones **127** and **128** on treatment with NaH in a DMF/THF mixture.

Both these compounds were deprotected to produce **129** and **130**, convenient substrates for the stereoselective alkylation at C-3 with various electrophiles.

Thus, the enolates generated by treatment with *tert*-BuLi (2.0 equiv) in THF at −78 °C in the presence of HMPA reacted with halogeno compounds to provide derivatives **131** and **132** with very high chiral induction (>90% de).

The observed diastereoselectivity has been accounted for by the rigid intermediate that forces the approach of the electrophile from the face opposite to a lithium chelate involving N_1 and the alcohol appended to the 1′-substituent.[70,72]

However, only one diastereomer is directly accessible since the configuration at the 3-position of the 2-oxopiperazine is totally governed by the configuration of the chiral inductor.

This limitation has been overcome by using orthogonally protected serinol-based 2-oxopiperazines **136** and **137**[71] (Scheme 26).

The synthetic pathway required the conversion of the *O*-benzyl-L-serine methyl ester to compound **133**, which was transformed into **134** by a number of steps including: (a) concomitant amide and ester lithium aluminum hydride reduction; (b) silyl etherification; and (c) coupling with bromoacetic acid. Subsequent base-induced cyclization of intermediate **134** furnished piperazinone **135**. Its selective O-deprotection could give rise to compounds **136** and **137**, which underwent C-3 alkylation with halide derivatives to yield (3*S*)- or (3*R*)-1,3-disubstituted 2-oxopiperazines **138** and **139**, respectively, in high diastereomeric purity (>95% de).

Unfortunately, the chiral auxiliary cannot be removed, and this represents a major drawback of this interesting methodology.

Highly stereoselective approaches based on synthetic elaboration of amino acids have been used to obtain enantiomerically enriched 5-substituted 2-oxopiperazines, which are further functionalized at C-3.[24,73]

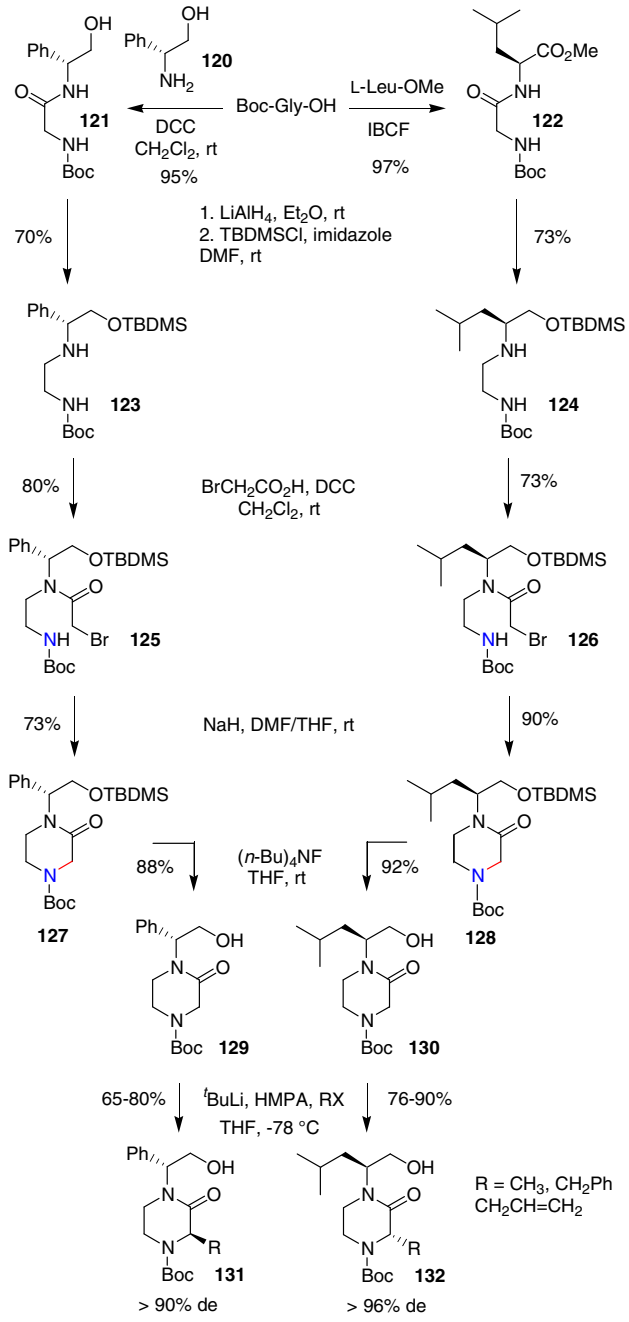

Scheme 25.

Key intermediates in these processes were vicinal diamines, a class of compounds commonly encountered as synthons, easily prepared by the reductive amination of enantiomerically pure α-amino aldehydes with suitable amines.

Thus, α-amino aldehyde **140** derived from Boc-(*S*)-allylglycine was used in a reductive amination with 2,4-dimethoxybenzylamine to produce **141**.[24] Its chloroacetylation produced **142** which provided the 5-allyl 2-oxopiperazine **143** through base-promoted cyclization, as shown in Scheme 27. Subsequent alkylation at the 3-position with benzyl bromide provided the *trans*-disubstituted derivative **144** (diastereoselectivity ⩾ 95:5). This compound is a convenient precursor of the constrained bicyclic analogue **145** featuring a 3,8-diazabicyclo[3.2.1]octan-2-one framework.

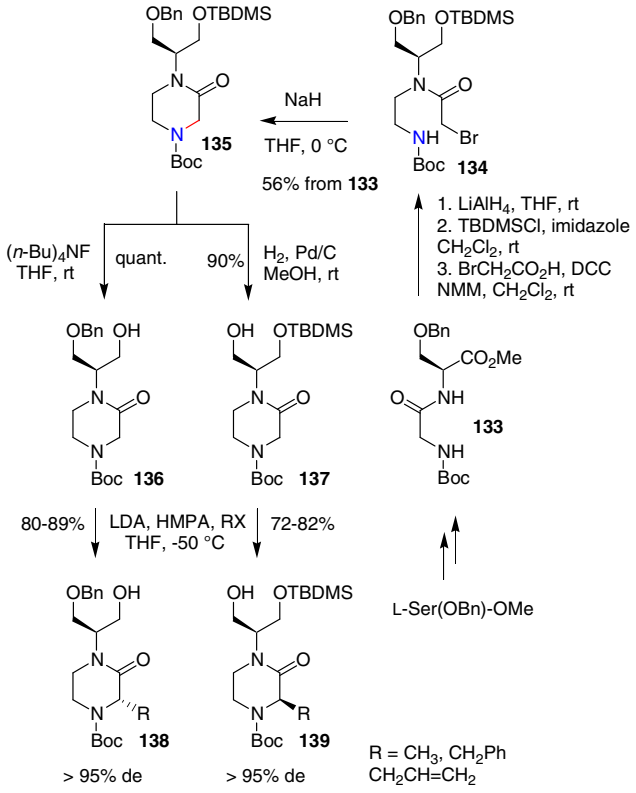

Scheme 26.

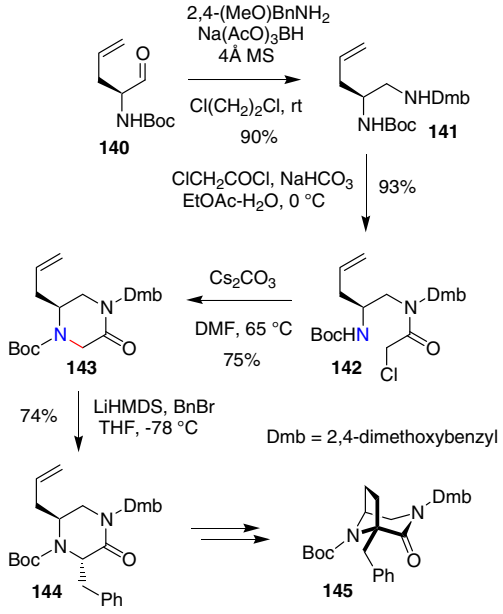

Scheme 27.

A similar approach based on the use of α-amino aldehydes derived from Boc protected naturally occurring amino acids[73] is shown in Scheme 28.

Thus, reductive amination of Boc-L-alaninal **146** with benzylamine produced diamine **147**, which was reacted with bromoacetic acid to give the intermediate amide **148**. The latter was used to obtain 5-methyl 2-oxopiperazine **149** by base-promoted cyclization.

Treatment of the derived enolate [*tert*-BuLi (2 equiv)/HMPA (4 equiv) mixture in THF at −78 °C] with allylbromide quantitatively

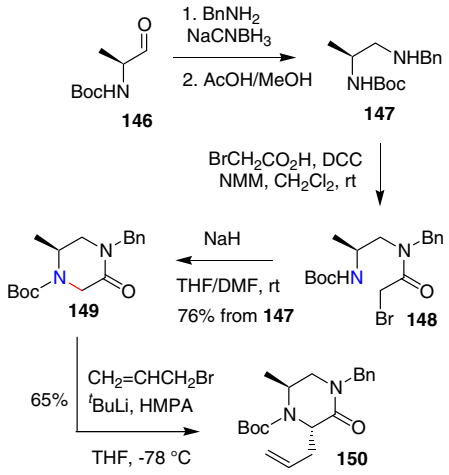

Scheme 28.

afforded the 3-allylated 2-oxopiperazine **150**. Remarkably, only one diastereoisomer could be found in the final reaction mixture. The relative *anti* stereochemistry between substituents at C-3 and C-5 was deduced by NOE difference experiments, accounting for a conventional 1,3-asymmetric induction.[74]

This approach allowed differently decorated 3-substituted 5-methyl-2-oxopiperazines to be obtained by using suitable electrophiles, a double functionalization at the 3-position also being accomplished.

The reductive alkylation of amino aldehydes derived for natural amino acids with appropriate amine counterparts has been widely used as a convenient tool for the assembly of chiral 2-oxopiperazine precursors.[75,65]

The solid-phase preparation of 1,4,5-substituted 2-oxopiperazines has been achieved via on-bead intramolecular cyclization of suitable precursors obtained by a reductive alkylation of resin-bound amino acids with N-protected α-amino aldehydes,[75] followed by acylation with α-chloroacetyl chloride.

The synthesis of 2-oxopiperazine **161** serves as an illustrative example of this synthetic route (Scheme 29).

The Wang resin-immobilized Fmoc-L-leucine **151** was deprotected to amine **152** which in turn was treated with Fmoc-L-phenylalaninal **73**. The resulting imine could be removed from the excess aldehyde by filtration. The subsequent reduction produced a 1:1 diastereomeric mixture of pseudodipeptides **153** and **154**, owing to epimerization of the α-amino aldehyde during the amination step. After acylation to **155** and **156**, Fmoc deprotection produced a mixture of primary amines **157** and **158**.

At this stage, on-bead intramolecular cyclization, treatment with *p*-toluenesulfonylchloride and TFA cleavage allowed piperazinone (2*S*,5′*R*)-**161** to be obtained as the sole product, while the corresponding (2*S*,5′*S*) diastereomer was not obtained.

This result has been explained as being due to the conversion of amine (2*S*,5′*S*)-**158** into cleaved piperazinone **160** through an intramolecular N-acylation process which is likely to proceed faster than on-bead S_N2 intramolecular cyclization. The detection of compound **160** in the filtrate (LC–MS analysis) corroborated this hypothesis.

The Fmoc/Alloc orthogonally protected 1,5-disubstituted 2-oxopiperazine **165** was prepared starting from the pseudodipeptide **162** simply obtained by reductive amination between glycine *tert*-butyl ester and α-amino aldehyde **104** derived from L-ornithine (Scheme 30).[65]

Treatment of **162** with α-bromoacetyl chloride gave the corresponding acylated derivative **163**, which underwent smooth cycli-

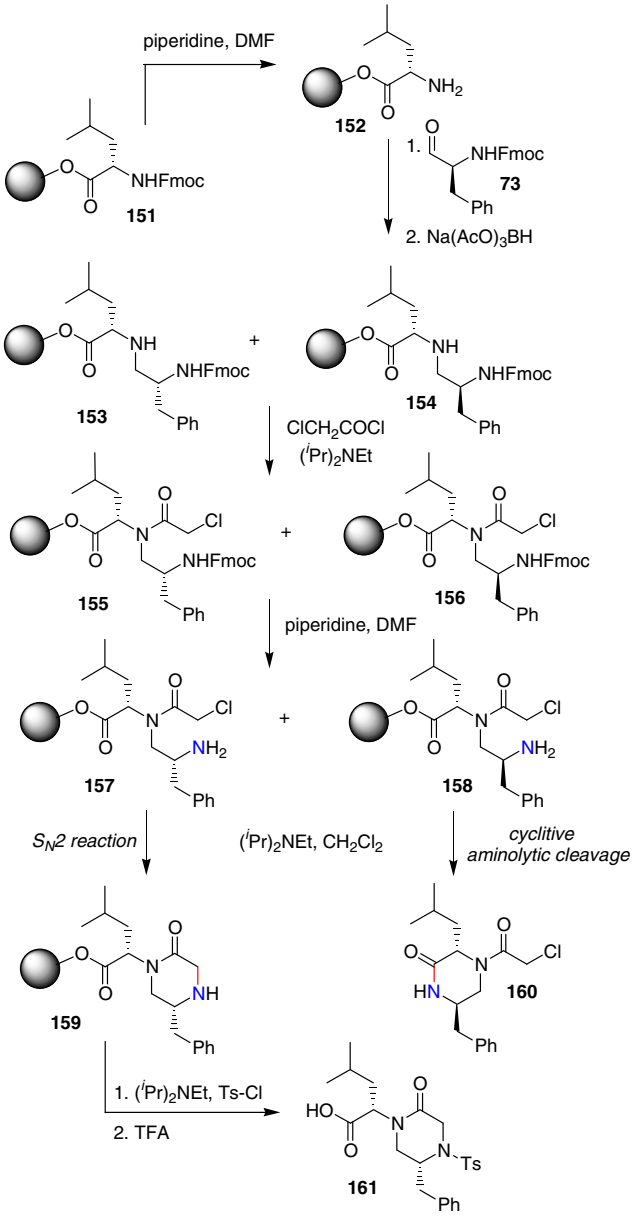

Scheme 29.

zation upon heating in the presence of Cs_2CO_3 in DMF to give the Boc/Alloc-protected ketopiperazine **164**, suitable for Boc chemistry.

This compound can be adapted to Fmoc chemistry (Fmoc on the secondary ring amine and Alloc on the side chain primary amine) through the interchange of Boc/Fmoc-protecting groups accomplished by standard Boc removal and subsequent Fmoc reprotection of the crude-derived amine to yield piperazinone **165**. Similar results have been obtained using L-lysinal as the starting amino acid.

An efficient route for the preparation of piperazinones featuring a C_3–N_4 ring-forming reaction involves a tandem reductive coupling and S_N2-cyclization of a 2-chloro-*N*-(2-oxoalkyl)acetamide and a primary amine.[76]

This approach has been adopted to achieve the asymmetric synthesis of (5*R*)-1-benzyl-5-methyl-2-oxopiperazine **168** starting from β-amidoketone **166** and (*R*)-α-methylbenzylamine as the chiral auxiliary (Scheme 31).

Thus, the tandem process proceeded smoothly to give a 6:1 diastereomeric mixture from which the major isomer **167** can be eas-

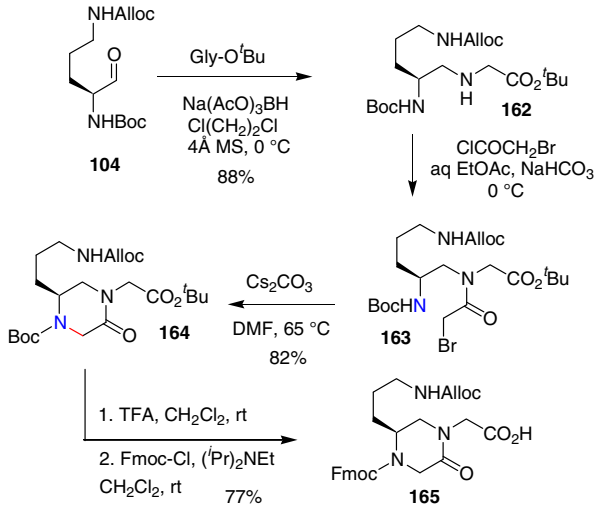

Scheme 30.

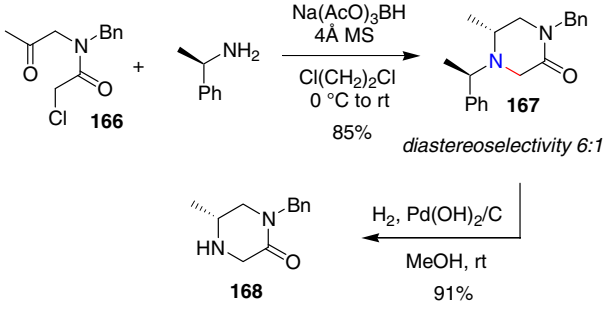

Scheme 31.

ily separated. Its hydrogenolysis allowed **168** to be obtained, with the stereochemical assignment being made by the analysis of Mosher's amide derivatives.

Interestingly, the use of an α-amino ester instead of a simple amine component in the reductive amination step led to the formation of a mixture of piperazinones, as shown in Scheme 32.

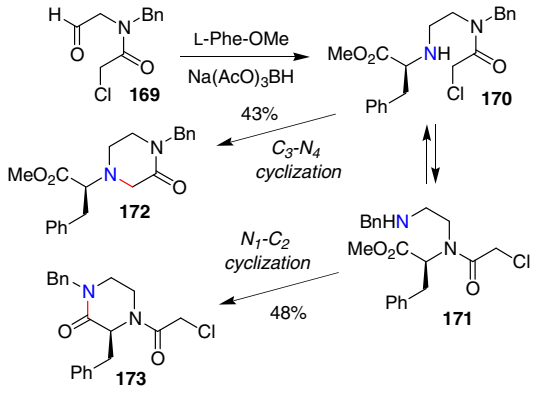

Scheme 32.

Accordingly, the reductive amination of **169** with L-phenylalanine methyl ester produced **170**, its cyclization leading to the formation of the same amounts of the expected product **172**, as well as of the piperazinone **173**.

The formation of the latter has been ascribed to an intramolecular *N*,*N*′-acyl transfer converting the intermediate **170** into **171**,

which gave rise to a concurrent N_1–C_2 cyclization occurring via N-acylation rather than N-alkylation.

Chiral sulfinimines, readily available in both enantiomeric forms, have proven to be valuable intermediates for the synthesis of different nitrogen-containing targets.[77]

Viso et al.[78–80] reported the asymmetric synthesis of enantiopure *N*-sulfinyl imidazolidines **176** via a diastereoselective 1,3-dipolar cycloaddition between readily available *p*-toluenesulfinimines **174** and glycine iminoester enolates **175** (Scheme 33).

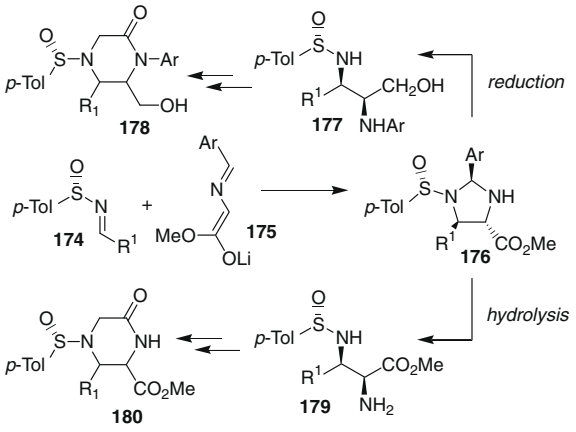

Scheme 33.

The enantiopure *p*-toluenesulfinimines displayed a moderate to high facial selectivity producing the corresponding *N*-sulfinyl imidazolidines in good to excellent diastereomeric excess. The chirality of sulfur has been transferred to three asymmetric centers in a single synthetic operation with almost complete stereocontrol.

Reductive[78–80] or hydrolytic cleavage[81] of the aminal moiety transformed *N*-sulfinyl imidazolidines **176** into differently protected vicinal diamino alcohols **177** and *N*-sulfinyl diamino esters **179**, respectively. These classes of compounds are potential substrates for the synthesis of enantiopure *N*-sulfinyl piperazinones **178** and **180**, respectively, bearing suitable arms for further functionalizations.

This synthetic pathway could give access to a wide range of *N*-sulfinyl-5,6-disubstituted 2-oxopiperazines[82,83] by varying the nature of the *p*-toluenesulfinimines and glycine iminoester enolates. A representative example is shown in Scheme 34.

Thus, substrate **186** has been obtained by a five-step sequence featuring cycloaddition between **181** and **182** to produce **183**, then taken to **184** by reduction[80] and silylation.[83] This compound was N-acylated to **185** and cyclized in basic media to produce **186**.[83]

It is noteworthy that the treatment of **186** with NaH in refluxing THF promoted a clean elimination of the sulfur moiety to give 5,6-dihydropyrazin-2(1*H*)-one **187**, useful intermediate for further functionalization of the heterocyclic nucleus through nucleophilic additions[83,84] and Staudinger reactions.[85]

Attempts to obtain *N*-sulfinyl ketopiperazines from *N*-sulfinyl diamino esters,[83] available via a selective imidazoline hydrolysis, failed in most cases, although the N-acylation step gave good yields. The authors speculated on the origin of these results, a plausible explanation was the acidity of the amide and the hydrogen bound to the carbon α- to the ester group.

The 2-oxopiperazine nucleus is widely found as a core fragment in a variety of natural and biologically important products, their synthesis representing a test bed for new methods for the construction of the piperazinone moiety.

The asymmetric total synthesis of guadinomine C_2, an inhibitor of type III secretion system (TTSS) of bacteria, has been successfully

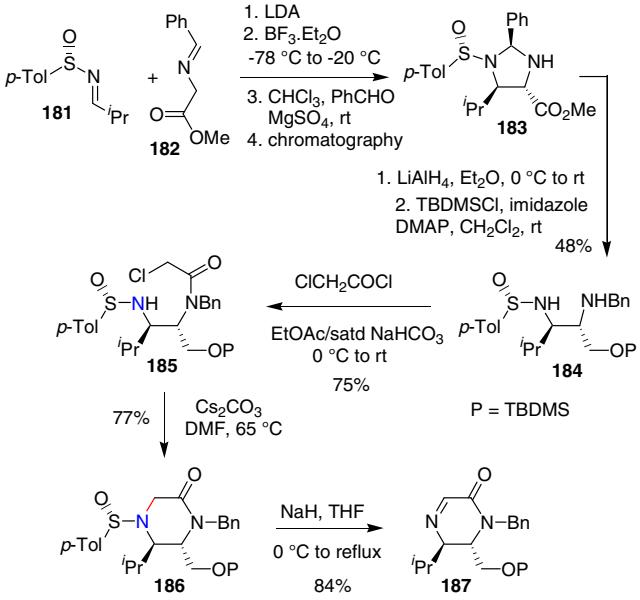

Scheme 34.

achieved through a novel concise entry to 3,5,6-trisubstituted piperazinone cores in enantiomerically pure forms.[22]

As shown in the selected example depicted in Scheme 35, the Evans aldol reaction of valeraldehyde with (*R*)-oxazolidinone **188**, followed by hydrolytic removal of the chiral auxiliary, produced the α-chloro-β-hydroxy acid **189** as a single enantiomer which was condensed with the known peptide section NH_2-L-Ala-L-Val-O^{t}Bu to give **190**.

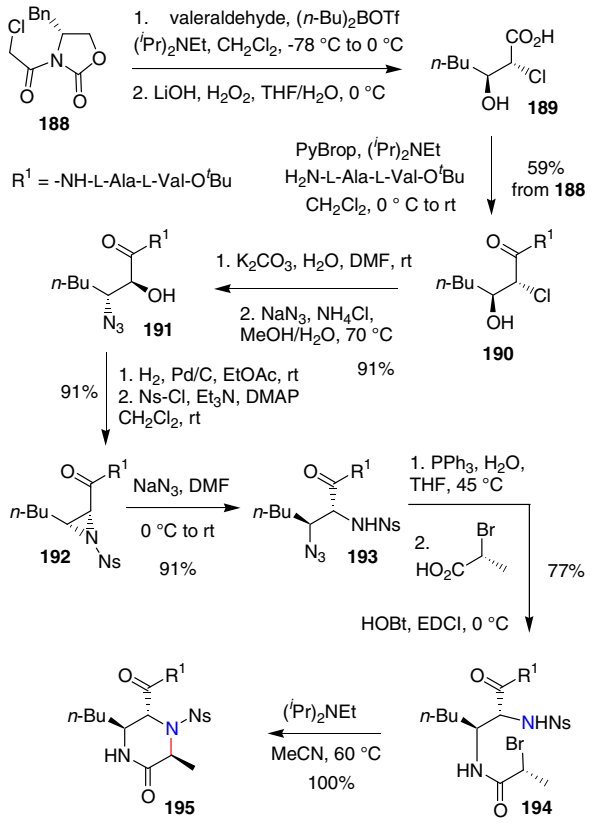

Scheme 35.

Subsequent epoxide formation under mild basic conditions and azidolysis produced intermediate **191**, which on reduction and aziridination gave rise to the Ns-aziridine **192**. Its regioselective azidolysis furnished the corresponding β-azide **193**. Staudinger amination and condensation of the released amine with (*R*)-2-bromopropionic acid yielded the intermediate derivative **194**, which took part in an intramolecular S_N2 cyclization leading to the formation of piperazinone **195**.

A similar reaction sequence has been used for the preparation of a structurally related (3*R*,5*R*,6*R*)-5,6-*cis*-3,6-*syn*-diastereomer.

The piperazinone core of (*R*)-(−)-praziquantel **16**, a powerful anti-worm drug, has been assembled through a six-step sequence starting with the easily available *N*-phthaloylglycine chloride **196** and phenethylamine to give imine **197** (Scheme 36).[45]

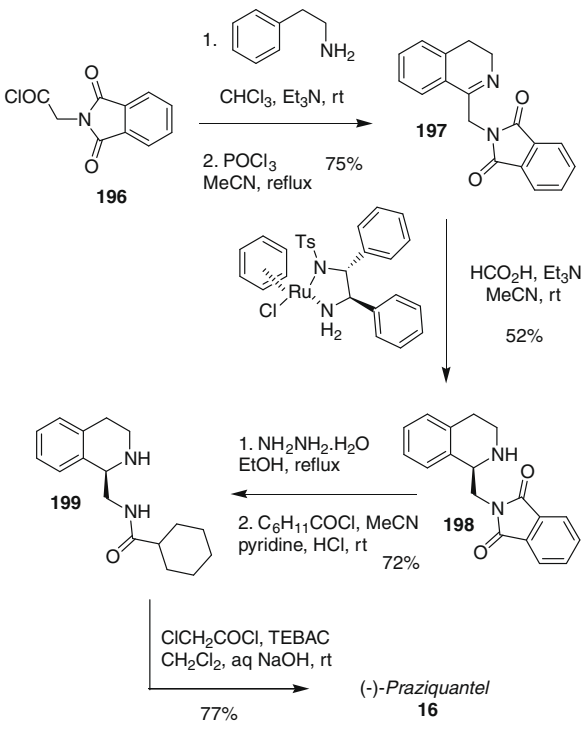

Scheme 36.

The asymmetric transfer hydrogenation of **197**, in the presence of a ruthenium catalyst, gave rise to the formation of **198**. Deprotection and amidation of the derived primary amine furnished compound **199**. Its reaction with α-chloroacetyl chloride under Schotten–Baumann conditions completed the synthesis of **16**.

4. Cyclization at N_4–C_5

The synthetic approaches to 2-oxopiperazine ring systems featuring N_4–C_5 bond formation have been organized in sub-sections according to the different strategies by which the C–N bond has been formed.

4.1. Reductive amination

DiMaio and Belleau[86] described the enantiospecific synthesis of two interesting piperazinone synthons, (3*S*,6*R*)-6-ethoxycarbonyl-3-(*p*-hydroxybenzyl)piperazin-2-one **203** and (3*S*)-1-(ethoxycarbonylmethyl)-3-(*p*-hydroxybenzyl)piperazin-2-one hydrochloride **207**, used as peptidomimetics for the first and second residue of Leu-enkephalin.

Synthon **203** was prepared as described in Scheme 37. Coupling between *Z*-L-tyrosine and ethyl 2-amino-3,3-diethoxypropionate

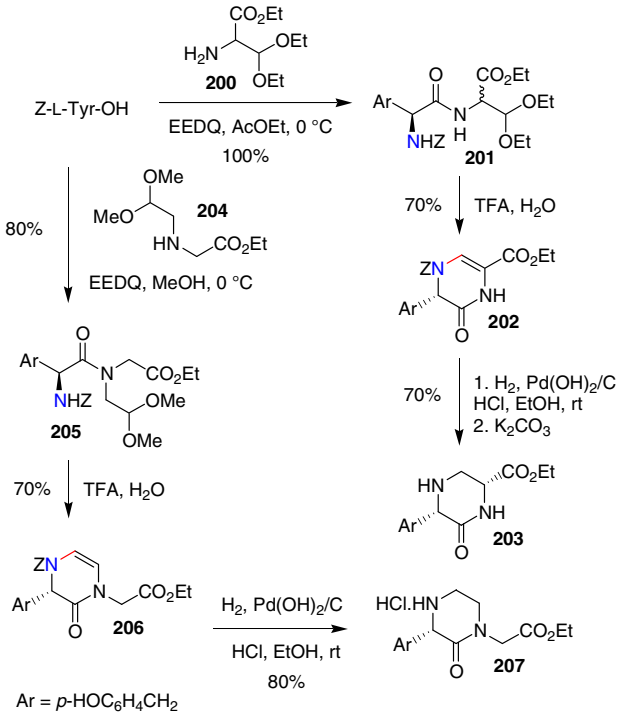

Scheme 37.

200 in the presence of 2-ethoxy-1-ethoxycarbonyl-1,2-dihydroquinoline (EEDQ) produced the dipeptide **201** as a diastereomeric mixture. Acid hydrolysis afforded vinylogous amide **202**, with the best results being observed with TFA, while the use of AcOH or HCl promoted partial hydrolysis of the acetal and no cyclization. The catalytic reduction of **202** in the presence of a slight excess of HCl and subsequent neutralization gave 3,6-disubstituted piperazin-2-one **203**.

Only one diastereoisomer was detected in the product mixture, its formation being accounted for the removal of the *Z* group followed by enantiospecific electrophilic attack of the proton α to the ethoxycarbonyl group and catalytic reduction of the intermediate iminium ion.[87]

Similarly, the TFA-promoted cyclization of the dipeptide **205**, in turn obtained from *Z*-L-tyrosine and ethyl *N*-(2,2-dimethoxyethyl)glycinate **204**, followed by one-pot deprotection and reduction of the cyclic enamide **206**, afforded the amine hydrochloride **207** in 80% yield.

Since then, the incorporation of these synthons into biologically active peptides has gained wide acceptance, with the 2-oxopiperazine ring being used as a model template in which two nitrogen atoms of the dipeptide backbone are linked by an ethylene bridge and consequently the torsion angles ω, φ, and ϕ are restricted compared to the parent peptide (Fig. 4).

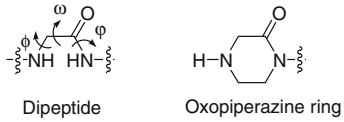

Figure 4.

The original DiMaio's route[86] has been successfully extended to the preparation of a large variety of substituted piperazinones.[25,28,34,35,88]

A representative application of this approach is illustrated in Scheme 38.

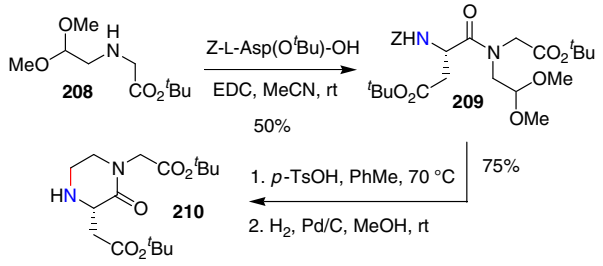

Scheme 38.

Thus, condensation of *Z*-L-aspartic acid *tert*-butyl ester with *tert*-butyl *N*-(2,2-dimethoxyethyl)glycinate **208** produced the acetal amide **209**, which underwent an acid-catalyzed cyclization/reduction sequence to afford 1,3-disubstituted piperazin-2-one **210**.[34]

This chemistry has been successfully applied to the synthesis of enantiomerically pure 1,3-disubstituted 2-oxopiperazine derivatives, used as precursors of non-peptide glycoprotein (GP) IIb–IIIa antagonists,[34,35] starting from diverse N-substituted *N*-(2,2-dialcoxyethyl)-amides derived from *Z*-protected L-amino acids.

Recently, 2,2-dimethoxyethylamine derivatives have been used as convenient starting materials for the preparation of 1,3-disubstituted piperazinone precursors of PGGTase-I inhibitors.[25]

As an example, the secondary amine **211** obtained by a reductive amination of 2,2-dimethoxyethylamine with *p*-fluorobenzaldehyde was coupled with *Z*-L-leucine to give intermediate **212**. Acid-promoted cyclization to enamide **213** followed by one-pot deprotection and reduction produced 2-oxopiperazine **214** (Scheme 39).

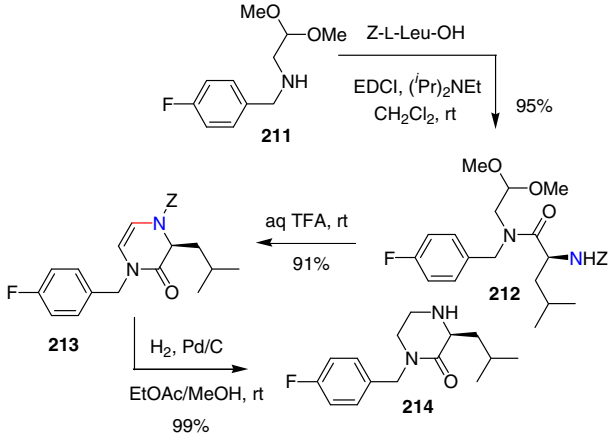

Scheme 39.

An alternative approach to the synthesis of the piperazinone nucleus involves the use of suitable *N*-allylic amides, with the aldehyde required for the cyclization step being generated by oxidation of the alkene functionality.[23,90]

As reported by Just et al.,[89] $NaBH_4$ reduction of the imine **215** resulting by reductive amination of 4-methoxycinnamaldehyde with L-valine methyl ester furnished *N*-allyl derivative **216** (Scheme 40). Its coupling with *Z*-L-phenylalanine by activating the carboxylic acid as the corresponding fluoride proceeded smoothly to give the derivatized dipeptide **217**. Ozonolysis followed by hydrogenation produced the 1,3-disubstituted 2-oxopiperazine **218**, thus accounting for an intramolecular reductive amination reaction.

In a parallel synthetic pathway, a suitable *N*-allyl derivative has been prepared via a sulfonamide approach, based on the use of *N*-4-nitrosulfonamide as an activating group for achieving mono-*N*-allylation.[89]

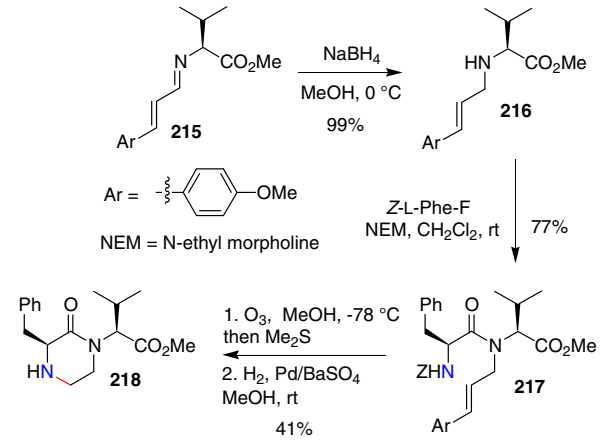

Scheme 40.

These methods seem to represent valuable alternatives to the classical reaction of dipeptides with 1,2-dibromoethane, which failed to give high yields of the desired products.

The synthetic strategy based on intramolecular amination reaction via a *N*-allyl substrate has been used to obtain a piperazinone-based building block precursor of a substance P analogue having the Phe[7]-Phe[8] region constrained.[23]

As illustrated in Scheme 41, the protection of (3*R*)-phenylproline **219** followed by electrochemical oxidation gave the methoxylated product **220**. Its treatment with $BF_3{\cdot}Et_2O$ and allyltrimethylsilane produced compound **221**, with the allyl substituent *trans* to the phenyl ring and *cis* to the methyl ester. Cleavage of the double bond by ozonolysis, reduction of the resulting aldehyde and elimination allowed the installation of a vinyl substituent at C-5 leading to **222**.

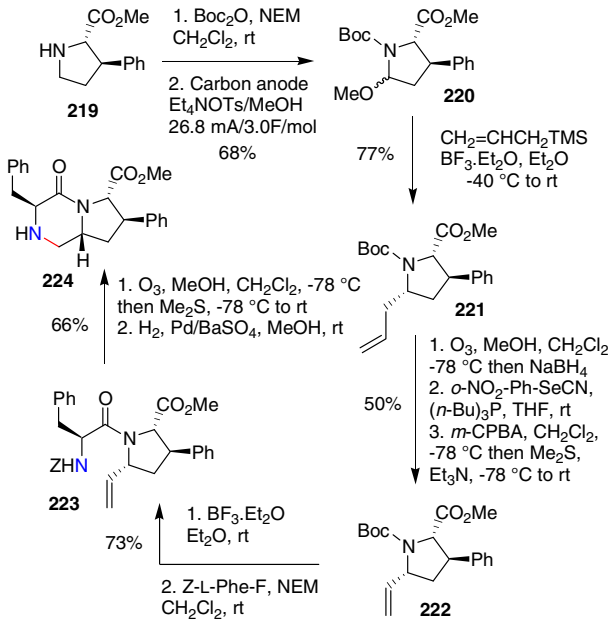

Scheme 41.

Deprotection of **222** and coupling of the released amine with *Z*-L-phenylalanine acid fluoride gave access to dipeptide **223**, which underwent ozonolysis/reduction sequence to furnish the bicyclopiperazine building block **224**, removal of the *Z* protecting group occurring during the reductive step.

Intramolecular reductive amination entailing on the use of D-glucosamine-derived amide **225** as the starting material repre-

sented the key step in the preparation of scaffolds **49** and **53**,[55] already obtained through a N_1–C_2 bond-forming strategy.

As shown in Scheme 42, compound **225** underwent a one-pot hydrogenolytic removal of the *Z* group, cyclization and reduction of the intermediately formed imine. Boc protection to give **48** followed by an oxidation/reduction sequence yielded the piperazinone **49** without any detectable racemization.

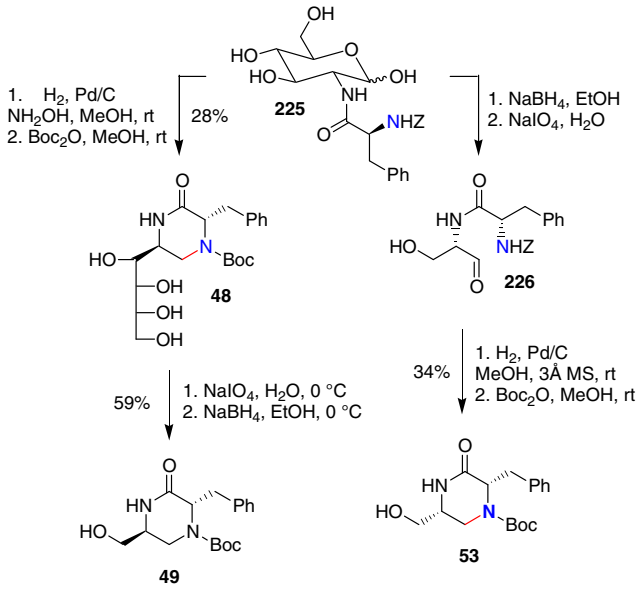

Scheme 42.

It is noteworthy that the ring-closure step could be efficiently promoted by the addition of molar or catalytic amounts (10%) of hydroxylamine.

Moreover, the sequential transformation of **225** into configurationally stable α-amino aldehyde **226**, hydrogenation and Boc protection gave access to (6*R*)-configured piperazinone **53**.

4.2. Nucleophilic substitution

The N_4–C_5 bond-forming strategy centered on an intramolecular Mitsunobu reaction was firstly used by Jacobsen et al.[57] for the preparation of (3*R*)-1-benzyl-3-methyl-piperazin-2-one **229** starting from amide **227** prepared by coupling Boc-D-alanine and *N*-benzylethanolamine (Scheme 43). Removal of the Boc-protecting group produced an intermediate amine **228**, which underwent Mitsunobu cyclization (PPh_3, DEAD) to give **229**.

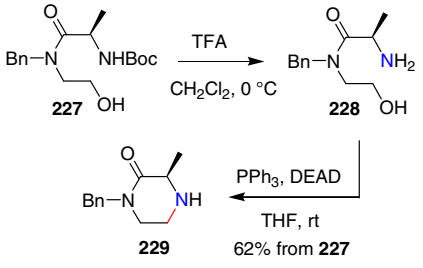

Scheme 43.

Later, Schofield et al.[27] further assessed the Jacobsen approach as a straightforward and flexible route for the synthesis of *N*-benzyl piperazinones bearing variable substituents at C-3 starting from protected α-amino acids and *N*-benzylethanolamine.

The Mitsunobu reaction has been successfully applied to install the N_4–C_5 bond of 1,3-disubstituted 2-oxopiperazine **234** through cyclization of the key amino alcohol **233**,[88] its preparation being achieved by a six-step sequence starting from (*S*)-α-methylbenzylamine (Scheme 44).

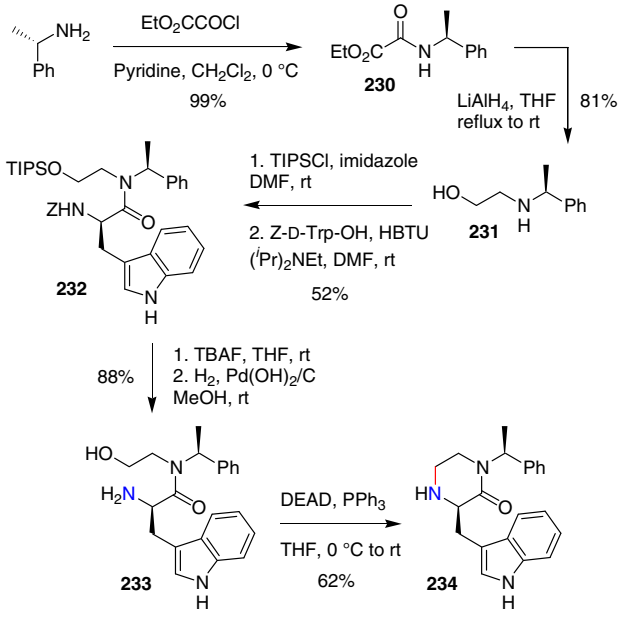

Scheme 44.

Thus, the reaction of (*S*)-α-methylbenzylamine with chloroethyl oxalate and reduction of the derived amide **230** furnished alcohol **231**, which was sequentially protected and coupled to *Z*-D-tryptophan. The resulting amide **232** was deprotected to release both the alcohol and amino groups to give **233** which in turn was submitted to Mitsunobu conditions to give piperazinone **234**.

Recently, a library of spirocyclopropanated 2-oxopiperazine-5-carboxylates has been developed starting from methyl 2-chloro-2-cyclopropylidene-acetate **235**[90] by sequential conjugate addition, acylation, and tandem nucleophilic substitution. A typical application of this approach is outlined in Scheme 45.

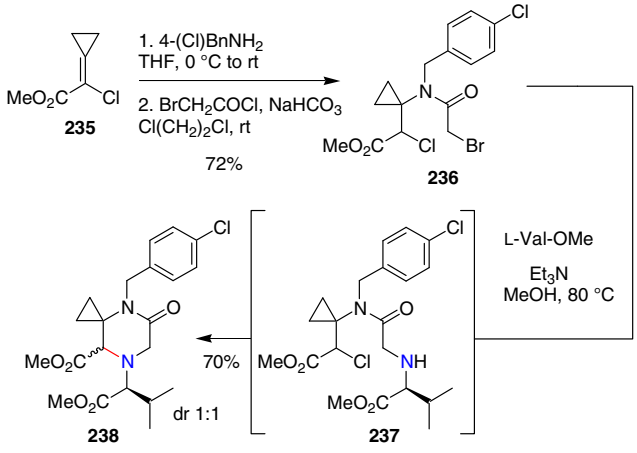

Scheme 45.

Thus, the Michael addition of 4-chlorobenzylamine onto **235** followed by coupling with α-bromoacetyl chloride under modified Schotten–Baumann conditions yielded the stable acyclic bishalide **236**.

Subsequent treatment with L-valine methyl ester triggered a tandem nucleophilic substitution occurring via intermolecular substitution of the bromide giving transient **237** followed by a

ring-closing intramolecular nucleophilic substitution of the chlorine atom to produce piperazinone **238** as a 1:1 diastereomeric mixture, which could be separated by column chromatography.

Bicyclic oxopiperazines were obtained when **236** was reacted with pure β-amino alcohols, with an intramolecular transesterification taking place after piperazinone ring formation.

4.3. Michael addition

Intramolecular Michael addition has been established as a convenient tool for piperazinone synthesis through N_4–C_5 cyclization.

In this context, Goff and Zuchermann[91,92] have reported the efficient synthesis of piperazinones on solid support with an intramolecular Michael ring closure as the key step.

As shown in Scheme 46, the acylation of dipeptoid **239** with Fmoc-L-phenylalanine produced **240**. Removal of the Fmoc group produced resin-bound derivative **241** through Michael addition of the released amine onto the α,β-unsaturated system. Subsequent detachment of the solid support produced piperazinones **242** (3:1 diastereomeric mixture) which contain two ring substituents and a free secondary amino group to be used for further functionalization.

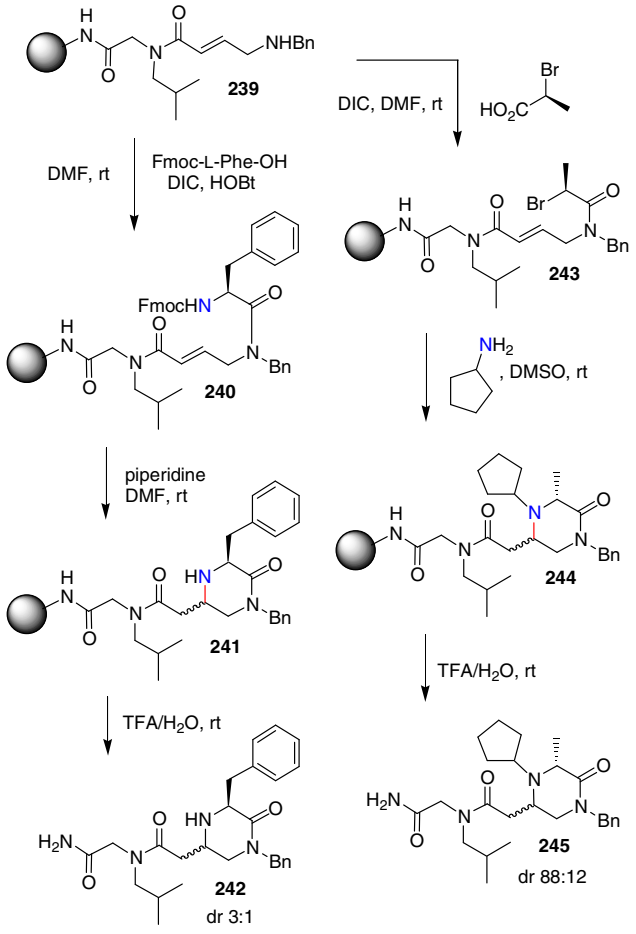

Scheme 46.

Alternatively, compound **239** was coupled with (*S*)-2-bromopropionic acid to furnish the supported amide **243**. Subsequent reaction with cyclopentylamine promoted a tandem S_N2 displacement/Michael addition leading to solid-supported intermediate **244**. Final acid treatment gave 3,4,5-trisubstituted 2-oxopiperazine **245** as a 88:12 mixture of two diastereomers, which were easily separated.

This chemistry was feasible for combinatorial synthesis, since the substitution around the ring could be varied by the appropriate choice of the starting peptoid, the Fmoc amino acid, the α-haloacid, and the amine used for the cyclization step. Furthermore, the free secondary amine of the intermediate **241** permitted further substitution by reaction with different acylating agents.

The tricyclic A–B–C ring system of (−)-agelastatin A **10** featuring a piperazinone core has been assembled by a Cs_2CO_3-mediated intramolecular Michael cyclization of compound **249** to produce the key intermediate **250** (Scheme 47).[15] The preparation of **249** has been achieved by ring-closing metathesis of diamino ketodiene **248**, in turn obtained from compound **246** via **247**.

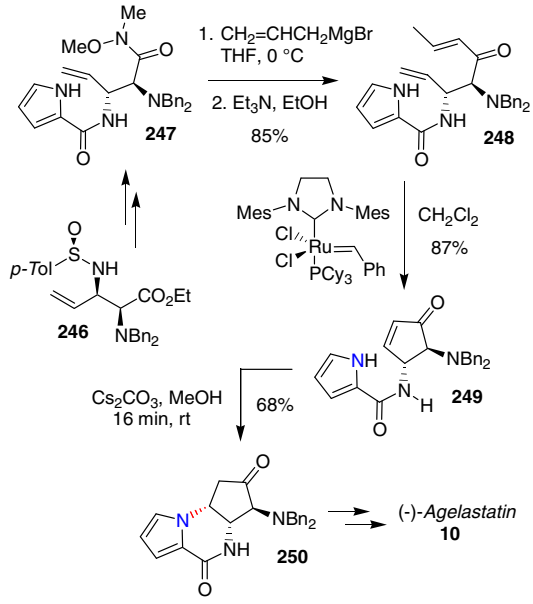

Scheme 47.

Recently, Dickson and Wardrop[17] reported a similar approach based on an intramolecular Michael reaction for the assemblage of the A–B–C ring system of racemic agelastatin A, the key ring-closure step being achieved using K_2CO_3 as the base in DMSO at 100 °C for 1 h.

An efficient synthesis of the piperazinone fragment of pseudotheonamide A_1, a potent serine protease inhibitor, has been accomplished via a stereoselective intramolecular Michael ring closure of dipeptide **253**,[14] which has been obtained starting from *O*-2,6-dichlorobenzyl(Cl_2Bn)-Boc-L-tyrosine (Scheme 48). Thus, conversion into γ-amino-α,β-unsaturated ester **251** followed by coupling with Boc-D-phenylalanine afforded **252**. The subsequent Boc-deprotection gave **253**, which took part in an intramolecular Michael reaction by stirring in methanol at room temperature to yield **254**.

4.4. Miscellaneous

During their studies toward the synthesis of pseudotheonamides A_1 and A_2, Gurjar et al.[13] developed a novel approach for the construction of the 3,5,6-trisubstituted piperazinone ring system of the natural products using an intramolecular [3+2] cycloaddition reaction between an azide and an α,β-unsaturated ester. The azido ester **259** was the key intermediate in this approach summarized in Scheme 49.

Its preparation has been conveniently accomplished by coupling between the (*R*)-α-azido acid **255** and *p*-methoxyphenylalaninol **256** to provide dipeptide **257** along with the corresponding dipeptide ester as a minor component, which could furnish additional **257** upon hydrolysis.

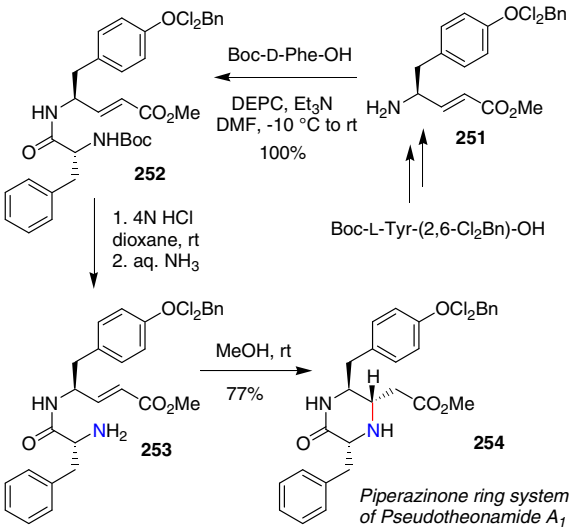

Scheme 48.

Oxidation of the primary alcohol with Dess–Martin periodinane reagent gave the corresponding aldehyde **258** which underwent a two-carbon homologation via a Wittig reaction to give the α,β-unsaturated ester **259**.

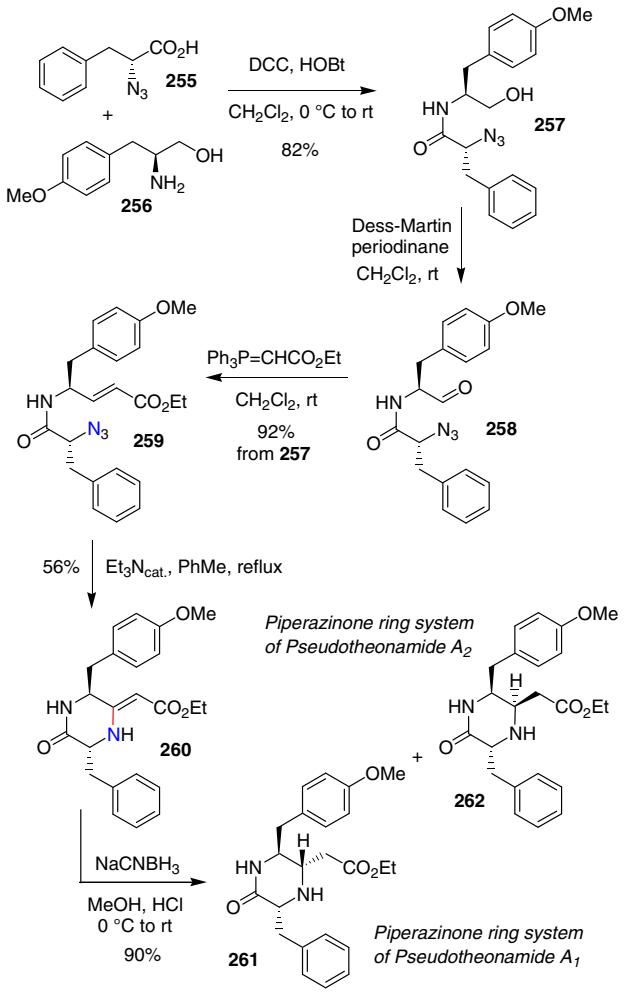

Scheme 49.

The latter was subjected to the key cycloaddition step to produce the enamine **260** which was subsequently reduced with sodium cyanoborohydride to give an easily separated 3:7 mixture of piperazin-2-ones **261** and **262**.

The piperazinone ring B moiety of dibromophakellstatin[19,20] and related marine sponges alkaloids bromophakellin and phakellin[21] has been assembled through a two-step synthetic sequence entailing a key oxidative cyclization.

Thus, condensation of 2-(trichloroacetyl) pyrrole with L-prolinol followed by oxidation of intermediate amide **263** produced a 3:1 diastereomeric mixture of *N,O*-hemiacetals **264** (Scheme 50). These compounds have been successfully converted into **265**, which has been used as a common starting material to give the first enantioselective synthesis of (+)-bromophakellin *ent*-**13** and (+)-phakellin *ent*-**14**.[21]

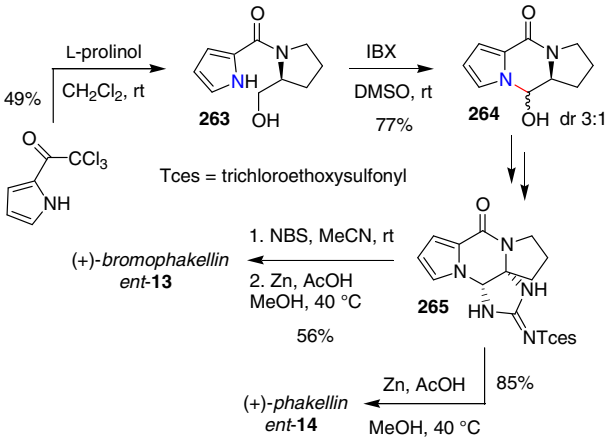

Scheme 50.

Poli et al.[93] developed an elegant and original strategy for the synthesis of piperazin-2-one derivatives entailing on a 6-*exo* intramolecular Pd(0)-catalyzed allylic amination of *N*-tosyl derivatives **266** giving rise to cyclic compounds **267** as a mixture of the two possible diastereomers in high yield (Scheme 51).

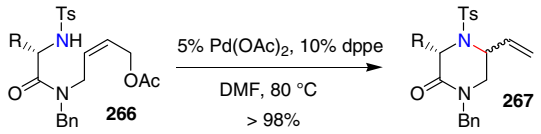

Scheme 51.

The authors presented convincing evidence that this cyclization is a reversible process, constantly favoring the thermodynamically more stable *cis* isomer, and that the *cis*/*trans* ratio increases with the size of the amino acid residue.

In order to enhance the diastereoselectivity of the cyclization process and to circumvent the equilibration between the two epimers, the same authors envisioned an alternative route,[94] the intramolecular Pd(II)-catalyzed allylic amination in the presence of LiCl and without a reoxidizing system. These conditions allowed higher diastereoselectivities than those reported using Pd(0) and produced an irreversible process, with the stereoselectivity being conveniently reversed when the reaction was performed in the absence of LiCl.

5. Cyclization at C_6–N_1

The cyclization of suitable dipeptides with 1,2-dielectrophiles has been extensively used to achieve the synthesis of substituted

2-oxopiperazines.[33,70,95–97] This approach usually takes place via a two-step sequence involving an initial intermolecular N_4–C_5 bond-forming reaction followed by an intramolecular C_6–N_1 bond-forming step.

The reaction of dipeptide **122** with ethylene glycol bis-triflate gives 2-oxopiperazine **268** (Scheme 52),[70] while other 1,2-dielectrophiles, such as ethylene sulfate, were completely uneffective.

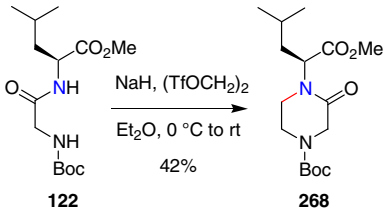

Scheme 52.

The preparation of 1,3-disubstituted 2-oxopiperazines by the cyclization of sulfonamide dipeptides with 1,2-dibromoethane was reported 20 years ago by Just et al.[95] along the pathway illustrated in Scheme 53 as a selected example.

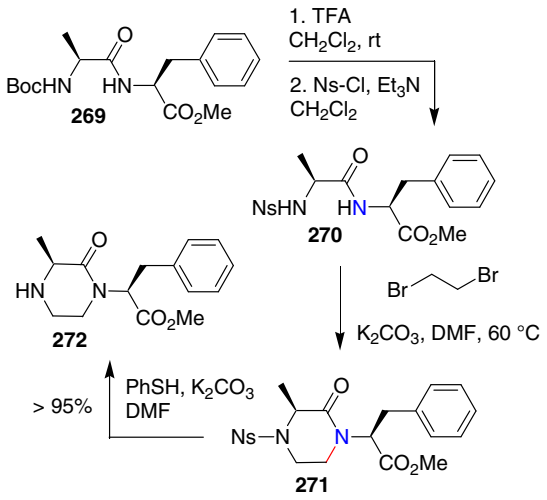

Scheme 53.

Removal of the Boc-protecting group from peptide **269**, obtained by classical peptide coupling between Boc-L-alanine and L-phenylalanine methyl ester, followed by sulfonamide formation gave the key sulfonamide dipeptide **270**. This compound underwent reaction with excess 1,2-dibromoethane and K_2CO_3 in DMF at 60 °C to yield the sulfonamide 2-oxopiperazine **271**, which was eventually deprotected to give **272**.

Interestingly, the same compound **272** has been prepared starting from the 2-nitrobenzenesulfonamide analogue of **270** through a sequential Mitsunobu reaction with 2-bromoethanol, base-promoted cyclization and deprotection.

A successful application of the approach based on cyclization of sulfonamides with 1,2-dibromoethane has been achieved by the same authors on solid support (Scheme 54).[95] Resin-bound 2-nitrobenzenesulfonamide dipeptide **274**, in turn obtained from Fmoc derivative **273**, reacted with excess 1,2-dibromoethane. Subsequent deprotection furnished the resin-bound piperazinone **275**, which could be converted into 1,3,4-trisubstituted 2-oxopiperazine **276** through sequential functionalization of the free secondary amino group and cleavage of the resin.

Similar routes via piperazinone ring assembly by treatment of a suitable sulfonamide dipeptide with 1,2-dibromoethane have been used to obtain key intermediates for the synthesis of a thyrotropin

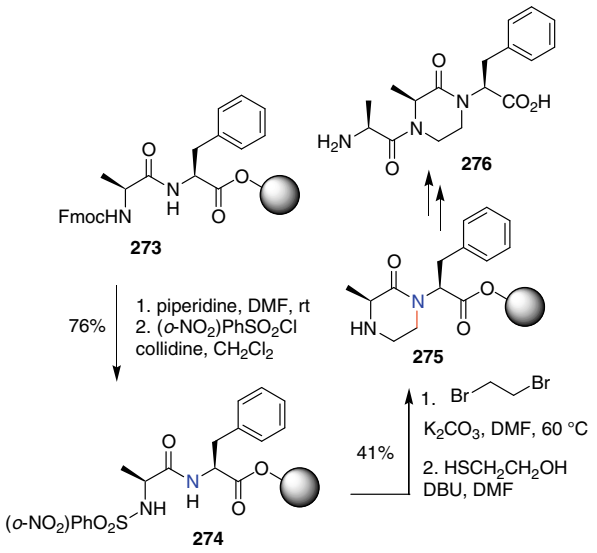

Scheme 54.

releasing hormone (TRH) analogue[96] and 1,3,4-trisubstituted 2-oxopiperazine based melanocortin-4 (MC4) agonists.[33]

Studies directed toward the development of a short and efficient route for the preparation of piperazinone **136**,[97] led to the discovery of the synthetic pathway outlined in Scheme 55.

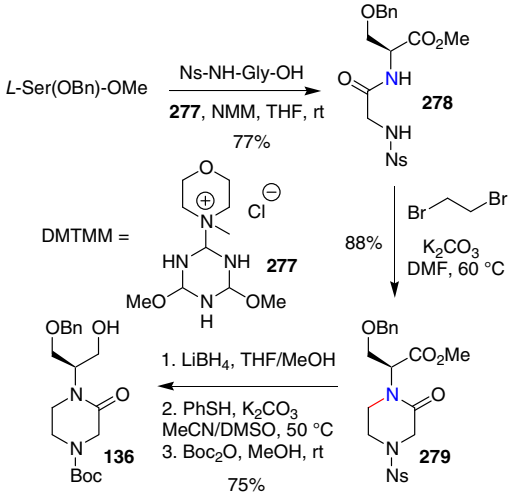

Scheme 55.

Condensation of *O*-benzyl-L-serine methyl ester with *N*-nosyl glycine in the presence of 4-(4,6-dimethoxy-1,3,5-triazin-2-yl)-4-methylmorpholinium chloride (DMTMM) **277** produced sulfonamide **278**, which was reacted with an excess of 1,2-dibromoethane producing satisfactorily the 1-substituted piperazin-2-one **279**. Reduction of the ester group, deprotection, and Boc-reprotection completed the synthesis of **136**.

It is noteworthy that the direct cyclization of the Boc analogue of **278** using ethylene glycol bis-triflate as a dielectrophile proved to be unsuccessful, as the hydrogen bound to the carbamate nitrogen was not acidic enough.

An operationally simple 6-*exo* epoxide ring-opening cyclization allowed chiral 1-aryl-6-(hydroxymethyl)-2-ketopiperazine **283** to be obtained in high yields and with excellent enantiomeric purity,[62] through the synthetic pathway depicted in Scheme 56.

This approach utilized (*S*)-epichlorohydrin instead of Garner's aldehyde as the source of the C-6 chirality as previously illustrated for the N_1–C_2 bond-forming reaction depicted in Scheme 19.

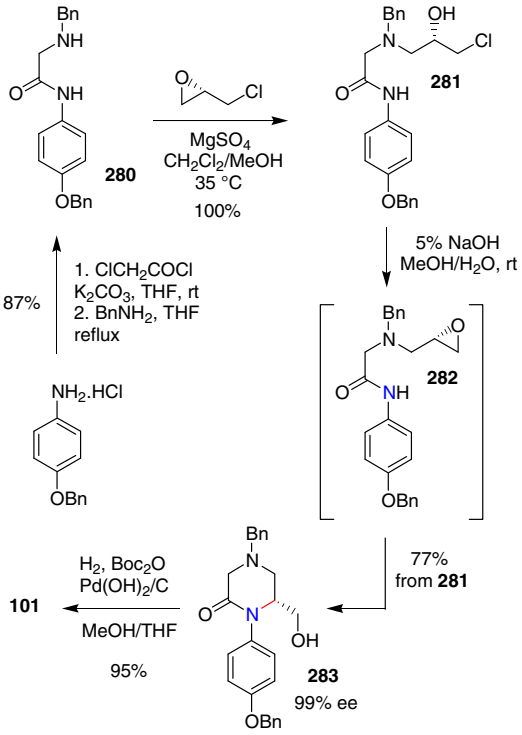

Scheme 56.

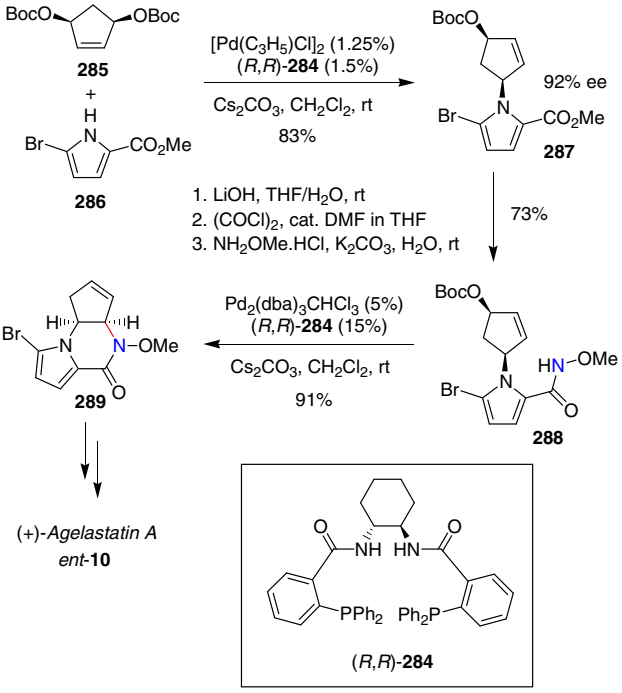

Scheme 57.

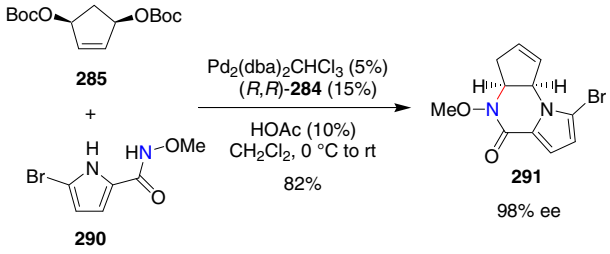

Scheme 58.

Thus, the reaction of 4-benzyloxyaniline with α-chloroacetyl chloride followed by alkylation of the intermediate chloromethylacylated derivative with benzylamine gave an 87% overall yield of the secondary amine **280**. Its reaction with (*S*)-epichlorohydrin in the presence of $MgSO_4$ produced chlorohydrin **281**, which was used in the next step without further purification. Basic treatment of crude **281** (5% NaOH, room temperature) allowed the rapid formation of epoxide **282** which took part in a slow cyclization to give ketopiperazine **283** in 77% yield over the two steps. Finally, hydrogenation of **283** in the presence of Boc_2O proceeded smoothly to yield compound **101**.

The authors outlined that the treatment of **281** with an aqueous NaOH solution followed by NaH-promoted cyclization in anhydrous DMF produced the desired piperazinone **283** in 26% yield together with 4-benzyloxyaniline and various unidentified polar byproducts, while other solvents exclusively gave the formation of polar byproducts.

A noteworthy application to natural product synthesis of C_6–N_1 bond-forming reaction has been described by Trost and Dong[16] who demonstrated that pyrroles and *N*-methoxyamides could be employed as nucleophiles in the functionalization of cyclopentenes through Pd-catalyzed asymmetric allylic alkylation reactions in the presence of C_2-symmetric bisphosphine ligand (*R*,*R*)-**284**.

As shown in Scheme 57, the Pd-catalyzed reaction between Boc-activated cyclopentene 1,4-diol **285** and methyl 5-bromopyrrole-2-carboxylate **286** in the presence of Cs_2CO_3 gave *N*-alkyl pyrrole **287** in 83% yield and 92% ee. A two-step hydrolysis/condensation process allowed the transformation of **287** into *N*-methoxyamide **288** which underwent an intramolecular Pd-catalyzed asymmetric allylic alkylation leading to piperazin-2-one **289**, eventually elaborated to the potent cytotoxic agent (+)-agelastatin A *ent*-**10**.

It is noteworthy that the chiral ligand was not necessary to achieve piperazinone formation. However, the use of (*R*,*R*)-**284** as a catalyst gave higher yields (91%) compared to dppp (70%).

Furthermore, when *N*-methoxyamide **290** was used as the counterpart of **285** (Scheme 58), a palladium-catalyzed cascade reaction using two sequential allylic displacement reactions led to a highly enantioselective, one-pot assemblage of the regioisomeric piperazinone **291** (98% ee), which allowed to obtain the natural (−)-enantiomer of agelastatin A.

Note added in proof: after submission of the manuscript to the Editor, an additional nice paper has appeared (Baran et al. *Angew. Chem., Int. Ed.* **2010**, *49*, 1095–1098). This work reported the total synthesis of palau'amine using a remarkable transannular cyclization of a suitable macrocycle as the key step to assemble the piperazinone moiety of the natural compound.

6. Outlook

The present report highlights the synthetic routes toward chiral 2-ketopiperazines, which feature a particular backbone which can be assembled in different and complementary ways. This greatly helps medicinal, combinatorial, and natural product chemists to cover a certain activity space in an optimum fashion. Moreover it can be anticipated that even more routes toward piperazines as privileged scaffolds will be discovered in the future.

References

1. Horton, D. A.; Bourne, G. T.; Smythe, M. L. *Chem. Rev.* **2003**, *103*, 893–930.
2. Tullberg, M.; Grøtli, M.; Luthman, K. *J. Org. Chem.* **2007**, *72*, 195–199.
3. Vacca, J. P.; Dorsey, B. D.; Schleif, W. A.; Levin, R. B.; McDaniel, S. L.; Darke, P. L.; Zugay, J.; Quintero, J. C.; Blahy, O. M.; Roth, E.; Sardana, V. V.; Schlabach, A. J.;

Graham, P. I.; Condra, J. H.; Gotlib, L.; Holloway, M. K.; Lin, J.; Chen, I.-W.; Vastag, K.; Ostovic, D.; Anderson, P. S.; Emini, E. A.; Huff, J. R. *Proc. Natl. Acad. Sci. U.S.A.* **1994**, *91*, 4096–4100.
4. Capdeville, R.; Buchdunger, E.; Zimmermann, J.; Matter, A. *Nat. Rev. Drug Disc.* **2002**, *1*, 493–502.
5. López-Rodríguez, M. L.; Ayala, D.; Benhamú, B.; Morcillo, M. J.; Viso, A. *Curr. Med. Chem.* **2002**, *9*, 443–469.
6. López-Rodriguez, M. L.; Salama, B. B. *Arylpiperazine Derivative and Use thereof as 5Ht1a Receptor Ligands*. U.S. Patent 2009/036455 (Feb 05, 2009).
7. Ward, S. E.; Eddershaw, P.; Flynn, S. T.; Gordon, L.; Lovell, P. J.; Moore, S. H.; Scott, C. M.; Smith, P. W.; Thewlis, K. M.; Wyman, P. A. *Bioorg. Med. Chem. Lett.* **2009**, *19*, 428–432.
8. Ashley, E. R.; Cruz, E. G.; Stoltz, B. M. *J. Am. Chem. Soc.* **2003**, *125*, 15000–15001.
9. Rikimaru, K.; Mori, K.; Toshiyuki, K.; Fukuyama, T. *Chem. Commun.* **2005**, 394–396.
10. Amador, M. L.; Jimeno, J.; Paz-Ares, L.; Cortes-Funes, H.; Hidalgo, M. *Ann. Oncol.* **2003**, *14*, 1607–1615.
11. Nagumo, S.; Matoba, A.; Ishii, Y.; Yamaguchi, S.; Akutsu, N.; Nishijima, H.; Nishida, A.; Kawahara, N. *Tetrahedron* **2002**, *58*, 9871–9877.
12. Garg, N. K.; Stoltz, B. M. *Tetrahedron Lett.* **2005**, *46*, 2423–2426.
13. Gurjar, M. K.; Karmakar, S.; Mohapatra, D. K.; Phalgune, U. D. *Tetrahedron Lett.* **2002**, *43*, 1897–1900.
14. Shioiri, T.; Irako, N. *Chem. Lett.* **2002**, 130–131.
15. Davis, F. A.; Deng, J. *Org. Lett.* **2005**, *7*, 621–623.
16. Trost, B. M.; Dong, G. *J. Am. Chem. Soc.* **2006**, *128*, 6054–6055.
17. Dickson, D. P.; Wardrop, D. J. *Org. Lett.* **2009**, *11*, 1341–1344.
18. Trost, B. M.; Cramer, N.; Bernsmann, H. *J. Am. Chem. Soc.* **2007**, *129*, 3086–3087.
19. Jacquot, D. E. N.; Hoffmann, H.; Polborn, K.; Lindel, T. *Tetrahedron Lett.* **2002**, *43*, 3699–3702.
20. Chung, R.; Yu, E.; Incarvito, C. D.; Austin, D. J. *Org. Lett.* **2004**, *6*, 3881–3884.
21. Wang, S.; Romo, D. *Angew. Chem., Int. Ed.* **2008**, *47*, 1284–1286.
22. Hirose, T.; Sunazuka, T.; Tsuchiya, S.; Tanaka, T.; Kojima, Y.; Mori, R.; Iwatsuki, M.; Omura, S. *Chem. Eur. J.* **2008**, *14*, 8220–8238.
23. Tong, Y.; Fobian, Y. M.; Wu, M.; Boyd, N. D.; Moeller, K. D. *J. Org. Chem.* **2000**, *65*, 2484–2493.
24. Dinsmore, C. J.; Bergman, J. M.; Bogusky, M. J.; Culberson, J. C.; Hamilton, K. A.; Graham, S. L. *Org. Lett.* **2001**, *3*, 865–868.
25. Peng, H.; Carrico, D.; Thai, V.; Blaskovich, M.; Bucher, C.; Pusateri, E. E.; Sebti, S. M.; Hamilton, A. D. *Org. Biomol. Chem.* **2006**, *4*, 1768–1784.
26. Dinsmore, C. J.; Zartman, C. B.; Bergman, J. M.; Abrams, M. T.; Buser, C. A.; Culberson, J. C.; Davide, J. P.; Ellis-Hutchings, M.; Fernandes, C.; Graham, S. L.; Hartman, G. D.; Huber, H. E.; Lobell, R. B.; Mosser, S. D.; Robinson, R. G.; Williams, T. M. *Bioorg. Med. Chem. Lett.* **2004**, *14*, 639–643.
27. Seibel, J.; Brown, D.; Amour, A.; Macdonald, S. J.; Oldham, N. J.; Schofield, C. J. *Biorg. Med. Chem. Lett.* **2003**, *13*, 387–389.
28. Su, T.; Yang, H.; Volkots, D.; Woolfrey, J.; Dam, S.; Wong, P.; Sinha, U.; Scarborough, R. M.; Zhu, B.-Y. *Bioorg. Med. Chem. Lett.* **2003**, *13*, 729–732.
29. Holsworth, D. D.; Powell, N. A.; Downing, D. M.; Cai, C.; Cody, W. L.; Ryan, J. M.; Ostroski, R.; Jalaie, M.; Bryant, J. W.; Edmunds, J. J. *Bioorg. Med. Chem.* **2005**, *13*, 2657–2664.
30. Powell, N. A.; Clay, E. H.; Holsworth, D. D.; Bryant, J. W.; Ryan, J. M.; Jalaie, M.; Zhang, E.; Edmunds, J. J. *Bioorg. Med. Chem. Lett.* **2005**, *15*, 2371–2374.
31. Holsworth, D. D.; Cai, C.; Cheng, X.-M.; Cody, W. L.; Downing, D. M.; Erasga, N.; Lee, C.; Powell, N. A.; Edmunds, J. J.; Stier, M.; Jalaie, M.; Zhang, E.; McConnell, P.; Ryan, J. M.; Bryant, J.; Li, T.; Kasani, A.; Hall, E.; Subedi, R.; Rahim, M.; Maiti, S. *Bioorg. Med. Chem. Lett.* **2006**, *16*, 2500–2504.
32. Cumming, J. N.; Le, T. X.; Babu, S.; Carroll, C.; Chen, X.; Favreau, L.; Gaspari, P.; Guo, T.; Hobbs, D. W.; Huang, Y.; Iserloh, U.; Kennedy, M. E.; Kuvelkar, R.; Li, G.; Lowrie, J.; McHugh, N. A.; Ozgur, L.; Pan, J.; Parker, E. M.; Saionz, K.; Stamford, A. W.; Strickland, C.; Tadesse, D.; Voigt, J.; Wang, L.; Wu, Y.; Zhang, L.; Zhang, Q. *Bioorg. Med. Chem. Lett.* **2008**, *18*, 3236–3241.
33. Tian, X.; Mishra, R. K.; Switzer, A. G.; Hu, X. E.; Kim, N.; Mazur, A. W.; Ebetino, F. H.; Wos, J. A.; Crossdoersen, D.; Pinney, B. B.; Farmer, J. A.; Sheldon, R. J. *Bioorg. Med. Chem. Lett.* **2006**, *16*, 4668–4673.
34. Sugihara, H.; Fukushi, H.; Miyawaki, T.; Imai, Y.; Terashita, Z.-I.; Kawamura, M.; Fujisawa, Y.; Kita, S. *J. Med. Chem.* **1998**, *41*, 489–502.
35. Kitamura, S.; Fukushi, H.; Miyawaki, T.; Kawamura, M.; Konishi, N.; Terashita, Z.-I.; Naka, T. *J. Med. Chem.* **2001**, *44*, 2438–2450.
36. Okamura, N.; Habay, S. A.; Zeng, J.; Chamberlin, A. R.; Reinscheid, R. K. *JPET* **2008**, *325*, 893–901.
37. Zhang, Y.; Gilmour, B. P.; Navarro, H. A.; Runyon, S. P. *Bioorg. Med. Chem. Lett.* **2008**, *18*, 4064–4067.
38. Maryanoff, B. E.; Costanzo, M. J. *Bioorg. Med. Chem.* **2008**, *16*, 1562–1595.
39. Kim, H.; So, S. M.; Chin, J.; Kim, B. M. *Aldrichim. Acta* **2008**, *41*, 77–88.
40. Dinsmore, C. J.; Beshore, D. C. *Tetrahedron* **2002**, *58*, 3297–3312.
41. Dinsmore, C. J.; Beshore, D. C. *Org. Prepar. Proced. Int.* **2002**, *34*, 367–404.
42. Quirion, J.-C. Asymmetric Synthesis of Substituted Piperazines. In *Targets in Heterocyclic Systems*; Attanasi, O. A., Spinelli, D., Eds.; Italian Society of Chemistry: Roma, 2008; Vol. 12, pp 438–459.
43. Petasis, N. A.; Patel, Z. D. *Tetrahedron Lett.* **2000**, *41*, 9607–9611.
44. Hulme, C.; Ma, L.; Kumar, V.; Krolikowski, P. H.; Allen, A. C.; Labaudiniere, R. *Tetrahedron Lett.* **2000**, *41*, 1509–1514.
45. Roszkowski, P.; Maurin, J. K.; Czarnocki, Z. *Tetrahedron: Asymmetry* **2006**, *17*, 1415–1419.
46. Takenaka, H.; Miyake, H.; Kojima, Y.; Yasuda, M.; Gemba, M.; Yamashita, T. *J. Chem. Soc., Perkin Trans. 1* **1993**, 933–937.
47. Yamashita, T.; Tsuru, E.; Banjyo, E.; Doe, M.; Shibata, K.; Yasuda, M.; Gemba, M. *Chem. Pharm. Bull.* **1997**, *45*, 1940–1944.
48. Yamashita, T.; Hatamoto, E.; Takenaka, H.; Kojima, Y.; Inoue, Y.; Gemba, M.; Yasuda, M. *Chem. Pharm. Bull.* **1996**, *44*, 856–859.
49. Hansen, T. K.; Schlienger, N.; Hansen, B. S.; Andersen, P. H.; Bryce, M. R. *Tetrahedron Lett.* **1999**, *40*, 3651–3654.
50. Shreder, K.; Zhang, L.; Goodman, M. *Tetrahedron Lett.* **1998**, *39*, 221–224.
51. Shreder, K.; Zhang, L.; Gleeson, J.-P.; Ericsson, J. A.; Yalamoori, V. V.; Goodman, M. *J. Comb. Chem.* **1999**, *1*, 383–387.
52. Herrero, S.; García-López, M. T.; Latorre, M.; Cenarruzabeitia, E.; Del Río, J.; Herranz, R. *J. Org. Chem.* **2002**, *67*, 3866–3873.
53. Herrero, S.; Suárez-Gea, M. L.; García-López, M. T.; Herranz, R. *Tetrahedron Lett.* **2002**, *43*, 1421–1424.
54. Guitot, K.; Carboni, S.; Reiser, O.; Piarulli, U. *J. Org. Chem.* **2009**, *74*, 8433–8436.
55. Kolter, T.; Dahl, C.; Giannis, A. *Liebigs Ann.* **1995**, 625–629.
56. Rübsam, F.; Mazitschek, R.; Giannis, A. *Tetrahedron* **2000**, *56*, 8481–8487.
57. Mickelson, J. W.; Belonga, K. L.; Jacobsen, E. J. *J. Org. Chem.* **1995**, *60*, 4177–4183.
58. Mickelson, J. W.; Jacobsen, E. J. *Tetrahedron: Asymmetry* **1995**, *6*, 19–22.
59. González-Goméz, J. C.; Uriarte-Villares, E.; Figueroa-Pérez, S. *Synlett* **2002**, 1085–1088.
60. Beshore, D. C.; Dinsmore, C. J. *Org. Lett.* **2002**, *4*, 1201–1204.
61. Williams, A. J.; Chakthong, S.; Gray, D.; Lawrence, R. M.; Gallagher, T. *Org. Lett.* **2003**, *5*, 811–814.
62. Powell, N. A.; Ciske, F. L.; Clay, E. C.; Cody, W. L.; Downing, D. M.; Blazecka, P. G.; Holsworth, D. D.; Edmunds, J. J. *Org. Lett.* **2004**, *6*, 4069–4072.
63. Pollini, G. P.; Baricordi, N.; Benetti, S.; De Risi, C.; Zanirato, V. *Tetrahedron Lett.* **2005**, *46*, 3699–3701.
64. Gellerman, G.; Hazan, E.; Brider, T.; Traube, T.; Albeck, A.; Shatzmiler, S. *Int. J. Pept. Res. Ther.* **2008**, *14*, 183–192.
65. Gellerman, G.; Hazan, E.; Kovaliov, M.; Albeck, A.; Shatzmiler, S. *Tetrahedron* **2009**, *65*, 1389–1396.
66. Gallicchio, S. N.; Bell, I. M. *Tetrahedron Lett.* **2009**, *50*, 3817–3819.
67. Berst, F.; Holmes, A. B.; Ladlow, M. *Org. Biomol. Chem.* **2003**, *1*, 1711–1719.
68. Schanen, V.; Riche, C.; Chiaroni, A.; Quirion, J.-C.; Husson, H.-P. *Tetrahedron Lett.* **1994**, *35*, 2533–2536.
69. Schanen, V.; Cherrier, M.-P.; de Melo, S. J.; Quirion, J.-C.; Husson, H.-P. *Synthesis* **1996**, 833–837.
70. Pohlmann, A.; Schanen, V.; Guillaume, D.; Quirion, J.-C.; Husson, H.-P. *J. Org. Chem.* **1997**, *62*, 1016–1022.
71. Franceschini, N.; Sonnet, P.; Guillaume, D. *Org. Biomol. Chem.* **2005**, *3*, 787–793.
72. Micouin, L.; Jullian, V.; Quirion, J.-C.; Husson, H.-P. *Tetrahedron: Asymmetry* **1996**, *7*, 2839–2846.
73. Reginato, G.; Di Credico, B.; Andreotti, D.; Mingardi, A.; Paio, A.; Donati, D. *Tetrahedron: Asymmetry* **2007**, *18*, 2680–2688.
74. Bull, S. D.; Davies, S. G.; Fox, D. J.; Garner, A. C.; Sellers, T. G. R. *Pure Appl. Chem.* **1998**, *70*, 1501–1506.
75. Khan, N. M.; Cano, M.; Balasubramanian, S. *Tetrahedron Lett.* **2002**, *43*, 2439–2443.
76. Dinsmore, C. J.; Zartman, C. B. *Tetrahedron Lett.* **2000**, *41*, 6309–6312.
77. For a review on sulfinimines, see: Zhou, P.; Chen, B. C.; Davis, F. A. *Tetrahedron* **2004**, *60*, 8003–8030.
78. Viso, A.; Fernández de la Pradilla, R.; Guerrero-Strachan, C.; Alonso, M.; Martínez-Ripoll, M.; André, I. *J. Org. Chem.* **1997**, *62*, 2316–2317.
79. Viso, A.; Fernández de la Pradilla, R.; García, A.; Alonso, M.; Guerrero-Strachan, C.; Fonseca, I. *Synlett* **1999**, 1543–1546.
80. Viso, A.; Fernández de la Pradilla, R.; García, A.; Guerrero-Strachan, C.; Alonso, M.; Tortosa, M.; Flores, A.; Martínez-Ripoll, M.; Fonseca, I.; André, I.; Rodríguez, A. *Chem. Eur. J.* **2003**, *9*, 2867–2876.
81. Viso, A.; Fernández de la Pradilla, R.; López-Rodríguez, M. L.; García, A.; Flores, A.; Alonso, M. *J. Org. Chem.* **2004**, *69*, 1542–1547.
82. Viso, A.; Fernández de la Pradilla, R.; López-Rodríguez, M. L.; García, A.; Tortosa, M. *Synlett* **2002**, 755–758.
83. Viso, A.; Fernández de la Pradilla, R.; Flores, A.; García, A.; Tortosa, M.; López-Rodríguez, M. L. *J. Org. Chem.* **2006**, *71*, 1442–1448.
84. Viso, A.; Fernández de la Pradilla, R.; Flores, A.; del Águila, M. A. *Tetrahedron* **2008**, *64*, 11580–11588.
85. Viso, A.; Fernández de la Pradilla, R.; Flores, A. *Tetrahedron Lett.* **2006**, *47*, 8911–8915.
86. DiMaio, J.; Belleau, B. *J. Chem. Soc., Perkin Trans. 1* **1989**, 1687–1689.
87. Ficini, J.; Krief, A. *Tetrahedron Lett.* **1970**, *17*, 1397–1400.
88. Horwell, D. C.; Lewthwaite, R. A.; Pritchard, M. C.; Ratcliffe, G. S.; Rubin, J. R. *Tetrahedron* **1998**, *54*, 4591–4606.
89. Bhatt, U.; Mohamed, N.; Just, G.; Roberts, E. *Tetrahedron Lett.* **1997**, *38*, 3679–3682.
90. Limbach, M.; Lygin, A. V.; Korotkov, V. S.; Es-Sayed, M.; de Meijere, A. *Org. Biomol. Chem.* **2009**, *7*, 3338–3342.
91. Goff, D. A.; Zuckermann, R. N. *Tetrahedron Lett.* **1996**, *37*, 6247–6250.
92. Goff, D. A. *Tetrahedron Lett.* **1998**, *39*, 1473–1476.
93. Ferber, B.; Lemaire, S.; Mader, M. M.; Prestat, G.; Poli, G. *Tetrahedron Lett.* **2003**, *44*, 4213–4216.
94. Ferber, B.; Prestat, G.; Vogel, S.; Madec, D.; Poli, G. *Synlett* **2006**, 2133–2135.
95. Mohamed, N.; Bhatt, U.; Just, G. *Tetrahedron Lett.* **1998**, *39*, 8213–8216.
96. Bhatt, U.; Just, G. *Helv. Chim. Acta* **2000**, *83*, 722–727.
97. Lencina, C. L.; Dassonville-Klimpt, A.; Sonnet, P. *Tetrahedron: Asymmetry* **2008**, *19*, 1689–1697.

Synthesis and separation of the enantiomers of the Neuropeptide S receptor antagonist (9R/S)-3-Oxo-1,1-diphenyl-tetrahydro-oxazolo[3,4-a]pyrazine-7-carboxylic acid 4-fluoro-benzylamide (SHA 68)

Journal:	*Journal of Medicinal Chemistry*
Manuscript ID:	jm-2011-00138r
Manuscript Type:	Article
Date Submitted by the Author:	28-Feb-2011
Complete List of Authors:	Trapella, Claudio; University of Ferrara, Department of Pharmaceutial Sciences and Biotechnology Center Pela', Michela; University of Ferrara, Department of Pharmaceutial Sciences and Biotechnology Center Del Zoppo, Luisa; University of Ferrara, Department of Pharmaceutial Sciences and Biotechnology Center Calo', Girolamo; University of Ferrara, Pharmacology Camarda, Valeria; University of Ferrara, Department of Pharmacology Ruzza, Chiara; University of Ferrara, Department of Pharmacology Cavazzini, Alberto; University of Ferrara, Department of Chemistry Costa, Valentina; University of Ferrara, Department of Chemistry Bertolasi, Valerio; University of Ferrara, Department of Chemistry Reinscheid, Rainer; University of California Irvine, Department of Pharmaceutical Sciences Salvadori, Severo; University of Ferrara, Dept. of Pharmaceutical Sciences Guerrini, Remo; University of Ferrara, Department of Pharmaceutical Sciences

Synthesis and separation of the enantiomers of the Neuropeptide S receptor antagonist (9R/S)-3-Oxo-1,1-diphenyl-tetrahydro-oxazolo[3,4-*a*]pyrazine-7-carboxylic acid 4-fluoro-benzylamide (SHA 68)

Claudio Trapella[§Ŧ], Michela Pela'[§Ŧ], Luisa Del Zoppo[§], Girolamo Calo'[#], Valeria Camarda[#], Chiara Ruzza[#], Alberto Cavazzini[¶], Valentina Costa[¶], Valerio Bertolasi[¶¥], Rainer K. Reinscheid[≠], Severo Salvadori[§] and Remo Guerrini[§*]

[§]*Department of Pharmaceutical Sciences and Biotechnology Center, and* [#]*Department of Experimental and Clinical Medicine, Section of Pharmacology and Neuroscience center, and National Institute of Neuroscience, University of Ferrara, via Fossato di Mortara 19, 44100 Ferrara, Italy.* [¶]*Department of Chemistry and* [¥]*Centre for Structural Diffractometry, University of Ferrara, via L. Borsari 46, 44100 Ferrara, Italy.* [≠]*Department of Pharmaceutical Sciences, University of California Irvine, 2214 Natural Sciences I, Irvine, CA 92697, USA.*

[Ŧ] These authors contributed equally to this work

*To whom Correspondence should be addressed.
Remo Guerrini
Phone: +39-0532-455-988; Fax: +39-0532-455953
E-mail: r.guerrini@unife.it

Abbreviations used:
DBU, 1,8-Diazabicyclo[5.4.0]undec-7-ene; DMEM, Dulbecco's modified Eagle's medium; DMF, *N,N*-Dimethylformamide; Fmoc-Cl, 9-Fluorenylmethyl chloroformate; HBSS, Hank's Balanced Salt Solution; HEK, Human Embryonic Kidney; HEPES, 4-(2-hydroxyethyl)-1-piperazineethanesulfonic acid; MS-ESI,electron spray ionization mass spectrometry; NMDA, *N*-Methyl-D-aspartic acid; PFTE, Polytetrafluoroethylene; RP-HPLC, reversed-phase high-performance liquid chromatography; THF, tetrahydrofuran; TMEDA, tetramethylethylenediamine ; WSC, 1-Ethyl-3-(3'-dimethylaminopropyl)carbodiimide.

Abstract

This study reports the synthesis, chromatographic separation and pharmacological evaluation of the two enantiors of the neuropeptide S receptor (NPSR) antagonist (9R/S)-3-oxo-1,1-diphenyl-tetrahydro-oxazolo[3,4-a]pyrazine-7-carboxylic acid 4-fluoro-benzylamide (SHA 68). The (9R)-3-oxo-1,1-diphenyl-tetrahydro-oxazolo[3,4-a]pyrazine-7-carboxylic acid 4-fluoro-benzylamide (compound **10**) and (9S)-3-oxo-1,1-diphenyl-tetrahydro-oxazolo[3,4-a]pyrazine-7-carboxylic acid 4-fluoro-benzylamide (compound **10a**) were synthesized and their purity assessed by chiral chromatography. The absolute configuration of the enantiomer **10** has been assigned from the crystal structure of the corresponding (S)-phenyl ethyl amine derivative **8.** Calcium mobilization studies performed on cells expressing the recombinant NPSR demonstrated that compound **10** is the active enantiomer while the contribution of **10a** to the NPSR antagonist properties of the racemic mixture is negligible.

Introduction

Neuropeptide S (NPS) is the last neuropeptide identified via the reverse pharmacology approach.[1] NPS selectively binds and activates a previously orphan GPCR receptor now referred to as NPSR.[1] NPSR is widely distributed in the brain while the expression of the NPS peptide precursor is limited to few discrete brain areas.[1, 2] The supraspinal administration of NPS in rodents produces a rather unique pattern of actions: stimulation of wakefulness associated with anxiolytic-like effects.[1] In addition, NPS has been reported to inhibit food intake, facilitate memory, elicit antinociceptive effects, and recent evidence suggests an involvement of the NPS/NPSR system in drug addiction (see for a review [3]).

Potent and NPSR selective antagonists are now required for understanding the biological functions controlled by the NPS/NPSR system. As far as peptide antagonists are concerned, these molecules

were recently discovered by replacing Gly[5] in the natural peptide sequence with a D-amino acid. Examples of such compounds are [D-Cys(tBu)[5]]NPS[4], [D-Val[5]]NPS[5] and more recently [[t]Bu-D-Gly[5]]NPS.[6] The first example of non-peptide molecules able to interact with the NPSR was reported in the patent literature by Takeda researchers.[7] Among the different molecules described in the patent, the compound (9R/S)-3-oxo-1,1-diphenyl-tetrahydro-oxazolo[3,4-a]pyrazine-7-carboxylic acid 4-fluoro-benzylamide (SHA 68; compound **1**) has been pharmacologically characterized. In vitro, compound **1** behaves as a selective, potent ($pA_2 \cong 8$) and competitive antagonist at human[8] and murine[9] NPSR. In vivo, compound **1** has been reported to prevent the arousal promoting and anxiolytic-like effects elicited by NPS in mice and rats.[8, 9] In addition, compound **1** reversed the protective effect of NPS on the NMDA receptor antagonist MK-801-induced neurotoxicity in rats.[10] Finally recent findings indicate that in the rat intracerebroventricular injection of NPS increased conditioned reinstatement of cocaine seeking, whereas peripheral administration of compound **1** reduced it.[11] These pharmacological investigations were performed using the racemic compound **1**. Molecular modelling studies investigated non-peptide ligand binding to NPSR.[12] In the frame of these studies, docking analyses were performed and a defined NPSR binding pocked was proposed; of note, only the (S) enantiomer of compound **1** was used in such simulations. The importance of ligand chirality for NPSR interaction has been recently supported by the identification of two novel classes of non-peptide NPSR antagonists: the quinoline[13] and the tricyclic imidazole[14] based compounds. In both cases, a single bioactive enantiomer was obtained by chiral chromatography separation from the corresponding racemic mixture.

In the present study, we report the synthesis, chiral HPLC analysis, X-ray crystallographic assignment and in vitro pharmacological evaluation of the two compound **1** enantiomers.

Results and Discussion

The reference compound **1** was synthesized following the procedures reported by Okamura et al.[8] In Scheme 1 is described the synthetic approach adopted for the synthesis of **10** and **10a** starting from

(S)-phenyl ethyl amine. As reported in literature[15, 16] the use of phenyl ethyl amine was expected to induce the stereochemistry of C9 of the tetrahydro-oxazolo[3,4-*a*]pyrazine nucleus. Unfortunately, we obtained only a slight chiral induction corresponding approximately to a 60 / 40% ratio determined by NMR spectroscopy. Similar results were obtained using (R)-phenyl ethyl amine as chiral auxiliary. Nevertheless, diastereomers **8** and **8a** were successfully separated in good yield by flash chromatography. The removal of the chiral auxiliary to obtain **9** and **9a** and the acylation of N7 with *p*-fluoro-benzylisocyanate to obtain final compounds were achieved using the procedure reported by Okamura et al.[8] The purity grade and enantiomeric excess of **10** and **10a** were determined by chiral HPLC analysis. The top panel of Figure 1 shows the chromatogram for the single enantiomer **10a** (first eluted component), the middle panel that of **10** (second eluted species) and the bottom panel of the figure displays the chromatogram for the racemate. As it is evident from this figure, there is no trace of **10** in the chromatogram corresponding to the elution of **10a**, nor of **10a** in that of **10**. In order to define the absolute configuration of the C9 chiral centre, we explored different crystallization conditions for compounds **8**, **8a**, **9**, **9a** and for the final products. Only with compound **8** we were able to obtain crystals suitable for further X-ray investigation. In particular, compound **8** was crystallized from ethanol/ ethyl acetate and its X-ray analysis demonstrated the absolute configuration R at the chiral center C9. The absolute C9 configuration of compound **8** has been assigned by reference to the unchanged chiral centre C10 in configuration S (Figure 2). On the basis of the absolute configuration of **8**, we were able to assign the absolute C9 configuration to compounds **8a**, **9**, **9a** and that to the final products **10** and **10a**.

In parallel, we performed a series of NMR experiments. In Figure 3 the enlarged [^{1}H]NMR spectra of the C9 proton region of the **10a** and **10** isomers are depicted. The coupling constant analysis between Hx and Ha/Hb C8 protons are very similar (11.3/3.7 Hz for **10a**, panel A and 11.2/3.7 Hz

for **10**, panel B) in both compounds. This result together with X-ray data of **8** (see Figure 2), confirms the axial position of C9 proton in both enantiomers.

Next, we evaluated and compared the in vitro NPSR antagonist properties of compound **1**, compound **10**, and compound **10a**. The three samples were tested in calcium mobilization studies performed on HEK293 cells expressing the murine NPSR or the two isoforms of the human receptor (hNPSRAsn107 and hNPSRIle107).[17]

The natural peptide NPS was able to induce calcium mobilization in a concentration dependent manner in HEK 293 mNPSR (pEC_{50} 8.97 ± 0.11; E_{max} 250 ± 11%), hNPSRAsn107 (pEC_{50}: 9.07 ± 0.11; E_{max} 316 ± 13%) and hNPSRIle107 (pEC_{50}: 9.17 ± 0.15; E_{max} 333 ± 17%). The three samples were challenged against the stimulatory effect of 10 nM NPS in inhibition response curves (Figure 4). Compound **1**, compound **10**, and compound **10a** did not stimulated per se calcium mobilization up to 10 μM. Compound **1** inhibited in a concentration dependent manner the stimulatory effect of NPS showing similar high values of potency ($pK_B \cong 8$). These values of potency are superimposable to those previously published.[8, 9] Compound **10** was also able to antagonize in a concentration dependent manner the stimulatory effect of NPS displaying values of potency similar or slightly higher than the racemic mixture. By contrast, compound **10a** showed a slight inhibitory effect only at micromolar concentrations. The values of potency of the three compounds in the three cells lines are summarized in Table 1. Collectively, these results demonstrated that compound **10** is the active enantiomer while the contribution of compound **10a** to the biological activity of the racemic mixture is negligible. This information can be extremely useful for the refinement of the recently proposed molecular models of NPSR and its binding pocket.[12] As already mentioned in the introduction, the relevance of ligand chirality for NPSR binding is also corroborated by the fact that the biological activity of chemically different molecules, such as the quinoline[13] and the tricyclic imidazole[14] compounds, could be attributed to a single bioactive enantiomer.

In conclusion, the present study described the synthesis and separation of the two compound **1** enantiomers. The synthetic scheme we used can be easily scaled up to multi-grams. Compound **10** was demonstrated to be the bioactive enantiomer. Nowadays this molecule represents the standard non peptide NPSR antagonist that has been, and surely will be, used to investigate the biological functions controlled by the NPS / NPSR system and to evaluate the therapeutic potential of innovative drugs acting as NPSR selective ligands.

Experimental Section

Materials. HPLC grade solvent were purchased from Sigma Aldrich (Steinheim, Germany). The purity of the tested compound **1**, compound **10** and compound **10a** has been assessed by RP-HPLC. All compounds showed >95% purity. One-dimensional and two dimensional NMR spectra were recorded on a VARIAN 400 MHz instrument. Chemical shifts are given in ppm (δ) relative to TMS and coupling constants are in Hz. MS analyses were performed on a ESI-Micromass ZMD 2000. Optical rotation data were recorded on a Perkin-Elmer polarimeter 241. Flash chromatography was carried out on a silica gel (Merck, 230–400 Mesh). Silica gel (Polygram SIL G/UV254) was used for thin layer chromatography.

Typical Procedures for the Synthesis of 10 and 10a.

[(1-Phenyl-ethylcarbamoyl)-methyl]-carbamic acid *tert*-butyl ester (3). To a stirred solution of Boc-Gly-OH (5 g, 28.5 mmol) in CH_2Cl_2 (50 mL), WSC (3.64 g, 19 mmol) and (S)-phenylethyl amine (3.45 g, 28.5 mmol) were added. After 24 h at room temperature the reaction was monitored by TLC (EtOAc/light petroleum 2:1). The organic layer was washed with 10% citric acid (20 mL), 5% $NaHCO_3$ (20 mL) and brine (20 mL). The organic phase was dried, concentrated in vacuo and purified by flash chromatography (EtOAc/light petroleum 2:1) to obtain **3** in 60% yield. ^{1}H NMR (400MHz, $CDCl_3$): δ 7.31-7.24 (m, 5H, Ar); 6.62 (bs, 1H, N*H*-CO); 5.31 (bs, 1H, N*H*-Boc); 5.11 (m, 1H, C*H*-CH_3); 3.75 (m, 2H, CH_2-NH-Boc); 1.47 (d, 3H, CH_3-CH-Ar, J=6.8 Hz); 1.42 (s, 9H,

^{t}bu-); ^{13}C NMR (100MHz, $CDCl_3$): δ 168.6, 156.2, 143.0, 128.7, 127.4, 126.1, 80.2, 48.7, 44.6, 28.3, 21.9; MS (ESI): $[M+H]^+$ =279; $[\alpha]_D^{20}$ = -41 (c = 0.121g/100 ml, chloroform).

[2-(1-Phenyl-ethylamino)-ethyl]-carbamic acid *tert*-butyl ester (4). To a stirred suspension of $LiAlH_4$ (0.85g, 22.38mmol) at 0 °C in anhydrous THF, a solution of **3** (3.11 g, 11.19 mmol) was added drop wise. The reaction was monitored by TLC (EtOAc/light petroleum 3:1) and after 24 hours the excess of hydride was quenched with water and the salts were filtered trough a celite pad. The solvent was evaporated in vacuo to yield **4** (2.66 g, 10.07 mmol) in 90% yield. ^{1}H NMR (400MHz, $CDCl_3$): δ 7.32-7.27 (m, 5H, Ar); 4.96 (bs, 1H, N*H*-Boc); 3.77-3.73 (q, 1H, CH_3-C*H*-Ar, J=6.6 Hz); 3.16-3.13 (m, 2H, NH-C*H*$_2$-CH_2); 2.59-2.51 (m, 2H, NH- CH_2-C*H*$_2$); 1.75 (bs, 1H, -N*H*); 1.42 (s, 9H, ^{t}bu-); 1.36-1.33 (d, 3H, C*H*$_3$-CH-Ar, J=6.6 Hz);. MS (ESI): $[M+H]^+$ = 265; $[\alpha]_D^{20}$ = -29° (c = 0.11 g/100 mL, chloroform).

{2-[(2-Chloro-acetyl)-(1-phenyl-ethyl)-amino]-ethyl}-carbamic acid *tert*-butyl ester (5). To a stirred solution of **4** (1.94 g, 7.34 mmol) in EtOAc (50 mL) at 0 °C, satured solution of $NaHCO_3$ (5 mL) was added. After 10 min, chloroacetyl chloride (1.17 mL, 14.68 mmol) was added drop wise. The reaction was monitored by TLC (EtOAc/light petroleum 3:1) and after 24 h at room temperature, $NaHCO_3$ (2 mL) was added to the organic phase. The organic layer was separated and the aqueous phase was extracted twice with EtOAc (50 mL). The combined organic phases were concentrate to dryness to obtain **5** in quantitative yield. ^{1}H NMR (400MHz, $CDCl_3$): δ 7.22-6.98 (m, 5H, Ar); 5.59-5.43 (q, 1H, CH_3-C*H*-Ar, J=8 Hz); 4.85 (bs, 1H, N*H*-Boc); 4.10-3.97 (m, 2H, NH-C*H*$_2$-CH_2); 3.76 (s, 2H, C=O-C*H*$_2$-Cl); 3.18-3.15 (m, 2H, NH- CH_2-C*H*$_2$); 1.40-1.25 (d, 3H, C*H*$_3$-CH-Ar, J=8 Hz); 1.06 (s, 9H, ^{t}bu). ^{13}C NMR (100MHz, $CDCl_3$): δ 170.12, 155.85, 139.47, 128.45, 128.20, 128.03, 80.69, 59.44, 42.86, 41.14, 38.24, 27.48, 19.98. MS (ESI): $[M+H]^+$ = 341.

3-oxo-4-(1-phenyl-ethyl)-piperazine-1-carboxylic acid *tert*-butyl ester (6). To a stirred suspension of 60% NaH (1.14 g, 28.61 mmol) in a mixture of THF/DMF 1/1 (20 mL) at 0 °C, a solution of **5** (3.25 g, 9.54 mmol) in THF/DMF 1/1 (10 mL) was added. After 24 h the reaction was

quenched by adding NH_4Cl satured solution (15 mL) and the solvent was removed in vacuo. The residue was dissolved in EtOAc (50 mL) and washed twice with water (20 mL). The organic layer was dried, evaporated under reduced pressure and the crude product purified by flash chromatography (eluent: EtOAc/light petroleum 1:1) to obtain **6** in 45% yield. ^{1}H NMR (400MHz, $CDCl_3$): δ 7.36-7.28 (m, 5H, Ar); 6.08 (q, 1H, CH_3-C*H*-Ar, J=8Hz); 4.23-4.18 (d, 1H, N-C*He*Ha-C=O, J=20Hz); 4.10 (d, 1H, N-CHe*Ha*-C=O, J=20Hz); 3.62 (bs, 1H, CH_2 Piperazine); 3.27 (bs, 1H, CH_2 Piperazine); 3.19 (bs, 1H, CH_2 Piperazine); 2.83 (bs, 1H, CH_2 Piperazine); 1.53-1.51 (d, 3H, C*H*$_3$-CH-Ar, J=8Hz); 1.45 (s, 3H, ^{t}bu-). ^{13}C NMR (100MHz, $CDCl_3$): δ 165.44, 153.78, 139.41, 128.63, 127.68, 127.36, 80.69, 50.08, 47.98, 40.24, 28.32, 15.34. MS (ESI): $[M+H]^+$ = 305; $[\alpha]_D^{20}$ = -116.0 ° (c = 0.318 g/100 mL, chloroform).

4-(1-phenyl-ethyl)-piperazine-carboxylic acid *tert*-butyl ester (7). To a stirred suspension of $LiAlH_4$ (453 mg, 18.9 mmol) in anhydrous THF (20 mL) at room temperature, a solution of **6** (1.15 g, 3.78 mmol) in THF (10 mL) was added. After 30 minutes the reaction was completed as showed by TLC analysis (EtOAc/light petroleum 1:2). The reaction was quenched by adding 15% NaOH (1 mL) and Et_2O (20 mL). The resulting precipitate was filtered through a Celite pad and the solvent was concentrate to dryness. The crude product was purified by flash chromatography (eluent: EtOAc/light petroleum 1:2) to give **7** (920 mg, 3.17 mmol) in 84% yield. ^{1}H NMR (400MHz, $CDCl_3$): δ 7.31-7.25 (m, 5H, Ar); 3.41-3.35 (m, 5H, C*H*$_2$-N-Boc, *CH*-CH_3); 2.41-2.33 (m, 4H, C*H*$_2$-N); 1.43 (s, 9H, ^{t}bu-); 1.36 (d, 3H, C*H*$_3$-CH-Ar). ^{13}C NMR (100MHz, $CDCl_3$): δ 146.80, 134.13, 128.38, 127.74, 127.10, 85.27, 50.36, 29.78, 28.49, 27.48. MS (ESI): $[M+H]^+$ = 291; $[\alpha]_D^{20}$ = -32° (c = 0.0104 g/100 mL, chloroform).

1,1-Diphenyl-7-(1-phenyl-ethyl)-hexahydro-oxazolo[3,4-*a*] pyrazin-3-one (8 and 8a). To a stirred solution of **7** (380 mg, 1.31 mmol) in anhydrous THF (5 mL), TMEDA (0.53 mL, 3.54 mmol) was added. The reaction was cooled at -78 °C and *sec*-BuLi 1.4M in exane (2.53 mL, 3.54 mmol) was added. The reaction was heated at -35 °C and after 2 h a solution of benzophenone (480

mg, 2.62 mmol) in anhydrous THF (7 mL) was added drop wise. The reaction became green and was stirred at room temperature for 24 h. After this time the reaction was monitorated by TLC (EtOAc/light petroleum 1:2) and quenched by adding NH_4Cl satured solution (20 mL). The solvent was removed in vacuo and the aqueous phase extracted 3 times with EtOAc (30 mL). The combined organic layer was dried and evaporated to dryness. The crude diastereomers mixture was purified by flash chromatography using EtOAc/light petroleum 1:2 as eluent to obtain the fast running diastereomer **8a** in 40% yield and the low running distereomer **8** in 45% yield.

8a: ^{1}H NMR (400 MHz, $CDCl_3$): δ 7.55 - 7.49 (m, 2H), 7.41 - 7.21 (m, 11H), 7.19 - 7.14 (m, 2H), 4.51 (dd, 1H, *J* = 10.9, 3.6 Hz), 3.74 (ddd, 1H, *J* = 13.2, 3.5, 1.3 Hz), 3.34 (q, 1H, *J* = 6.7 Hz), 3.04 (ddd, 1H, *J* = 13.0, 12.1, 3.6 Hz), 2.70 - 2.61 (m, 2H), 1.86 (td, 1H, *J* = 11.9, 3.6 Hz), 1.50 - 1.41 (m, 1H), 1.22 (d, 3H, *J* = 6.7 Hz). ^{13}C NMR (100 MHz, $CDCl_3$): δ 156.17, 142.85, 142.52, 138.91, 128.69, 128.58, 128.50, 128.35, 128.01, 127.51, 127.37, 126.19, 125.95, 85.50, 64.52, 61.56, 52.66, 49.30, 42.07, 19.34. MS ESI [M+H$^+$]= 399; $[\alpha]_D^{20}$= +216 (c = 0.108 g/100 mL, chloroform).

8: ^{1}H NMR (400 MHz, $CDCl_3$): δ 7.50 - 7.45 (m, 2H), 7.39 - 7.20 (m, 11H), 7.18 - 7.14 (m, 2H), 4.44 (dd, 1H, *J* = 3.56, 10.93 Hz), 3.86 - 3.79 (m, 1H), 3.48 (q, 1H, *J* = 6.8 Hz), 3.11 (ddd, 1H, *J* = 13.0, 12.0, 3.81 Hz), 2.80 - 2.73 (m, 1H), 2.44 (ddd, 1H, *J* = 11.5, 3.5, 1.6 Hz,), 2.07 - 1.97 (m, 1H), 1.50 (m, 1H), 1.27 (d, 3H, *J* = 6.8 Hz). ^{13}C NMR (100 MHz, $CDCl_3$): δ 156.20, 142.48, 142.28, 138.81, 128.65, 128.51, 128.32, 127.98, 127.59, 127.28, 126.11, 125.92, 125.84, 85.39, 63.86, 61.67, 53.24, 47.58, 42.11, 17.16; MS ESI [M+H$^+$]= 399; $[\alpha]_D^{20}$= -132°(c = 0.11 g/100 mL, chloroform).

3-Oxo-1,1-diphenyl-tetrahydro-oxazolo[3,4-*a*]pyrazine-7-carboxylic acid 9*H*-fluoren-9-ylmethyl ester (9 and 9a). To a stirred solution of **8** or **8a** (200 mg, 0.52 mmol) in acetonitrile (10 mL) at reflux, Fmoc-Cl (148 mg, 0.57 mmol) dissolved in acetonitrile (7 mL) was added. The reaction, monitored by TLC (EtOAc/light petroleum 1:2), was completed in 12 h. The desired

precipitate was filtered off to obtain **9** or **9a** in about 67% yield and pure enough to be used in the next reaction.

3-Oxo-1,1-diphenyl-tetrahydro-oxazolo[3,4-*a*]pyrazine-7-carboxylic acid 4-fluoro-benzylamide (10 and 10a). To a stirred solution of **9** (59 mg, 0.11 mmol) in anhydrous THF (15 mL) *p*-fluoro-benzylisocianate (34.4 mg, 0.228 mmol) and DBU (19.2 mg, 0.126 mmol) were added. The reaction was monitored by TLC (EtOAc/light petroleum 1:2) and by mass spectrometry. After 24 h the reaction was treated as for **8** and **8a**. The organic phase was dried and evaporate to dryness to give **10** in 76% yield after column chromatography using EtOAc/light petroleum 1/1 as eluent. ^{1}H NMR (400 MHz, $CDCl_3$): δ 7.51 - 7.47 (m, 2H), 7.41 - 7.18 (m, 10H), 7.03 - 6.94 (m, 2H), 4.95 (t, 1H, *J* = 5.5 Hz), 4.45 - 4.27 (m, 3H), 4.03 (ddd, 1H, *J* = 13.5, 3.5, 1.2 Hz), 3.81 (dd, 1H, *J* = 13.1, 2.7 Hz), 3.69 - 3.60 (m, 1H), 3.05 (td, 1H, *J* = 12.7, 3.7 Hz), 2.93 - 2.82 (m, 1H), 2.14 (dd, 1H, *J* = 13.3, 11.3 Hz). ^{13}C NMR (100 MHz, $CDCl_3$): δ 157.20, 156.11, 141.81, 138.30, 134.91, 129.48, 129.41, 129.17, 129.09, 128.82, 128.72, 128.37, 125.99, 125.85, 115.70, 115.48, 85.90, 60.55, 46.58, 44.47, 43.76, 41.37. MS ESI [M+H$^+$]= 445.9; $[\alpha]_D^{20}$= +92 (c= 0.1 g/100 mL, MeOH). Compound **10a** was obtained in the same manner, starting from **9a**. Analytical data: Yield: 83%; ^{1}H NMR (400 MHz, $CDCl_3$): δ 7.51 - 7.47 (m, 2H), 7.41 - 7.18 (m, 10H), 7.03 - 6.94 (m, 2H), 4.95 (t, 1H, *J* = 5.5 Hz), 4.45 - 4.27 (m, 3H), 4.03 (ddd, 1H, *J* = 13.3, 3.6, 1.3 Hz), 3.81 (dd, 1H, *J* = 13.1, 2.7 Hz), 3.69 - 3.60 (m, 1H), 3.05 (td, 1H, *J* = 12.7, 3.7 Hz), 2.93 - 2.82 (m, 1H), 2.14 (dd, 1H, *J* = 13.3, 11.3 Hz). ^{13}C NMR (100 MHz, $CDCl_3$): δ 157.20, 156.11, 141.81, 138.30, 134.91, 129.48, 129.41, 129.17, 129.09, 128.82, 128.72, 128.37, 125.99, 125.85, 115.70, 115.48, 85.90, 60.55, 46.58, 44.47, 43.76, 41.37. MS ESI [M+H$^+$]= 445.9; $[\alpha]_D^{20}$= -91 (c= 0.12 g/100 mL, MeOH).

Chiral chromatography analysis. A micro HPLC (Agilent 1100 micro series, Agilent Technologies) equipped with a micro diode array detector was employed. A 150mm × 2mm stainless steel column packed with Lux Cellulose-1 (cellulose tris 3,5-dimethylphenylcarbamate from Phenomenex) was used for all the measurements. The average size of the packing material

was 3 µm. The mobile phase was a binary mixture of hexane/isopropyl alcohol (80/20 v/v). Flow rate was 200uL/min. Injection volume was 3µL. Analyte solutions were filtered with PFTE filters (0.45µm, Supelco, Bellefonte, PA, USA) before injection. All chromatograms were recorded at 230 nm. The retention times for the first (**10a**) and second (**10**) eluted enantiomers were 6.5 and 7.9 min, respectively.

Crystal structure determination of compound 8.

The crystal data of compound **8** were collected at room temperature using a Nonius Kappa CCD diffractometer with graphite monochromated Mo-Kα radiation. The data sets were corrected for Lorentz and polarization effects. The structure was solved by direct methods[18] and refined using full-matrix least-squares with all non-hydrogen atoms anisotropically and hydrogens included on calculated positions, riding on their carrier atoms. All calculations were performed using SHELXL-97[19]and PARST[20]implemented in WINGX[21] system of programs.

Crystal Data: $C_{26}H_{26}N_2O_2$, orthorhombic, space group $P2_12_12_1$, a = 11.2339(2), b = 11.6808(3), c = 16.4783(5) Å, V = 2162.30(9) Å^3, Z = 4, D_c = 1.224 g cm^{-3}, intensity data collected with $\theta \leq 26°$, 4215 independent reflections measured, 3460 observed reflections [$I > 2\sigma(I)$], final R index = 0.0365 (observed reflections), R_w = 0.0904 (all reflections), S = 1.048. The absolute configuration has not been established by anomalous dispersion effects in diffraction measurements on the crystal. The enantiomer has been assigned by reference to an unchanging chiral centre in the synthetic procedure. ORTEP[22] view of compound **8** is shown in Figure 2.

CCDC deposition number: 810351.

Calcium mobilization experiments. HEK293 cells stably expressing the murine NPSR or the human receptor isosforms NPSRIle107 and NPSRAsn107 were generated as previously described.[17] $HEK293_{mNPSR}$ and $HEK293_{hNPSRIle107}$ cells were maintained in DMEM medium supplemented with 10% fetal bovine serum, 2mM l-glutamine, hygromycin B (100 mg/L). $HEK293_{hNPSRAsn107}$ cells were maintained in DMEM medium supplemented with 10% fetal bovine serum, 2 mM glutamine,

zeocin (100 mg/L). Cells were cultured at 37 °C in 5% CO_2 humidified air. Cells were seeded at a density of 50,000 cells/well into poly-D-lysine coated 96-well black, clear-bottom plates. The following day, the cells were incubated with medium supplemented with 2.5 mM probenecid, 3 μM of the calcium sensitive fluorescent dye Fluo-4 AM and 0.01% pluronic acid, for 30 min at 37 °C. After that time the loading solution was aspirated and 100 μL/well of assay buffer (Hank's Balanced Salt Solution; HBSS) supplemented with 20 mM 4-(2-hydroxyethyl)-1-piperazineethanesulfonic acid (HEPES), 2.5 mM probenecid and 500 μM Brilliant Black (Aldrich) was added. Concentrated solutions (1 mM) of NPS were made in bidistilled water and kept at −20 ◦C. Compound **1**, compound **10** and compound **10a** were dissolved DMSO at a final concentration of 10 mM and stock solutions were kept at -20 °C until use. The successive dilutions were carried out in HBSS/HEPES (20mM) buffer (containing 0.02% bovine serum albumin fraction V). After placing both plates (cell culture and master plate) into the fluorometric imaging plate reader FlexStation II (Molecular Devices, Sunnyvale, CA), fluorescence changes were measured. On-line additions were carried out in a volume of 50 μL/well. To facilitate drug diffusion into the wells in antagonist type experiments, the present studies were performed at 37 °C and three cycles of mixing (25 μL from each well moved up and down 3 times) were performed immediately after antagonist injection to the wells. Inhibition response curves were determined against the stimulatory effect of 10 nM NPS. Compound **1**, compound **10** and compound **10a** were injected into the wells 24 min before adding NPS.

Data analysis and terminology. The pharmacological terminology adopted in this paper is consistent with IUPHAR recommendations. Data were expressed as mean ± sem of at least four independent experiments made in duplicate. Maximum change in fluorescence, expressed in percent of baseline fluorescence, was used to determine agonist response. Non-linear regression analysis using GraphPad Prism software (v.4.0) allowed logistic iterative fitting of the resultant responses and the calculation of agonist potencies and maximal effects. Agonist potencies are given as pEC_{50}

(the negative logarithm to base 10 of the molar concentration of an agonist that produces 50% of the maximal possible effect). Compound **1**, compound **10** and compound **10a** antagonist properties were evaluated in inhibition response curve experiments; the antagonist potency, expressed as pK_B, was derived from the following equation:

$K_B = IC_{50}/([2 + ([A]/EC_{50})^n]^{1/n} - 1)$

where IC_{50} is the concentration of antagonist that produces 50% inhibition of the agonist response, [A] is the concentration of agonist, EC_{50} is the concentration of agonist producing a 50% maximal response and n is the Hill coefficient of the concentration response curve to the agonist.

Acknowledgments. We are grateful to Dr. Alberto Casolari and Dr Elisa Durini for the NMR analysis and Professor Vinicio Zanirato for the helpful discussion about NMR spectra of compound 8. This work was supported by funds from the University of Ferrara (FAR grants to GC and SS), the Italian Ministry of the University (PRIN grant to GC and SS and CHEM-PROFARMA-NET grant to AC), the Compagnia di S. Paolo Foundation (NPSNP grant to GC), and the National Institute of Mental Health (MH-71313 grant to RKR).

Supporting Information Available: monodimensional and bidimensional NMR spectra of compounds **8**, **8a**, and final products and crystal data of compound **8** (cif file) are available free of charge via the internet at http://pubs.acs.org

References

(1) Xu, Y. L.; Reinscheid, R. K.; Huitron-Resendiz, S.; Clark, S. D.; Wang, Z.; Lin, S. H.; Brucher, F. A.; Zeng, J.; Ly, N. K.; Henriksen, S. J.; de Lecea, L.; Civelli, O. Neuropeptide S: a neuropeptide promoting arousal and anxiolytic-like effects. *Neuron* **2004,** 43, 487-497.

(2) Xu, Y. L.; Gall, C. M.; Jackson, V. R.; Civelli, O.; Reinscheid, R. K. Distribution of neuropeptide S receptor mRNA and neurochemical characteristics of neuropeptide S-expressing neurons in the rat brain. *J. Comp. Neurol.* **2007,** 500, 84-102.

(3) Guerrini, R.; Salvadori, S.; Rizzi, A.; Regoli, D.; Calo, G. Neurobiology, pharmacology, and medicinal chemistry of neuropeptide S and its receptor. *Med. Res. Rev.* **2010,** 30, 751-777.

(4) Camarda, V.; Rizzi, A.; Ruzza, C.; Zucchini, S.; Marzola, G.; Marzola, E.; Guerrini, R.; Salvadori, S.; Reinscheid, R. K.; Regoli, D.; Calo, G. In vitro and in vivo pharmacological characterization of the neuropeptide s receptor antagonist [D-Cys(tBu)5]neuropeptide S. *J. Pharmacol. Exp. Ther.* **2009,** 328, 549-555.

(5) Guerrini, R.; Camarda, V.; Trapella, C.; Calo, G.; Rizzi, A.; Ruzza, C.; Fiorini, S.; Marzola, E.; Reinscheid, R. K.; Regoli, D.; Salvadori, S. Synthesis and biological activity of human neuropeptide S analogues modified in position 5: identification of potent and pure neuropeptide S receptor antagonists. *J. Med. Chem.* **2009,** 52, 524-529.

(6) Guerrini, R.; Camarda, V.; Trapella, C.; Calo, G.; Rizzi, A.; Ruzza, C.; Fiorini, S.; Marzola, E.; Reinscheid, R. K.; Regoli, D.; Salvadori, S. Further studies at neuropeptide s position 5: discovery of novel neuropeptide S receptor antagonists. *J. Med. Chem.* **2009,** 52, 4068-4071.

(7) Fukatsu, K.; Nakayama, Y.; Tarui, N.; Mori, M.; Matsumoto, H.; Kurasawa, O.; Banno, H. Bicyclic piperazine compound and use thereof. *PCT Int. Appl., WO2005021555.*

(8) Okamura, N.; Habay, S. A.; Zeng, J.; Chamberlin, A. R.; Reinscheid, R. K. Synthesis and pharmacological in vitro and in vivo profile of 3-oxo-1,1-diphenyl-tetrahydro-oxazolo[3,4-a]pyrazine-7-carboxylic acid 4-fluoro-benzylamide (SHA 68), a selective antagonist of the neuropeptide S receptor. *J. Pharmacol. Exp. Ther.* **2008,** 325, 893-901.

(9) Ruzza, C.; Rizzi, A.; Trapella, C.; Pela, M.; Camarda, V.; Ruggieri, V.; Filaferro, M.; Cifani, C.; Reinscheid, R. K.; Vitale, G.; Ciccocioppo, R.; Salvadori, S.; Guerrini, R.; Calo, G.

Further studies on the pharmacological profile of the neuropeptide S receptor antagonist SHA 68. *Peptides* **2010,** 31, 915-925.

(10) Okamura, N.; Reinscheid, R. K.; Ohgake, S.; Iyo, M.; Hashimoto, K. Neuropeptide S attenuates neuropathological, neurochemical and behavioral changes induced by the NMDA receptor antagonist MK-801. *Neuropharmacology* **2010,** 58, 166-172.

(11) Kallupi, M.; Cannella, N.; Economidou, D.; Ubaldi, M.; Ruggeri, B.; Weiss, F.; Massi, M.; Marugan, J.; Heilig, M.; Bonnavion, P.; de Lecea, L.; Ciccocioppo, R. Neuropeptide S facilitates cue-induced relapse to cocaine seeking through activation of the hypothalamic hypocretin system. *Proc. Natl. Acad. Sci. U S A* **2010,** 107, 19567-19572.

(12) Dal Ben, D.; Antonini, I.; Buccioni, M.; Lambertucci, C.; Marucci, G.; Vittori, S.; Volpini, R.; Cristalli, G. Molecular modeling studies on the human neuropeptide S receptor and its antagonists. *ChemMedChem.* **2010,** 5, 371-383.

(13) Melamed, J. Y.; Zartman, A. E.; Kett, N. R.; Gotter, A. L.; Uebele, V. N.; Reiss, D. R.; Condra, C. L.; Fandozzi, C.; Lubbers, L. S.; Rowe, B. A.; McGaughey, G. B.; Henault, M.; Stocco, R.; Renger, J. J.; Hartman, G. D.; Bilodeau, M. T.; Trotter, B. W. Synthesis and evaluation of a new series of Neuropeptide S receptor antagonists. *Bioorg. Med. Chem. Lett.* **2010,** 20, 4700-4703.

(14) Trotter, B. W.; Nanda, K. K.; Manley, P. J.; Uebele, V. N.; Condra, C. L.; Gotter, A. L.; Menzel, K.; Henault, M.; Stocco, R.; Renger, J. J.; Hartman, G. D.; Bilodeau, M. T. Tricyclic imidazole antagonists of the Neuropeptide S Receptor. *Bioorg. Med. Chem. Lett.* **2010,** 20, 4704-4708.

(15) Juaristi, E.; Leon-Romo, J. L.; Reyes, A.; Escalante, J. Recent applications of alpha-phenylethylamine (alpha-PEA) in the preparation of enantiopure compounds. Part 3: alpha-PEA as chiral auxiliary. Part 4: alpha-PEA as chiral reagent in the stereodifferentiation of prochiral substrates. *Tetrahedron Asymmetry* **1999,** 10, 2441-2495.

(16) Guizzetti, S.; Benaglia, M.; Rossi, S. Highly stereoselective metal-free catalytic reduction of imines: an easy entry to enantiomerically pure amines and natural and unnatural alpha-amino esters. *Org. Lett.* **2009,** 11, 2928-2931.

(17) Reinscheid, R. K.; Xu, Y. L.; Okamura, N.; Zeng, J.; Chung, S.; Pai, R.; Wang, Z.; Civelli, O. Pharmacological Characterization of Human and Murine Neuropeptide S Receptor Variants. *J. Pharmacol. Exp. Ther.* **2005,** 315, 1338-1345.

(18) Altomare, A.; Burla, M. C.; Camalli, M.; Cascarano, G. L.; Giacovazzo, C.; Guagliardi, A.; Moliterni, A. G.; Polidori, G.; Spagna, R. SIR97: a new tool for crystal structure determination and refinement. *J. Appl. Crystallogr.* **1999**, 32, 115-119.

(19) Sheldrich, G. M. Program for the crystal structure refinement. University of Gottingen, Germany. http://shelx.uni-ac.gwdg.de/SHELX/ **1997**.

(20) Nardelli, M. PARST95- an updata to PARST: a system of Fortran routines for calculating molecular structure parameters from the results of crystal structure analyses. *J. Appl. Crystallogr.* **1995**, 28, 659.

(21) Farrugia, L. J. WinGX suite for small-molecule single crystal crystallography. *J. Appl. Crystallogr.* **1999**, 32, 837-838.

(22) Farrugia, L. J. ORTEP-3 for Windows – a version of ORTEP-III with a Graphical User Interface (GUI). *J. Appl. Crystallogr.* **1997**, 30, 565.

Table 1. Potencies (pK_B) of compound **1** (SHA 68), compound **10** and compound **10a** in HEK293 cells expressing the murine NPSR and the human NPSR isoforms

Compound	mNPSR	hNPSR Ile107	hNPSR Asn107
	pK_B	pK_B	pK_B
1	8.16 (7.79 - 8.53)	8.03 (7.77 - 8.37)	7.99 (7.73 - 8.25)
10	8.29 (7.93 - 8.65)	8.18 (7.90 - 8.46)	8.28 (7.72 - 8.84)
10a	<6	<6	<6

Figure 1. Chromatograms of compound **10a** (top panel) and **10** (middle panel) in comparison with the racemate (bottom panel).

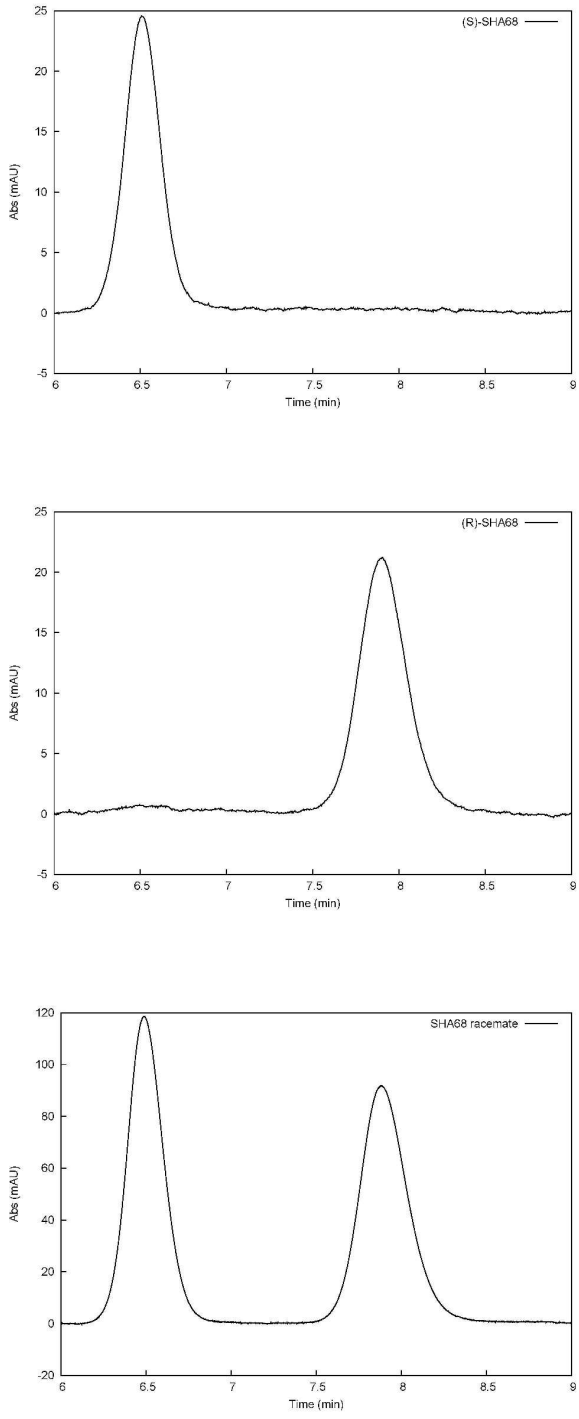

Figure 2. ORTEP view of compound **8**. The thermal ellipsoids are drawn at 30% probability level.

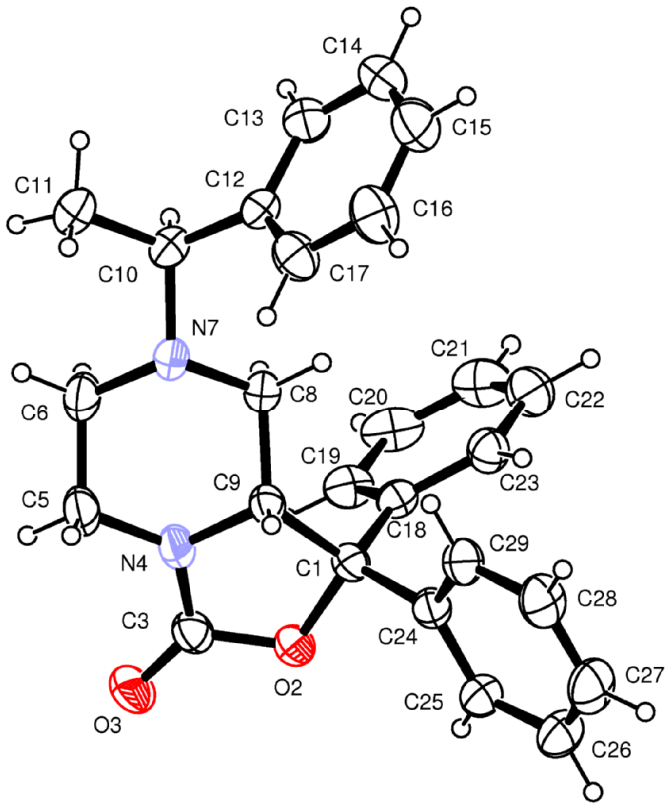

Figure 3. Enlarged [^{1}H]NMR spectra of the C9 proton region of the **10a** (panel A) and **10** (panel B) isomers

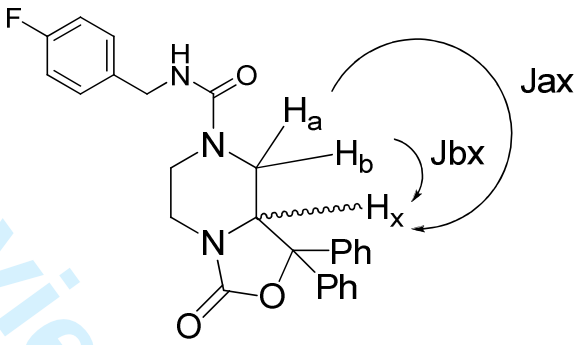

Panel A

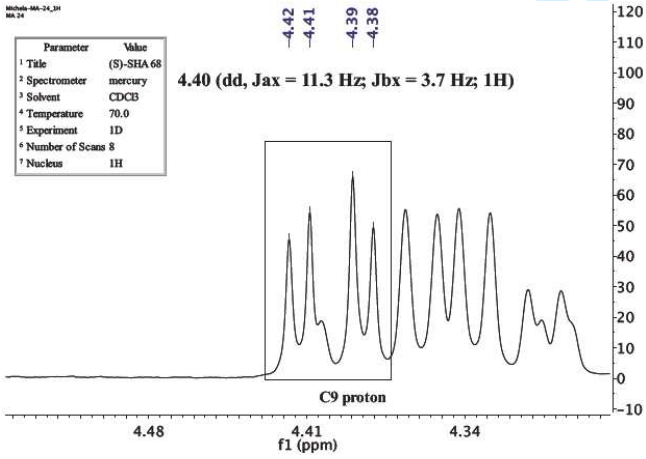

Panel B

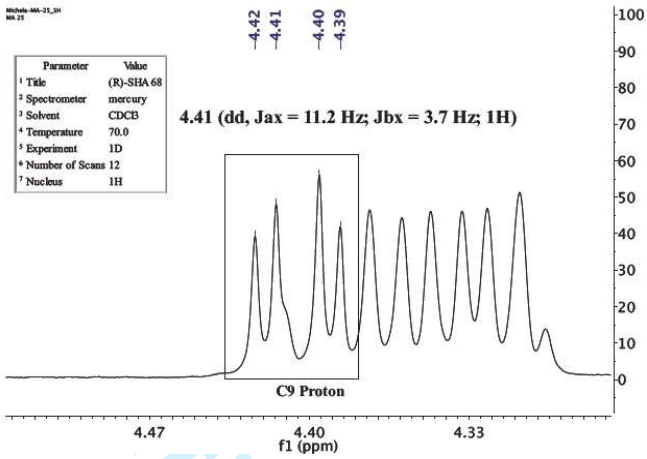

Figure 4. Inhibition response curves to compound **1** (SHA 68), compound **10** and compound **10a** in HEK293 cells expressing the murine NPSR and the human NPSR isoforms. Data are mean ± s.e.m. of four separate experiments made in duplicate.

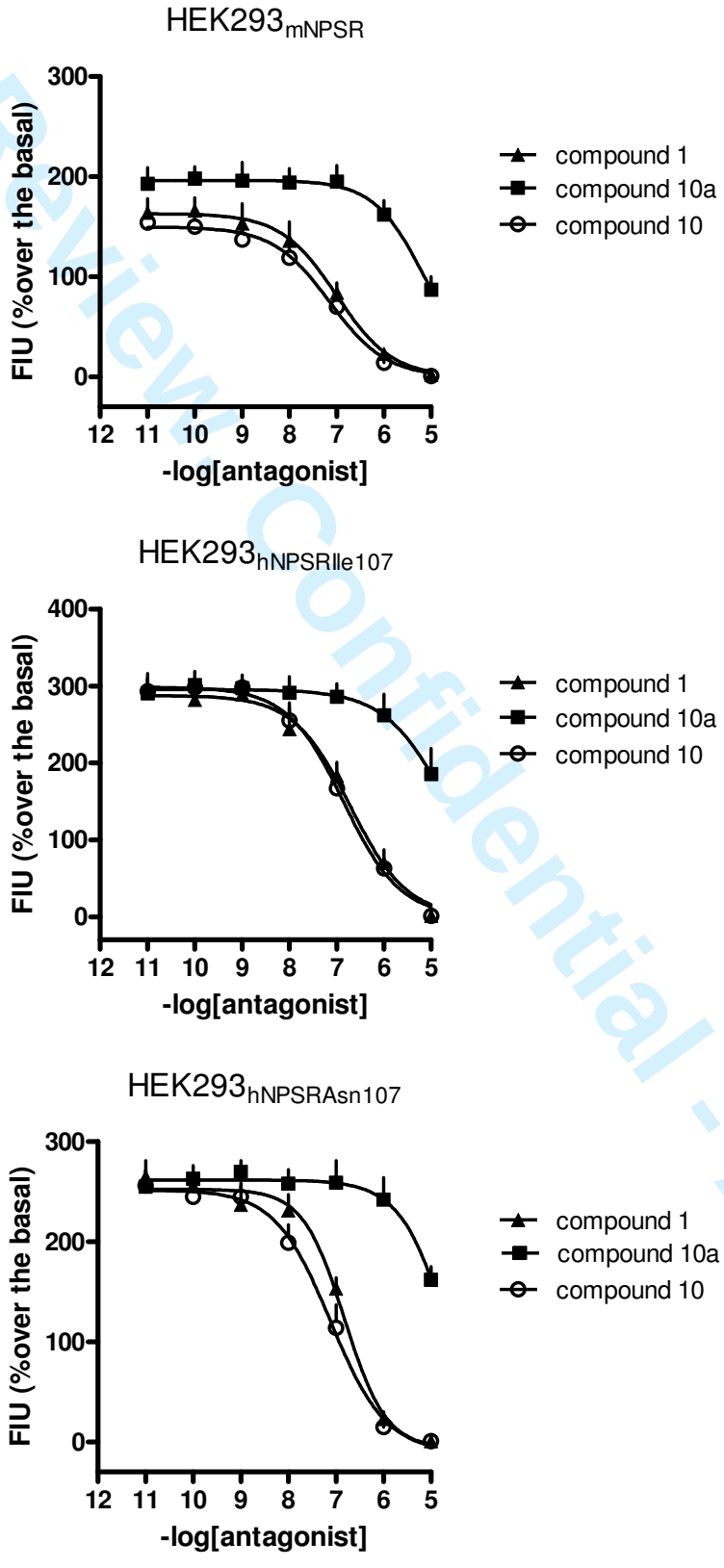

Scheme 1. Synthesis of compound **10** and **10a**

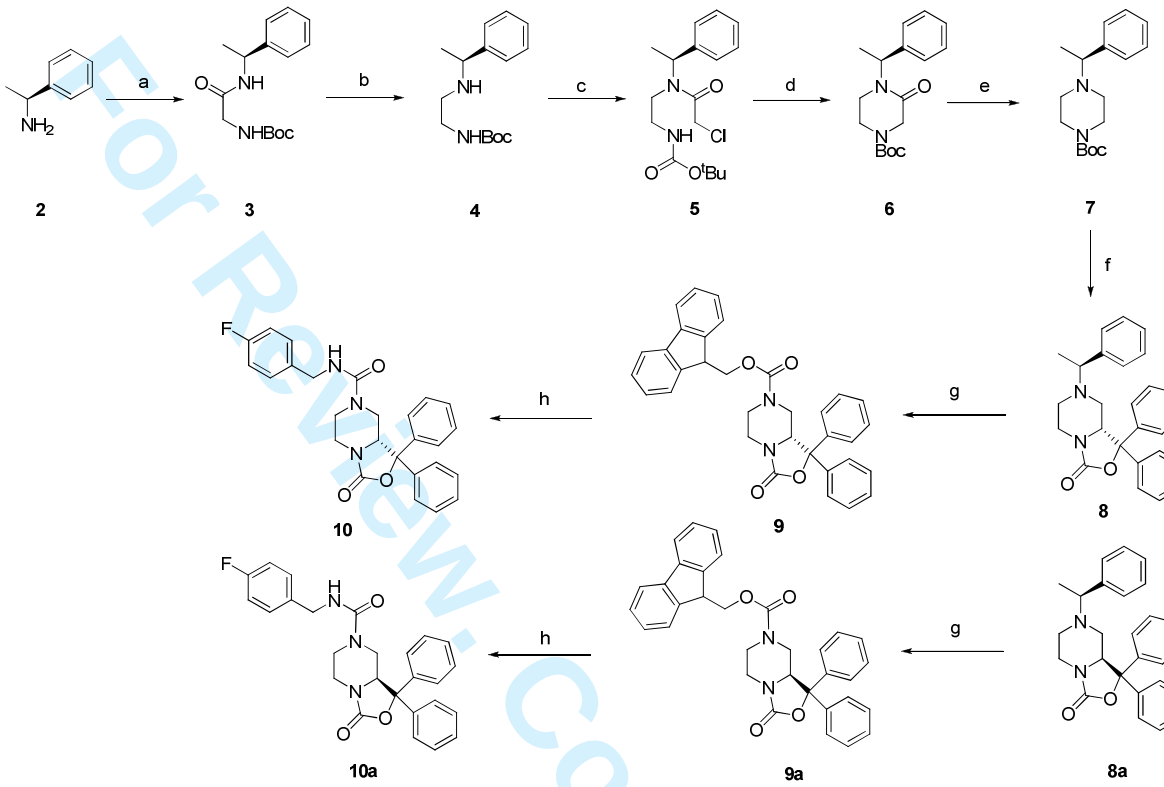

Reagents and conditions: (a) CH_2Cl_2, WSC, Boc-Gly-OH, room temp, 12h; (b) $LiAlH_4$, THF, 0°C, 1h; (c) Chloroacetyl-chloride, EtOAc, $NaHCO_3$, 0°C to room temp., 24h; (d) THF/DMF 1/1, NaH, 0°C to room temp, 24h; (e) THF, $LiAlH_4$, room temp, 4h; (f) THF, Benzophenone, *sec*-BuLi, TMEDA, -78°C to -30°C to room temp, 24h; (g) CH_3CN, Fmoc-Cl, reflux, 12h; (h) THF, DBU, *p*-fluoro-benzylisocyanate, room temp, 12h.

Table of Contents Graphic

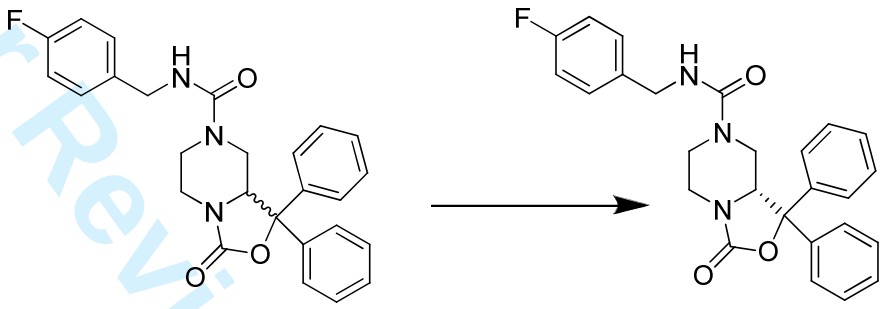

SHA-68 **10**

Compound **10** is the bioactive enantiomer